

Existence and Stability of Periodic Waves in the
Fractional Korteweg–de Vries Type Equations

EXISTENCE AND STABILITY OF PERIODIC WAVES IN
THE FRACTIONAL KORTEWEG–DE VRIES TYPE
EQUATIONS

BY
UYEN LE, M.A, B.Sc

A THESIS
SUBMITTED TO THE DEPARTMENT OF DEPARTMENT OF MATHEMATICS
AND STATISTICS
AND THE SCHOOL OF GRADUATE STUDIES
OF MCMASTER UNIVERSITY
IN PARTIAL FULFILMENT OF THE REQUIREMENTS
FOR THE DEGREE OF
DOCTOR OF PHILOSOPHY

© Copyright by Uyen Le, 2021
All Rights Reserved

Doctor of Philosophy (2021)
(Department of Mathematics and Statistics)

McMaster University
Hamilton, Ontario, Canada

TITLE: Existence and Stability of Periodic Waves in the
Fractional Korteweg–de Vries Type Equations

AUTHOR: Uyen Le
M.A(University of Kansas)
B.Sc(Seattle University)

SUPERVISOR: Dr. Dmitry Pelinovsky

NUMBER OF PAGES: x, 143

Abstract

This thesis is concerned with the existence and spectral stability of periodic waves in the fractional Korteweg–de Vries (KdV) equation and the fractional modified Korteweg–de Vries (mKdV) equation. We study the existence of periodic travelling waves using various tools such as Green’s function for fractional Laplacian operator, Petviashvili fixed point method, and a new variational characterization in which the periodic waves in fractional KdV and fractional mKdV are realized as the constrained minimizers of the quadratic part of the energy functional subject to fixed L^3 and L^4 norm respectively. This new variational framework allows us to identify the existence region of periodic travelling waves and to derive the criterion for spectral stability of the periodic waves with respect to perturbations of the same period.

Acknowledgements

First and foremost, I would like to express my sincere gratitude to my advisor, Dr. Dmitry Pelinovsky for his patience and unwavering support through my graduate studies. It has been a challenging and rewarding journey to study under his guidance. I can only hope that one day I will be able to emulate his work ethics and his vast amount knowledge.

I would like to thank Dr. Bartosz Protas, Dr. Stanley Alama, Dr. Lia Bronsard and Dr. Eric Sawyer for their wonderful and inspiring courses. I must also extend my thanks to Dr. Aaron Childs, Christopher McLean and the administrative staff members, Paula Marcoux and Taryn Sutton, who have guided me through my teaching duties.

I want to thank my peers in the department especially Lorena, Alexander, Adilbek, Priptal "Pip", Szymon, Anthony, Elkin, Jie, Subhajit and Neela. Their kindness and friendships have made my four years at McMaster University full of good memories.

Last but not least, I would like to thank my mother who is my constant source of comfort. Without her unconditional love and trust I could not have made it this far.

To my parents

Contents

Abstract	iii
Acknowledgements	iv
1 Introduction	1
1.1 Nonlinear Dispersive Waves	1
1.2 Stability Theory	5
1.3 Numerical Methods	8
1.4 Background Literature	10
1.5 Future Study	11
1.6 Outline of the Thesis	12
2 The Green's Function For The Fractional KdV Equation	15
2.1 Main Results	16
2.2 Properties of the Mittag-Leffler Function	17
2.3 Integral Representation	20
2.4 Properties of Green's function for $\alpha \leq 2$	22
2.5 Properties of Green's function $\mathcal{G}_{\mathbb{T}}$ for $\alpha > 2$	27
2.6 Numerical Illustrations	30
3 Existence Of Periodic Waves Of The Fractional KdV Equation	35
3.1 Main Results	36
3.2 Proof of Theorem 3.1	39
3.3 Proof of Theorem 3.2	41
3.4 Proof of Theorem 3.3	45
3.5 Periodic Waves for $\alpha = 1$ and 2	49
4 Convergence Of the Petviashvili Method	51
4.1 Main Results	53
4.2 Proof of Theorem 4.1	55
4.3 Proof of Theorem 4.2	57
4.4 Proof of Theorem 4.3	62
4.5 Numerical Illustrations	63

5	Spectral Stability Of Periodic Waves In Fractional KdV Equation	71
5.1	Main Results	72
5.2	Proof of Theorem 5.1	73
5.3	Proof of Theorem 5.2	78
5.4	Proof of Theorem 5.3	85
5.5	Numerical Illustrations	87
6	Periodic Waves In Fractional Modified KdV Equation	94
6.1	Main Results	95
6.2	Odd Periodic Waves	98
6.3	Even Periodic Waves	106
6.4	Examples and Numerical Illustrations	113
A	Preliminary Results	132
B	Periodic Waves In The KdV And BO Equation	135

List of Figures

1.1	Phase Portrait of the KdV equation (1.4): ψ' vs ψ with $b = 0$ and $c = 1$	3
2.1	Countable sequence of zeros $\{a_n\}_{n \in \mathbb{N}}$ of 2.47	29
2.2	Left: areas on (a, x) plane where $\mathcal{G}_{\mathbb{T}}$ is positive (yellow) and negative (blue). Right: the same but for $\mathcal{G}'_{\mathbb{T}}$	31
2.3	Profiles of $\mathcal{G}_{\mathbb{T}}$ for $\alpha = 0.5$ (left) and $\alpha = 1.5$ (right) for specific values of c	31
2.4	Profiles of G on \mathbb{T} for $\alpha = 2.5$ (top) and $\alpha = 3.5$ (bottom) at specific values of c	32
2.5	Difference between computations of $\mathcal{G}_{\mathbb{T}}(\pi)$ in (2.51) and (2.52) for $\alpha = 2.5$ (left) and $\alpha = 3.5$ (right) versus parameter c	33
2.6	Top: Location of the first five roots of $\mathcal{G}_{\mathbb{T}}(\pi)$ on the (c, α) plane. Bottom left: The first root of $\mathcal{G}_{\mathbb{T}}(\pi)$ relative to the boundary c_{α} (left). Bottom right: Coalescence of the 2nd and 3rd roots (upper right) and the 4th and 5th roots (lower right).	34
3.1	Schematic representation of the constant fixed point ψ_c and pairs of non-trivial fixed points on the $(c, \ \psi\ _{L^2_{\text{per}}})$ plane for $\alpha = 2$	48
3.2	Left: profile ψ in (3.40), $\alpha = 2$ and $k = 0.5$, Right: profile ψ in (3.42), $\alpha = 1$ and $\gamma = 1.0884$	50
4.1	Plot of Λ_2 versus α	61
4.2	Left: Eigenvalues of the operator $\tilde{\mathcal{L}}_{c,\alpha}^{-1} \tilde{\mathcal{H}}_{c,\alpha}$ for $\alpha = 2$. The blue curves and green curves represent the five largest and five smallest eigenvalues respectively. Right: Zoom in with the asymptotic dependence given by (4.38) and (4.39).	64
4.3	The plot of $ 1 - \lambda $ for the complex eigenvalues λ . The insert shows that the complex eigenvalues do not reach the boundary of the unit disk.	65
4.4	Iterations for $c = 2$ and $\alpha = 2$. (a) The last iteration versus x . (b) Computational errors versus n	65
4.5	Iterations for $c = 2.3$ and $\alpha = 2$. (a) The last iteration versus x . (b) Computational errors versus n	66

4.6	Iterations for $c = 3$ and $\alpha = 2$. (a) The last two iterations versus x . (b) Computational errors versus n	66
4.7	Left: Eigenvalues of the operator $\tilde{\mathcal{L}}_{c,\alpha}^{-1}\tilde{\mathcal{H}}_{c,\alpha}$ for $\alpha = 1$. Right: Zoom in with the asymptotic dependence given by (4.38) and (4.39).	67
4.8	Iterations for $c = 1.1$ and $\alpha = 1$. (a) The last four iterations versus x . (b) Computational errors versus n	67
4.9	Iterations for $c = 1.3$ and $\alpha = 1$. (a) The last four iterations versus x . (b) Computational errors versus n	68
4.10	Iterations for $c = 1.6$ and $\alpha = 1$. (a) The last two iterations versus x . (b) Computational errors versus n	68
4.11	Iterations for $c = 3$ and $\alpha = 2$. (a) The last iteration versus x . (b) Computational errors versus n	70
4.12	Iterations for $c = 1.6$ and $\alpha = 1$. (a) The last iteration versus x . (b) Computational errors versus n	70
5.1	The dependence of b versus c (left) and μ versus ω (right) for $\alpha = 1$	88
5.2	Left: the dependence of b versus c for $\alpha = 2$. Right: the difference between the numerical and exact values of b versus c . . .	89
5.3	Left: the dependence of b versus c for $\alpha = 0.6$ obtained with the Petviashvili method. Right: Profiles of ψ for two values of c . . .	90
5.4	Left: the dependence of b versus c for $\alpha = 0.55$ obtained with the Petviashvili method. Right: The number of Fourier modes versus c	91
5.5	The dependence of b versus c for $\alpha = 0.5$ (left) and $\alpha = 0.45$ (right) obtained with the Newton's method.	92
5.6	The dependence of μ versus ω for $\alpha = 0.6$ (left) and $\alpha = 0.5$ (right) obtained with the Newton's method.	92
6.1	Normalized eigenfunctions of \mathcal{H} on \mathbb{T} for $\alpha = 2$ computed from the exact expression of equations (6.71)–(6.73) and (6.75)–(6.76)	102
6.2	Periodic waves for $\alpha = 2$. Top left: Profiles of ψ with $b = 0$ for three different values of c . Top right: Profiles of ψ with $b \neq 0$ for three values of c . Middle left: Dependence of b versus c showing the pitchfork bifurcation point c_* . Middle right: Dependence of the momentum $F(\psi)$ versus c . Bottom left: Dependence of σ_0 versus c . Bottom right: The lowest eigenvalues of \mathcal{H} versus c . The blue (red) line corresponds to the family with $b = 0$ ($b \neq 0$).	120
6.3	The same as Figure 6.2 but for $\alpha = 1$	121
6.4	Periodic waves for $\alpha = 2$. Top: Profiles of ψ for three different values of c . Bottom: Dependence of the momentum $F(\psi)$ versus c (left) and $F(\phi)$ versus ω (right).	128

6.5	Periodic waves for $\alpha = 1$. Top: Profiles of ψ for three different values of c (left). Dependence of the momentum $F(\psi)$ versus c (right). Bottom: Dependence of $F(\phi)$ versus ω (left). and derivatives of $F(\phi)$ in ω (right). The solid (dashed) line shows the partial (ordinary) derivative in ω	129
6.6	The same as Figure 6.5 but for $\alpha = 0.6$	131

Chapter 1

Introduction

1.1 Nonlinear Dispersive Waves

The study of dispersive waves has long and rich history dating back to the work of Airy, Boussinesq and Stokes, where Airy developed the linear theory for water waves and Boussinesq and Stokes pioneered the nonlinear theory [3, 4, 22, 90]. Informally, the dispersing effect refers to the phenomenon where waves at different frequency propagate at different speed. This effect is readily seen via the Airy equation, which is a linear partial differential equation of the form

$$u_t + u_{xxx} = 0 \tag{1.1}$$

where $u(t, x) : \mathbb{R} \times \mathbb{R} \rightarrow \mathbb{R}$. The equation admits the plane wave solution

$$u(x, t) = e^{i(\xi x + \xi^3 t)}. \tag{1.2}$$

Hence, the dispersion relation obtained from $u(t, x) = e^{i\xi x - i\omega(\xi)t}$ is given by $\omega(\xi) = -\xi^3$. Since the phase velocity of the wave is given by $c = \frac{\omega(\xi)}{\xi}$, the solution implies that waves move to the left and waves with higher wave number propagate at higher speed. An example of nondispersive wave is the transport equation $u_t + v u_x = 0$; the solution is $u(t, x) = f(x - vt)$ and the dispersion relation of which is $\omega = v\xi$, implying that for any frequency, the wave travels at the same speed v .

The nonlinear counterpart of the Airy equation is the Korteweg–de Vries equation

$$u_t + u_{xxx} + 2uu_x = 0 \tag{1.3}$$

Although equation (1.3) was first introduced by Boussinesq in 1877 [23], it bears the name of Diederik Korteweg and Gustav de Vries, who rediscovered and studied the equation in depth about twenty years later [61].

The KdV equation has a wide range of applications in various fields. In

the context of water waves, it is used to model unidirectional propagation of shallow surface waves in a canal, internal solitons in the ocean, propagation of nonlinear acoustic waves in bubbly liquids.

Equation (1.3) is completely integrable, which can be solved explicitly using the method of IST (Inverse Scattering Transform). It is known that equation (1.3) admits travelling wave solution of the form $u(t, x) = \psi(x - ct)$ where c is a real valued constant representing the wave speed. When the travelling wave $\psi(x - ct) = \psi(\xi)$ is substituted to equation (1.3), we obtain the third order ordinary differential equation

$$\psi''' - c\psi' + 2\psi\psi' = 0.$$

Integrating the equation above once yields a nonlinear second order differential equation

$$\psi'' - c\psi + \psi^2 - b = 0, \quad (1.4)$$

where b is a constant of integration. Viewing the above as Newton's law, we obtain the potential function

$$V(\psi) = \frac{1}{3}\psi^3 - \frac{c}{2}\psi^2 - b\psi,$$

whose critical points occur when $\psi^2 - c\psi - b = 0$ corresponding to the equilibrium solutions of (1.4). Setting the constant of integration b to zero, we have two equilibria at $\psi = 0$ and $\psi = c$. There are two types of travelling waves solutions of (1.3): solitary and periodic waves. Fig 1.1 shows the phase portrait of (1.4) with $b = 0$ and $c = 1$ where we see a homoclinic orbit (red curve) to the saddle point $(0, 0)$ and a family of periodic orbits surrounding the center point $(1, 0)$. The homoclinic orbit defines a solitary wave as a bounded solution on the line and decaying to zero at infinity. The periodic orbits define periodic waves. It is well-known [2] that the solitary wave solution of equation (1.3) takes the form

$$u(t, x) = \frac{3c}{2} \operatorname{sech}^2 \left(\frac{\sqrt{c}}{2}(x - ct) \right),$$

and the periodic solutions are expressed as cnoidal waves [61].

This thesis focuses on the existence and stability of nonlinear, periodic travelling waves with nonlocal dispersion, that is, the dispersion relation $\omega(\xi)$ is no longer a polynomial in $i\xi$. Models of the form

$$u_t - \mathcal{M}u_x + f'(u)u_x = 0 \quad (1.5)$$

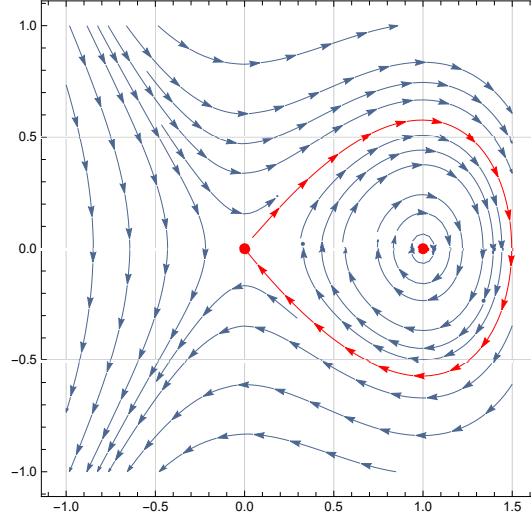


Figure 1.1: Phase Portrait of the KdV equation (1.4): ψ' vs ψ with $b = 0$ and $c = 1$

where \mathcal{M} is a constant coefficient, pseudodifferential operator and f is a general function were first studied in [1]. The equation can be used to describe unidirectional wave motion, and dynamics of dislocation in crystals. We are particularly interested in the case when $\mathcal{M} = D^\alpha = (-\Delta)^{\alpha/2}$ is the fractional Laplacian defined via Fourier series by

$$f(x) = \sum_{n \in \mathbb{Z}} f_n e^{inx}, \quad (D^\alpha f)(x) = \sum_{n \in \mathbb{Z}} |n|^\alpha f_n e^{inx}. \quad (1.6)$$

The fractional KdV and fractional mKdV equations are given respectively by

$$u_t + 2uu_x - (D^\alpha u)_x = 0, \quad (1.7)$$

$$u_t + 6u^2 u_x - (D^\alpha u)_x = 0, \quad (1.8)$$

where $u(t, x) : \mathbb{R} \times \mathbb{T} := [-\pi, \pi]$. From the travelling wave ansatz $u(t, x) = \psi(x - ct)$, we obtain the stationary equations for (1.7) and (1.8)

$$D^\alpha \psi + c\psi - p\psi^{p+1} + b = 0, \quad \psi \in H_{\text{per}}^\alpha(\mathbb{T}) \quad (1.9)$$

where $p = 1, 2$ respectively, the constant of integration b is another parameter of (1.9) in addition to the wave speed c , and the space $H_{\text{per}}^\alpha(\mathbb{T})$ is the class of $L_{\text{per}}^2(\mathbb{T})$ functions, whose derivatives up to order α also belong to $L_{\text{per}}^2(\mathbb{T})$ and

satisfying

$$H_{\text{per}}^{\alpha}(\mathbb{T}) = \left\{ f \in L_{\text{per}}^2(\mathbb{T}) : \sum_{n \in \mathbb{Z}} (1 + |n|^2)^{\alpha} |f_n|^2 < \infty \right\}.$$

For simplicity, in what follows, we will write H_{per}^{α} and L_{per}^2 instead of $H_{\text{per}}^{\alpha}(\mathbb{T})$ and $L_{\text{per}}^2(\mathbb{T})$. The subspace of odd (even) periodic functions in is denoted $H_{\text{per,odd}}^{\alpha}$ ($H_{\text{per,even}}^{\alpha}$). Similarly, the subspace of odd (even) functions in L^2 is denoted by $L_{\text{per,odd}}^2$ ($L_{\text{per,even}}^2$).

We are interested in the single-lobe, periodic waves ψ satisfying the following definition.

Definition 1.1. *We say the periodic wave ψ satisfying (1.9) has a single lobe profile if there exists only one maximum and minimum of ψ on \mathbb{T} .*

In equation (1.7), when $\alpha = 2$ we recover the KdV equation (1.3), and when $\alpha = 1$, we recover the Benjamin-Ono (BO) equation [19, 77], which models unidirectional propagation of small amplitude, internal waves in deep water. Similarly in equation (1.8), the two special cases are when $\alpha = 1$ and 2, corresponding to the modified KdV and modified BO equations.

Equation (1.7) has the following conserved quantities

$$M(u) = \int_{-\pi}^{\pi} u dx, \quad (1.10)$$

$$F(u) = \frac{1}{2} \int_{-\pi}^{\pi} u^2 dx, \quad (1.11)$$

$$E(u) = \frac{1}{2} \int_{-\pi}^{\pi} (D^{\frac{\alpha}{2}} u)^2 dx - \frac{1}{3} \int_{-\pi}^{\pi} u^3 dx, \quad (1.12)$$

representing mass, momentum and energy respectively. Equation (1.8) also admits the same conserved quantities with the mass and momentum defined similarly to (1.10) and (1.11) respectively, whereas the energy of equation (1.8) is given by

$$E(u) = \frac{1}{2} \int_{-\pi}^{\pi} \left((D^{\frac{\alpha}{2}} u)^2 - u^4 \right) dx, \quad (1.13)$$

Moreover, the stationary equation (1.9) is the Euler-Lagrange equation of the augmented Lyapunov functional

$$G_{c,b}(u) = E(u) + cF(u) + bM(u), \quad (1.14)$$

so that the solution ψ of (1.9) is a critical point of $G_{c,b}(u)$ satisfying $G'_{c,b}(\psi) = 0$. The conserved quantities in (1.10)-(1.12) and (1.13) are defined in $H_{\text{per}}^{\frac{\alpha}{2}}$. By Sobolev inequality, it follows that the last term of the energy in (1.12) is

bounded if $\alpha > \frac{1}{3}$. Similarly, to control the second term of the energy in (1.13), we require $\alpha > \frac{1}{2}$.

1.2 Stability Theory

After well-posedness theory of the initial value problem, stability theory plays an important role in the analysis of partial differential equations. Since the equations aim to model physical phenomena, their solutions are only useful if they can actually manifest in real life. Therefore, it is of special interest that we have a theory which can determine the robustness of the solutions, i.e., whether the solutions can persist under perturbations.

In general, we can give four definitions of stability of solutions in nonlinear evolution equations: spectral stability, linearized stability, orbital stability and asymptotic stability. However, in this thesis, we focus mainly on spectral stability. In order to explain the formalism of spectral stability for the travelling wave, let us consider the stationary equation (1.9) when $p = 1$. We compute the Hessian operator from (1.14) and find the linearized operator around the wave ψ in the form

$$\mathcal{H} := G''_{c,b}(\psi) = D^\alpha + c - 2\psi. \quad (1.15)$$

We note that \mathcal{H} is related to the (1.9). Indeed, when we take the derivative in (1.9) with respect to the spatial variable, we get $\mathcal{H}(\partial_x \psi) = 0$. It follows that the zero is an eigenvalue of \mathcal{H} with eigenfunction $\partial_x \psi$. The property that zero is a simple eigenvalue turns out to be important in our analysis.

The linearized operator \mathcal{H} determines the spectral stability of the periodic wave with the profile ψ . By using $u(t, x) = \psi(x - ct) + v(t, x - ct)$ and substituting equation (1.9) for ψ , we obtain

$$v_t + 2vv_x + 2(\psi v)_x - cv_x - D^\alpha v_x = 0. \quad (1.16)$$

Replacing the nonlinear equation (1.16) by its linearization at the zero solution yields the linearized evolution equation

$$v_t = \partial_x \mathcal{H}v, \quad (1.17)$$

where \mathcal{H} is given by (1.15). Since ψ depends only on x , separation of variables in the form $v(t, x) = e^{\lambda t} \eta(x)$ with some $\lambda \in \mathbb{C}$ and $\eta(x) : \mathbb{T} \rightarrow \mathbb{C}$ reduces the linear equation (1.17) to the spectral stability problem

$$\partial_x \mathcal{H} \eta = \lambda \eta. \quad (1.18)$$

Definition 1.2 (Spectral stability of periodic wave).

The periodic wave with profile ψ is said to be spectrally stable with respect to

perturbations of the same period if $\sigma(\partial_x \mathcal{H}) \subset i\mathbb{R}$ in L_{per}^2 . Otherwise, it is spectrally unstable if $\sigma(\partial_x \mathcal{H})$ in L_{per}^2 contains a point λ with $\text{Re}(\lambda) > 0$.

In fact, since the operator ∂_x is not one-to-one in the periodic case, the spectral problem (1.18) with $\lambda \neq 0$ is restricted to the space of zero mean functions

$$\partial_x \mathcal{H}|_{X_0} v = \lambda v, \quad X_0 := \{f \in L_{\text{per}}^2 : \langle f(x), 1 \rangle = 0\}, \quad (1.19)$$

where $\langle \cdot, \cdot \rangle$ denotes the standard inner product in L_{per}^2 . In [36, 50], it is shown that the periodic wave with profile ψ is spectrally and orbitally stable if it is the constrained minimizer of the energy (1.12) subject to fixed momentum (1.11) and mass (1.10). The mass constraint is given by the zero mean function space X_0 and the momentum constraint provides an additional orthogonality condition $\langle f, \psi \rangle = 0$. Since \mathcal{H} is the Hessian operator of $G(u)$ in (1.14), ψ is the constrained minimizer if the operator \mathcal{H} satisfies

$$\mathcal{H}|_{L_c^2} > 0, \quad \ker(\mathcal{H}|_{L_c^2}) = \ker(\mathcal{H}) = \text{span}(\partial_x \psi) \quad (1.20)$$

where $L_c^2 := \{f \in L_{\text{per}}^2 : \langle f, 1 \rangle = 0 = \langle f, \psi \rangle\}$ is a constrained subspace of L_{per}^2 . Then, Theorem A.3 provides the count for the number of negative eigenvalues of $\mathcal{H}|_{L_c^2}$ by relating to the number of negative and zero eigenvalues of the matrix $D(\lambda)$, which is constructed from the two constraints of L_c^2

$$D(\lambda) := \begin{bmatrix} \langle (\mathcal{H} - \lambda I)^{-1} \psi, \psi \rangle & \langle (\mathcal{H} - \lambda I)^{-1} \psi, 1 \rangle \\ \langle (\mathcal{H} - \lambda I)^{-1} 1, \psi \rangle & \langle (\mathcal{H} - \lambda I)^{-1} 1, 1 \rangle \end{bmatrix}, \quad \lambda \notin \sigma(\mathcal{H}). \quad (1.21)$$

By using Lagrange multipliers theorem we can show that the constrained minimizers are indeed solutions to the boundary value problem (1.9) but this leads to a delicate issue of determining if the solutions can be smoothly continued with respect to the Lagrange multipliers, which incidentally is the wave speed c and the integration constant b . In [53], it was claimed that for all $\alpha \in [1/3, 2]$, the solution of (1.9) with $p = 2$ obtained from minimizing the energy subject to fixed mass and momentum is smoothly differentiable with respect to both b and c and that the kernel of the operator \mathcal{H} is one dimensional. However, from Stokes expansion argument (see Chapter 3) we observe a threshold $\alpha_0 := \frac{\log 3}{\log 2} - 1$ for which the number of negative eigenvalue of \mathcal{H} changes from 1 to 2 as α crosses α_0 from above. If $\alpha < \alpha_0$, we show that the solution ψ to the boundary value problem (1.9) continued with respect to parameters c and b may pass the fold point in the sense of the following definition.

Definition 1.3. *We say that the solution ψ to the stationary equation (1.9) is at the fold point if the linearized operator \mathcal{H} at ψ has a double zero eigenvalue.*

To ensure the smooth continuation of the solution with respect to parameter c and b , in Chapter 5 we develop a new variational method which characterizes the solution as minimizer of the quadratic part of the energy functional subject to the zero mean condition and the fixed L^3 norm (see [65] for similar approach for the fifth order KdV equation). By using the new variational method, we are able to establish the sharp condition for stability of the periodic waves of the fractional KdV equation (1.7) based the monotonicity of the map between the wave speed c and the momentum. Furthermore, this variational characterization allows us to classify the entire region of existence of the periodic waves for α near α_0 .

Although spectral stability does not imply other modes of stability, the spectral information are important for the study of linear or nonlinear stability. If the periodic wave ψ is spectrally unstable, one can conclude that ψ is also linearly unstable. One mode of stability that is closely related to spectral stability is orbital stability. In order to define orbital stability we first have to define an orbit of ψ , that is, the family of $T(\omega)\psi$, where $\omega \in \mathbb{R}$ belongs to an open set and $T(\omega)$ is a generator of the group related to the symmetry of the evolution equation. We will use the following definition for the orbital stability of the periodic wave with the profile ψ .

Definition 1.4 (Orbital Stability of periodic wave).

The periodic wave with profile ψ is said to be orbitally stable in Banach space X with norm $\|\cdot\|_X$ if for any $\varepsilon > 0$, there is a $\delta > 0$ such that if $\|u(t) - \psi\|_X < \delta$ then

$$\inf_{\omega \in \mathbb{R}} \|u(t) - T(\omega)\psi\|_X < \varepsilon \quad (1.22)$$

for all $t \in \mathbb{R}^+$. Otherwise, ψ is orbitally unstable in X .

In the context of the fractional KdV and the fractional mKdV equations, the orbit of ψ is generated by the translation invariance, i.e $T(\omega)\psi = \psi(\cdot + \omega)$ and the Banach space X is given by the energy space $H_{per}^{\alpha/2}$. In the case of the fractional KdV equation, given global well-posedness in the space H_{per}^s for $s > \frac{\alpha}{2}$, if a periodic wave with profile ψ is spectrally stable then it is also orbitally stable according to the technique developed in [9].

Stability of the periodic waves in the cubic case with $p = 2$ has been unexplored for $\alpha < 2$. In Chapter 6, we use the similar approach to that of Chapter 5 and construct the periodic waves as the minimizers of the quadratic part of the energy functional subject to the zero mean condition and the fixed L^4 norm. Unlike the fractional KdV case, we are not able to classify all possible periodic, single-lobe solutions in the cubic case because the Galilean transformation in the cubic case generates an additional quadratic term. However, we are still able to consider the periodic waves satisfying (1.9) with $p = 2$ and $b = 0$ and establish the criteria for their spectral stability and instability.

1.3 Numerical Methods

Due to the pseudo-differential operator D^α , (1.7) and (1.8) are not integrable except when $\alpha = 1, 2$. Thus, explicit solutions are difficult to obtain. Here, we outline two fixed point methods which will be employed to numerically generate solutions of (1.7) and (1.8) in later chapters.

1.3.1 Petviashvili method

First introduced in Petviashvili's seminal paper in 1976 [82], the iteration method is robust for capturing solitary wave solutions in nonlinear evolution equations. In recent years, renewed interest in the method has resulted in several convergence analysis and modifications of the iteration, [8, 32, 39, 41]. While the convergence analysis of the Petviashvili method applied to the periodic fractional KdV equation is the main topic of Chapter 4, we briefly explain the iteration scheme here. Let us motivate the formulation of the Petviashvili method by first considering a nonlinear equation of the form

$$\mathcal{L}(u) = u^p, \quad (1.23)$$

where \mathcal{L} is a positive operator and $p > 1$. The stationary equations (1.9) with the constant of integration $b = 0$ can be formulated in the form of (1.23) with

$$\mathcal{L} = D^\alpha + c \quad (1.24)$$

Since \mathcal{L} is a positive operator, it is invertible; an intuitive, although naive, fixed point iteration of (1.23) reads

$$u_{n+1} = \mathcal{L}^{-1}u_n^p, \quad n \in \mathbb{N}. \quad (1.25)$$

However, it is easy to see that if ϕ is a solution of (1.23), then the scheme (1.25) fails to converge for the sequence $u_n = a_n\phi$ where $\{a_n\} \subset \mathbb{R}$ satisfying

$$a_{n+1} = a_n^p$$

since $a_* = 1$ is an unstable fixed point of the above for $p > 1$. To circumvent this difficulty, Petviashvili method introduces the stabilizing factor M_n to the naive iteration (1.25) as follows

$$u_{n+1} = M_n^\gamma \mathcal{L}^{-1}u_n$$

where

$$M_n = \frac{\langle \mathcal{L}u_n, u_n \rangle}{\langle u_n^s, u_n \rangle},$$

and γ is a constant which can be chosen to be $\frac{p}{p-1}$ for optimal convergence. This can be observed by taking $u_n = a_n \phi$. Then, $M_n = a_n^{1-p}$ and the iteration gives $a_{n+1} = a_n^{p+\gamma(1-p)}$ so the value of $\gamma = \frac{p}{p-1}$ reduces the power to 0 and the iterations converge in a single iteration.

Although Petviashvili method is favored for approximating solitary waves [31, 40], empirical experiments have shown it to diverge for periodic waves in finite depth, particularly sign indefinite, periodic waves. In [87], Petviashvili method was modified and it successfully approximated the periodic waves in infinite depth, however, the iteration did not work in finite depth. In [32], to overcome this drawback, the authors suggest rewriting the Euler equations in the form of a Babenko equation [16], then use a variable transform which makes the Babenko equation suitable for the classical Petviashvili method. The work [41] explores the generalization of Petviashvili method for non-power nonlinearities proposed originally in [63].

The rigorous analysis for the convergence (or divergence) of the classical Petviashvili method for periodic waves is one of the main results of Chapter 4. By using Stokes expansion and perturbation analysis, we are able to demarcate the specific range of c and α for which the Petviashvili iteration converges (or diverges) for both left propagating and right propagating waves. Moreover, we discover an important threshold $\alpha_0 = \frac{\log 3}{\log 2} - 1 \approx 0.585$. As α changes from $\alpha > \alpha_0$ to $\alpha < \alpha_0$, the number of negative eigenvalues of the operator \mathcal{H} increases from 1 to 2, which implies a double zero eigenvalue at $\alpha = \alpha_0$. Since the operator \mathcal{H} coincides with Hessian operator of the action functional G in (1.14), the number of zero eigenvalues has important implication in stability of the periodic waves [53] and in the solution continuation argument in Chapter 5.

1.3.2 Newton's method

We recast equation (1.23) as a root finding problem

$$F(u) := \mathcal{L}(u) - u^p = (c + D^\alpha)u - u^p = 0, \quad (1.26)$$

then given an initial guess u_0 , the Newton's method is defined by

$$u_{n+1} = u_n - [F'(u_n)]^{-1} F(u_n), \quad n \in \mathbb{N}, \quad (1.27)$$

where $F' := (c + D^\alpha)u - pu^{p-1}$ denotes the Jacobian operator of equation (1.26). Note that when $p = 2$, $F' = \mathcal{H}$ in equation (1.15). It is well known that the Newton's method converges quadratically whenever the operator F' is invertible. By differentiating in x we see that if ψ is the solution then ψ' belongs to $\ker(F')$, corresponding to the a zero eigenvalue of \mathcal{H} induced by translational symmetry. Thus, using parity between ψ and ψ' we need to restrict F' to appropriate subspace in order to guarantee its invertibility.

One drawback of the Newton's method is that it requires a good initial guess whereas the Petviashvili method is not as sensitive to the initial guess. Hence, it makes sense to use the Petviashvili method and the Newton's method in tandem. In bifurcation and solution continuation problems, which we encounter in Chapter 5 and 6, the Petviashvili method is used first to approximate the periodic wave, then this solution is set to be the initial seed for the Newton's method.

1.4 Background Literature

We list the important results in local well-posedness, stability theory and numerical analysis of (1.7) and (1.8).

1.4.1 Fractional KdV

Local well-posedness of the Cauchy problem for fractional KdV equation (1.7) was proven in [1] for the initial data in Sobolev space $H^s(\mathbb{R})$ or $H^s(\mathbb{T})$ for $s \geq \frac{3}{2}$. Local well-posedness in $H^s(\mathbb{R})$ for $s > \frac{3}{2} - \frac{3}{8}\alpha$ was proven in [67], where the authors also showed existence of weak global solutions in energy space $H^{\frac{\alpha}{2}}(\mathbb{R})$ for $\alpha > \frac{1}{2}$ and for $\alpha = \frac{1}{2}$ and small data. More recently, local well-posedness in $H^s(\mathbb{R})$ was proven in [73] for $\alpha > 0$ and $s > \frac{3}{2} - \frac{5}{4}\alpha$. Together with the conservation of energy, the latter result implies global well-posedness in the energy space $H^{\frac{\alpha}{2}}(\mathbb{R})$ for $\alpha > \frac{6}{7}$. Traveling solitary waves were characterized as minimizers of energy subject to the fixed momentum in [68] for $\alpha \in (\frac{1}{2}, 1)$ and in [5] for $\alpha \geq 1$.

Existence and stability of traveling periodic waves were analyzed by using perturbative [54], variational [25, 27, 53], and fixed-point [26] methods. From the variational point of view, the traveling periodic waves are characterized as constrained minimizers of energy $E(u)$ subject to fixed momentum $F(u)$ and mass $M(u)$ for every $\alpha \in (\frac{1}{3}, 2]$ [53]. Spectral stability of periodic waves with respect to perturbations of the same period follows from computations of eigenvalues of a 2-by-2 matrix involving derivatives of momentum and mass with respect to two parameters of the periodic waves, see [36, 50] for review. Recently, a different approach was developed in [48] where the periodic waves

with single-lobe profile were constructed by minimizing the energy $E(u)$ using the fixed momentum $F(u)$ as the only constraint. It was shown that such minimizers were degenerate up to the translation symmetry and were spectrally stable.

1.4.2 Fractional mKdV

In the case of equation (1.8), the well-posedness and stability theory are limited to the local cases $\alpha = 1, 2$. The global well-posedness results for the initial data in $H^s(\mathbb{R})$ with $s > \frac{1}{4}$ and in $H^s(\mathbb{T})$ with $s \geq \frac{1}{2}$ were obtained for $\alpha = 2$ in [33]. Local well-posedness results for initial data in $H^s(\mathbb{R})$ with $s \geq \frac{1}{2}$ were obtained for $\alpha = 1$ in [59]. Energy and momentum are conserved in the time evolution of such solutions. Local solutions with sufficiently large initial data in $H^{\frac{1}{2}}(\mathbb{R})$ blow up in a finite time [58, 70].

Spectral and orbital stability of the periodic waves of the stationary equation (1.9) with $p = 2$ were studied in the local case $\alpha = 2$. Employing the arguments in [21] and [92, 93], orbital stability of sign-definite dnoidal waves was proven in [12]. Spectral stability of sign-indefinite cnoidal waves was studied in [36] by using the count of negative eigenvalues of the operator \mathcal{H} restricted to the orthogonal complement of $\text{span}(1, \psi)$ (also also [50, 80]). It was discovered in [36] that the cnoidal waves were spectrally stable for smaller speeds c and spectrally unstable for larger speeds c . Spectral and orbital stability and instability of the cnoidal waves was proven in [15] by adopting the arguments of [66] in the periodic context and employing the approach in [51] based on the existence of a sufficiently smooth data-to-solution-map. Orbital stability of a particular family of positive periodic waves of the dnoidal type with $b \neq 0$ was proven in [11] by adopting the arguments of [47].

1.5 Future Study

We address possible avenues for future research, which arise from the results this thesis.

- In Chapter 2, we formulate two conjectures which are supported numerically. Since the Green's function was formulated using integral representation with the Mittag-Leffler functions, one possible route to pursue analytical evidence for the conjectures is to study the asymptotic expansion of the Mittag-Leffler function and to investigate how to control the associating error.
- The variational problem with one constraint (fixed L^4 norm), (6.5) and

(6.9) presented in Chapter 6 only describes only two particular families of periodic solution of the stationary equation (6.2) with $b = 0$. These families generalize the sign-indefinite cnoidal and the sign-definite dnoidal elliptic solutions of the local case $\alpha = 2$. However, it remains an open problem to characterize the most general solution of the stationary equation (6.2) with arbitrary b . Further studies are needed to investigate if the variational problem with two constraints

$$\inf_{u \in H_{\text{per}}^{\frac{\alpha}{2}}} \left\{ \int_{-\pi}^{\pi} [(D^{\frac{\alpha}{2}} u)^2 + c_0 u^2] dx : \int_{-\pi}^{\pi} u^4 dx = 1, \quad \frac{1}{2\pi} \int_{-\pi}^{\pi} u dx = m \right\}$$

can recover the most general periodic solution to (6.2).

1.6 Outline of the Thesis

Chapter 2,3 and 4 focus on the existence and positivity property of the periodic waves of the fractional KdV (1.7) while Chapter 5 and 6 deal with the spectral stability of the periodic waves of the fractional KdV (1.7) and the fractional mKdV (1.8). The brief overview of each chapter is as follows.

- In **Chapter 2**, we study the Green’s function, $G_{\mathbb{T}}$, of the shifted fractional Laplacian operator $c + (-\Delta)^{\frac{\alpha}{2}} := c + D^{\alpha}$, with $c > 0$, on periodic domain, which arises from the stationary equation of the fractional KdV. We show that $G_{\mathbb{T}}$ is positive and has single-lobe profile for $\alpha \in (0, 2]$. In particular, we give explicit formulation of the Green’s function in terms of the Mittag–Leffler functions. The Mittag–Leffler functions are important special functions of mathematical physics and often used in the context of Riemann–Liouville and Caputo’s fractional derivatives. The positivity result of the Green’s function is going to provide an important ingredient for the proof of the existence of positive, periodic waves of the fractional KdV in Chapter 3.

The content of Chapter 2 is based on:

U. Le and D. Pelinovsky, “Green’s Function for the Fractional KDV Equation on the Periodic Domain via Mittag–Leffler’s Function”.
arXiv:2101.02269

- In **Chapter 3**, our main goal is to establish the existence of single-lobe, periodic, travelling waves of (1.7). First, we make use of the perturbative argument to review existence of periodic waves in small amplitude

limits. We identify the left travelling waves bifurcation from zero solution via Stokes expansion. We also connect the left propagating waves to the right propagating waves using the speed parameter c . Then, we use the property of the Green's function obtained in Chapter 2 to show that the right moving waves are positive. This task is achieved by utilizing the Kranoselskii's fixed point theorem in a positive cone, and applying a homotopy argument with the Leray–Schauder index to distinguish single lobe solution from constant solution. Finally, we will also verify that the right-propagating waves are minimizers of the constrained energy functional.

- In **Chapter 4**, we recast the stationary equation of (1.9) with $p = 1$ as a fixed point problem to study the Petviashvili method. We explain the divergence (convergence) of the fixed point iterations from unstable eigenvalues of the generalized eigenvalue problem. We also show that a simple modification of the iterative method after the mean value shift results in the unconditional convergence of Petviashvili method. Then, we will illustrate the results numerically for the classical Korteweg–de Vries and Benjamin–Ono equations.

The content of Chapter 3 and Chapter 4 is based on:

*U. Le, D. Pelinovsky, “Convergence of the Petviashvili’s Method Near Periodic Waves in the Fractional Korteweg–De Vries Equation”. SIAM J. Math. Anal. **51** (2019), 2850–2883.*

- In **Chapter 5**, we put forth a new variational method where the periodic waves are realized constrained minimizers of the quadratic form of energy subject to fixed cubic part of energy and the zero mean. This new variational characterization allows us to unfold the existence region of travelling periodic waves and to give a sharp criterion for spectral stability of periodic waves with respect to perturbations of the same period. The sharp stability criterion is given by the monotonicity of the map from the wave speed to the wave momentum similarly to the stability criterion for solitary waves.

The content of Chapter 5 is based on:

*F. Natali, U. Le and D. Pelinovsky, “New Variational Characterization of Periodic Waves in the Fractional Korteweg–de Vries Equation”. Nonlinearity **33**, 2020, 1956–1986.*

- In **Chapter 6**, we extend the variational framework in Chapter 5 to the fractional mKdV equation (1.8). Two families of solutions in the local case are given by the sign-definite dnoidal and sign-indefinite cnoidal solutions. Both solutions can be characterized in the general fractional case as global minimizers of the quadratic part of the energy functional subject to the fixed L^4 norm: the sign-definite (sign-indefinite) solutions are obtained in the subspace of even (odd) functions. Morse index is computed for both solutions and the spectral stability criterion is derived. We show numerically that the family of sign-definite solutions has a generic fold bifurcation for the fractional Laplacian of lower regularity and the family of sign-indefinite solutions has a generic symmetry-breaking bifurcation both in the fractional and local cases. The content of Chapter 6 is based on:

F. Natali, U. Le and D. Pelinovsky, “Periodic Waves in the Fractional Modified Korteweg–de Vries Equation”. In print. arXiv:2006.14398

Chapter 2

The Green's Function For The Fractional KdV Equation

This chapter covers the strict positivity and single-lobe profile properties of the Green's function for the linear operator

$$\mathcal{L}_{c,\alpha} := c + (-\Delta)^{\alpha/2}, \quad (2.1)$$

where $(-\Delta)^{\frac{\alpha}{2}} = D^\alpha$ as defined in (1.6), $c > 0$ is a parameter and $\alpha > 0$. Our goal is to provide a new formulation of the Green's function $\mathcal{G}_{\mathbb{T}}$ using the Mittag-Leffler function [72] and to prove the positivity of $\mathcal{G}_{\mathbb{T}}$ using this new representation.

Properties of the fractional Laplacian on the d -dimensional torus \mathbb{T}^d were studied in [86]. Recent review of boundary-value problems for the fractional Laplacian and related applications can be found in [69].

The Green's function satisfies the periodic boundary value problem

$$[c + (-\Delta)^{\alpha/2}] \mathcal{G}_{\mathbb{T}}(x) = \delta(x), \quad x \in \mathbb{T}, \quad (2.2)$$

where δ is the Dirac delta distribution. The solution is represented via Fourier series by

$$\mathcal{G}_{\mathbb{T}}(x) = \frac{1}{2\pi} \sum_{n \in \mathbb{Z}} \frac{\cos(nx)}{c + |n|^\alpha} = \frac{1}{2\pi} \left(\frac{1}{c} + 2 \sum_{n=1}^{\infty} \frac{\cos(nx)}{c + n^\alpha} \right). \quad (2.3)$$

Green's function $\mathcal{G}_{\mathbb{T}}$ arises in the study of the nonlinear equation

$$[c + (-\Delta)^{\alpha/2}] \psi(x) = \psi(x)^{1+p}, \quad x \in \mathbb{T}, \quad (2.4)$$

where $p \in \mathbb{N}$. The nonlinear equation (2.4) defines the travelling periodic waves of the fractional Korteweg-de Vries (fKdV) equation with the speed c

[26, 27, 53, 54, 74, 75] and the standing periodic waves of the fractional nonlinear Schrödinger (fNLS) equation with the frequency c [30, 48]. Periodic solutions in other nonlinear elliptic equations associated with the fractional Laplacian were also considered, i.e., in [10, 38].

The plan for this chapter is as follows. The main results of the chapter are stated in Section 2.1. In Section 2.2, we mention properties of the Mittag–Leffler function which are important to the proof of the main results. Section 2.3 and 2.4 are devoted to proving the two main theorems of this chapter. We discuss the conjectures which extends of the main results to the case $\alpha \in (2, 4]$ in Section 2.5. Finally, numerical illustrations and numerical evidence to support the conjectures are collected in Section 2.6.

2.1 Main Results

We prove strict positivity and single-lobe profile properties of Green’s function $\mathcal{G}_{\mathbb{T}}$ satisfying the boundary-value problem (2.2) on \mathbb{T} for every $c > 0$ and every $\alpha \in (0, 2]$. Moreover, the main novelty of our approach is to relate $\mathcal{G}_{\mathbb{T}}$ and the Mittag–Leffler functions [72]. The positivity of $\mathcal{G}_{\mathbb{T}}$ for $\alpha \in (0, 2]$ are crucial for the existence of positive periodic, travelling waves of the fractional KDV equation (1.7), see Remark 2.5 and Chapter 3 for more details.

The following theorems summarize our results. The Green’s function $\mathcal{G}_{\mathbb{T}}$ can be rewritten from its Fourier series definition in (2.3) to the integral form involving the Mittag–Leffler function $E_{\alpha, \alpha}$ according to the following theorem

Theorem 2.1. *For every $c > 0$ and every $\alpha \in (0, 2]$ and $x \in \mathbb{T}$ it is true that*

$$\mathcal{G}_{\mathbb{T}}(x) = \frac{1}{2\pi c} + \frac{1}{\pi} \int_0^{\infty} \left(\frac{e^t \cos(x) - 1}{1 - 2e^t \cos(x) + e^{2t}} \right) t^{\alpha-1} E_{\alpha, \alpha}(-ct^{\alpha}) dt. \quad (2.5)$$

Furthermore, the representation (2.5) holds for $\alpha > 2$ provided that $c \in (0, c_{\alpha})$, where c_{α} is given by

$$c_{\alpha} := \left[\cos \left(\frac{\pi}{\alpha} \right) \right]^{-\alpha}, \quad (2.6)$$

Remark 2.1. *Several equivalent forms of the fractional Laplacian operator on \mathbb{R}^d with $d = \{1, 2, 3, \dots\}$ were shown in [62]. However, to the best of our knowledge, the fractional Laplacian has not been expressed in terms of the Mittag–Leffler function.*

Theorem 2.2. *For every $c > 0$ and every $\alpha \in (0, 2]$, Green’s function $\mathcal{G}_{\mathbb{T}}$ defined by (2.2) and (2.3) is even, strictly positive on \mathbb{T} , and monotonically decreasing on $(0, \pi)$.*

Remark 2.2. *The property of strict positivity of Green’s function was proven for different boundary-value problems associated with the fractional operators*

in [76] for $\alpha \in (0, 1)$ and in [17] for $\alpha \in (1, 2)$; however, the fractional derivatives were considered in the Riemann–Liouville sense (see [60, 83] for review of fractional derivatives).

Remark 2.3. We note that strict positivity and single-lobe profile property of the Green’s function on the real line, $\mathcal{G}_{\mathbb{R}}$, has been shown in [42] (see Lemma A.4) using similar properties of the heat kernel related to the fractional Laplacian $(-\Delta)^{\alpha/2}$ (see Lemma A.1 in [42]). The constant $c > 0$ in $\mathcal{L}_{c,\alpha}$ can be normalized to unity when $\mathcal{L}_{c,\alpha}$ is considered on the real line \mathbb{R} . We observe that the same properties hold for Green’s function $\mathcal{G}_{\mathbb{T}}$ on the periodic domain \mathbb{T} because it can be written as the following periodic superposition of Green’s function $\mathcal{G}_{\mathbb{R}}$ on the real line \mathbb{R} :

$$\mathcal{G}_{\mathbb{T}}(x) = \sum_{n \in \mathbb{Z}} \mathcal{G}_{\mathbb{R}}(x - 2\pi n), \quad x \in \mathbb{T}. \quad (2.7)$$

Hence, if $\mathcal{G}_{\mathbb{R}}(x) > 0$ for $x \in \mathbb{R}$, then $\mathcal{G}_{\mathbb{T}}(x) > 0$ for $x \in \mathbb{T}$ and if $\mathcal{G}'_{\mathbb{R}}(x) \leq 0$ and $\mathcal{G}''_{\mathbb{R}}(x) \leq 0$ for $x \geq 0$, then $\mathcal{G}'_{\mathbb{T}}(x) \leq 0$ for $x \in [0, \pi]$. However, here the parameter c in $\mathcal{G}_{\mathbb{T}}$ cannot be normalized to unity.

Remark 2.4. In [88], the author gave an alternative proof of Theorem 2.2 using probabilistic argument and proved complete monotonicity property of $\mathcal{G}_{\mathbb{T}}$ on $(0, \pi)$.

Remark 2.5. Equation (2.4) coincides with the travelling wave reduction of the fractional KdV equation (1.9) for $p = 1$ and $b = 0$. The positive solution ψ of (2.4) can be realized as a fixed point of the nonlinear operator $A_{c,\alpha}(\psi) : L^2_{\text{per}}(\mathbb{T}) \rightarrow L^2_{\text{per}}(\mathbb{T})$

$$A_{c,\alpha}(\psi) := \int_{-\pi}^{\pi} \mathcal{G}_{\mathbb{T}}(x - s) \psi(s)^2 ds. \quad (2.8)$$

Choosing an appropriate positive cone, and the positivity of the Green’s function implies that the operator $A_{c,\alpha}$ is closed in the cone. Then, application of the Krasnoselskii’s fixed point theorem verifies the existence of a fixed point of $A_{c,\alpha}$ in the cone, see Section 3.4.

2.2 Properties of the Mittag–Leffler Function

We first review some important properties of the Mittag–Leffler function which will be used for the proof of Theorem 2.1. The Mittag–Leffler function is defined by

$$E_{\alpha}(x) = \sum_{k=0}^{\infty} \frac{x^k}{\Gamma(k\alpha + 1)}, \quad \alpha > 0, \quad (2.9)$$

and its two-parametric generalization is defined by

$$E_{\alpha,\beta}(x) = \sum_{k=0}^{\infty} \frac{x^k}{\Gamma(k\alpha + \beta)}, \quad \alpha, \beta > 0. \quad (2.10)$$

Mittag–Leffler functions were introduced in the theory of analytic functions [72]. In recent years, they have become popular due to their applications in fractional differential equations [60]. In depth studies of the Mittag–Leffler functions can be found in [18] and [46]. Mittag–Leffler functions are typically used to represent solutions of initial-value problems for the fractional differential equations defined by the Riemann–Liouville or Caputo fractional derivatives [60].

Lemma 2.1. *For every $\alpha > 0$ and every $x \in \mathbb{R}$, it is true that*

$$E_{\alpha,\alpha}(x) = \alpha \frac{d}{dx} E_{\alpha}(x). \quad (2.11)$$

Proof. The result is obtained by differentiating (2.9) and using (2.10):

$$\frac{d}{dx} E_{\alpha}(x) = \sum_{k=1}^{\infty} \frac{x^{k-1}}{\alpha \Gamma(\alpha k)} = \frac{1}{\alpha} \sum_{k=0}^{\infty} \frac{x^k}{\Gamma(\alpha k + \alpha)} = \frac{1}{\alpha} E_{\alpha,\alpha}(x).$$

The series converges absolutely for every $x \in \mathbb{R}$ since E_{α} and $E_{\alpha,\alpha}$ are entire functions. \square

Lemma 2.2. [84] *For every $\alpha \in (0, 1]$, the function $x \mapsto E_{\alpha}(-x)$ is positive and completely monotonic for $x \geq 0$, that is*

$$(-1)^m \frac{d^m}{dx^m} E_{\alpha}(-x) \geq 0, \quad m \in \mathbb{N}, \quad x \geq 0. \quad (2.12)$$

Consequently, $E_{\alpha,\alpha}(-x) \geq 0$ for every $x \geq 0$.

Remark 2.6. *A necessary and sufficient condition for the function $x \mapsto E_{\alpha}(-x)$ to be completely monotonic for $x \geq 0$ is that $E_{\alpha}(-x)$ can be expressed in the form*

$$E_{\alpha}(-x) = \int_0^{\infty} e^{-xt} dF_{\alpha}(t), \quad x \geq 0,$$

where F_{α} is a non decreasing and bounded on $(0, \infty)$. The proof of [84] is based on the representation of $E_{\alpha}(-x)$ given by

$$E_{\alpha}(-x) = \frac{1}{2i\pi\alpha} \int_C \frac{e^{t^{1/\alpha}}}{t+x} dt,$$

with a specially selected the contour C in \mathbb{C} .

Lemma 2.3. [46] *For every $\alpha \in (0, 2)$, $E_\alpha(-x^\alpha)$ admits the asymptotic expansion*

$$E_\alpha(-x^\alpha) = - \sum_{k=1}^N \frac{(-1)^k}{\Gamma(1 - \alpha k) x^{\alpha k}} + \mathcal{O}\left(\frac{1}{|x|^{\alpha N + \alpha}}\right) \quad \text{as } x \rightarrow \infty, \quad (2.13)$$

where $N \in \mathbb{N}$ is arbitrarily fixed. For every $\alpha \geq 2$, $E_\alpha(-x^\alpha)$ admits the asymptotic expansion

$$E_\alpha(-x^\alpha) = \frac{1}{\alpha} \sum_{n=-N+1}^N e^{a_n x} + \mathcal{O}\left(\frac{1}{|x|^\alpha}\right) \quad \text{as } x \rightarrow \infty, \quad (2.14)$$

where $a_n = e^{\frac{i\pi(2n-1)}{\alpha}}$ and N is the largest integer satisfying the bound $2N - 1 \leq \frac{\alpha}{2}$.

Remark 2.7. *Asymptotic expansions (2.13) and (2.14) can be differentiated term by term.*

Remark 2.8. *We list the explicit cases of the Mittag-Leffler function $E_\alpha(-x^\alpha)$ for the first integers:*

$$\begin{aligned} \alpha = 1, & \quad E_1(-x) = e^{-x}, \\ \alpha = 2, & \quad E_2(-x^2) = \cos(x), \\ \alpha = 3, & \quad E_3(-x^3) = \frac{1}{3}e^{-x} + \frac{2}{3}e^{\frac{x}{2}} \cos\left(\frac{\sqrt{3}x}{2}\right), \\ \alpha = 4, & \quad E_4(-x^4) = \cos\left(\frac{x}{\sqrt{2}}\right) \cosh\left(\frac{x}{\sqrt{2}}\right). \end{aligned}$$

For $\alpha = 1$, the asymptotic representation (2.13) admits zero leading-order terms for every $N \in \mathbb{N}$. The asymptotic representation (2.14) is also obvious from the exact expressions for $\alpha = 2, 3, 4$, moreover, the remainder term is zero for $\alpha = 2$ and can be included to the summation by increasing N by one for $\alpha = 3$ and $\alpha = 4$.

Lemma 2.4. [46] *For every $\alpha \in (0, 2)$ and every $x \in \mathbb{R}$, $E_\alpha(-x)$ satisfies the following integral representation,*

$$E_\alpha(-x^\alpha) = \frac{2}{\pi} \sin\left(\frac{\pi\alpha}{2}\right) \int_0^\infty \frac{t^{\alpha-1} \cos(xt)}{1 + 2t^\alpha \cos\left(\frac{\pi\alpha}{2}\right) + t^{2\alpha}} dt. \quad (2.15)$$

Remark 2.9. *It is claimed in [46] that the integral representation (2.15) is true for all $\alpha > 0$, however, the integral is singular for $\alpha = 2$ and a discrepancy*

exists at $x = 0$ for $\alpha > 2$. For example, when $\alpha = 3$, it follows from (2.9) that $E_3(0) = 1$ whereas computing the integral given in (2.15) via the change of variable $u = t^3$ gives

$$E_3(0) = -\frac{2}{3\pi} \int_0^\infty \frac{du}{1+u^2} = -\frac{1}{3} \neq 1.$$

Hence, the integral representation (2.15) can only be used for $\alpha \in (0, 2)$, for which $E_\alpha(-x^\alpha)$ is bounded and decaying as $x \rightarrow +\infty$.

2.3 Integral Representation

The goal of this Section is to prove Theorem 2.1.

Proof. Assume first that $x \neq 0$ and $c \in (0, 1)$. Expanding each term of the trigonometric sum in (2.3) into absolutely convergent geometric series and interchanging the two series, we obtain

$$\sum_{n=1}^{\infty} \frac{\cos(nx)}{c+n^\alpha} = \sum_{n=1}^{\infty} \frac{\cos(nx)}{n^\alpha} \sum_{k=0}^{\infty} \left(\frac{-c}{n^\alpha}\right)^k = \sum_{k=0}^{\infty} (-c)^k \sum_{n=1}^{\infty} \frac{\cos(nx)}{n^{\alpha(k+1)}}. \quad (2.16)$$

It is known from the integral representation (1) in [85, Section 5.4.2] that for every $x \neq 0$ and $\alpha > 0$ that

$$\sum_{n=1}^{\infty} \frac{\cos(nx)}{n^{\alpha(k+1)}} = \frac{1}{\Gamma(\alpha k + \alpha)} \int_0^\infty \frac{t^{\alpha(k+1)-1} (e^t \cos(x) - 1)}{1 - 2e^t \cos(x) + e^{2t}} dt, \quad (2.17)$$

where $k \geq 0$. Substituting (2.17) into (2.16) and interchanging formally the summation and the integration yields the following representation:

$$\sum_{n=1}^{\infty} \frac{\cos(nx)}{c+n^\alpha} = \sum_{k=0}^{\infty} \frac{(-c)^k}{\Gamma(\alpha k + \alpha)} \int_0^\infty \frac{t^{\alpha(k+1)-1} (e^t \cos(x) - 1)}{1 - 2e^t \cos(x) + e^{2t}} dt, \quad (2.18)$$

$$= \int_0^\infty \left(\frac{e^t \cos(x) - 1}{1 - 2e^t \cos(x) + e^{2t}} \right) t^{\alpha-1} \sum_{k=0}^{\infty} \frac{(-ct^\alpha)^k}{\Gamma(\alpha k + \alpha)} dt, \quad (2.19)$$

$$= \int_0^\infty \left(\frac{e^t \cos(x) - 1}{1 - 2e^t \cos(x) + e^{2t}} \right) t^{\alpha-1} E_{\alpha, \alpha}(-ct^\alpha) dt. \quad (2.20)$$

This yields formally the integral formula (2.5). Let us now justify the interchange of summation and integration in (2.18). Using the chain rule and

Lemma 2.1, we get

$$t^{\alpha-1}E_{\alpha,\alpha}(-ct^\alpha) = -\frac{1}{c}\frac{d}{dt}E_\alpha(-ct^\alpha). \quad (2.21)$$

It follows from (2.21) that for every $\alpha \in (0, 2]$, the asymptotic expansion (2.13) in Lemma 2.3 for $\alpha \in (0, 2)$ and Remark 2.8 for $\alpha = 2$ imply that

$$\sup_{t \in [0, \infty)} t^{\alpha-1}|E_{\alpha,\alpha}(-t^\alpha)| < \infty. \quad (2.22)$$

Hence, the integral in (2.5) converges absolutely for every $x \neq 0$ and $\alpha \in (0, 2]$. Similarly, the integral in (2.18) converges absolutely for every $x \neq 0$ and $\alpha \in (0, 2]$, whereas the numerical series converges absolutely for every $c \in (0, 1)$. Thus, the interchange of summation and integration in (2.18) is justified by Fubini's theorem.

For $x = 0$, we note that $\mathcal{G}_\mathbb{T}(0) < \infty$ if $\alpha > 1$ and $\mathcal{G}_\mathbb{T}(0) = \infty$ if $\alpha \in (0, 1]$. Since $E_{\alpha,\alpha}(-x^\alpha) = 1 + \mathcal{O}(x^\alpha)$ as $x \rightarrow 0$, the integral in (2.5) converges absolutely for $x = 0$ and $\alpha \in (1, 2]$ and diverges for $x = 0$ and $\alpha \in (0, 1]$. Hence, the integral representation (2.5) holds again for $x = 0$, $c \in (0, 1)$, and $\alpha \in (0, 2]$. In order to extend the integral representation (2.5) from $c \in (0, 1)$ to every $c > 0$, we use real analyticity of Green's function $\mathcal{G}_\mathbb{T}$ and the integral in (2.5) in c for $c > 0$. Due to uniqueness of the analytical continuation of both $\mathcal{G}_\mathbb{T}$ and the integral in (2.5) in c , the equality in (2.5) is uniquely continued from $c \in (0, 1)$ to $c > 0$.

Next, we verify that the integral representation (2.5) extends to $\alpha > 2$ if c is sufficiently small. The asymptotic expansion (2.14) in Lemma 2.3 implies for every $c > 0$ and $\alpha > 2$ that

$$\sup_{t \in [0, \infty)} e^{-t \cos(\frac{\pi}{\alpha})} t^{\alpha-1} |E_{\alpha,\alpha}(-t^\alpha)| < \infty, \quad (2.23)$$

where we have used again the connection formula (2.21). In addition, $E_{\alpha,\alpha}(-x^\alpha) = 1 + \mathcal{O}(x^\alpha)$ as $x \rightarrow 0$. Due to the above properties, the integral in (2.5) converges absolutely for every $x \in \mathbb{T}$ if $c \in (0, c_\alpha)$, where c_α is given by (2.6). This justifies the formal computations similarly to those in the case when $\alpha \in (0, 2]$. \square

Remark 2.10. For $c \geq c_\alpha$ and $\alpha > 2$, the Fourier series representation (2.3) suggests that $|\mathcal{G}_\mathbb{T}(x)| < \infty$ for every $x \in \mathbb{T}$. However, the integral in (2.5) does not converge absolutely, hence it is not clear if the integral representation (2.5) can be used in this case. Our numerical results in Section 2.6 show that the integral representation (2.5) cannot be used for $c > c_\alpha$.

2.4 Properties of Green's function for $\alpha \leq 2$

Here, we prove Theorem 2.2 by incorporating the integral representation (2.5) in Theorem 2.1. It follows from (2.3) that $\mathcal{G}_{\mathbb{T}}$ is even for every $c > 0$ and $\alpha > 0$. Furthermore, if $\alpha \in (0, 1]$, then $\lim_{x \rightarrow 0} \mathcal{G}_{\mathbb{T}}(x) = +\infty$, and if $\alpha > 1$, then

$$\mathcal{G}_{\mathbb{T}}(0) = \frac{1}{2\pi} \left(\frac{1}{c} + 2 \sum_{n=1}^{\infty} \frac{1}{c + n^{\alpha}} \right) > 0.$$

We shall prove that $\mathcal{G}'_{\mathbb{T}}(x) \leq 0$ for $x \in (0, \pi)$ and $\mathcal{G}_{\mathbb{T}}(\pi) > 0$ for every $c > 0$ and $\alpha \in (0, 2]$. The proof of $\mathcal{G}'_{\mathbb{T}}(x) \leq 0$ on $(0, \pi)$ is broken into Propositions 2.2, 2.3 and 2.4 corresponding to $\alpha \in (0, 1]$, $\alpha \in (1, 2)$ and $\alpha = 2$ respectively. Proposition 2.1 gives an integral representation for $\mathcal{G}_{\mathbb{T}}(\pi)$ which implies its strict positivity for every $c > 0$ and $\alpha \in (0, 2)$. For $\alpha = 2$, this result follows from the exact analytical representation of $\mathcal{G}_{\mathbb{T}}$.

Proposition 2.1. *For every $c > 0$ and every $\alpha \in (0, 2)$, it is true that*

$$\mathcal{G}_{\mathbb{T}}(\pi) = \frac{\sin(\frac{\alpha\pi}{2})}{\pi c^{1-\frac{1}{\alpha}}} \int_0^{\infty} \frac{s^{\alpha} \operatorname{csch}(\pi c^{\frac{1}{\alpha}} s)}{1 + 2^{\alpha} \cos(\frac{\alpha\pi}{2}) + s^{2\alpha}} ds, \quad (2.24)$$

which implies $\mathcal{G}_{\mathbb{T}}(\pi) > 0$.

Proof. Evaluating the integral representation (2.5) at $x = \pi$, we obtain

$$\mathcal{G}_{\mathbb{T}}(\pi) = \frac{1}{2\pi c} - \frac{1}{\pi} \int_0^{\infty} \frac{1}{1 + e^t} t^{\alpha-1} E_{\alpha, \alpha}(-ct^{\alpha}) st \quad (2.25)$$

Substituting (2.21) into (2.25), integrating by parts, and using the asymptotic representation (2.13) to get zero contribution in the limit of $t \rightarrow \infty$, we obtain

$$\mathcal{G}_{\mathbb{T}}(\pi) = \frac{1}{\pi c} \int_0^{\infty} \frac{e^t}{(1 + e^t)^2} E_{\alpha}(-ct^{\alpha}) st, \quad (2.26)$$

where the integral converges absolutely for every $c > 0$ and $\alpha \in (0, 2)$. Substituting the integral representation (2.15) for $E_{\alpha}(-ct^{\alpha})$ from Lemma 2.4 into (2.26), we obtain

$$\mathcal{G}_{\mathbb{T}}(\pi) = \frac{2}{\pi^2 c} \sin\left(\frac{\alpha\pi}{2}\right) \int_0^{\infty} \frac{e^t}{(1 + e^t)^2} \int_0^{\infty} \frac{s^{\alpha-1} \cos(c^{\frac{1}{\alpha}} ts)}{1 + 2^{\alpha} \cos(\frac{\pi\alpha}{2}) + s^{2\alpha}} ds dt \quad (2.27)$$

Since both integrates belong to $L^1(0, \infty)$, the order of integration in (2.27) can

be interchanged to get

$$\mathcal{G}_{\mathbb{T}}(\pi) = \frac{2}{\pi^2 c} \sin\left(\frac{\alpha\pi}{2}\right) \int_0^\infty \frac{s^{\alpha-1}}{1 + 2^\alpha \cos\left(\frac{\pi\alpha}{2}\right) + s^{2\alpha}} \int_0^\infty \frac{e^t \cos(c^{\frac{1}{\alpha}} st)}{(1 + e^t)^2} dt ds \quad (2.28)$$

The inner integral is evaluated exactly with the help of integral (7) in [85, Section 2.5.46]:

$$\int_0^\infty \frac{e^t \cos(c^{\frac{1}{\alpha}} st)}{(1 + e^t)^2} dt = \frac{\pi}{2} c^{\frac{1}{\alpha}} s \operatorname{csch}(\pi c^{\frac{1}{\alpha}} s),$$

When it is substituted into (2.28), it yields the integral representation (2.24). The integrand is positive and absolutely integrable for every $c > 0$ and $\alpha \in (0, 2)$, which implies that $\mathcal{G}_{\mathbb{T}}(\pi) > 0$. \square

Remark 2.11. *positivity of $\mathcal{G}_{\mathbb{T}}(\pi)$ for $c > 0$ and $\alpha \in (0, 1]$ also follows from the representation (2.26) due to positivity of $E_\alpha(-ct^\alpha)$ for every $t > 0$ in Lemma 2.2. However, $E_\alpha(-ct^\alpha)$ is not positive for all $t > 0$ when $\alpha > 1$, hence, the representation (2.26) is not sufficient for the proof of positivity of $\mathcal{G}_{\mathbb{T}}(\pi)$ if $\alpha \in (1, 2)$.*

It remains to prove that $\mathcal{G}'_{\mathbb{T}}(x) \leq 0$ for every $x \in (0, \pi)$. The proof is carried differently for $\alpha \in (0, 1]$, for $\alpha \in (1, 2)$, and for $\alpha = 2$. In the first case, we obtain the integral representation for $\mathcal{G}'_{\mathbb{T}}(x)$, which is strictly negative for $x \in (0, \pi)$. In the second case, we employ the variational method to verify that the unique solution $\mathcal{G}_{\mathbb{T}}$ of the boundary-value problem (2.2) admits the single lobe profile, with the only maximum located at the point of symmetry at $x = 0$. In the case $\alpha = 2$, we rely on the exact analytic form of $\mathcal{G}_{\mathbb{T}}$.

The next two propositions give results for the case $\alpha \in (0, 1]$ and $\alpha \in (1, 2)$.

Proposition 2.2. *For every $c > 0$ and every $\alpha \in (0, 1]$, $\mathcal{G}'_{\mathbb{T}}(x) < 0$ for every $x \in (0, \pi)$.*

Proof. Differentiating the integral representation (2.5) in x yields

$$\begin{aligned} \mathcal{G}'_{\mathbb{T}}(x) &= \frac{1}{\pi c} \int_0^\infty t^{\alpha-1} E_{\alpha,\alpha}(-ct^\alpha) \frac{d}{dx} \left(\frac{e^t \cos(x) - 1}{1 - 2e^t \cos(x) + e^{2t}} \right) dt, \\ &= -\frac{\sin(x)}{\pi c} \int_0^\infty t^{\alpha-1} E_{\alpha,\alpha}(-ct^\alpha) \frac{e^t (e^{2t} - 1)}{(1 - 2e^t \cos(x) + e^{2t})^2} dt, \end{aligned} \quad (2.29)$$

where the integrand is absolutely integrable. It follows by Lemma 2.2 that $E_{\alpha,\alpha}(-ct^\alpha) \geq 0$ for $t > 0$. Since $\sin(x) > 0$ for $x \in (0, \pi)$, and the integrand is positive, it follows from the integral representation (2.29) that $\mathcal{G}'_{\mathbb{T}}(x) < 0$ for $x \in (0, \pi)$. \square

Proposition 2.3. *For every $c > 0$ and every $\alpha \in (1, 2)$, $\mathcal{G}'_{\mathbb{T}}(x) \leq 0$ for every $x \in (0, \pi)$.*

Proof. The proof consists of the following two steps. First, we obtain a variational solution to the boundary-value problem (2.2). Second, we use the fractional Polya–Szegő inequality to show that the solution $\mathcal{G}_{\mathbb{T}}$ has a single-lobe profile on \mathbb{T} with the only maximum located at the point of symmetry at $x = 0$.

Step 1: Let us consider the following minimization problem,

$$\mathcal{B}_c := \min_{u \in H_{\text{per}}^{\frac{\alpha}{2}}} \{B_c(u) - u(0)\}, \quad (2.30)$$

where the quadratic functional $B_c(u)$ is given by

$$B_c(u) = \frac{1}{2} \int_{\mathbb{T}} \left[(D^{\frac{\alpha}{2}} u)^2 + cu^2 \right] dx. \quad (2.31)$$

Since $c > 0$, we have

$$\frac{1}{2} \min(1, c) \|u\|_{H_{\text{per}}^{\frac{\alpha}{2}}} \leq B_c(u) \leq \frac{1}{2} \max(1, c) \|u\|_{H_{\text{per}}^{\frac{\alpha}{2}}},$$

hence, $B_c(u)$ is equivalent to the squared $H_{\text{per}}^{\frac{\alpha}{2}}$ norm. Moreover, for $\alpha \in (1, 2)$, $\delta \in H_{\text{per}}^{-\frac{\alpha}{2}}$, the dual of $H_{\text{per}}^{\frac{\alpha}{2}}$ since

$$\|\delta\|_{H_{\text{per}}^{-\frac{\alpha}{2}}} = \sum_{\xi \in \mathbb{Z}} \frac{1}{(1 + |\xi|^2)^{\frac{\alpha}{2}}} < \infty.$$

Thus, by Lax–Milgram theorem (see Corollary 5.8 in [24]), there exists a unique $\mathcal{G}_{\mathbb{T}} \in H_{\text{per}}^{\frac{\alpha}{2}}$ such that $\mathcal{G}_{\mathbb{T}}$ is the global minimizer of the variational problem (2.30), for which the Euler–Lagrange equation is equivalent to the boundary-value problem (2.2). By uniqueness of solutions of the two problems, $\mathcal{G}_{\mathbb{T}}$ is equivalently written as the Fourier series (2.3), from which it follows that $\mathcal{G}_{\mathbb{T}}(\pi) < \mathcal{G}_{\mathbb{T}}(0)$. Hence, $\mathcal{G}_{\mathbb{T}}$ is different from a constant function on \mathbb{T} .

Remark 2.12. *The variational method and in particular the Lax–Milgram theorem cannot be applied to the case $\alpha \in (0, 1]$ since the Dirac delta distribution δ does not belong to the dual space of $H_{\text{per}}^{\frac{\alpha}{2}}$ when $\alpha \in (0, 1]$.*

Step 2: We utilize the fractional Polya–Szegő inequality, proved in the appendix of [30], to show that a symmetric decreasing rearrangement of the minimizer $\mathcal{G}_{\mathbb{T}}$ on \mathbb{T} does not increase $B_c(u)$. For completeness, we state the following definition and lemma.

Definition 2.1. Let m be the Lebesgue measure on \mathbb{T} and $f(x) : \mathbb{R} \rightarrow \mathbb{R}$ be a 2π periodic function. The symmetric and decreasing rearrangement \tilde{f} of f on \mathbb{T} is given by

$$\tilde{f}(x) = \inf\{t : m(\{z \in \mathbb{T} : f(z) > t\}) \leq 2|x|\}, \quad x \in \mathbb{T}. \quad (2.32)$$

The rearrangement \tilde{f} satisfies the following properties:

- i) $\tilde{f}(-x) = \tilde{f}(x)$ and $\tilde{f}'(x) \leq 0$ for $x \in (0, \pi)$.
- ii) $\tilde{f}(0) = \max_{x \in \mathbb{T}} f(x)$.
- iii) $\|\tilde{f}\|_{L^2(\mathbb{T})} = \|f\|_{L^2(\mathbb{T})}$.

Lemma 2.5. [30] For every $\alpha > 1$ and every $f \in H_{per}^{\frac{\alpha}{2}}(\mathbb{T})$, it is true that

$$\int_{-\pi}^{\pi} |D^{\frac{\alpha}{2}} \tilde{f}|^2 dx \leq \int_{-\pi}^{\pi} |D^{\frac{\alpha}{2}} f|^2 dx. \quad (2.33)$$

The argument of the proof in the second step goes as follows. Suppose $\tilde{G}_{\mathbb{T}}$ is the symmetric and decreasing rearrangement of $\mathcal{G}_{\mathbb{T}}$, then by Lemma 2.5 and by property (iii) of Definition 2.1 we have $B_c(\tilde{G}_{\mathbb{T}}) \leq B_c(\mathcal{G}_{\mathbb{T}})$. Since the global minimizer of the variational problem (2.30) is uniquely given by $\mathcal{G}_{\mathbb{T}}$, $\tilde{G}_{\mathbb{T}}$ coincides with $\mathcal{G}_{\mathbb{T}}$ up to a translation on \mathbb{T} . However, it follows from (2.3) that $\mathcal{G}_{\mathbb{T}}(-x) = \mathcal{G}_{\mathbb{T}}(x)$ and $\mathcal{G}_{\mathbb{T}}(\pi) < \mathcal{G}_{\mathbb{T}}(0)$, hence an internal maximum at $x_0 \in (0, \pi)$ would contradict to the single-lobe profile of $\mathcal{G}_{\mathbb{T}}$ and the only maximum of $\mathcal{G}_{\mathbb{T}}$ is located at 0, so that $\mathcal{G}_{\mathbb{T}}(x) = \tilde{G}_{\mathbb{T}}(x)$ for every $x \in \mathbb{T}$. It follows from property (i) of Definition 2.1 that $\mathcal{G}'_{\mathbb{T}}(x) \leq 0$ for $x \in (0, \pi)$. \square

Finally, we derive the explicit form of $\mathcal{G}_{\mathbb{T}}$ for $\alpha = 2$. The proposition below verifies Theorem 2.2 for $\alpha = 2$.

Proposition 2.4. For every $c > 0$, Green's function $\mathcal{G}_{\mathbb{T}}$ at $\alpha = 2$ is even, strictly positive on \mathbb{T} , and strictly monotonically decreasing on $(0, \pi)$.

Proof. For $\alpha = 2$, Green's function $\mathcal{G}_{\mathbb{T}}$ satisfies the second-order differential equation

$$-\mathcal{G}_{\mathbb{T}}''(x) + c\mathcal{G}_{\mathbb{T}}(x) = \delta(x), \quad x \in \mathbb{T}, \quad (2.34)$$

where $c > 0$. It follows from the theory of Dirac delta distributions that $\mathcal{G}_{\mathbb{T}}$ is continuous, even, periodic on \mathbb{T} , and have a jump discontinuity of the first derivative at $x = 0$.

To see the jump condition of $\mathcal{G}'_{\mathbb{T}}(x)$ across $x = 0$, we integrate (2.34) on $(-\varepsilon, \varepsilon)$ and then take the limit as $\varepsilon \rightarrow 0$.

$$\lim_{\varepsilon \rightarrow 0} \int_{-\varepsilon}^{\varepsilon} (-\mathcal{G}_{\mathbb{T}}''(x) + c\mathcal{G}_{\mathbb{T}}(x)) dx = \lim_{\varepsilon \rightarrow 0} \int_{-\varepsilon}^{\varepsilon} \delta(x) dx = 1, \quad (2.35)$$

where the last equality follows from properties of δ . Since $\mathcal{G}_{\mathbb{T}} \in C^0(\mathbb{R})$, the second term on the left hand side vanishes as $\varepsilon \rightarrow 0$, which yields $-\mathcal{G}'_{\mathbb{T}}(0^+) + \mathcal{G}'_{\mathbb{T}}(0^-) = 1$. Since $\mathcal{G}_{\mathbb{T}}$ is even on \mathbb{R} , we obtain

$$\mathcal{G}'_{\mathbb{T}}(0^+) = -\frac{1}{2}. \quad (2.36)$$

Additionally, it follows from the Fourier series representation (2.3) with $\alpha = 2$ that

$$\mathcal{G}_{\mathbb{T}}(0) = \frac{1}{2\pi} \sum_{n \in \mathbb{Z}} \frac{1}{c + n^2} = \frac{\coth(\sqrt{c}\pi)}{2\sqrt{c}}, \quad (2.37)$$

where we have used numerical series (4) in [85, Section 5.1.25].

The differential equation (2.34) is solved for even $\mathcal{G}_{\mathbb{T}}$ as follows:

$$\mathcal{G}_{\mathbb{T}}(x) = \mathcal{G}_{\mathbb{T}}(0) \cosh(\sqrt{c}x) + \mathcal{G}'_{\mathbb{T}}(0^+) \frac{\sinh(\sqrt{c}|x|)}{\sqrt{c}}, \quad x \in \mathbb{T}.$$

Due to (2.36) and (2.37), this can be rewritten in the closed form as

$$\mathcal{G}_{\mathbb{T}}(x) = \frac{\cosh(\sqrt{c}(\pi - |x|))}{2\sqrt{c} \sinh(\sqrt{c}\pi)}, \quad x \in \mathbb{T}. \quad (2.38)$$

It follows from (2.38) that

$$\mathcal{G}'_{\mathbb{T}}(x) = -\frac{\sinh(\sqrt{c}(\pi - x))}{2 \sinh(\sqrt{c}\pi)} < 0, \quad x \in (0, \pi), \quad (2.39)$$

and hence $\mathcal{G}_{\mathbb{T}}$ is strictly monotonically decreasing on $(0, \pi)$. On the other hand,

$$\mathcal{G}_{\mathbb{T}}(\pi) = \frac{1}{2 \sinh(\sqrt{c}\pi)} > 0, \quad c > 0, \quad (2.40)$$

and hence $\mathcal{G}_{\mathbb{T}}$ is strictly positive on \mathbb{T} . Note that the exact expression for $\mathcal{G}_{\mathbb{T}}(\pi)$ in (2.40) also follows from numerical series (6) in [85, Section 5.1.25]. \square

Remark 2.13. *It follows from (2.38) that $\mathcal{G}'_{\mathbb{T}}(\pi) = 0$, due to smoothness and periodicity of even $\mathcal{G}_{\mathbb{T}}(x)$ across $x = \pm\pi$. Therefore, the exact expression in (2.38) and the relation for $\mathcal{G}_{\mathbb{T}}(0)$ in (2.37) can be alternatively found by solving the differential equation (2.34) for even $\mathcal{G}_{\mathbb{T}}$ subject to the boundary conditions*

$$\mathcal{G}'_{\mathbb{T}}(0^\pm) = \mp \frac{1}{2} \text{ and } \mathcal{G}'_{\mathbb{T}}(\pm\pi) = 0.$$

2.5 Properties of Green's function $\mathcal{G}_{\mathbb{T}}$ for $\alpha > 2$

From the results of previous sections, we see that the properties of $\mathcal{G}_{\mathbb{T}}$ for $\alpha \in (0, 2)$ is similar to those of $\alpha = 2$ (the same is true for $G_{\mathbb{R}}$). However, it is an open question if the properties of $\mathcal{G}_{\mathbb{T}}$ for $\alpha \in (2, 4)$ is similar to those of $\alpha = 4$, for which $G_{\mathbb{R}}$ has infinitely many oscillations, whereas the number of oscillations of $\mathcal{G}_{\mathbb{T}}$ only becomes infinite in the limit of $c \rightarrow \infty$. We make the following conjectures.

Conjecture 2.1. *For each $\alpha \in (2, 4]$, there exists $c_0 > 0$ such that for $c \in (0, c_0)$, Green's function $\mathcal{G}_{\mathbb{T}}$ defined by (2.2) and (2.3) is even, strictly positive on \mathbb{T} , and monotonically decreasing on $(0, \pi)$. For $c \in [c_0, \infty)$, $\mathcal{G}_{\mathbb{T}}$ has a finite number of zeros on \mathbb{T} . The number of zeros is bounded in the limit of $c \rightarrow \infty$ if $\alpha \in (2, 4)$ and unbounded as $c \rightarrow \infty$ if $\alpha = 4$.*

Since the limit $c \rightarrow \infty$ for Green's function $\mathcal{G}_{\mathbb{T}}$ can be re-scaled as Green's function $\mathcal{G}_{\mathbb{R}}$ with c normalized to unity, Conjecture 2.1 implies the following conjecture (which is relevant for interactions of strongly localized waves in [34, 35]).

Conjecture 2.2. *For every $c > 0$ and every $\alpha \in (2, 4]$, Green's function $\mathcal{G}_{\mathbb{R}}$ is not strictly positive on \mathbb{R} and is not monotonically decreasing on $(0, \infty)$. It has a finite number of zeros on \mathbb{R} if $\alpha \in (2, 4)$ and an infinite number of zeros if $\alpha = 4$.*

Since we can obtain the exact analytical form of $\mathcal{G}_{\mathbb{T}}$ for $\alpha = 4$, we prove Conjecture 2.1 for $\alpha = 4$ in Proposition 2.5. For the case $\alpha \in (2, 4)$, numerical approximations of $\mathcal{G}_{\mathbb{T}}$ to support Conjecture 2.1 are given in Section 2.6.

Proposition 2.5. *There exists $c_0 > 0$ such that for $c \in (0, c_0)$, Green's function $\mathcal{G}_{\mathbb{T}}$ at $\alpha = 4$ is even, strictly positive on \mathbb{T} , and strictly monotonically decreasing on $(0, \pi)$. For $c \in [c_0, \infty)$, $\mathcal{G}_{\mathbb{T}}$ has a finite number of zeros on \mathbb{T} , which becomes unbounded as $c \rightarrow \infty$.*

Proof. For $\alpha = 4$, Green's function $\mathcal{G}_{\mathbb{T}}$ satisfies the fourth-order differential equation

$$\mathcal{G}_{\mathbb{T}}''''(x) + c\mathcal{G}_{\mathbb{T}}(x) = \delta(x), \quad x \in \mathbb{T}, \quad (2.41)$$

where $c > 0$. It follows from the theory of Dirac delta distributions that $\mathcal{G}_{\mathbb{T}}$ is continuous, even, periodic on \mathbb{T} , and have a jump discontinuity of the third derivative at $x = 0$. Similarly to the computation in (2.35), it follows

that Green's function solves the boundary-value problem with the boundary conditions

$$\mathcal{G}'_{\mathbb{T}}(0) = \mathcal{G}'_{\mathbb{T}}(\pm\pi) = \mathcal{G}'''_{\mathbb{T}}(\pm\pi) = 0, \quad \mathcal{G}'''_{\mathbb{T}}(0^{\pm}) = \pm\frac{1}{2}. \quad (2.42)$$

Due to the boundary conditions (2.42), it is easier to solve the differential equation (2.41) for $\mathcal{G}'_{\mathbb{T}}$ on $[0, \pi]$. By using the parametrization $c = 4a^4$, we obtain

$$\begin{aligned} \mathcal{G}'_{\mathbb{T}}(x) = & c_1 \cosh(ax) \cos(ax) + c_2 \cosh(ax) \sin(ax) \\ & + c_3 \sinh(ax) \cos(ax) + c_4 \sinh(ax) \sin(ax), \quad x \in [0, \pi], \end{aligned}$$

where c_1, c_2, c_3 , and c_4 are some coefficients. We can find $c_1 = 0$ and $c_4 = \frac{1}{4a^2}$ from the two boundary conditions (2.42) at $x = 0^+$. The other two boundary conditions (2.42) at $x = \pi$ gives the linear system for c_2 and c_3 :

$$\begin{bmatrix} \cosh(\pi a) \sin(\pi a) & \sinh(\pi a) \cos(\pi a) \\ \sinh(\pi a) \cos(\pi a) & -\cosh(\pi a) \sin(\pi a) \end{bmatrix} \begin{bmatrix} c_2 \\ c_3 \end{bmatrix} = -c_4 \begin{bmatrix} \sinh(\pi a) \sin(\pi a) \\ \cosh(\pi a) \cos(\pi a) \end{bmatrix}.$$

By Cramer's rule, we find the unique solution

$$c_2 = -c_4 \frac{\sinh(2\pi a)}{\cosh(2\pi a) - \cos(2\pi a)}, \quad c_3 = c_4 \frac{\sin(2\pi a)}{\cosh(2\pi a) - \cos(2\pi a)},$$

which results in the exact analytical expression

$$\mathcal{G}'_{\mathbb{T}}(x) = \frac{1}{4a^2} \frac{\sinh(ax) \sin a(2\pi - x) - \sin(ax) \sinh a(2\pi - x)}{\cosh(2\pi a) - \cos(2\pi a)}, \quad x \in [0, \pi]. \quad (2.43)$$

Integrating (2.43) in x yields the exact analytical expression for $\mathcal{G}_{\mathbb{T}}$:

$$\mathcal{G}_{\mathbb{T}}(x) = \frac{1}{8a^3} \frac{g(x)}{\cosh(2\pi a) - \cos(2\pi a)}, \quad x \in [0, \pi], \quad (2.44)$$

where

$$\begin{aligned} g(x) := & \sinh(ax) \cos a(2\pi - x) + \cosh(ax) \sin a(2\pi - x) \\ & + \sin(ax) \cosh a(2\pi - x) + \cos(ax) \sinh a(2\pi - x) \end{aligned}$$

and the constant of integration is set to zero due to the differential equation (2.41).

We verify the validity of the exact solution (2.44) by comparing $\mathcal{G}_{\mathbb{T}}(0)$ and

$\mathcal{G}_{\mathbb{T}}(\pi)$ with the Fourier series representation (2.3) for $\alpha = 4$:

$$\mathcal{G}_{\mathbb{T}}(0) = \frac{1}{2\pi} \sum_{n \in \mathbb{Z}} \frac{1}{4a^4 + n^2} = \frac{1}{8a^3} \frac{\sinh(2\pi a) + \sin(2\pi a)}{\cosh(2\pi a) - \cos(2\pi a)} \quad (2.45)$$

and

$$\mathcal{G}_{\mathbb{T}}(\pi) = \frac{1}{2\pi} \sum_{n \in \mathbb{Z}} \frac{(-1)^n}{4a^4 + n^2} = \frac{1}{4a^3} \frac{\sinh(\pi a) \cos(\pi a) + \sin(\pi a) \cosh(\pi a)}{\cosh(2\pi a) - \cos(2\pi a)}. \quad (2.46)$$

Indeed, the exact expressions coincide with those found from the numerical series (1) and (2) in [85, Section 5.1.27].

It follows from (2.46) that $\mathcal{G}_{\mathbb{T}}(\pi)$ vanishes for $c = 4a^4 > 0$ if and only if $a > 0$ is a solution of the transcendental equation

$$\tanh(\pi a) + \tan(\pi a) = 0. \quad (2.47)$$

Elementary graphical analysis on Figure 2.1 shows that there exist a countable sequence of zeros $\{a_n\}_{n \in \mathbb{N}}$ such that $a_n \in (n - \frac{1}{4}, n)$, $n \in \mathbb{N}$. Hence, $\mathcal{G}_{\mathbb{T}}$ is not positive for $a \in (a_1, \infty)$.

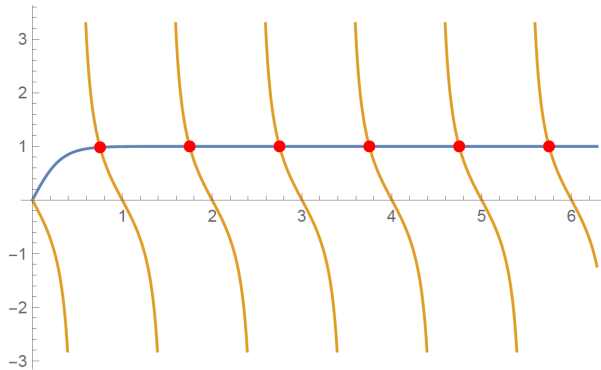


Figure 2.1: Countable sequence of zeros $\{a_n\}_{n \in \mathbb{N}}$ of 2.47

Let us now show that the profile of $\mathcal{G}_{\mathbb{T}}$ is strictly, monotonically decreasing on $(0, \pi)$ for small a . It follows from (2.43) that $\mathcal{G}'_{\mathbb{T}}(x) < 0$ for $x \in (0, \pi)$ if and only if

$$\frac{\sin(ax)}{\sinh(ax)} > \frac{\sin a(2\pi - x)}{\sinh a(2\pi - x)}, \quad x \in (0, \pi). \quad (2.48)$$

The function

$$x \mapsto \frac{\sin(ax)}{\sinh(ax)}$$

is monotonically decreasing on $[0, 2\pi]$ as long as

$$\cos(ax) \sinh(ax) - \sin(ax) \cosh(ax) \leq 0, \quad x \in [0, 2\pi], \quad (2.49)$$

which is true at least for $a \in (0, \frac{1}{2})$. Hence, $\mathcal{G}_{\mathbb{T}}$ is strictly monotonically decreasing on $(0, \pi)$ with $\mathcal{G}_{\mathbb{T}}(\pi) > 0$ for $a \in (0, a_0)$, where $a_0 \in (\frac{1}{2}, 1)$. On the other hand, it is obvious that there exists $a_* \in (1, \frac{3}{2})$ such that the inequality (2.49) [and hence the inequality (2.48)] is violated at $x = \pi$ for $a \in (a_*, 2)$, for which $\mathcal{G}'_{\mathbb{T}}(x) > 0$ at least near $x = \pi$.

The first part of the proposition is proven due to the relation $c = 4a^4$. It remains to prove that $\mathcal{G}_{\mathbb{T}}$ has a finite number of zeros on \mathbb{T} for fixed $a \in [a_0, \infty)$ which becomes unbounded as $a \rightarrow \infty$. To do so, we simplify the expression (2.44) for $\mathcal{G}_{\mathbb{T}}$ in the asymptotic limit of large a for every fixed $x \in (0, \pi)$:

$$\mathcal{G}_{\mathbb{T}}(x) = \frac{1}{8a^3} [e^{-ax} \cos(ax) + e^{-ax} \sin(ax) + \mathcal{O}(e^{-a(2\pi-x)})] \quad \text{as } a \rightarrow \infty. \quad (2.50)$$

Thus, as a gets large, there are finitely many zeros of $\mathcal{G}_{\mathbb{T}}$ on $(0, \pi)$ but the number of zeros of $\mathcal{G}_{\mathbb{T}}$ grows unbounded as $a \rightarrow \infty$. \square

Remark 2.14. *The leading-order term in the asymptotic expansion (2.50) represents Green's function $\mathcal{G}_{\mathbb{R}}$. The proof of Conjecture 2.2 for $\alpha = 4$ follows from this explicit expression.*

Remark 2.15. *Figure 2.2 shows boundaries on the (a, x) plane between positive (yellow) and negative (blue) values of $\mathcal{G}_{\mathbb{T}}$ (left) and $\mathcal{G}'_{\mathbb{T}}$ (right). It follows from the figure that the zeros of $\mathcal{G}_{\mathbb{T}}$ and $\mathcal{G}'_{\mathbb{T}}$ are monotonically decreasing with respect to parameter a and the number of zeros only grows as a increases. In other words, zeros of $\mathcal{G}_{\mathbb{T}}$ cannot coalesce and disappear. We were not able to prove these properties for every $a > 0$ inside $(0, \pi)$.*

2.6 Numerical Illustrations

In this section, we present graphical illustrations for Theorem 2.2 and Conjecture 2.1 as well as numerical approximations of the Green's function (2.3), and its the first five roots.

Figure 2.3 illustrates the statement of Theorem 2.1. It shows the single-lobe positive profile of $\mathcal{G}_{\mathbb{T}}$ for two values of c in the case $\alpha = 0.5$ (left) and $\alpha = 1.5$ (right). The only difference between these two cases is that $\mathcal{G}_{\mathbb{T}}(0)$ is bounded for $\alpha > 1$ and is unbounded for $\alpha \leq 1$.

Figure 2.4 supports the statement of Conjecture 2.1. For $\alpha = 2.5$ (top), Green's function G has the single-lobe positive profile for $c = 2$ (red curve) but it is not positive for $c = 10$ (blue curve). For $\alpha = 3.5$ (bottom), it is positive

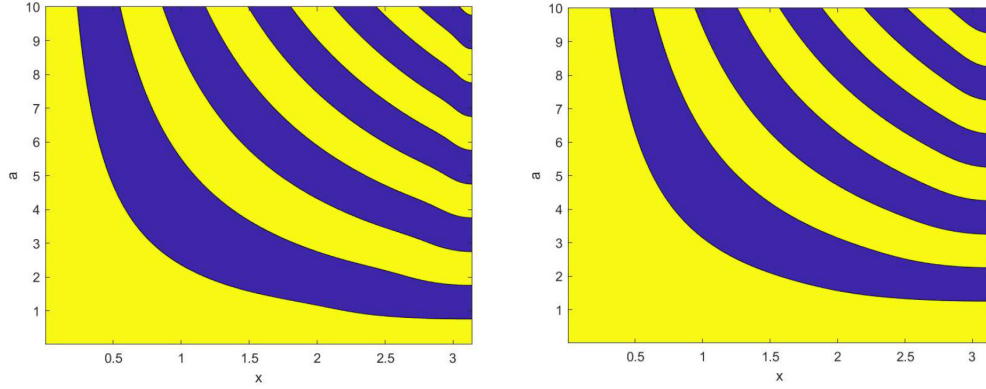


Figure 2.2: Left: areas on (a, x) plane where \mathcal{G}_T is positive (yellow) and negative (blue). Right: the same but for \mathcal{G}'_T .

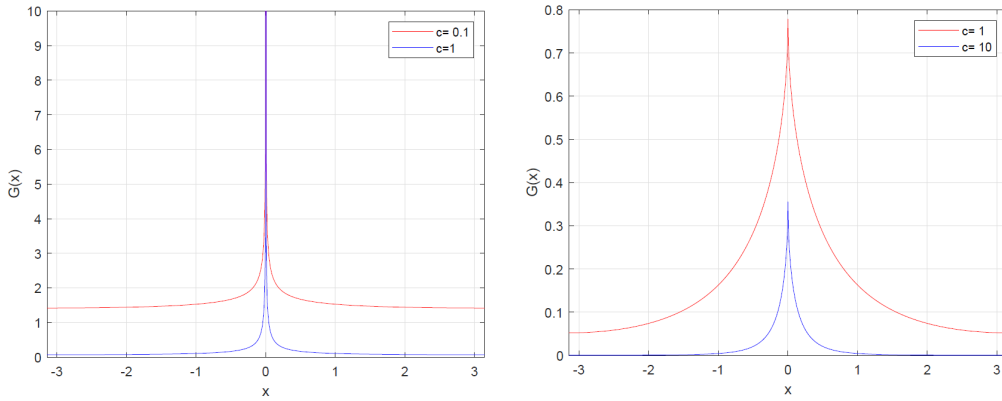


Figure 2.3: Profiles of \mathcal{G}_T for $\alpha = 0.5$ (left) and $\alpha = 1.5$ (right) for specific values of c .

for $c = 1$ (red curve), has one pair of zeros for $c = 10$ (blue curve), and has two pairs of zeros for $c = 60$ (black curve).

Next, we study how zeros of $G_T(\pi)$ depend on parameters (c, α) , which supports Conjecture 2.1. The profiles of \mathcal{G}_T are depicted on Figure 2.4.

It follows from the Fourier series (2.3) that $\mathcal{G}_T(\pi)$ can be computed by the numerical series

$$\mathcal{G}_T(\pi) = \frac{1}{2\pi} \left(\frac{1}{c} + 2 \sum_{n=1}^{\infty} \frac{(-1)^n}{c + n^\alpha} \right), \tag{2.51}$$

where the series converges absolutely if $\alpha > 1$. On the other hand, $\mathcal{G}_T(\pi)$ can also be computed from the integral representation (2.5), that is,

$$\mathcal{G}_T(\pi) = \frac{1}{\pi c} \int_0^{\infty} \frac{e^t}{(1 + e^t)^2} E_\alpha(-ct^\alpha) dt, \tag{2.52}$$

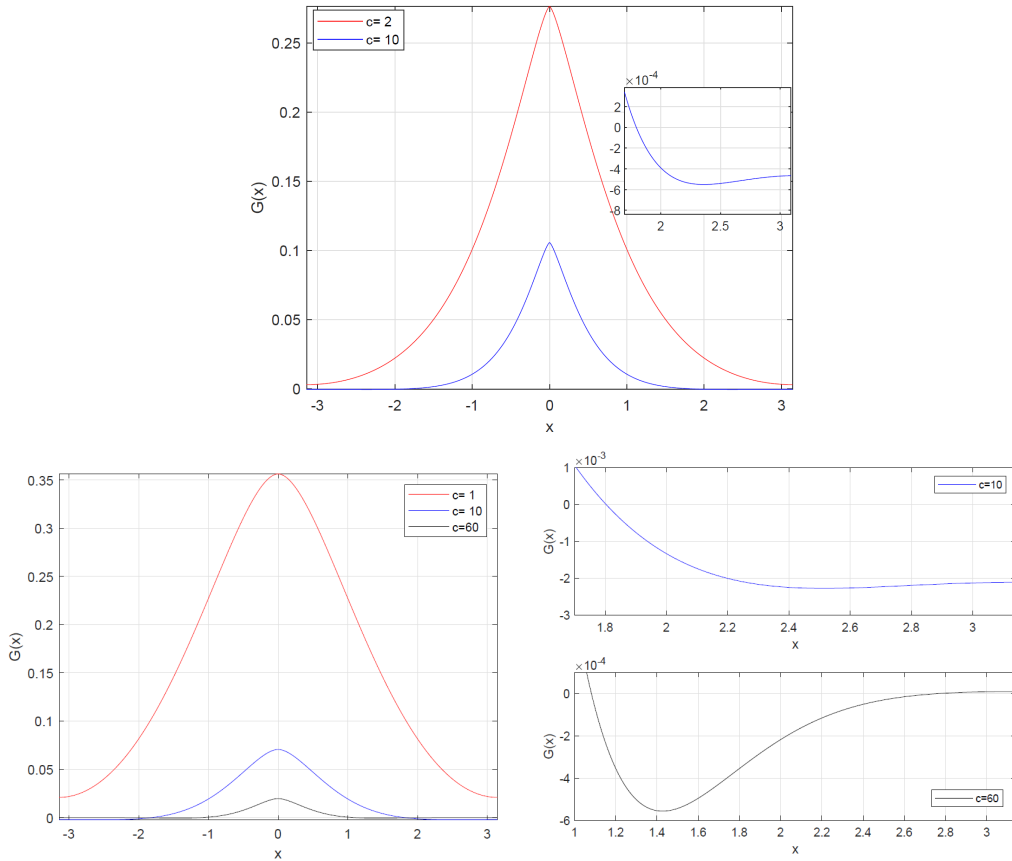


Figure 2.4: Profiles of G on \mathbb{T} for $\alpha = 2.5$ (top) and $\alpha = 3.5$ (bottom) at specific values of c .

which converges absolutely for $c \in (0, c_\alpha)$, see Theorem 2.1, where c_α is given by (2.6). Figure 2.5 shows the difference of $\mathcal{G}_{\mathbb{T}}(\pi)$ computed from (2.51) and (2.52) for $\alpha = 2.5$ (left) and $\alpha = 3.5$ (right) in logarithmic scale versus parameter c . The Fourier series (2.51) is truncated such that the remainder is of the size $\mathcal{O}(10^{-10})$. For the integral representation of $\mathcal{G}_{\mathbb{T}}(\pi)$ in (2.52), we numerically compute the Mittag–Leffler function $E_\alpha(-ct^\alpha)$ on the half line; this task is accomplished by using the Matlab code provided in [44], where the Mittag–Leffler functions are approximated with relative errors of the size $\mathcal{O}(10^{-15})$. As follows from Fig. 2.5, the difference between the two computations is constantly small if $c < c_\alpha$, when the integral representation (2.52) converges absolutely, where $c_{\alpha=2.5} \approx 18.8$ and $c_{\alpha=3.5} \approx 5.2$. However, the accuracy of numerical computations based on the integral representation (2.52) deteriorates for c approaching c_α and as a result, the difference between two computations quickly grows for $c > c_\alpha$.

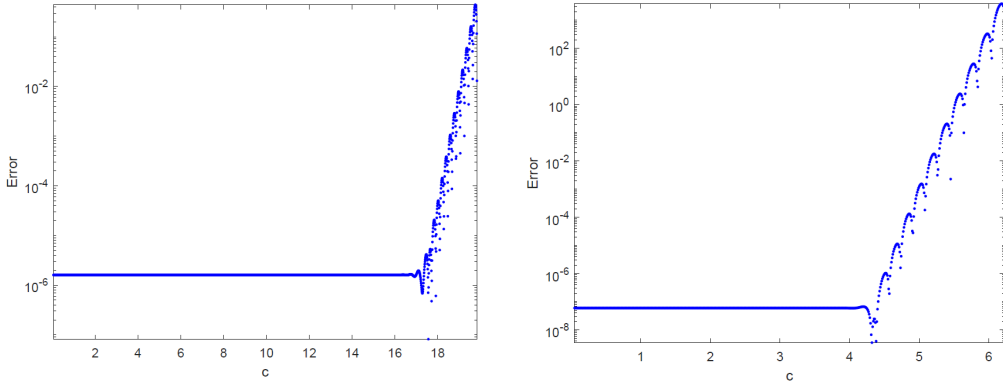


Figure 2.5: Difference between computations of $\mathcal{G}_{\mathbb{T}}(\pi)$ in (2.51) and (2.52) for $\alpha = 2.5$ (left) and $\alpha = 3.5$ (right) versus parameter c .

Green’s function $\mathcal{G}_{\mathbb{T}}$ was computed versus x using the Fourier series representation (2.3) for fixed values of (c, α) . The plots of $\mathcal{G}_{\mathbb{T}}$ are shown in Figures 2.3 and 2.4. The roots of $\mathcal{G}_{\mathbb{T}}(\pi)$ in c for each fixed $\alpha > 2$ are computed using the bisection method. Figure 2.6 (top) shows the first five zeros of $\mathcal{G}_{\mathbb{T}}(\pi)$ on the (c, α) plane, where the dots show the roots of $\mathcal{G}_{\mathbb{T}}(\pi)$ computed from the exact solutions in using the transcendental equation (2.47) for $\alpha = 4$. The first root exists for every $\alpha > 2$ and is located inside $(0, c_{\alpha})$, in particular, the first root of $\mathcal{G}_{\mathbb{T}}(\pi)$ occurs at $c \approx 2.507$ for $\alpha = 2.5$ and at $c \approx 1.446$ for $\alpha = 3.5$, see Fig. 2.6 (bottom left panel). The threshold c_0 in Conjecture 2.1 reduces with the larger value of α . The other roots are located outside $(0, c_{\alpha})$ and disappear via pairwise coalescence as α is reduced towards $\alpha = 2$, see the bottom right panels. The 2nd and 3rd roots coalesce at $\alpha \approx 3.325$ and the 4th and 5th roots coalesce at $\alpha \approx 3.89$. The number of terms in the Fourier series of $\mathcal{G}_{\mathbb{T}}(\pi)$ is increased to compute the 4th and 5th roots such that the remainder is of the size of $\mathcal{O}(10^{-14})$ because $\mathcal{G}_{\mathbb{T}}(\pi)$ becomes very small near the location of these roots.

Table 2.1 compares the error between the numerically detected roots at $\alpha = 4$ and the roots of $\mathcal{G}_{\mathbb{T}}(\pi)$ obtained from solving the transcendental equation (2.47).

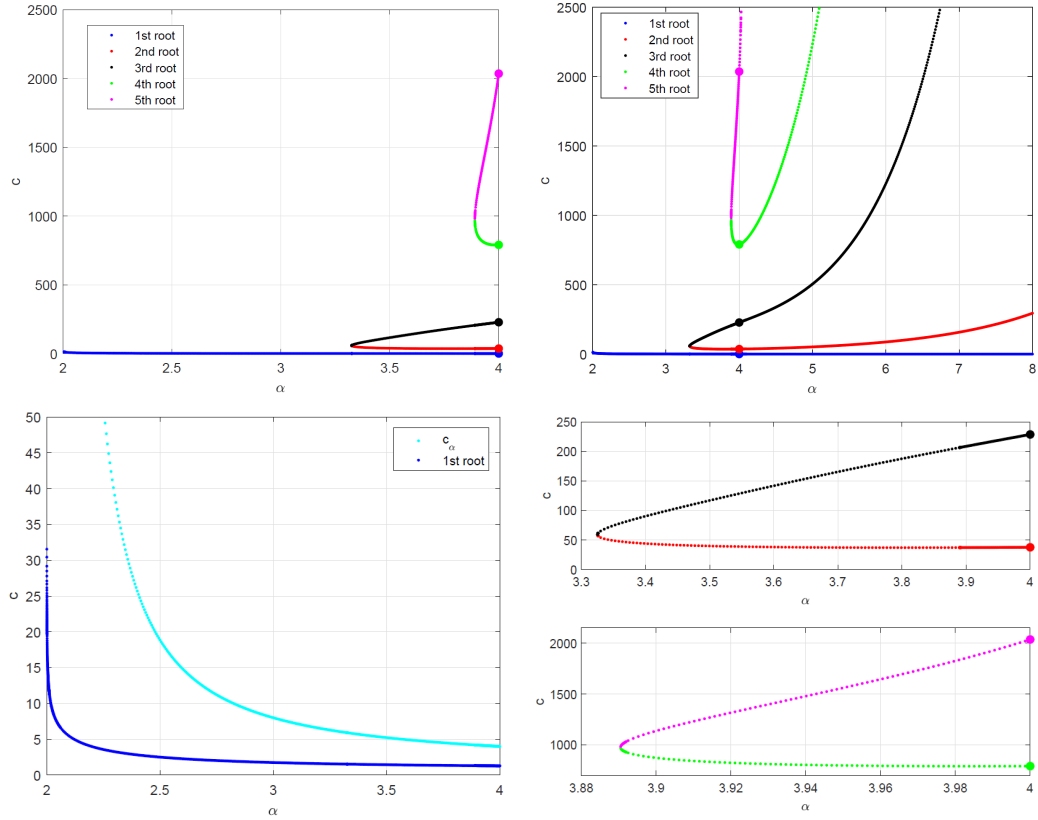


Figure 2.6: Top: Location of the first five roots of $\mathcal{G}_T(\pi)$ on the (c, α) plane. Bottom left: The first root of $\mathcal{G}_T(\pi)$ relative to the boundary c_α (left). Bottom right: Coalescence of the 2nd and 3rd roots (upper right) and the 4th and 5th roots (lower right).

Root	Error
1st	1.9915 e-11
2nd	7.1495 e-08
3rd	3.3182 e-06
4th	0.0031
5th	0.0156

Table 2.1: Difference between locations of the first five roots of $\mathcal{G}_T(\pi)$ for $\alpha = 4$ computed from (2.3) and (2.47).

Chapter 3

Existence Of Periodic Waves Of The Fractional KdV Equation

In this chapter, we turn our attention to the existence of periodic, travelling waves of the fractional KdV equation (1.7). Our goal is to prove the existence of periodic waves in the small-amplitude limit, and to verify that these solutions are the local minimizers of the energy(1.12) subject to fixed mass (1.10) and momentum (1.11). Moreover, we prove a new result stating that the periodic waves, travelling to the right, are positive by using the positivity result of the Green's function in Theorem 2.1.

We recall the fractional KdV equation (1.7) taken in the normalized form

$$u_t + 2uu_x - (D^\alpha u)_x = 0, \quad (3.1)$$

where $u(t, x) : \mathbb{R} \times \mathbb{T} \mapsto \mathbb{R}$, $\mathbb{T} := [-\pi, \pi]$, and the fractional Laplacian D^α is defined via Fourier series by

$$f(x) = \sum_{n \in \mathbb{Z}} f_n e^{inx}, \quad (D^\alpha f)(x) = \sum_{n \in \mathbb{Z}} |n|^\alpha f_n e^{inx}. \quad (3.2)$$

Periodic traveling waves are solutions of the fractional KdV equation (3.1) in the form $u(t, x) = \psi(x - ct)$, where ψ is a periodic function in its argument and c is the speed parameter. Without loss of generality, due to scaling and translation invariance of the fractional KdV equation (3.1), we scale the period of ψ to 2π and translate ψ to become an even function of its argument. The wave profile ψ is a 2π -periodic even solution to the following boundary-value problem (1.9) with $p = 1$ and the constant of integration $b = 0$ due to Galilean invariance

$$(D^\alpha + c)\psi = \psi^2, \quad \psi \in H_{\text{per}}^\alpha. \quad (3.3)$$

We say that the periodic wave has a *single-lobe* profile accordingly to Definition 1.1, that is, if there exist only one maximum and minimum of ψ on the period.

For uniqueness of solutions, we place the maximum of ψ at $x = 0$ and the minimum of ψ at $x = \pm\pi$. If $c > 0$, then the wave with profile ψ propagates to the right. In addition, we can also consider 2π -periodic waves with profile ϕ propagating to the left. These are solutions of the KdV equation (3.1) in the form $u(t, x) = \phi(x + ct)$, with $c > 0$ satisfying the following boundary-value problem:

$$(c - D^\alpha)\phi + \phi^2 = 0, \quad \phi \in H_{\text{per}}^\alpha. \quad (3.4)$$

A very simple formula connects the right-propagating waves with the left-propagating waves:

$$\phi(x) = -c + \psi(x). \quad (3.5)$$

The wave profile ϕ is a solution to the boundary-value problem (3.4) with some $c > 0$ if and only if ψ is a solution to the boundary-value problem (3.3) with the same $c > 0$.

Although recent works in the literature (see Section 1.4.1, particularly [14, 26, 27, 53, 54]) are devoted the right-propagating waves with profile ψ , there are no a priori reasons to prefer these waves over the left-propagating waves with profile ϕ . As we are going to show in Theorem 3.1, the perturbative expansions for waves of small amplitudes are more easily developed for the left-propagating waves with profile ϕ since they arise in the local bifurcation theory from linearization of the zero equilibrium. On the other hand, the right-propagating waves with profile ψ are more suitable for the proof of positivity result in Theorem 3.3. Moreover, we are going to prove in Theorem 3.2 that these right travelling waves in the small-amplitude limit are the constrained minimizers of the energy functional (1.12) subject to fixed mass (1.10) and momentum (1.11).

The chapter is organized as follows. In Section 3.1 we present the main results of the chapter. Section 3.2 is dedicated to the proof of the Stokes expansion for the solution of the boundary value problem (3.4). Section 3.3 presents the proof that the periodic, small-amplitude, single-lobe solutions are the local minimizers of the energy subject to fixed mass and momentum; we also state the closed form solutions for the integrable cases $\alpha = 1$ and $\alpha = 2$. Section 3.4 presents the proof of the existence of the positive periodic wave with profile ψ of the boundary value problem (3.3). Section 3.5 provides explicit solution of the classical KdV and BO equations as examples of Theorem 3.3.

3.1 Main Results

Here, we state the main results for this chapter. Let us define the following operators and important thresholds of α which will be referred to throughout the rest of the chapter. The Jacobian operator of the boundary value problem

(3.3) is given by

$$\mathcal{H}_{c,\alpha} := D^\alpha + c - 2\psi, \quad (3.6)$$

the Jacobian operator of the boundary value problem (3.4) is given by

$$\tilde{\mathcal{H}}_{c,\alpha} := D^\alpha - c - 2\phi, \quad (3.7)$$

and the thresholds for α are

$$\alpha_0 := \frac{\log 3}{\log 2} - 1, \quad \alpha_1 := \frac{\log 5}{\log 2} - 1. \quad (3.8)$$

Theorem 3.1. *For every $\alpha > \alpha_0$, there exists $c_0 > 1$ such that for every $c \in (1, c_0)$ there exists a unique single-lobe solution ϕ of the boundary-value problem (3.4) with the global maximum at $x = 0$. The wave profile ϕ and the wave speed c are real-analytic functions of the wave amplitude a satisfying the following Stokes expansions:*

$$\phi_{a,\alpha}(x) = a \cos(x) + a^2 \phi_2(x) + a^3 \phi_3(x) + a^4 \phi_4(x) + \mathcal{O}(a^5), \quad (3.9)$$

where

$$\phi_2(x) = -\frac{1}{2} + \frac{1}{2(2^\alpha - 1)} \cos(2x), \quad (3.10)$$

$$\phi_3(x) = \frac{1}{2(2^\alpha - 1)(3^\alpha - 1)} \cos(3x), \quad (3.11)$$

$$\phi_4(x) = \frac{1}{4} - \frac{1}{4(2^\alpha - 1)} - \frac{1}{8(2^\alpha - 1)^2} + \frac{1}{4(2^\alpha - 1)^2} \left[\frac{2}{3^\alpha - 1} - \frac{1}{2^\alpha - 1} \right] \cos(2x) \quad (3.12)$$

$$+ \frac{1}{8(2^\alpha - 1)(4^\alpha - 1)} \left[\frac{4}{3^\alpha - 1} + \frac{1}{2^\alpha - 1} \right] \cos(4x),$$

and

$$c_{a,\alpha} = 1 + c_2 a^2 + c_4 a^4 + \mathcal{O}(a^6), \quad (3.13)$$

with the correction terms given by

$$c_2 = 1 - \frac{1}{2(2^\alpha - 1)}, \quad (3.14)$$

$$c_4 = -\frac{1}{2} + \frac{1}{2(2^\alpha - 1)} + \frac{1}{4(2^\alpha - 1)^2} + \frac{1}{4(2^\alpha - 1)^3} - \frac{3}{4(2^\alpha - 1)^2(3^\alpha - 1)}. \quad (3.15)$$

Remark 3.1. *The small-amplitude periodic waves bifurcate from the constant zero solution to the boundary-value problem (3.4). The construction of the*

small-amplitude periodic waves is nearly identical to Lemma 2.1 in [54] subject to the following two changes. First, the constant of integration is set to zero, while in [54] the constant was carried as an additional (redundant) parameter of the problem. Second, the speed c is used as the main parameter of the periodic solution while the period is set to 2π , whereas in [54] c was set to 1 and the period was taken as the main parameter of the periodic solution.

Remark 3.2. Although the formal computations of the periodic waves in the small-amplitude limit hold for every $\alpha > 0$, the justification of the perturbative expansions requires $\alpha > 1/2$, for which H_{per}^α is a Banach algebra with respect to multiplication with a continuous embedding into L_{per}^∞ . A typical justification of the perturbative expansions is based on the method of Lyapunov–Schmidt reductions (see Appendix A of [54]) which requires smoothness of the nonlinear mappings. This smoothness is guaranteed in H_{per}^α with $\alpha > 1/2$. Since refinement to $\alpha \in (0, 1/2)$ is not important for the subject of our work, we leave the restriction $\alpha > 1/2$ in the same way as it was used in Theorem A.1 in [54].

The next theorem shows that the small-amplitude single-lobe solutions to Theorem 3.1 agree with the variational characterization of single-lobe solutions as minimizers of energy subject to fixed mass and momentum as in Proposition 2.1 shown in [53].

Theorem 3.2. Let $\psi = c_{a,\alpha} + \phi_{a,\alpha}$ be the locally unique single-lobe solution of the boundary value problem (3.3) for $\alpha > \alpha_0$ and $c > 1$ defined by Theorem 3.1. Then, ψ is a local minimizer of the energy

$$E(u) = -\frac{1}{2} \int_{-\pi}^{\pi} u (D^\alpha u) dx - \frac{1}{3} \int_{-\pi}^{\pi} u^2 dx, \quad (3.16)$$

subjected to the fixed momentum $F(u) = \frac{1}{2} \int_{-\pi}^{\pi} u^2 dx$ and mass $M(u) = \int_{-\pi}^{\pi} u dx$.

Remark 3.3. In Proposition 2.1 of [53], the variational results are obtained in the energy space $H_{\text{per}}^{\alpha/2}$ for $\alpha \in (1/3, 2]$ and for every $c > 0$, however, it is overlooked that the local minimizer may coincide with the nonzero constant solution $\psi_c(x) = c$ for all $x \in \mathbb{T}$ to the boundary-value problem (3.3). The same problem is present in Proposition 12 in [25].

Lastly, the following theorem proves the existence of positive, periodic and single-lobe wave with profile ψ in the boundary value problem (3.3) for all $c > 1$ and $\alpha \in (\alpha_0, 2]$ by using the positivity result of the Green’s function obtained in Theorem 2.1.

Theorem 3.3. Assume that the spectrum of the Jacobian operator $\mathcal{H}_{c,\alpha}$ in L_{per}^2 consists of one simple negative eigenvalue and a simple zero eigenvalue bounded

away from the rest of its spectrum for every $c > 1$ and $\alpha \in (\alpha_0, 2]$. Then, there exists a unique single-lobe solution ψ of the boundary-value problem (3.3) such that $\psi(x) > 0$ for every $x \in \mathbb{T}$.

Remark 3.4. *The result has not appeared in the literature, e.g. a remark in the proof of Proposition 2.1 in [53] states that a periodic solution need not be positive everywhere. On the other hand, positivity of the Fourier coefficients in the Fourier series for the periodic wave ψ is proven in Theorem 3.5 of [26] for every $\alpha > 1/2$ and for sufficiently large periods (which is equivalent to $c > 1$ at the 2π -period).*

Remark 3.5. *In Lemma 3.1, we show that there exists $c_0 > 1$ such that the assumption of Theorem 3.3 is satisfied for $c \in (1, c_0)$ and $\alpha \in (\alpha_0, 2]$. See Section 4.5.2 for numerical evidence supporting the assumption of Theorem 3.3 for all $c > 1$.*

Remark 3.6. *Our proof has similarity to the work of [91] on the second-order differential equations. However, the existence of constant solutions is eliminated in [91] by the space-dependent coefficients in the boundary-value problem. Since the boundary value problem (3.3) has space independent coefficients, we have to use the Leray–Schauder index to single out single-lobe periodic solutions from the constant solutions.*

3.2 Proof of Theorem 3.1

We prove Theorem 3.1 by employing algorithmic computations of the higher order coefficients to the periodic wave.

Proof. From the classical Stokes expansions:

$$\phi(x) = \sum_{k=1}^{\infty} a^k \phi_k(x), \quad c = 1 + \sum_{k=1}^{\infty} c_{2k} a^{2k},$$

the correction terms satisfy recursively,

$$\begin{cases} \mathcal{O}(a) : & (1 - D^\alpha)\phi_1 = 0, \\ \mathcal{O}(a^2) : & (1 - D^\alpha)\phi_2 + \phi_1^2 = 0, \\ \mathcal{O}(a^3) : & (1 - D^\alpha)\phi_3 + c_2\phi_1 + 2\phi_1\phi_2 = 0, \\ \mathcal{O}(a^4) : & (1 - D^\alpha)\phi_4 + c_2\phi_2 + 2\phi_1\phi_3 + \phi_2^2 = 0, \\ \mathcal{O}(a^5) : & (1 - D^\alpha)\phi_5 + c_2\phi_3 + c_4\phi_1 + 2\phi_1\phi_4 + 2\phi_2\phi_3 = 0, \end{cases}$$

For the single-lobe wave profile ϕ with the global maximum at $x = 0$, we select uniquely $\phi_1(x) = \cos(x)$ since $\text{Ker}_{\text{even}}(1 - D^\alpha) = \text{span}\{\cos(\cdot)\}$ in the space of even functions in L^2_{per} . In order to select uniquely all other corrections to

the Stokes expansion (3.9), we require the corrections terms $\{\phi_k\}_{k \geq 2}$ to be orthogonal to ϕ_1 in L^2_{per} .

Solving the inhomogeneous equation at $\mathcal{O}(a^2)$ yields the exact solution in H^α_{per} :

$$\phi_2(x) = -\frac{1}{2} + \frac{1}{2(2^\alpha - 1)} \cos(2x).$$

The inhomogeneous equation at $\mathcal{O}(a^3)$ admits a solution $\phi_3 \in H^\alpha_{\text{per}}$ if and only if the right-hand side is orthogonal to ϕ_1 , which selects uniquely the correction c_2 by

$$c_2 = 1 - \frac{1}{2(2^\alpha - 1)}.$$

After the resonant term is removed, the inhomogeneous equation at $\mathcal{O}(a^3)$ yields the exact solution in H^α_{per} :

$$\phi_3(x) = \frac{1}{2(2^\alpha - 1)(3^\alpha - 1)} \cos(3x).$$

By continuing the algorithm, we find the exact solution of the inhomogeneous equation at $\mathcal{O}(a^4)$ in H^α_{per} :

$$\begin{aligned} \phi_4(x) &= \frac{1}{4} - \frac{1}{4(2^\alpha - 1)} - \frac{1}{8(2^\alpha - 1)^2} + \frac{1}{4(2^\alpha - 1)^2} \left[\frac{2}{3^\alpha - 1} - \frac{1}{2^\alpha - 1} \right] \cos(2x) \\ &\quad + \frac{1}{8(2^\alpha - 1)(4^\alpha - 1)} \left[\frac{4}{3^\alpha - 1} + \frac{1}{2^\alpha - 1} \right] \cos(4x). \end{aligned}$$

Finally, the inhomogeneous equation at $\mathcal{O}(a^5)$ admits a solution $\phi_5 \in H^\alpha_{\text{per}}$ if and only if the right-hand side is orthogonal to ϕ_1 , which selects uniquely the correction c_4 by

$$c_4 = -\frac{1}{2} + \frac{1}{2(2^\alpha - 1)} + \frac{1}{4(2^\alpha - 1)^2} + \frac{1}{4(2^\alpha - 1)^3} - \frac{3}{4(2^\alpha - 1)^2(3^\alpha - 1)}.$$

Thus, we obtain the higher order correction terms for ϕ and c as stated in equations (3.10) to (3.14).

Note that $c_2 > 0$ if $\alpha > \alpha_0 := \log 3 / \log 2 - 1 \approx 0.585$, which implies that the small-amplitude periodic wave with profile ϕ exists in the boundary-value problem (3.4) for $c \in (1, c_0)$ with $c_0 > 1$, and $\alpha > \alpha_0$. The periodic wave has a global maximum at $x = 0$ for small a since $x = 0$ is the only maximum of $\phi_1(x) = \cos(x)$ and $\phi'(0) = 0$ with $\phi''(0) = -a + \mathcal{O}(a^2) < 0$.

Justification of the existence, uniqueness, and analyticity of the Stokes expansions (3.9) and (3.13) is performed with the method of Lyapunov–Schmidt reductions for $\alpha > 1/2$, see Lemma 2.1 and Theorem A.1 in [54]. Since

$\alpha_0 > 1/2$, the justification procedure applies for every $\alpha > \alpha_0$. □

Remark 3.7. *If $\alpha < \alpha_0$, then $c_2 < 0$ so that the small-amplitude periodic wave exists for $c \in (c_0, 1)$ with some $c_0 < 1$. The critical value α_0 can also be seen in the expansion of the wave period T (for fixed $c = 1$) with respect to the wave amplitude a in Lemma 2.1 of [54].*

3.3 Proof of Theorem 3.2

Here, we are going to verify that the small-amplitude, periodic and single-lobe solution $\psi = c_{a,\alpha} + \phi_{a,\alpha}$ with $\phi_{a,\alpha}$ given in Theorem 3.1 are the local minimizers of the energy subject to fixed mass and momentum.

Let us consider the Euler–Lagrange equation

$$(D^\alpha + c)\psi - \psi^2 + b = 0, \tag{3.17}$$

which is associated with the action functional (1.14)

$$G_{c,b}(u) := E(u) + cF(u) + bM(u).$$

Note that the Euler–Lagrange equation (3.17) coincides with the equation (3.3) for $b = 0$. With the transformation

$$\psi(x) = \frac{1}{2} \left(c - \sqrt{c^2 + 4b} \right) + \tilde{\psi}(x), \tag{3.18}$$

the Euler–Lagrange equation (3.17) transforms to the form

$$(D^\alpha + \tilde{c})\tilde{\psi} - \tilde{\psi}^2 = 0,$$

with $\tilde{c} := \sqrt{c^2 + 4b}$. By expansion (3.13) in Theorem 3.1, we have the following Stokes expansion for the new speed

$$\tilde{c} = 1 + c_2 a^2 + \mathcal{O}(a^4),$$

from which the parameter $a = a(c, b)$ near $(1, 0)$ is defined by

$$c_2 a^2 = c - 1 + 2b + \mathcal{O}((c - 1)^2 + b^2). \tag{3.19}$$

A single-lobe periodic solution of the Euler–Lagrange equation (3.17) for (c, b) near $(1, 0)$ is defined by the expansion (3.10) in Theorem 3.1 as follows:

$$\psi(x) = 1 - b + a \cos(x) + a^2 (c_2 + \phi_2(x)) + \mathcal{O}(a^3 + b^2). \tag{3.20}$$

This single-lobe periodic solution is a critical point of the action functional

$G_{c,b}(u)$ in (1.14); hence we denote it as $\psi_{c,b}(x)$. The Hessian operator of the action functional $G_{c,b}(u)$ at the critical point $u = \psi_{c,b}$ is given by $G''_{c,b}(\psi_{c,b}) = D^\alpha + c - 2\psi_{c,b}$. We observe that $G''_{c,b}(\psi_{c,b})$ has one zero eigenvalue which persists with respect to b since $G_{c,b}(\psi_{c,b})\psi'_{c,b}(x) = 0$ for every $b \in \mathbb{R}$.

When the critical point $\psi_{c,b}$ of $G_{c,b}(u)$ is considered as a critical point of $E(u)$ subject to the fixed $F(u)$ and $M(u)$, the space $L^2_{per}(\mathbb{T})$ is constrained by two orthogonality conditions

$$\langle \psi_{c,b}, v \rangle = 0, \quad \langle 1, v \rangle = 0, \quad (3.21)$$

imposed on the perturbation $v \in H^\alpha_{per}(\mathbb{T})$ to the periodic wave $\psi_{c,b} \in H^\alpha_{per}(\mathbb{T})$. By Theorem A.3, the number of negative eigenvalues of $G''_{c,b}(\psi_{c,b})$ in $L^2_{per}(\mathbb{T})$ is reduced under the constraints (3.21) by the number of negative eigenvalues of the matrix

$$\begin{bmatrix} \langle [G''_{c,b}(\psi_{c,b})]^{-1} \psi_{c,b}, \psi_{c,b} \rangle & \langle [G''_{c,b}(\psi_{c,b})]^{-1} 1, \psi_{c,b} \rangle \\ \langle [G''_{c,b}(\psi_{c,b})]^{-1} \psi_{c,b}, 1 \rangle & \langle [G''_{c,b}(\psi_{c,b})]^{-1} 1, 1 \rangle \end{bmatrix} = - \begin{bmatrix} \frac{\partial \mathcal{F}_{c,b}}{\partial c} & \frac{\partial \mathcal{F}_{c,b}}{\partial b} \\ \frac{\partial \mathcal{M}_{c,b}}{\partial c} & \frac{\partial \mathcal{M}_{c,b}}{\partial b} \end{bmatrix},$$

where we denote $\mathcal{F}_{c,b} := F(\psi_{c,b})$ and $\mathcal{M}_{c,b} := M(\psi_{c,b})$, and have used the derivative equations

$$G''_{c,b}(\psi_{c,b})\partial_c \psi_{c,b} = -\psi_{c,b}, \quad G''_{c,b}(\psi_{c,b})\partial_b \psi_{c,b} = -1,$$

assuming that $\psi_{c,b}$ is differentiable with respect to c and b . It follows from (3.19) and (3.20) that $\psi_{c,b}$ is differentiable in c and b if $c_2 \neq 0$ ($\alpha \neq \alpha_0$). Thanks to the expansion (3.20) for (c, b) near $(1, 0)$, we compute

$$\mathcal{F}_{c,b} = \pi \left[1 - 2b + a^2 \left(2c_2 - \frac{1}{2} \right) + \mathcal{O}(a^4 + b^2) \right],$$

and

$$\mathcal{M}_{c,b} = 2\pi \left[1 - b + a^2 \left(c_2 - \frac{1}{2} \right) + \mathcal{O}(a^4 + b^2) \right],$$

from which we obtain

$$\begin{bmatrix} \frac{\partial \mathcal{F}_{c,b}}{\partial c} & \frac{\partial \mathcal{F}_{c,b}}{\partial b} \\ \frac{\partial \mathcal{M}_{c,b}}{\partial c} & \frac{\partial \mathcal{M}_{c,b}}{\partial b} \end{bmatrix} = \frac{\pi}{c_2} \begin{bmatrix} \frac{3}{2} - \frac{1}{2^{\alpha-1}} & 1 - \frac{1}{2^{\alpha-1}} \\ 1 - \frac{1}{2^{\alpha-1}} & -\frac{1}{2^{\alpha-1}} \end{bmatrix}, \quad (3.22)$$

where the chain rule with the expression (3.19) has been used. Since the determinant of the matrix above is $-\frac{\pi^2}{c_2}$ and $c_2 > 0$ thanks to $\alpha > \alpha_0 > \frac{1}{2}$, there exists exactly one positive and one negative eigenvalues. Hence, the number of negative eigenvalues of $G''_{c,b}(\psi_{c,b})$ in the constrained $L^2_{per}(\mathbb{T})$ is reduced by one. Therefore, $\psi_{c,b}$ is a local minimizer of $E(u)$ subject to the fixed $F(u)$ and

$M(u)$ for (c, b) near $(1, 0)$ if we can show that $\sigma(G''_{c,b}(\psi_{c,b}))$ has only one simple negative eigenvalue.

Notice that when $b = 0$, $\psi_{c,b=0}$ coincides with $\psi = c_{c,\alpha} + \phi_{a,\alpha}$ so $G''_{c,b=0}(\psi)$ coincides with the Jacobian operator $\mathcal{H}_{c,\alpha}$ (3.6). Moreover, using the transformation (3.5), we have also that the Jacobian operator $\mathcal{H}_{c,\alpha}$ of the boundary value problem (3.3) is identical to the Jacobian operator $\tilde{\mathcal{H}}_{c,\alpha}$ of the boundary value problem (3.4)

$$\mathcal{H}_{c,\alpha} = D^\alpha + c - 2\psi = D^\alpha + c - 2(c + \phi) = D^\alpha - c - 2\phi = \tilde{\mathcal{H}}_{c,\alpha}. \quad (3.23)$$

Hence, the assertion of Theorem 3.2 is obtained once we prove Lemma 3.1 which verifies that for $\alpha > \alpha_0$ and $c \in (1, c_0)$ with $c_0 > 1$, $\sigma(\tilde{\mathcal{H}}_{c,\alpha})$ has only one simple negative eigenvalue, one simple zero eigenvalue and the rest of its spectrum bounded away from zero.

Remark 3.8. *Another periodic wave solution of the boundary value problem (3.3) is the constant wave $\psi_c(x) = c$. It is also a critical point of the action functional $G_{c,b=0}(u)$ with the Hessian operator $G''_{c,b=0}(\psi_c)$ has only one simple negative eigenvalue for $c \in (0, 1)$ and three more negative eigenvalues for $c > 1$. The constraints of fixed momentum $F(u)$ and fixed mass $M(u)$ impose only one orthogonality condition $\langle 1, v \rangle = 0$ since $\psi_c(x) = c$. Computing $\mathcal{P}_c := P(\psi_x) = \pi c^2$ shows that the constraint removes exactly one negative eigenvalue of $G''_{c,b=0}(\psi_c)$. Hence, the constant wave ψ_c is a local constrained minimizer of $E(u)$ subject to fixed $F(u)$ and $M(u)$ for $c \in (0, 1)$, but it is a saddle point of $E(u)$ for $c > 1$.*

Lemma 3.1. *For every $\alpha > \alpha_0$, there exists $c_0 > 1$ such that for every $c \in (1, c_0)$, $\sigma(\tilde{\mathcal{H}}_{c,\alpha})$ in L^2_{per} consists of one simple negative eigenvalue, a simple zero eigenvalue, and a countable sequence of positive eigenvalues bounded away from zero.*

Proof. Note that $\sigma(\tilde{\mathcal{H}}_{c,\alpha})$ in L^2_{per} is purely discrete for every $c > 1$, thanks to the compactness of $[-\pi, \pi]$ and boundedness of $\phi \in L^\infty_{\text{per}}$. Let us consider the linear operator

$$\tilde{\mathcal{L}}_{c,\alpha} := D^\alpha - c \quad (3.24)$$

in L^2_{per} with domain in H^α_{per} . For $c = 1$, $\tilde{\mathcal{H}}_{c=1,\alpha}$ coincide with $\tilde{\mathcal{L}}_{c=1,\alpha}$, whose spectrum in L^2_{per} is obtained for every $\alpha > 0$ as $\sigma(\tilde{\mathcal{L}}_{c=1,\alpha}) = \{|n|^\alpha - 1, n \in \mathbb{Z}\}$.

Hence, it follows that $\sigma(\tilde{\mathcal{H}}_{c=1,\alpha})$ has a simple negative eigenvalue, a double zero eigenvalue, and a countable sequence of positive eigenvalues bounded away from zero.

Since $\tilde{\mathcal{H}}_{c,\alpha} - \tilde{\mathcal{L}}_{c,\alpha} = -2\phi$ is a bounded perturbation and (ϕ, c) depend analytically on a , the analytic perturbation theory (Theorem VII.1.7 in [57])

guarantees continuity of eigenvalues for $c > 1$ close to their limiting values as $c \rightarrow 1$. Therefore, the proof is achieved if we can show that the double zero eigenvalue of $\tilde{\mathcal{H}}_{c,\alpha}$ in L^2_{per} splits as $c > 1$ into a simple zero eigenvalue and a simple positive eigenvalue.

Since $\text{Ker}(\tilde{\mathcal{H}}_{c=1,\alpha}) = \text{span}\{\cos(\cdot), \sin(\cdot)\}$ and $\tilde{\mathcal{H}}_{c,\alpha}\phi' = 0$ for every $c > 1$ with odd ϕ , the zero eigenvalue associated with the subspace $\text{Ker}_{\text{odd}}(\tilde{\mathcal{H}}_{c=1,\alpha}) = \text{span}\{\sin(\cdot)\}$ persists for $c > 1$. It remains to check the shift of the zero eigenvalue associated with the subspace $\text{Ker}_{\text{even}}(\tilde{\mathcal{H}}_{c=1,\alpha}) = \text{span}\{\cos(\cdot)\}$. Hence, we expand $\tilde{\mathcal{H}}_{c,\alpha}$ in powers of a by using (3.9):

$$\tilde{\mathcal{H}}_{c,\alpha} = -1 - D_\alpha - 2a \cos(x) - \frac{a^2}{2^\alpha - 1} \left[\cos(2x) - \frac{1}{2} \right] + \mathcal{O}(a^3) \quad (3.25)$$

and look for solutions $(\lambda, v) \in \mathbb{R} \times H_{\text{per}}^\alpha$ of the eigenvalue problem $\tilde{\mathcal{H}}_{c,\alpha}v = \lambda v$ near $(\lambda, v) = (0, \cos(\cdot))$ by using the expansions

$$\begin{cases} v(x) = \cos(x) + av_1(x) + a^2v_2(x) + \mathcal{O}(a^3), \\ \lambda = a\lambda_1 + a^2\lambda_2 + \mathcal{O}(a^3). \end{cases}$$

The correction terms in H_{per}^α satisfy recursively,

$$\begin{cases} \mathcal{O}(a) : & (1 + D_\alpha)v_1 + 1 + \cos(2x) + \lambda_1 \cos(x) = 0, \\ \mathcal{O}(a^2) : & (1 + D_\alpha)v_2 + 2 \cos(x)v_1 + \frac{1}{2^\alpha - 1} \left[\cos(2x) - \frac{1}{2} \right] \cos(x) + \lambda_2 \cos(x) = 0. \end{cases}$$

In order to determine them uniquely, we impose orthogonality conditions of $\{v_k\}_{k \geq 1}$ to $\cos(\cdot)$ in L^2_{per} . The linear inhomogeneous equation at $\mathcal{O}(a)$ admits a solution $v_1 \in H_{\text{per}}^\alpha$ if and only if $\lambda_1 = 0$, after which the solution is found explicitly:

$$v_1(x) = \frac{1}{2^\alpha - 1} \cos(2x) - 1.$$

The linear inhomogeneous equation at $\mathcal{O}(a^2)$ admits a solution $v_2 \in H_{\text{per}}^\alpha$ if and only if $\lambda_2 = 2c_2$, where c_2 is defined by (3.14); c_2 is positive if $\alpha > \alpha_0$ and negative if $\alpha < \alpha_0$. Hence, if $\alpha > \alpha_0$, the small positive eigenvalue $\lambda = 2c_2a^2 + \mathcal{O}(a^3)$ bifurcates from the zero eigenvalue as $c > 1$. Functional-analytic setup for justification of perturbative expansions can be found in [54] (see also [52]) for $\alpha > 1/2$, which is met since $\alpha_0 > 1/2$. \square

Remark 3.9. *It was shown in Proposition 3.1 and Lemma 3.3 of [53] that $\text{Ker}(\tilde{\mathcal{H}}_{c,\alpha}) = \text{span}\{\phi'\}$ is one-dimensional, the zero eigenvalue is the lowest eigenvalue in the subspace of odd functions in L^2_{per} , and $\sigma(\tilde{\mathcal{H}}_{c,\alpha})$ has either one or two negative eigenvalues for every $c > 1$ and $\alpha \in (1/3, 2]$. By Lemma 3.1 above, for $c > 1$ $\sigma(\tilde{\mathcal{H}}_{c,\alpha})$ has one negative eigenvalue for $\alpha > \alpha_0$ and two negative eigenvalues for $\alpha < \alpha_0$.*

3.4 Proof of Theorem 3.3

In this section, we present the proof for Theorem 3.3, which states that the single-lobe wave profile ψ in the boundary-value problem (3.3) is positive for every $c > 1$ and $\alpha \in (\alpha_0, 2]$.

Proof. For $c \in (1, c_0)$ with some $c_0 > 1$, the assertion follows from Theorem 3.1 thanks to the transformation (3.5) and smallness of a in the Stokes expansion (3.9). In order to prove the same for every $c > 1$, we use Kranoselskii's fixed-point theorem in a positive cone and a homotopy argument with the Leray–Schauder index to trace a branch of the single-lobe positive solution in c . We divide the proof in five steps.

Step 1. The Green's function for $(D^\alpha + c)$.

We recall the Green's function $\mathcal{G}_\mathbb{T}$ which satisfies the equation (2.2), and is given by the Fourier series

$$\mathcal{G}_\mathbb{T}(x) = \frac{1}{2\pi} \sum_{n \in \mathbb{Z}} \frac{\cos(nx)}{c + |n|^\alpha}. \quad (3.26)$$

In what follows, we will denote the Green's function $\mathcal{G}_\mathbb{T}$ as $\mathcal{G}_{c,\alpha}$ to emphasize the dependence on the parameters c and a . It follows from (3.26) that $\mathcal{G}_{c,\alpha} \in L^2_{\text{per}}$ if $\alpha > 1/2$ but $\mathcal{G}_{c,\alpha}(0) = \infty$ if $\alpha \leq 1$. It has been proven in Theorem 2.1 that $\mathcal{G}_{c,\alpha}$ is positive for $\alpha \in (0, 2]$. There is a positive (c, α) -dependent constant $m_{c,\alpha}$ such that

$$\mathcal{G}_{c,\alpha}(x) \geq m_{c,\alpha}, \quad x \in \mathbb{T}. \quad (3.27)$$

In addition, for $\alpha > 1/2$, there exists a positive (c, α) -dependent constant $M_{c,\alpha}$ such that

$$\|\mathcal{G}_{c,\alpha}\|_{L^2_{\text{per}}} \leq M_{c,\alpha}.$$

Step 2. Nonlinear operator $A_{c,\alpha}$ in a positive cone $P_{c,\alpha}$.

Let us consider a positive cone in the space of L^2_{per} -functions defined by

$$P_{c,\alpha} := \left\{ \psi \in L^2_{\text{per}} : \psi(x) \geq \frac{m_{c,\alpha}}{M_{c,\alpha}} \|\psi\|_{L^2_{\text{per}}}, \quad x \in \mathbb{T} \right\}. \quad (3.28)$$

Define the following nonlinear operator $A_{c,\alpha}(\psi) : L^2_{\text{per}} \mapsto L^2_{\text{per}}$ for any $c > 0$:

$$A_{c,\alpha}(\psi) := (D^\alpha + c)^{-1} \psi^2 \quad \Rightarrow \quad A_{c,\alpha}(\psi)(x) = \int_{-\pi}^{\pi} \mathcal{G}_{c,\alpha}(x-s) \psi(s)^2 ds. \quad (3.29)$$

The operator $A_{c,\alpha}$ is bounded and continuous in L^2_{per} thanks to the generalized Young inequality:

$$\|A_{c,\alpha}(\psi)\|_{L^2_{\text{per}}} \leq \|\mathcal{G}_{c,\alpha}\|_{L^2_{\text{per}}} \|\psi^2\|_{L^1_{\text{per}}} \leq M_{c,\alpha} \|\psi\|_{L^2_{\text{per}}}^2. \quad (3.30)$$

Moreover, $A_{c,\alpha}$ is compact because it is the limit of compact operators $A_{c,\alpha}^{(N)}$ given by the first $2N + 1$ Fourier coefficients. Indeed, we have

$$\begin{aligned} \|A_{c,\alpha}(\psi) - A_{c,\alpha}^{(N)}(\psi)\|_{L^2_{\text{per}}}^2 &= \frac{1}{2\pi} \sum_{|n|>N} \frac{|(\psi^2)_n|^2}{(c + |n|^\alpha)^2} \\ &\leq \frac{1}{2\pi} \|(\psi^2)_n\|_{\ell^\infty}^2 \sum_{|n|>N} \frac{1}{(c + |n|^\alpha)^2} \\ &\leq \frac{1}{2\pi} \|\psi^2\|_{L^1_{\text{per}}}^2 \sum_{|n|>N} \frac{1}{(c + |n|^\alpha)^2} \\ &= \frac{1}{2\pi} \|\psi\|_{L^2_{\text{per}}}^4 \sum_{|n|>N} \frac{1}{(c + |n|^\alpha)^2}, \end{aligned}$$

where the numerical series converges for every $\alpha > 1/2$. Therefore, for every $\psi \in L^2_{\text{per}}$,

$$\lim_{N \rightarrow \infty} \|A_{c,\alpha}(\psi) - A_{c,\alpha}^{(N)}(\psi)\|_{L^2_{\text{per}}} = 0,$$

so that $A_{c,\alpha}$ maps bounded sets in L^2_{per} to pre-compact sets in L^2_{per} .

Thanks to the positivity of the Green function in (3.27), we confirm that the operator $A_{c,\alpha}(\psi)$ is closed in $P_{c,\alpha} \subset L^2_{\text{per}}$:

$$A_{c,\alpha}(\psi)(x) \geq m_{c,\alpha} \|\psi\|_{L^2_{\text{per}}}^2 \geq \frac{m_{c,\alpha}}{M_{c,\alpha}} \|A_{c,\alpha}(\psi)\|_{L^2_{\text{per}}}. \quad (3.31)$$

A fixed point ψ of $A_{c,\alpha}(\psi)$ in $P_{c,\alpha} \subset L^2_{\text{per}}$ corresponds to the positive function ψ such that $\psi(x) > 0$ for every $x \in \mathbb{T}$.

Step 3. Existence of a fixed point in the positive cone $P_{c,\alpha}$.

Let $B_r := \{\psi \in L^2_{\text{per}} : \|\psi\|_{L^2_{\text{per}}} < r\}$ be a ball of radius r in L^2_{per} . The existence of a fixed point of $A_{c,\alpha}(\psi)$ in $P_{c,\alpha} \cap (\bar{B}_{r_+} \setminus B_{r_-})$ for some $0 < r_- < r_+ < \infty$ follows from Krasnoselskii's fixed-point theorem if there exist r_- and r_+ such that

$$\|A_{c,\alpha}(\psi)\|_{L^2_{\text{per}}} < \|\psi\|_{L^2_{\text{per}}}, \quad \psi \in P_{c,\alpha} \cap \partial B_{r_-} \quad (3.32)$$

and

$$\|A_{c,\alpha}(\psi)\|_{L^2_{\text{per}}} > \|\psi\|_{L^2_{\text{per}}}, \quad \psi \in P_{c,\alpha} \cap \partial B_{r_+}. \quad (3.33)$$

The bound (3.32) follows from (3.30) with $M_{c,\alpha} r_- < 1$. The bound (3.33)

follows from (3.31) with $\sqrt{2\pi}m_{c,\alpha}r_+ > 1$, hence the two radii satisfy the constraints

$$0 < r_- < \frac{1}{M_{c,\alpha}} \leq \frac{1}{\sqrt{2\pi}m_{c,\alpha}} < r_+ < \infty, \quad (3.34)$$

where $\sqrt{2\pi}m_{c,\alpha} \leq M_{c,\alpha}$ follows from (3.27). Hence, there exists a fixed point of $A_{c,\alpha}(\psi)$ in $P_{c,\alpha} \cap (\bar{B}_{r_+} \setminus B_{r_-})$.

Step 4. Regularity of the fixed point.

We use bootstrapping arguments similar to those used in the proof of Proposition 2.1 in [53] and show that the fixed point of $A_{c,\alpha}$ in L_{per}^2 also exists in H_{per}^α , hence ψ is a positive solution of the boundary-value problem (3.3). Indeed, if $\psi \in L_{\text{per}}^4(\mathbb{T})$, then $\psi \in H_{\text{per}}^\alpha$ thanks to the estimate:

$$\|D_\alpha \psi\|_{L_{\text{per}}^2} = \|D_\alpha(D_\alpha + c)^{-1}\psi^2\|_{L_{\text{per}}^2} \leq \|\psi^2\|_{L_{\text{per}}^2} = \|\psi\|_{L_{\text{per}}^4}^2.$$

In order to show that $\psi \in L_{\text{per}}^4(\mathbb{T})$, we use the generalized Young and Hölder inequalities:

$$\|\psi\|_{L_{\text{per}}^r} \leq \|\mathcal{G}_{c,\alpha}\|_{L_{\text{per}}^p} \|\psi^2\|_{L_{\text{per}}^q}, \quad 1 + \frac{1}{r} = \frac{1}{p} + \frac{1}{q}, \quad p, q, r \geq 1, \quad (3.35)$$

$$\leq \|\mathcal{G}_{c,\alpha}\|_{L_{\text{per}}^p} \|\psi\|_{L_{\text{per}}^{sq}} \|\psi\|_{L_{\text{per}}^{sq/(s-1)}}, \quad s \geq 1. \quad (3.36)$$

By using the Hausdorff–Young inequality

$$\|\mathcal{G}_{c,\alpha}\|_{L_{\text{per}}^p} \leq C_p \|(|n|^\alpha + c)^{-1}\|_{\ell^{p/(p-1)}}, \quad p \geq 2,$$

we can see that $\|\mathcal{G}_{c,\alpha}\|_{L_{\text{per}}^p} < \infty$ if $\alpha p/(p-1) > 1$. If $\alpha \geq 1$, then $\mathcal{G}_{c,\alpha} \in L_{\text{per}}^p$ for every $p \in [2, \infty)$. Applying (3.35) with $r = p$ and $q = 1$, we have $\psi \in L_{\text{per}}^p$ for every $p \in [2, \infty)$.

If $\alpha \in (\alpha_0, 1)$, we set $p_0 = 1/(1 - \alpha_0) > 2$ and obtain with the same argument that $\mathcal{G}_{c,\alpha}, \psi \in L_{\text{per}}^{p_0}$. Then, using bound (3.36) with $sq = 2$ and $sq/(s-1) = p_0$, that is, with $s = 1 + 2/p_0$ and $q = 2p_0/(2 + p_0)$, we obtain $\psi \in L_{\text{per}}^r$ with $r = 2p_0/(4 - p_0) > p_0$ (because $p_0 > 2$). Iterating bound (3.36) with $sq = 2$ and $sq/(s-1) = r$, we obtain a bigger value for $r = p_0/(3 - p_0) > 2p_0/(4 - p_0)$, hence by further iterations, we get $\psi \in L_{\text{per}}^p$ for every $p \in [2, \infty)$ including $p = 4$.

Step 5. Leray–Schauder index along branches of fixed points.

The fixed point $\psi \in P_{c,\alpha} \cap (\bar{B}_{r_+} \setminus B_{r_-})$ for $r_- < r_+$ satisfying (3.34) exists for every $c > 0$. However, the constant periodic solution

$$\psi_c(x) = c, \quad x \in \mathbb{T} \quad (3.37)$$

is a fixed point of $A_{c,\alpha}$ in $P_{c,\alpha} \cap (\bar{B}_{r_+} \setminus B_{r_-})$ for every $c > 0$ and $\alpha > 0$. Indeed, $A_{c,\alpha}(\psi_c) = \psi_c$ for every $\alpha > 0$ and $\psi_c \in P_{c,\alpha} \cap (\bar{B}_{r_+} \setminus B_{r_-})$ for every $c > 0$ thanks to the condition $\sqrt{2\pi}m_{c,\alpha} \leq M_{c,\alpha}$. In order to be able to claim that there exists a non-trivial fixed point $\psi \in P_{c,\alpha} \cap (\bar{B}_{r_+} \setminus B_{r_-})$ for $c > 1$ in addition to the constant fixed point ψ_c , we look at the Leray–Schauder index of the fixed point in the subspace of even functions in L^2_{per} :

Definition 3.1. *The Leray–Schauder index of the fixed point ψ is defined as $(-1)^N$, where N is the number of unstable eigenvalues of $A'_{c,\alpha}(\psi)$ outside the unit disk with the account of their multiplicities.*

For the fixed point ψ_c in (3.37), we have $A'_{c,\alpha}(\psi_c) = 2c(D^\alpha + c)^{-1}$, hence there exists $N = K + 1$ unstable eigenvalues of $A'_{c,\alpha}(\psi_c)$ outside the unit disk for every $c \in (K^\alpha, (K + 1)^\alpha)$, where $K \in \mathbb{N}$. Therefore, the index of ψ_c changes sign every time c crosses values in the set $\{K^\alpha\}_{K \in \mathbb{N}}$, as is shown on Figure 3.1. On the other hand, for $K = 1$, $c = 1$ is a bifurcation value by Theorem 3.1 and two non-trivial fixed points $\psi \in P_{c,\alpha} \cap (\bar{B}_{r_+} \setminus B_{r_-})$ bifurcate for $c > 1$ if $\alpha > \alpha_0$, one is single-lobe with maximum at $x = 0$ and the other one is single-lobe with minimum at $x = 0$, both are strictly positive. For the non-trivial fixed points ψ , we have

$$A'_{c,\alpha}(\psi) = 2(D^\alpha + c)^{-1}\psi = \text{Id} - (D^\alpha + c)^{-1}\mathcal{H}_{c,\alpha},$$

where it follows from positivity of ψ that $A'_{c,\alpha}(\psi) \geq 0$. By the assumption that the spectrum of $\mathcal{H}_{c,\alpha}$ contains only one negative eigenvalue and a simple zero eigenvalue for all $c > 1$ and $\alpha \in (\alpha_0, 2]$, there exists $N = 1$ unstable eigenvalues of $A'_{c,\alpha}(\psi)$. Therefore, the pair of non-trivial fixed points $\psi \in P_{c,\alpha} \cap (\bar{B}_{r_+} \setminus B_{r_-})$ is distinct from the constant fixed point ψ_c for every $c \in (1, c_0)$, as is shown on Figure 3.1.

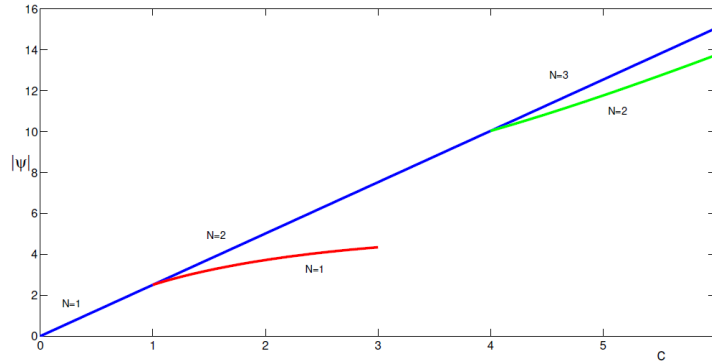


Figure 3.1: Schematic representation of the constant fixed point ψ_c and pairs of non-trivial fixed points on the $(c, \|\psi\|_{L^2_{\text{per}}})$ plane for $\alpha = 2$.

The pair of non-trivial fixed points for the single-lobe solution remains

inside $P_{c,\alpha} \cap (\bar{B}_{r_+} \setminus B_{r_-})$ in continuation of the solution family in c for a fixed $\alpha \in (\alpha_0, 2]$, thanks to the conditions (3.32), (3.33), and (3.34). Their indices also remain invariant with respect to c because no zero eigenvalue of \mathcal{H} are supposed to exist in the parameter continuations of the periodic waves. Therefore, these fixed points cannot coalesce with any other fixed points of $A_{c,\alpha}$ in $P_{c,\alpha} \cap (\bar{B}_{r_+} \setminus B_{r_-})$. By continuity, these fixed points coincide with the single-lobe solutions, existence of which is proven in Proposition 2.1 in [53]. \square

Remark 3.10. *At every bifurcation point $c = K^\alpha$ with $K \geq 2$, a pair of additional fixed points of $A_{c,\alpha}$ bifurcates in $P_{c,\alpha} \cap (\bar{B}_{r_+} \setminus B_{r_-})$, as is shown on Figure 3.1 for $K = 2$ and $\alpha = 2$. These fixed points are not single-lobe solutions for $K \geq 2$ but instead these are concatenations of the single-lobe solutions with K periods on $[-\pi, \pi]$.*

3.5 Periodic Waves for $\alpha = 1$ and 2

We give examples illustrating positivity of ψ for the classical cases $\alpha = 2$ and $\alpha = 1$. For the KdV equation (see, e.g., Proposition 4.1 in [49]), the solution ϕ to the boundary-value problem (3.4) with $\alpha = 2$ is given by

$$\phi(x) = \frac{2K(k)^2}{\pi^2} \left[1 - 2k^2 - \sqrt{1 - k^2 + k^4} + 3k^2 \operatorname{cn}^2 \left(\frac{K(k)}{\pi} x; k \right) \right] \quad (3.38)$$

where cn is the Jacobi elliptic function, $K(k)$ is a complete elliptic integral of the first kind, and $k \in (0, 1)$ is the elliptic modulus that parameterizes the wave speed c given by

$$c = \frac{4K(k)^2}{\pi^2} \sqrt{1 - k^2 + k^4}. \quad (3.39)$$

Using the relation between ϕ and ψ in equation (3.5), we obtain

$$\psi(x) = \frac{2K(k)^2}{\pi^2} \left[1 - 2k^2 + \sqrt{1 - k^2 + k^4} + 3k^2 \operatorname{cn}^2 \left(\frac{K(k)}{\pi} x; k \right) \right], \quad (3.40)$$

from which $\psi(x) \geq \psi(\pm\pi) > 0$ holds for every $x \in \mathbb{T}$ and every $k \in (0, 1)$, in accordance with Theorem 3.3 (see Figure 3.2, left panel). Indeed, if $\alpha = 2$, the boundary-value problem (3.3) can be formulated as a planar Hamiltonian system on the phase plane (ψ, ψ') and a set of closed orbits for periodic solutions is located on the phase plane between the saddle point $(0, 0)$ and the center point $(c, 0)$, hence, $\psi(x) > 0$ for every $x \in [-\pi, \pi]$.

For the BO equation (see, e.g., [71]), the solution ϕ to the boundary-value

problem (3.4) with $\alpha = 1$ is given by

$$\phi(x) = \frac{\cosh \gamma \cos x - 1}{\sinh \gamma (\cosh \gamma - \cos x)}, \quad c = \coth \gamma. \quad (3.41)$$

Again, we use equation (3.5) to obtain

$$\psi(x) = \frac{\sinh \gamma}{\cosh \gamma - \cos x}, \quad (3.42)$$

from which $\psi(x) \geq \psi(\pm\pi) = \tanh \gamma > 0$ holds for every $x \in \mathbb{T}$ and every $\gamma \in (0, \infty)$, in agreement with Theorem 3.3 (see Figure 3.2, right panel).

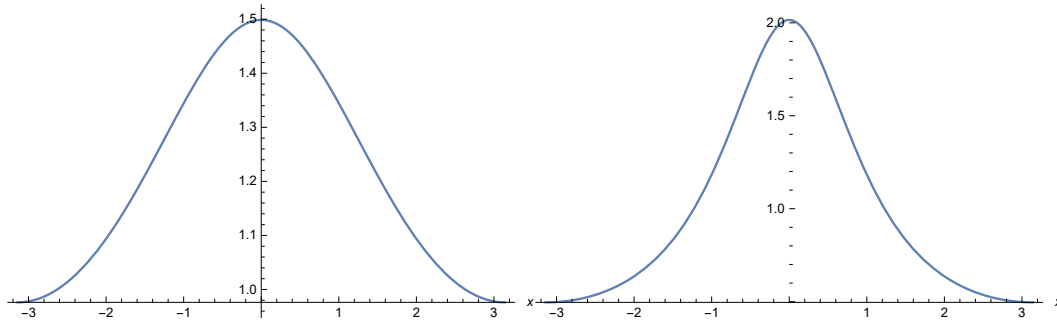


Figure 3.2: Left: profile ψ in (3.40), $\alpha = 2$ and $k = 0.5$, Right: profile ψ in (3.42), $\alpha = 1$ and $\gamma = 1.0884$

Chapter 4

Convergence Of the Petviashvili Method

In this chapter, our goal is to analyze the convergence of the Petviashvili method for approximating the solution of the boundary value problems:

$$(c - D^\alpha)\phi + \phi^2 = 0, \quad \phi \in H_{\text{per}}^\alpha, \quad (4.1)$$

and

$$(c + D^\alpha)\psi = \psi^2, \quad \psi \in H_{\text{per}}^\alpha. \quad (4.2)$$

Let us first explain the classical Petviashvili method applied to the equation (4.1). For $c \notin \{1, 2^\alpha, 3^\alpha, \dots\}$ and given a suitable initial guess $w_0 \in H_{\text{per}}^\alpha$, we define a sequence $\{w_n\}_{n \in \mathbb{N}} \subset H_{\text{per}}^\alpha$ by the iterative rule

$$w_{n+1} = \tilde{T}_{c,\alpha}(w_n) := [\tilde{M}(w_n)]^2 \tilde{\mathcal{L}}_{c,\alpha}^{-1}(w_n^2), \quad n \in \mathbb{N}. \quad (4.3)$$

where the Petviashvili quotient is given by

$$\tilde{M}(w) := \frac{\langle \tilde{\mathcal{L}}_{c,\alpha} w, w \rangle}{\langle w^2, w \rangle}, \quad w \in H_{\text{per}}^\alpha, \quad (4.4)$$

with the linear operator $\mathcal{L}_{c,\alpha} := D^\alpha - c$ and its spectrum in L_{per}^2 for $c \in \mathbb{R}$ and $\alpha > 0$ is given by

$$\sigma(\mathcal{L}_{c,\alpha}) = \{|n|^\alpha - c, \quad n \in \mathbb{Z}\}. \quad (4.5)$$

Here, we note that the exponent of $M(w_n)$ is chosen to be quadratic so that $\tilde{T}_{c,\alpha}(w)$ is a homogeneous power function in w of degree *zero*. This ensures the fastest convergence rate of the iterative method (4.3) near a solution of the nonlinear equation (4.1) [81].

Linearizing $\tilde{T}_{c,\alpha}$ at ϕ with $w_n = \phi + \omega_n$, where $\omega_n \in H_{\text{per}}^\alpha$, yields the

linearized iterative rule:

$$\omega_{n+1} = -\frac{2\langle \tilde{\mathcal{L}}_{c,\alpha}\phi, \omega_n \rangle}{\langle \tilde{\mathcal{L}}_{c,\alpha}\phi, \phi \rangle} \phi + \tilde{\mathcal{L}}_{c,\alpha}^{-1}(2\phi\omega_n), \quad n \in \mathbb{N}. \quad (4.6)$$

Since $\tilde{\mathcal{L}}_{c,\alpha}^{-1}(\phi^2) = \phi$ and $\tilde{\mathcal{L}}_{c,\alpha}^{-1}(2\phi\phi') = \phi'$, the linearized iterative rule (4.6) is invariant in the constrained space

$$L_c^2 := \{\omega \in L_{\text{per}}^2 : \langle \phi^2, \omega \rangle = \langle \phi\phi', \omega \rangle = 0\}. \quad (4.7)$$

To satisfy the two constraints, one can expand $\omega_n = a_n\phi + b_n\phi' + \beta_n$ with $\beta_n \in H_{\text{per}}^\alpha \cap L_c^2$ and derive the following from (4.6):

$$a_{n+1} = 0, \quad b_{n+1} = b_n, \quad \beta_{n+1} = \tilde{\mathcal{L}}_T\beta_n, \quad (4.8)$$

where

$$\tilde{\mathcal{L}}_T := \tilde{\mathcal{L}}_{c,\alpha}^{-1}(2\phi \cdot) = \text{Id} - \tilde{\mathcal{L}}_{c,\alpha}^{-1}\tilde{\mathcal{H}}_{c,\alpha} : H_{\text{per}}^\alpha \cap L_c^2 \mapsto H_{\text{per}}^\alpha \cap L_c^2 \quad (4.9)$$

with the Jacobian operator for (4.1) defined as $\tilde{\mathcal{H}}_{c,\alpha} := D^\alpha - c - 2\phi$. We call $\tilde{\mathcal{L}}_T$ the linearized iterative operator of the iterative rule (4.3).

As is well understood since the first proof of convergence in [81] (see also follow-up works in [6, 7, 29, 37, 63]), convergence of the iterative method is analyzed from the contraction of the linearized iterative operator $\tilde{\mathcal{L}}_T$ in (4.9). We observe that the operator $\tilde{\mathcal{L}}_T$ is necessarily a contraction if its spectrum is confined within the unit disk. Moreover, by Lemma 1.2 in [81], the set of fixed points of $\tilde{\mathcal{L}}_{c,\alpha}$ coincides with the set of solutions to the boundary-value problem (4.1). Thus, the contraction of the operator $\tilde{\mathcal{L}}_T$ is determined by the spectrum of the generalized eigenvalue problem

$$\tilde{\mathcal{H}}_{c,\alpha}v = \lambda\tilde{\mathcal{L}}_{c,\alpha}v, \quad v \in H_{\text{per}}^\alpha. \quad (4.10)$$

Similarly for the boundary value problem (4.2), for any suitable initial guess $w_0 \in H_{\text{per}}^\alpha$ we have the iteration rule

$$w_{n+1} = T_{c,\alpha}(w_n) := [M(w_n)]^2 \mathcal{L}_{c,\alpha}^{-1}(w_n^2), \quad n \in \mathbb{N}. \quad (4.11)$$

where

$$M(w) := \frac{\langle \mathcal{L}_{c,\alpha}w, w \rangle}{\langle w^2, w \rangle}, \quad w \in H_{\text{per}}^\alpha, \quad (4.12)$$

with the positive operator $\mathcal{L}_{c,\alpha} = D^\alpha + c$. We linearize $T_{c,\alpha}$ at ψ with $w_n = \psi + a_n\psi + b_n\psi' + \beta_n$ satisfying the two constraints in

$$L_c^2 := \{\omega \in L_{\text{per}}^2 : \langle \psi^2, \omega \rangle = \langle \psi\psi', \omega \rangle = 0\}, \quad (4.13)$$

and obtain the linearized iterative rule

$$a_{n+1} = 0, \quad b_{n+1} = b_n, \quad \beta_{n+1} = \mathcal{L}_T \beta_n, \quad (4.14)$$

where the linearized iterative operator is given by

$$\mathcal{L}_T := \mathcal{L}_{c,\alpha}^{-1}(2\psi \cdot) = \text{Id} - \mathcal{L}_{c,\alpha}^{-1} \mathcal{H}_{c,\alpha} : \quad H_{\text{per}}^\alpha \cap L_c^2 \mapsto H_{\text{per}}^\alpha \cap L_c^2 \quad (4.15)$$

with $\mathcal{H}_{c,\alpha} = D^\alpha + c - 2\psi$ is the Jacobian operator of the boundary value problem (4.2). We recall from Chapter 3 that $\mathcal{H}_{c,a}$ by the relation

$$\mathcal{H}_{c,\alpha} = D^\alpha + c - 2\psi = D^\alpha + c - 2(c + \phi) = D^\alpha - c - 2\phi = \tilde{\mathcal{H}}_{c,\alpha}.$$

Hence, the contraction of operator \mathcal{L}_T is also determined by the spectrum of the generalized eigenvalue problem

$$\mathcal{H}_{c,\alpha} v = \lambda \mathcal{L}_{c,\alpha} v, \quad v \in H_{\text{per}}^\alpha. \quad (4.16)$$

This chapter is organized as follows. In Section 4.1, we state the main results regarding the sufficient condition for convergence (divergence) of iterations (4.3) and (4.11); we also describe the specific range of parameters c and α for which the convergence (divergence) of the Petviashvili iteration occurs when applied to the boundary value problems (4.1) and (4.2). The proofs of the main results will be presented in Section 4.2, 4.3, and 4.4. Finally, we collect the numerical illustrations for iterations (4.3) and (4.11) in Section 4.5.

4.1 Main Results

Here, we provide the sufficient condition for convergence and divergence of the iterations (4.3) and (4.11). In order to make the statement less cumbersome, we only mention the iteration (4.3) in the Theorem 4.1. The same conclusion also holds when the iteration (4.11) replaces the iteration (4.3).

Theorem 4.1. *Assume*

$$\int_{-\pi}^{\pi} \phi^3 dx \neq 0, \quad \int_{-\pi}^{\pi} \phi(\phi')^2 dx \neq 0. \quad (4.17)$$

If $\sigma(\tilde{\mathcal{L}}_T)$ in L_c^2 includes at least one eigenvalue outside the unit disk, then there exists $w_0 \in H_{\text{per}}^\alpha$ near $\phi \in H_{\text{per}}^\alpha$ such that the iterative method (4.3) diverges from ϕ . Otherwise, if $\sigma(\tilde{\mathcal{L}}_T)$ in L_c^2 is located inside the unit disk, there exists a small $\epsilon_0 > 0$ such that for every $w_0 \in H_{\text{per}}^\alpha$ satisfying

$$\epsilon := \|w_0 - \phi\|_{H_{\text{per}}^\alpha} \leq \epsilon_0, \quad (4.18)$$

there exist b_* satisfying $|b_*| \leq C\epsilon$ for some ϵ -independent $C > 0$ such that the iterative method (4.3) converges to $\phi(\cdot - b_*)$.

We recall again the two thresholds of α , which were obtained through the perturbative argument in Chapter 3

$$\alpha_0 = \frac{\log 3}{\log 2 - 1} \approx 0.558,$$

and

$$\alpha_1 = \frac{\log 5}{\log 2} - 1.$$

The following two theorems describe the convergence (divergence) of the Petviashvili method when applied to the boundary value problems (4.1) and (4.2).

Theorem 4.2. *For every $c > 1$ and $\alpha \in (\alpha_0, 2]$, consider the unique, single-lobe solution $\phi \in H_{\text{per}}^\alpha$ obtained in Theorem 3.1. There is $c_0 > 0$ such that for every $c \in (1, c_0)$ this solution is an unstable fixed point of the iterative method (4.3) for $\alpha \in (\alpha_0, \alpha_1)$ and an asymptotically stable fixed point (up to a translation) for $\alpha \in (\alpha_1, 2]$.*

Remark 4.1. *Theorem 4.2 implies that the iterative method (4.3) diverges from ϕ for the classical BO equation with $\alpha = 1$. Although the iterative method (4.3) converges to ϕ for the classical KdV equation with $\alpha = 2$ for $c \in (1, c_0)$, we show numerically that it diverges from ϕ for $c > c_0$ with $c_0 \gtrsim 2.3$. Instabilities of the iterative method (4.3) are explained by the unstable eigenvalues of the generalized eigenvalue problem (4.10).*

Theorem 4.3. *Consider the unique, single-lobe solution $\psi \in H_{\text{per}}^\alpha$ obtained in Theorem 3.3. This unique solution is an asymptotically stable (up to a translation) fixed point of the iterative method (4.11) for every $c > 1$ and $\alpha \in (\alpha_0, 2]$.*

Remark 4.2. *We observe that the small-amplitude solution ϕ of the boundary value problem (4.1) obtained by Theorem 3.1 satisfies assumption (4.17). In fact, using the Stokes expansion of ϕ we have*

$$\int_{-\pi}^{\pi} \phi^3 dx = \frac{3\pi a^4}{4(2^\alpha - 1)}(3 - 2^{\alpha+1}) + \mathcal{O}(a^6)$$

and

$$\int_{-\pi}^{\pi} \phi(\phi')^2 dx = \frac{\pi a^4}{4(2^\alpha - 1)}(5 - 2^{\alpha+1}) + \mathcal{O}(a^6),$$

which imply that for α_0 and α_1 given in (3.8)

$$\left. \begin{aligned} \int_{-\pi}^{\pi} \phi^3 dx &< 0, & \alpha > \alpha_0, \\ &> 0, & \alpha < \alpha_0, \end{aligned} \right\} \quad (4.19)$$

and

$$\left. \begin{aligned} \int_{-\pi}^{\pi} \phi(\phi')^2 dx &< 0, & \alpha > \alpha_1, \\ &> 0, & \alpha < \alpha_1, \end{aligned} \right\}. \quad (4.20)$$

The solution ψ of the boundary value problem (4.2) defined in Theorem 3.3 also satisfies assumption (3.3) thanks to the positivity of ψ .

Remark 4.3. *The unconditional convergence of the iterative method (4.11) compared to the iterative method (4.3) has a well-known physical interpretation. The phase velocity of the linear waves of the fractional KdV equation (1.7) on the zero background is strictly negative, hence the travelling wave $u(x, t) = \phi(x + ct)$ propagating to the left is in resonance with the linear waves. On the other hand, the travelling wave on the constant background $b := -c < 0$ propagates to the right and avoids resonances with the linear waves on the background $b < 0$, which still have negative phase velocity.*

Remark 4.4. *The new iterative method (4.11) can be considered as a modification of the classical Petviashvili method (4.3) after the shift of the field variable proposed in [8]. The modified algorithm consists of three steps. In the first step, the constant value b is found from the constant solution of the stationary problem (4.1). Solving $cb + b^2 = 0$ for nonzero b yields $b = -c$. In the second step, the change of variables $\phi = b + \psi$ transforms the original problem (4.1) to the new problem (4.2), which is confirmed from the transformation formula (3.5) since $b = -c$. Finally, the third step is the iterative method for the transformed problem (4.2), which is defined by the new iterative operator $\tilde{T}_{c,\alpha}$ in (4.11).*

Remark 4.5. *In the case of solitary waves, the boundary-value problem (4.1) for ϕ and $c > 0$ admits no solutions and the iterative method (4.3) cannot be defined since $\tilde{\mathcal{L}}_{c,\alpha}$ is not invertible in $L^2(\mathbb{R})$ for $c > 0$. On the other hand, the boundary-value problem (4.2) for ψ and $c > 0$ admits solitary wave solutions and the iterative method (4.11) is well-defined to approximate this solution, as shown numerically in [39].*

4.2 Proof of Theorem 4.1

If $\sigma(\tilde{\mathcal{L}}_T)$ in L_c^2 admits at least one eigenvalue outside the unit disk, the corresponding eigenfunction of $\tilde{\mathcal{L}}_T$ defines a direction in H_{per}^α along which the sequence $\{w_n\}_{n \in \mathbb{N}}$ diverges from the fixed point ϕ , as follows from the unstable manifold theorem.

To show that the iteration (4.3) converges to a translation of ϕ if $\sigma(\tilde{\mathcal{L}}_T)$ in L_c^2 is confined inside the unit disk, we first prove it for an even initial guess w_0 then extend it to a general function.

Let us first assume that $w_0 \in H_{\text{per}}^\alpha$ is even, in which case the assertion is true with $b_* = 0$. Since $\tilde{\mathcal{L}}_{c,\alpha}$ maps even functions to even functions, the sequence of functions $\{w_n\}_{n \in \mathbb{N}}$ in H_{per}^α generated by iteration (4.3) is even. Therefore, the linearization $w_n = \phi + \omega_n$ and the decomposition $\omega_n = a_n\phi + b_n\phi' + \beta_n$ yields $b_n = 0$ for every $n \geq 0$. The linear iterative formula (4.8) yields $a_n = 0$ for every $n \geq 1$ even if $a_0 \neq 0$. The linearized operator $\tilde{\mathcal{L}}_T$ given by (4.9) is a strict contraction if $\sigma(\tilde{\mathcal{L}}_T)$ in L_c^2 is located inside the unit disk. Convergence of the sequence to ϕ follows by Banach's fixed-point theorem A.5.

Let us now relax the condition that the initial guess $w_0 \in H_{\text{per}}^\alpha$ is even. In order to control the projection b_n in the decomposition $\omega_n = a_n\phi + b_n\phi' + \beta_n$, we need to use tools of the modulation theory for periodic waves, see, e.g., Section 5 in [43]. Instead of defining b_n by $\omega_n = a_n\phi + b_n\phi' + \beta_n$, we define $b_n \in \mathbb{R}$ by using the decomposition

$$w_n(x) = \phi(x - b_n) + \omega_n(x - b_n) \quad (4.21)$$

and the orthogonality condition

$$\langle \phi\phi', \omega_n \rangle = 0. \quad (4.22)$$

By a standard application of the implicit function theorem, see, e.g., Lemma 6.1 in [43], for every $w_n \in H_{\text{per}}^\alpha$ satisfying

$$\epsilon_n := \inf_{b \in [-\pi, \pi]} \|w_n - \phi(\cdot - b)\|_{H_{\text{per}}^\alpha} \leq \epsilon_0, \quad (4.23)$$

the decomposition (4.21)–(4.22) is unique under the assumption $\int_{-\pi}^{\pi} \phi(\phi')^2 dx \neq 0$ with uniquely defined b_n near the argument of the infimum in (4.23) and uniquely defined ω_n satisfying

$$\|\omega_n\|_{H_{\text{per}}^\alpha} \leq C_0 \epsilon_n \quad (4.24)$$

for some ϵ_n -independent constant $C_0 > 0$.

Substituting the decomposition (4.21) into the iterative method (4.3) and using the translational invariance in x , we obtain the equivalent iterative scheme:

$$\omega_{n+1} = \phi(\cdot + \Delta b_n) - \phi + \tilde{T}'(\phi)(\phi(\cdot + \Delta b_n)\omega_n(\cdot + \Delta b_n) + N(\omega_n(\cdot + \Delta b_n))), \quad (4.25)$$

where $\Delta b_n := b_{n+1} - b_n$, $\tilde{T}'(\phi)\omega_n$ denotes the linearized iterative operator given by the right-hand side in (4.6), and $N(\omega_n)$ is the nonlinear terms satisfying

$$\|N(\omega_n)\|_{H_{\text{per}}^\alpha} \leq C \|\omega_n\|_{H_{\text{per}}^\alpha}^2, \quad (4.26)$$

for every $\omega_n \in B_\rho(0) := \{\omega \in H_{\text{per}}^\alpha : \|\omega\|_{H_{\text{per}}^\alpha} \leq \rho\}$, where the constant $C > 0$ does not depend on ρ provided the radius ρ of the ball $B_\rho(0)$ is small. Thanks to (4.18) and (4.24), we work with $\rho = C\epsilon$ for some positive ϵ -independent constant C .

By using the constraint (4.22) both for ω_n and ω_{n+1} , we derive the following equation for Δb_n :

$$0 = \langle \phi\phi', \phi(\cdot + \Delta b_n) - \phi \rangle + \langle \phi\phi', \tilde{T}'(\phi(\cdot + \Delta b_n)\omega_n(\cdot + \Delta b_n)) \rangle + \langle \phi\phi', N(\omega_n(\cdot + \Delta b_n)) \rangle. \quad (4.27)$$

This equation can be treated as the root-finding problem $F(\Delta b_n, \omega_n) = 0$, where

$$F : \mathbb{R} \times H_{\text{per}}^\alpha \mapsto \mathbb{R}$$

is a smooth function in its variables satisfying $F(0, 0) = 0$ and $\partial_{\Delta b_n} F(0, 0) \neq 0$ thanks to smoothness of $\phi \in H_{\text{per}}^\infty$ and $N(\omega_n)$ as well as the assumption $\int_{-\pi}^{\pi} \phi(\phi')^2 dx \neq 0$. By the implicit function theorem, the root-finding problem (4.27) is uniquely solvable in Δb_n for every $\omega_n \in B_\rho(0)$ with small $\rho > 0$. Moreover, thanks to $\langle \phi\phi', \tilde{T}'(\phi)\omega_n \rangle = \langle \phi\phi', \omega_n \rangle = 0$ and (4.26), the uniquely found Δb_n satisfies the bound

$$|\Delta b_n| \leq C \|\omega_n\|_{H_{\text{per}}^\alpha}^2, \quad (4.28)$$

for some constant $C > 0$ that does not depend on the small radius ρ .

Substituting Δb_n satisfying (4.28) into (4.25) and decomposing $\omega_n = a_n\phi + \beta_n$ with $a_n \in \mathbb{R}$ and $\beta_n \in H_{\text{per}}^\alpha \cap L_c^2$, we obtain the linearized problem

$$a_{n+1} = 0, \quad \beta_{n+1} = \tilde{\mathcal{L}}_T \beta_n. \quad (4.29)$$

Since $\tilde{\mathcal{L}}_T$ is a strict contraction in L_c^2 , convergence $a_n \rightarrow 0$, $\Delta b_n \rightarrow 0$, and $\beta_n \rightarrow 0$ as $n \rightarrow \infty$ follows by Banach's fixed-point theorem A.5. Moreover, these sequences converge exponentially fast so that the sequence $\{b_n\}_{n \in \mathbb{N}}$ converges to a limit denoted by b_* . Since $|b_* - b_0| \leq C\epsilon^2$ thanks to (4.24) and (4.28), whereas $|b_0| \leq C\epsilon$ thanks to (4.18), (4.23), and triangle inequality, we also have $|b_*| \leq C\epsilon$ for some ϵ -independent $C > 0$. The assertion is proven thanks to the decomposition (4.21) with $\omega_n = a_n\phi + \beta_n$.

4.3 Proof of Theorem 4.2

Here, we present the proof of convergence (divergence) results for the iteration (4.3). The proof is achieved through Lemma 4.1 and Corollary 4.1. In Lemma 4.1, we characterize the spectrum of the operator $\tilde{\mathcal{L}}_{c,\alpha}^{-1} \tilde{\mathcal{H}}_{c,\alpha}$ for $c \in (1, c_0)$ with some $c_0 > 1$, then in Corollary 4.1 we count the number of remaining unstable eigenvalues in the constrained space L_c^2 in (4.7).

We begin by determining the spectrum of the operator $\tilde{\mathcal{L}}_{c,\alpha}^{-1}\tilde{\mathcal{H}}_{c,\alpha}$ in L^2_{per} in the following lemma.

Lemma 4.1. *For every $\alpha > \alpha_0$ there exists $c_0 \in (1, 2^\alpha)$ such that for every $c \in (1, c_0)$, $\sigma(\tilde{\mathcal{L}}_{c,\alpha}^{-1}\tilde{\mathcal{H}}_{c,\alpha})$ in L^2_{per} consists of a countable sequence of eigenvalues in a neighborhood of 1 and simple eigenvalues $\{-1, 0, \lambda_1, \lambda_2\}$ with*

$$\lambda_1 \rightarrow \frac{2^{\alpha+1} - 5}{2^{\alpha+1} - 3} \quad \text{and} \quad \lambda_2 \rightarrow 2 \quad \text{as} \quad c \rightarrow 1.$$

Moreover, $\lambda_2 < 2$, whereas $\lambda_1 < 0$ if $\alpha \in (\alpha_0, \alpha_1)$ and $\lambda_1 \in (0, 1)$ if $\alpha > \alpha_1$.

Proof. It follows from (4.5) that for every $c \in (1, 2^\alpha)$, the operator $\tilde{\mathcal{L}}_{c,\alpha}$ in L^2_{per} is invertible and

$$\sigma(\tilde{\mathcal{L}}_{c,\alpha}^{-1}) = \{(|n|^\alpha - c)^{-1}, \quad n \in \mathbb{Z}\}.$$

Since the sequence of eigenvalues is squared summable if $\alpha > 1/2$, the linear bounded operator $\tilde{\mathcal{L}}_{c,\alpha}^{-1}$ is of the Hilbert-Schmidt class (see Example 2 in Section 5.16 of [94]), hence it is compact. The linear operator $\tilde{\mathcal{L}}_T$ in L^2_{per} is a composition of a bounded operator $2\phi \cdot$ and a compact (Hilbert-Schmidt) operator $\tilde{\mathcal{L}}_{c,\alpha}^{-1}$, hence $\tilde{\mathcal{L}}_T$ is a compact operator and $\sigma(\tilde{\mathcal{L}}_T)$ in L^2_{per} consists of a sequence of eigenvalues converging to 0. Thanks to the representation (4.9), $\sigma(\tilde{\mathcal{L}}_{c,\alpha}^{-1}\tilde{\mathcal{H}}_{c,\alpha})$ in L^2_{per} consists of a sequence of eigenvalues converging to 1.

Eigenvalues $\{-1, 0\}$ of $\tilde{\mathcal{L}}_{c,\alpha}^{-1}\tilde{\mathcal{H}}_{c,\alpha}$ in L^2_{per} follow from exact computations for every $c > 1$:

$$\tilde{\mathcal{L}}_{c,\alpha}^{-1}\tilde{\mathcal{H}}_{c,\alpha}\phi = -\phi \quad \text{and} \quad \tilde{\mathcal{L}}_{c,\alpha}^{-1}\tilde{\mathcal{H}}_{c,\alpha}\phi' = 0. \quad (4.30)$$

In order to identify other eigenvalues of $\tilde{\mathcal{L}}_{c,\alpha}^{-1}\tilde{\mathcal{H}}_{c,\alpha}$ in L^2_{per} , we consider the generalized eigenvalue problem (4.10) defined by linear operators $\tilde{\mathcal{L}}_{c,\alpha}$ and $\tilde{\mathcal{H}}_{c,\alpha}$ in L^2_{per} with the domains in H^α_{per} .

Since $\tilde{\mathcal{H}}_{c=1,\alpha}$ coincides with $\tilde{\mathcal{L}}_{c=1,\alpha}$, the generalized eigenvalue problem (4.10) for $c = 1$ admits only one solution $\lambda = 1$ for every $v \in H^\alpha_{\text{per}} \setminus \{e^{ix}, e^{-ix}\}$. Since (ϕ, c) depend analytically on a in Theorem 3.1, by the analytic perturbation theory (Theorem VII.1.7 in [57]), the eigenvalues of $\tilde{\mathcal{L}}_{c,\alpha}^{-1}\tilde{\mathcal{H}}_{c,\alpha}$ in L^2_{per} for every $c > 1$ are divided into two sets: a countable sequence of eigenvalues near 1 and converging to 1 related to the subspace $L^2_{\text{per}} \setminus \{e^{ix}, e^{-ix}\}$ and a finite number of eigenvalues related to the subspace $\{e^{ix}, e^{-ix}\}$. The second set includes eigenvalues $\{-1, 0\}$ due to the exact solutions (4.30) for every $c > 1$. The subspace $\{e^{ix}, e^{-ix}\}$ may be related to more than two simple eigenvalues in the generalized eigenvalue problem (4.10) because both $\tilde{\mathcal{H}}_{c=1,\alpha}$ and $\tilde{\mathcal{L}}_{c=1,\alpha}$ vanish on the subspace.

In order to study all possible eigenvalues of $\tilde{\mathcal{L}}_{c,\alpha}^{-1}\tilde{\mathcal{H}}_{c,\alpha}$ in L^2_{per} related to the subspace $\{e^{ix}, e^{-ix}\}$, we perform perturbation expansions. Since $\tilde{\mathcal{L}}_{c,\alpha}$ and $\tilde{\mathcal{H}}_{c,\alpha}$ are closed in the subspaces of even and odd functions in L^2_{per} , the generalized

eigenvalue problem (4.10) can be uncoupled in these subspaces. By using (5.15) and (3.25), we rewrite the generalized eigenvalue problem (4.10) in the perturbed form:

$$(\lambda - 1) [1 - D^\alpha + c_2 a^2 + c_4 a^4 + \mathcal{O}(a^6)] v - 2 [a \cos(x) + a^2 \phi_2(x) + a^3 \phi_3(x) + a^4 \phi_4(x) + \mathcal{O}(a^5)] v = 0. \quad (4.31)$$

Assuming $\lambda \neq 1$, we are looking for perturbative expansions of the eigenvalues related to the even and odd subspace of $\{e^{ix}, e^{-ix}\}$ separately from each other. For the even subspace, we set

$$v(x) = \cos(x) + av_1(x) + a^2 v_2(x) + \mathcal{O}(a^3) \quad (4.32)$$

and obtain recursively

$$\begin{cases} \mathcal{O}(a) : & (\lambda - 1)(1 - D^\alpha)v_1 = 1 + \cos(2x), \\ \mathcal{O}(a^2) : & (\lambda - 1)(1 - D^\alpha)v_2 + (\lambda - 1)c_2 \cos(x) = 2 \cos(x)(v_1 + \phi_2). \end{cases}$$

At $\mathcal{O}(a)$, we obtain the exact solution in H_{per}^α :

$$v_1(x) = \frac{1}{\lambda - 1} \left[1 - \frac{\cos(2x)}{2^\alpha - 1} \right]. \quad (4.33)$$

The linear inhomogeneous equation at $\mathcal{O}(a^2)$ admits a solution $v_2 \in H_{\text{per}}^\alpha$ if and only if λ satisfies

$$\left[\lambda - \frac{2}{\lambda - 1} \right] c_2 = 0.$$

If $\alpha > \alpha_0$, then $c_2 \neq 0$ and λ satisfies the quadratic equation $\lambda(\lambda - 1) = 2$ with two roots $\{-1, 2\}$. For each of the two roots, we obtain the exact solution in H_{per}^α :

$$v_2(x) = \frac{(3 - \lambda) \cos(3x)}{2(\lambda - 1)^2(2^\alpha - 1)(3^\alpha - 1)}. \quad (4.34)$$

For the odd subspace, we set

$$v(x) = \sin(x) + av_1(x) + a^2 v_2(x) + \mathcal{O}(a^3) \quad (4.35)$$

and obtain recursively

$$\begin{cases} \mathcal{O}(a) : & (\lambda - 1)(1 - D^\alpha)v_1 = \sin(2x), \\ \mathcal{O}(a^2) : & (\lambda - 1)(1 - D^\alpha)v_2 + (\lambda - 1)c_2 \sin(x) = 2(\cos(x)v_1 + \sin(x)\phi_2). \end{cases}$$

At $\mathcal{O}(a)$, we obtain the exact solution in H_{per}^α :

$$v_1(x) = -\frac{\sin(2x)}{(\lambda - 1)(2^\alpha - 1)}. \quad (4.36)$$

The linear inhomogeneous equation at $\mathcal{O}(a^2)$ admits a solution $v_2 \in H_{\text{per}}^\alpha$ if and only if λ satisfies

$$\lambda c_2 + \frac{\lambda}{(\lambda - 1)(2^\alpha - 1)} = 0.$$

If $\alpha > \alpha_0$, then $c_2 \neq 0$ and λ satisfies the quadratic equation

$$\lambda [(2^{\alpha+1} - 3)\lambda - (2^{\alpha+1} - 5)] = 0$$

with two roots $\{0, \frac{2^{\alpha+1}-5}{2^{\alpha+1}-3}\}$. For each of the two roots, we obtain the exact solution in H_{per}^α :

$$v_2(x) = \frac{(3 - \lambda) \sin(3x)}{2(\lambda - 1)^2(2^\alpha - 1)(3^\alpha - 1)}. \quad (4.37)$$

Summarizing, we have obtained four eigenvalues related to the subspace $\{e^{ix}, e^{-ix}\}$, which are located as $c \rightarrow 1$ at the points $\{-1, 0, \frac{2^{\alpha+1}-5}{2^{\alpha+1}-3}, 2\}$.

The eigenvalues $\{-1, 0\}$ are preserved for every $c > 1$ thanks to the exact solution (4.30). However, the eigenvalues $\{\lambda_1, \lambda_2\}$ near $\{\frac{2^{\alpha+1}-5}{2^{\alpha+1}-3}, 2\}$ depend generally on c . It follows by the perturbation theory that $\lambda_1 < 0$ if $\alpha \in (\alpha_0, \alpha_1)$ and $\lambda_1 \in (0, 1)$ if $\alpha > \alpha_1$. We now claim that $\lambda_2 < 2$ if $\alpha > \alpha_0$ and $c > 1$. To prove this claim, we use the extended spectral problem (4.31) up to the order $\mathcal{O}(a^4)$. Hence, instead of the expansion (4.32) with (4.33) and (4.34), we use the expansions

$$\begin{cases} v(x) = \cos(x) + av_1(x) + a^2v_2(x) + a^3v_3(x) + a^4v_4(x) + \mathcal{O}(a^5), \\ \lambda = 2 + \Lambda_2 a^2 + \mathcal{O}(a^4), \end{cases} \quad (4.38)$$

where

$$v_1(x) = 1 - \frac{\cos(2x)}{2^\alpha - 1}, \quad v_2(x) = \frac{\cos(3x)}{2(2^\alpha - 1)(3^\alpha - 1)}.$$

We obtain from the extended spectral problem (4.31) the linear inhomogeneous equations:

$$\begin{cases} \mathcal{O}(a^3): & (1 - D^\alpha)v_3 + \Lambda_2(1 - D^\alpha)v_1 + c_2v_1 = 2[\cos(x)(v_2 + \phi_3) + \phi_2v_1], \\ \mathcal{O}(a^4): & (1 - D^\alpha)v_4 + \Lambda_2(1 - D^\alpha)v_2 + c_2v_2 + (c_4 + c_2\Lambda_2)\cos(x) \\ & = 2[\cos(x)(v_3 + \phi_4) + \phi_2v_2 + \phi_3v_1]. \end{cases}$$

The linear inhomogeneous equation at $\mathcal{O}(a^3)$ admits the explicit solution:

$$\begin{aligned} v_3(x) &= \frac{3^\alpha - 2^{\alpha+1} + 1}{2(2^\alpha - 1)^2(3^\alpha - 1)(4^\alpha - 1)} \cos(4x) \\ &+ \left[\frac{\Lambda_2}{2^\alpha - 1} - \frac{1 + (2 + c_2)(3^\alpha - 1)}{(2^\alpha - 1)^2(3^\alpha - 1)} \right] \cos(2x) \\ &- \left(\Lambda_2 + c_2 + 1 + \frac{1}{2(2^\alpha - 1)^2} \right). \end{aligned}$$

The linear inhomogeneous equation at $\mathcal{O}(a^4)$ admits a solution $v_4 \in H_{\text{per}}^\alpha$ if and only if Λ_2 is given by

$$\Lambda_2 = -1 + \frac{3}{2^\alpha - 1} - \frac{7}{2^{\alpha+1} - 3}. \quad (4.39)$$

It is easy to see that Λ_2 has a vertical asymptote at $\alpha = \alpha_0$. By plotting Λ_2 versus α on Figure 4.1, we verify that $\Lambda_2 < 0$ for every $\alpha > \alpha_0$. Hence, the eigenvalue $\lambda = 2 + \Lambda_2 a^2 + \mathcal{O}(a^4)$ satisfies $\lambda < 2$ for every $\alpha > \alpha_0$. \square

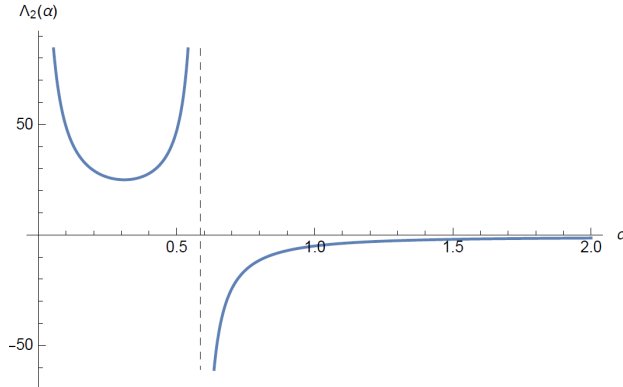


Figure 4.1: Plot of Λ_2 versus α .

The following Corollary describes the range of α for which the operator $\tilde{\mathcal{L}}_T$ is the strict contraction in the constrained space L_c^2 defined in (4.7), and thus determines the convergence of the iteration (4.3).

Corollary 4.1. *For every $c \in (1, c_0)$ in Lemma 4.1, the iterative method (4.3) converges to ϕ in H_{per}^α if $\alpha > \alpha_1$ and diverges from ϕ if $\alpha \in (\alpha_0, \alpha_1)$.*

Proof. If $\alpha > \alpha_1$, then $\lambda_1 \in (0, 1)$ by Lemma 4.1. By using the representation (4.9) and the count of eigenvalues of the generalized eigenvalue problem (4.10) in Lemma 4.1, we can see that $\sigma(\tilde{\mathcal{L}}_T)$ in L_{per}^2 consists of a countable sequence of eigenvalues in a neighborhood of 0 and converging to 0, two simple eigenvalues

inside the interval $(-1, 1)$, and two additional simple eigenvalues: 1 related to the eigenfunction ϕ' and 2 related to the eigenfunction ϕ . The two constraints in (4.7) remove the latter two eigenvalues so that the operator $\tilde{\mathcal{L}}_T$ is a strict contraction in L_c^2 for every $c \in (1, c_0)$ if $\alpha > \alpha_1$. Convergence of the iterative method (4.3) for $\alpha > \alpha_1$ follows by Theorem 4.1.

If $\alpha \in (\alpha_0, \alpha_1)$, then $\lambda_1 < 0$ by Lemma 4.1. Then, $\sigma(\tilde{\mathcal{L}}_T)$ in L_{per}^2 consists of a countable sequence of eigenvalues in a neighborhood of 0 and converging to 0, one simple eigenvalue inside the interval $(-1, 1)$, simple eigenvalue 1 related to the eigenfunction ϕ' , simple eigenvalue 2 related to the eigenfunction ϕ , and an additional simple eigenvalue bigger than 1 with an odd eigenfunction denoted by v_* . Because of the orthogonality conditions

$$\langle \tilde{\mathcal{L}}_{c,\alpha} v_j, v_k \rangle = 0, \quad j \neq k,$$

between eigenfunctions v_j and v_k of the generalized eigenvalue problem (4.10) for distinct eigenvalues, we verify that $\langle \phi^2, v_* \rangle = \langle \phi\phi', v_* \rangle = 0$, which implies that $v_* \in L_c^2$. Therefore, $\sigma(\tilde{\mathcal{L}}_T)$ in L_c^2 contains exactly one eigenvalue outside the unit disk for every $c \in (1, c_0)$ if $\alpha \in (\alpha_0, \alpha_1)$. Divergence of the iterative method (4.3) for $\alpha \in (\alpha_0, \alpha_1)$ follows by Theorem 4.1. \square

Remark 4.6. *Since the unstable eigenfunction v_* is odd, divergence of the iterative method (4.3) for $\alpha \in (\alpha_0, \alpha_1)$ is only observed if the initial guess $w_0 \in H_{\text{per}}^\alpha$ is not even but of a general form.*

4.4 Proof of Theorem 4.3

The proof of Theorem 4.3 is achieved from Lemma 4.2 and Corollary 4.2. In Lemma 4.2, we prove that the spectrum of the operator $\mathcal{L}_{c,\alpha}^{-1} \mathcal{H}_{c,\alpha}$ is confined in the unit disk for every $c > 1$. Then, Corollary 4.2 concludes that the operator \mathcal{L}_T is a strict contraction in the constrained space (4.13) and thus the iteration (4.11) converges to the single-lobe solution ψ of the boundary value problem (4.2).

Lemma 4.2. *For every $c > 1$ and $\alpha \in (\alpha_0, 2]$, $\sigma(\mathcal{L}_{c,\alpha}^{-1} \mathcal{H}_{c,\alpha}) \in (0, 1)$ in L_c^2 .*

Proof. We note that $\mathcal{L}_{c,\alpha}$ is positive for every $c > 1$ and $\alpha > 0$, whereas, by assumption given in Theorem 3.3, the operator $\mathcal{H}_{c,\alpha}$ has one simple negative eigenvalue and a simple zero eigenvalue for every $c > 1$ and $\alpha \in (\alpha_0, 2]$.

By Theorem 1 in [28], $\sigma(\mathcal{L}_{c,\alpha}^{-1} \mathcal{H}_{c,\alpha})$ in L_{per}^2 is real and contains one simple negative eigenvalue and a simple zero eigenvalue, the rest of the spectrum is positive and bounded away from zero. The negative and zero eigenvalues correspond to the exact solutions:

$$\mathcal{L}_{c,\alpha}^{-1} \mathcal{H}_{c,\alpha} \psi = -\psi \quad \text{and} \quad \mathcal{L}_{c,\alpha}^{-1} \mathcal{H}_{c,\alpha} \psi' = 0. \quad (4.40)$$

These eigenvalues are removed by adding two constraints in the definition of L_c^2 in (4.7). The positive eigenvalues are bounded from above by 1 because the operator

$$\mathcal{L}_T = \mathcal{L}_{c,\alpha}^{-1}(2\psi\cdot) = Id - \mathcal{L}_{c,\alpha}^{-1}\mathcal{H}_{c,\alpha}$$

is strictly positive due to positivity of $\mathcal{L}_{c,\alpha}$ and ψ . Hence, $\sigma(\mathcal{L}_{c,\alpha}^{-1}\mathcal{H}_{c,\alpha}) \in (0, 1)$ in L_c^2 . \square

Corollary 4.2. *For every $c > 1$ and $\alpha \in (\alpha_0, 2]$, the iterative method (4.11) converges to ψ in H_{per}^α .*

Proof. As mentioned in Remark 4.2, conditions $\int_{-\pi}^\pi \psi^3 dx > 0$ and $\int_{-\pi}^\pi \psi(\psi')^2 dx > 0$ follow by positivity of ψ in Theorem 3.3. By Lemma 4.2, the operator \mathcal{L}_T is a strict contraction in L_c^2 for every $c > 1$ and $\alpha \in (\alpha_0, 2]$. Convergence of the iterative method (4.11) follows by Theorem 4.1. \square

4.5 Numerical Illustrations

Here we address numerically convergence of the iterative method (4.3) and (4.11) near the single-lobe periodic wave for $c \in (1, 2^\alpha)$. For simplicity of computations, we only consider the classical KdV and BO equations.

4.5.1 Iteration (4.3)

In the case of the KdV equation with $\alpha = 2$, the following numerical results illustrate the convergence of the method for $c \in (1, c_0)$ with $c_0 \approx 2.3$ in agreement with Corollary 4.1, the transition to instability at $c = c_0$, and the divergence for $c \in (c_0, 4)$.

Figure 4.2 shows eigenvalues of the generalized eigenvalue problem (4.10) computed numerically with the Fourier method for $c \in (1, 4)$. Five largest and five smallest eigenvalues of the operator $\tilde{\mathcal{L}}_{c,\alpha}^{-1}\tilde{\mathcal{H}}_{c,\alpha}$ are shown on the left panel. In agreement with the result of Lemma 4.1, we observe eigenvalues λ near points $\{-1, 0, \frac{3}{5}, 2\}$ in addition to a countable sequence of eigenvalues near 1. The right panel zooms in eigenvalues near $c = 1$ and shows the asymptotic approximation of the eigenvalue near 2 given by (4.38) and (4.39) with $\alpha = 2$. For $c_* \approx 1.2$, two real eigenvalues coalesce to create a pair of complex eigenvalues that exist for every $c > c_*$. Figure 4.3 shows that $|1 - \lambda|$ for the eigenvalues of \mathcal{L}_T remains inside the unit disk for $c \in (c_*, 4)$. Therefore, the complex eigenvalue pair does not introduce additional instability to the iterative method.

For $c \in (1, c_0)$ with $c_0 \approx 2.3$, the spectrum of $\tilde{\mathcal{L}}_T$ in L_c^2 remains inside the unit disk for $c \in (1, c_0)$. However, the largest eigenvalue of $\tilde{\mathcal{L}}_{c,\alpha}^{-1}\tilde{\mathcal{H}}_{c,\alpha}$ crosses the

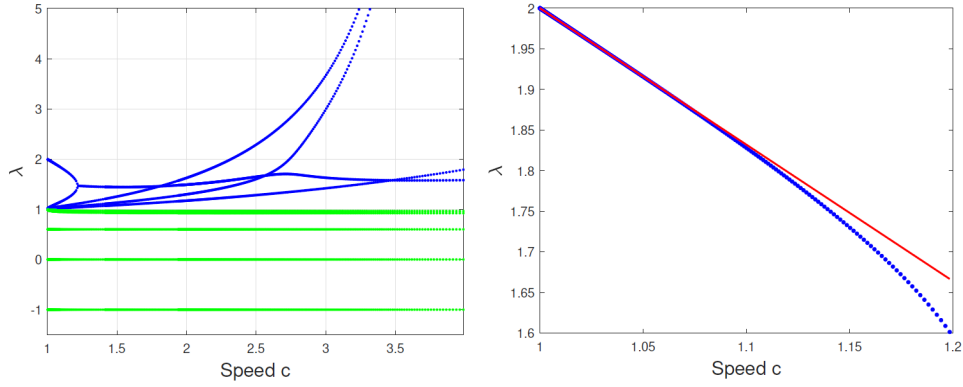


Figure 4.2: Left: Eigenvalues of the operator $\tilde{\mathcal{L}}_{c,\alpha}^{-1}\tilde{\mathcal{H}}_{c,\alpha}$ for $\alpha = 2$. The blue curves and green curves represent the five largest and five smallest eigenvalues respectively. Right: Zoom in with the asymptotic dependence given by (4.38) and (4.39).

level 2 for $c = c_0$ and the corresponding eigenvalue of $\tilde{\mathcal{L}}_T$ is smaller than -1 for $c \in (c_0, 4)$. This numerical result suggests that the iterative method (4.3) converges for $c \in (1, c_0)$ and diverge for $c \in (c_0, 4)$. Moreover, for $c_1 \approx 2.7$, the second largest eigenvalue of $\tilde{\mathcal{L}}_{c,\alpha}^{-1}\tilde{\mathcal{H}}_{c,\alpha}$ crosses the level 2, hence the iterative method (4.3) diverges with two unstable eigenvalues for $c \in (c_1, 4)$.

To illustrate convergence of the iterative method (4.3) for $\alpha = 2$, we use the initial function

$$u_0(x) = a \cos(x) + \frac{1}{2}a^2 (\cos(2x) - 3) + \varepsilon \sin(x), \quad (4.41)$$

where $a > 0$ and $\varepsilon \in \mathbb{R}$ are small parameters to our disposal. Notice that we include the $\mathcal{O}(a^2)$ correction term of the Stokes expansion (5.14) in the initial function (4.41) to avoid vanishing denominator in the Petviashvili quotient M defined by (4.4). Indeed, $\int_{-\pi}^{\pi} \cos(x)^3 dx = 0$, whereas $\int_{-\pi}^{\pi} \phi^3 dx < 0$ for every $c > 1$ and $\alpha = 2$, see Lemma B.1 Appendix B. Computations reported below correspond to $a = 0.4$ and $\varepsilon = 0$; we have checked that computations for other small values of a and ε return similar results. We measure the computational errors in three ways: the quantity $|1 - M_n|$, where $M_n = M(u_n)$, the distance between two successive approximations $\|u_{n+1} - u_n\|_{L^\infty}$, and the residual error $\|cu_n + u_n'' + u_n^2\|_{L^\infty}$. If iterations do not converge, we stop the algorithm after 500 iterations.

Figure 4.4 shows the profile of the last iteration and the three computational errors versus the number of iterations in the case $c = 2$. It is seen that the iterative method (4.3) converges to the single-lobe periodic wave, in agreement with Corollary 4.1. Since the exact periodic wave is known in (3.38)–(3.39), we can also compute the distance between the last iteration and

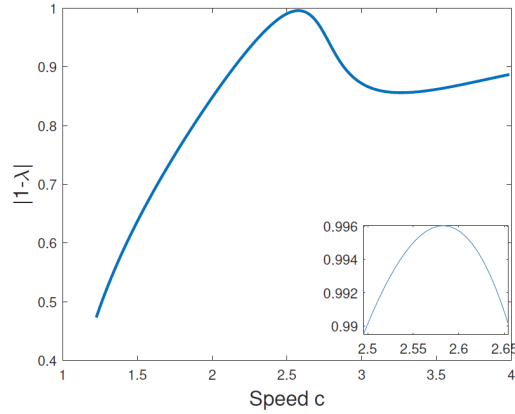


Figure 4.3: The plot of $|1 - \lambda|$ for the complex eigenvalues λ . The insert shows that the complex eigenvalues do not reach the boundary of the unit disk.

the exact solution, in which case we find $\|u - \phi\|_{L^\infty} \approx 2 \cdot 10^{-11}$. If $\varepsilon \neq 0$ in the initial function (4.41), the convergence to the periodic wave is still observed but the last iteration is shifted from $x = 0$, in agreement with Theorem 4.1.

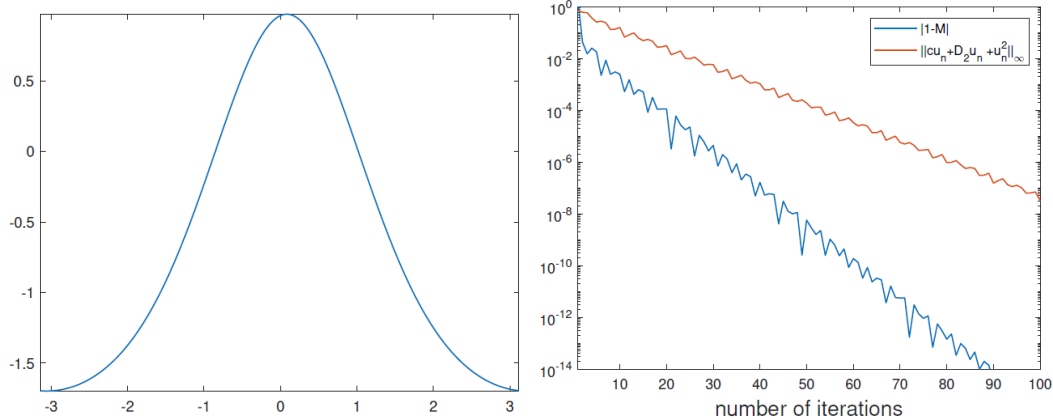


Figure 4.4: Iterations for $c = 2$ and $\alpha = 2$. (a) The last iteration versus x . (b) Computational errors versus n .

Figure 4.5 illustrates the case $c = 2.3$. Since the largest eigenvalue of $\tilde{\mathcal{L}}_{c,\alpha}^{-1} \tilde{\mathcal{H}}_{c,\alpha}$ crosses the level 2 at this value of c , see Figure 4.2, this case is marginal for convergence of iterations. As we can see from Figure 4.5, iterations still converge to a single-lobe periodic wave but the convergence is slow.

Figure 4.6 illustrates the case $c = 3$. The iterative method (4.3) diverges from the single-lobe periodic wave. The instability is related to the eigenvalue of \mathcal{L}_T which is smaller than -1 , hence the period-doubling instability leads to an alternating sequence which oscillates between two double-lobe profile

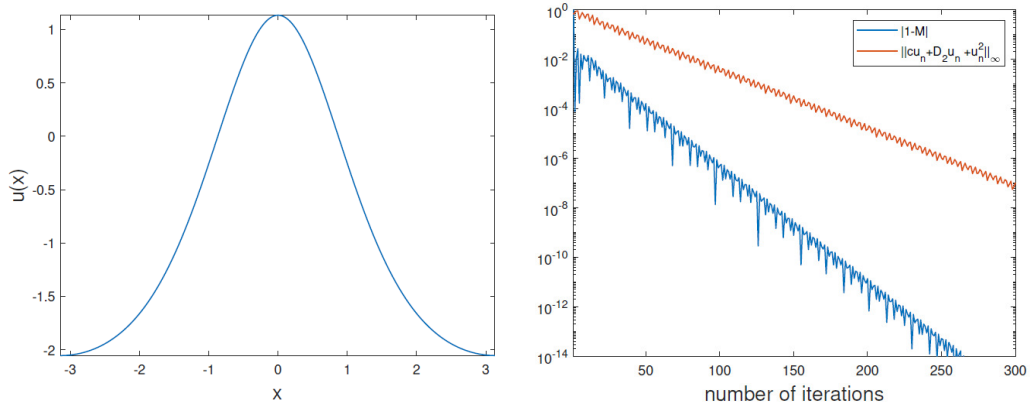


Figure 4.5: Iterations for $c = 2.3$ and $\alpha = 2$. (a) The last iteration versus x . (b) Computational errors versus n .

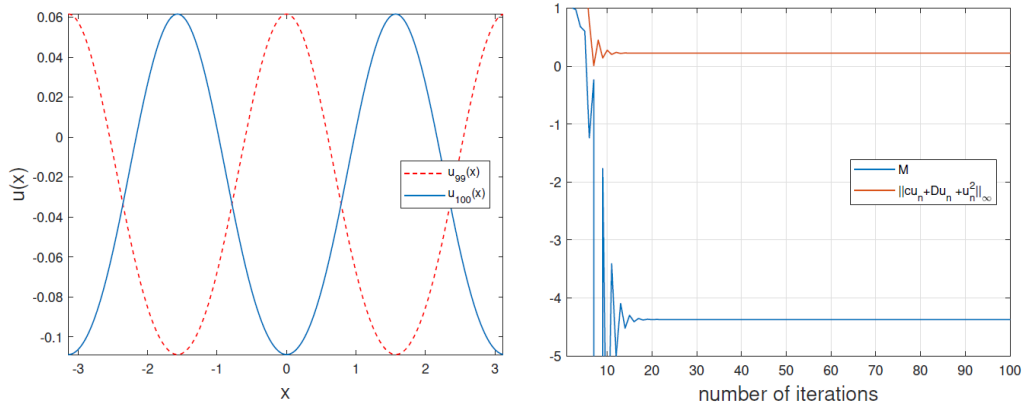


Figure 4.6: Iterations for $c = 3$ and $\alpha = 2$. (a) The last two iterations versus x . (b) Computational errors versus n .

shown on the left panel. The right panel shows that the factor M no longer converges to 1 but to -4.3737 and the residual errors does not converge to 0 but remains strictly positive with the number of iterations. Therefore, the two limiting states of the iterative method (4.3) in the 2-periodic orbit are not a periodic wave of the boundary-value problem (4.1).

In the case of BO equation with $\alpha = 1$, we show that the method diverges for $c \in (1, 2)$ in agreement with Corollary 4.1.

Figure 4.7 shows the eigenvalues of the generalized eigenvalue problem (4.10) for $\alpha = 1$. The eigenvalue $\lambda_1 = \frac{2^{\alpha+1}-5}{2^{\alpha+1}-3}$ in Lemma 4.1 yields $\lambda_1 = -1$ for $\alpha = 1$ in addition to the other eigenvalue -1 in $\{-1, 0, \lambda_1, \lambda_2\}$. Hence, $\lambda = -1$ is a double eigenvalue and the left panel shows that this double eigenvalue is preserved in c . The right panel zooms in eigenvalues near $c = 1$ and shows the asymptotic approximation of the eigenvalue near 2 given by (4.38) and (4.39)

with $\alpha = 1$.

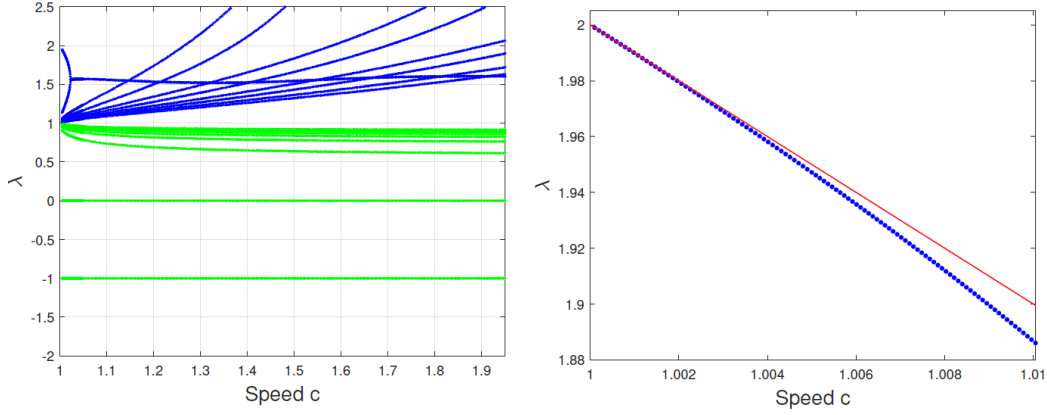


Figure 4.7: Left: Eigenvalues of the operator $\tilde{\mathcal{L}}_{c,\alpha}^{-1} \tilde{\mathcal{H}}_{c,\alpha}$ for $\alpha = 1$. Right: Zoom in with the asymptotic dependence given by (4.38) and (4.39).

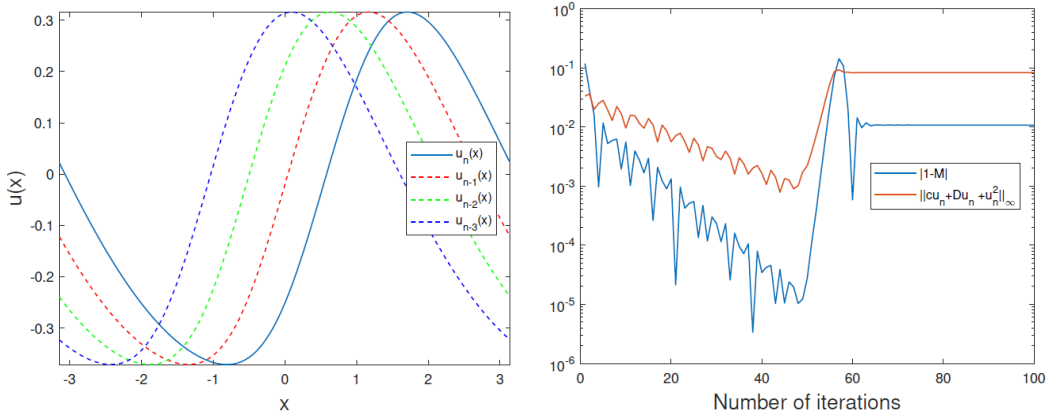


Figure 4.8: Iterations for $c = 1.1$ and $\alpha = 1$. (a) The last four iterations versus x . (b) Computational errors versus n .

To illustrate the divergence of the iterative method (4.3) for $\alpha = 1$, we use the initial function

$$u_0(x) = a \cos(x) + \frac{1}{2}a^2 (\cos(2x) - 1) + \varepsilon \sin(x), \quad (4.42)$$

where $a > 0$ and $\varepsilon \in \mathbb{R}$. We verify in Lemma B.2 in Appendix B that indeed, $\int_{-\pi}^{\pi} \phi^3 dx < 0$ for every $c > 1$ when $\alpha = 1$. We include the second term of the Stokes expansion (4.20) in the initial function (4.42) in order to ensure that $\int_{-\pi}^{\pi} u_0^3 dx < 0$. In computations below, we take $a = 0.4$.

As predicted by Corollary 4.1 for $\alpha = 1$, the iterative method (4.3) diverges

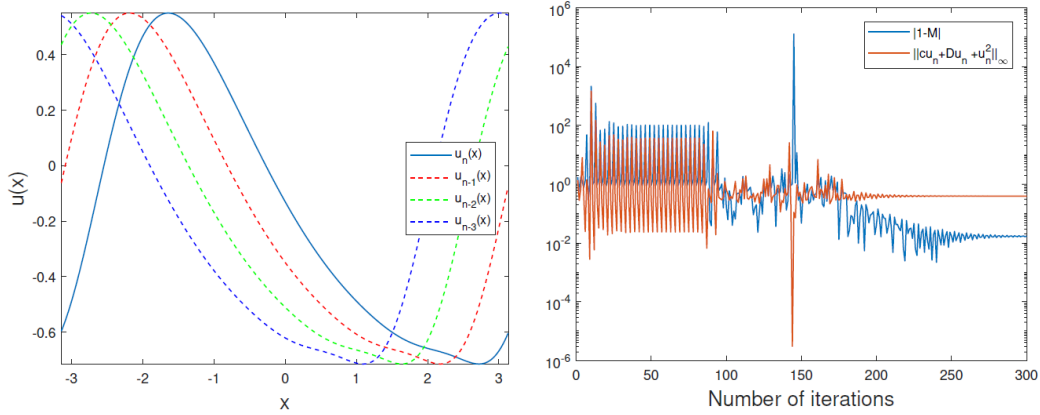


Figure 4.9: Iterations for $c = 1.3$ and $\alpha = 1$. (a) The last four iterations versus x . (b) Computational errors versus n .

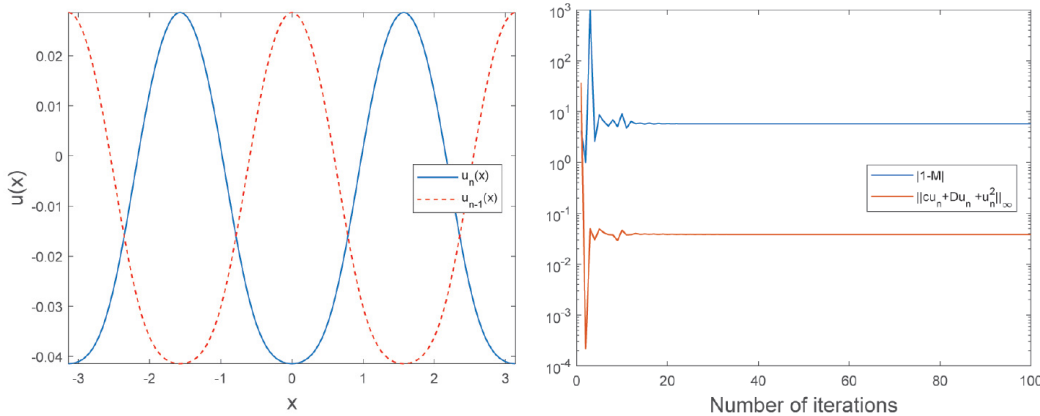


Figure 4.10: Iterations for $c = 1.6$ and $\alpha = 1$. (a) The last two iterations versus x . (b) Computational errors versus n .

for the BO equation and this divergence is due to an odd eigenfunction of the generalized eigenvalue problem (4.10) for the eigenvalue $\lambda_1 = -1$.

Figure 4.8 illustrates the case $c = 1.1$ showing the last four iterations in the left panel and the factor M converging to 1.0107 and the residual error converges to 0.0826 in the right panel. In this computation, we take $\varepsilon = 0$. Although the residual error starts to decrease initially due to contracting properties of $\tilde{\mathcal{L}}_T$ on the even subspace of L^2_{per} , round-off errors induce odd perturbations which result in slow instability. As a result, the periodic wave of amplitude 0.458 is not captured by the iterative method (4.3), instead iterations converge to the periodic profile of amplitude 0.344 which is drifted by every iteration to the right. This drifted periodic profile of the iterative method (4.3) is not a solution to the boundary-value problem (4.1). If $\varepsilon \neq 0$, the instability develops much faster and the drifted periodic profile is drifted

to the right if $\varepsilon > 0$ and to the left if $\varepsilon < 0$.

Figure 4.9 shows the marginal case $c = 1.3$ where another unstable eigenvalue of $\tilde{\mathcal{L}}_T$ related to the even eigenfunction crosses the level -1 . Although the instability pattern of Figure 4.8 is repeated on Figure 4.9, the periodic profile becomes more complicated and the instability process is accompanied by many intermediate oscillations. Here again we set $\varepsilon = 0$, if $\varepsilon \neq 0$, the drifted periodic profile is formed much faster and intermediate oscillations are reduced.

Figure 4.10 illustrates the case $c = 1.6$ when several eigenvalues of $\tilde{\mathcal{L}}_T$ are located below -1 . After short intermediate iterations, the iterative method starts to oscillate between two iterations, similarly to the pattern of Figure 4.6. The right panel of Figure 4.10 shows that the factor M converges to -5.1447 and the residual error remains strictly positive. The two limiting states of the iterative method (4.3) in the 2-periodic orbit are not a periodic wave of the boundary-value problem (4.1).

4.5.2 Iteration (4.11)

Finally, we demonstrate the convergence of the iterative method (4.11) using the initial condition

$$u_0(x) = c + a \cos(x)$$

with $a = 0.4$. This initial guess corresponds to the first two terms of the Stokes expansion (5.14) for $\psi(x) = c + \phi(x)$. We do not need to include the $\mathcal{O}(a^2)$ to the initial guess because $\int_{-\pi}^{\pi} u_0^3 dx > 0$ and the denominator of the Petviashvili quotient (4.12) does not vanish at u_0 .

Figure 4.11 shows the result of iterations for $c = 3$ and $\alpha = 2$. It is seen that iterations converge quickly to a positive, single-lobe periodic wave ψ in agreement with Corollary 4.2. Note that the iterative method (4.3) diverges for $c = 3$ and $\alpha = 2$, as is seen from Figure 4.6. We can also compute the distance between the last iteration and the exact solution, in which case we find $\|u - \phi\|_{L^\infty} \approx 1.3 \cdot 10^{-11}$.

Figure 4.12 reports similar results for $c = 1.6$ and $\alpha = 1$. Again, the iterative method (4.3) diverges for these values of c and α , as is seen from Figure 4.10. We can also compute the distance between the last iteration and the exact solution, in which case we find $\|u - \phi\|_{L^\infty} \approx 5.9 \cdot 10^{-11}$.

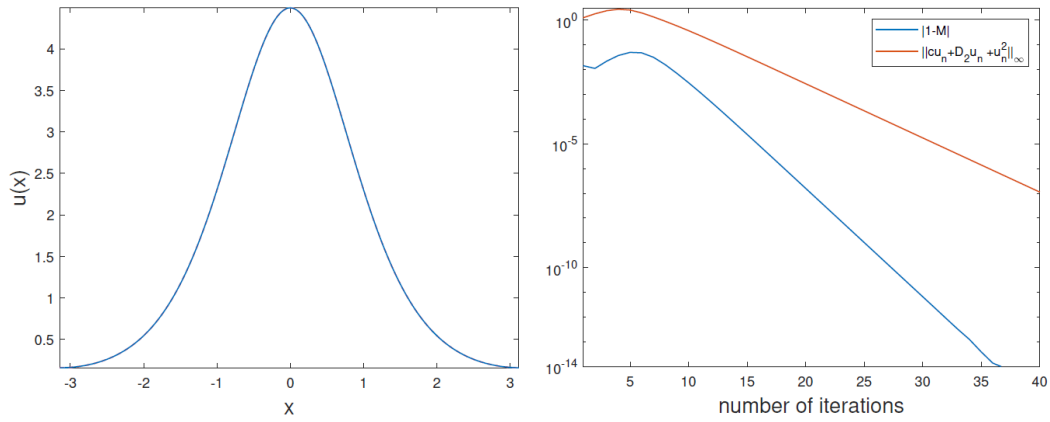


Figure 4.11: Iterations for $c = 3$ and $\alpha = 2$. (a) The last iteration versus x . (b) Computational errors versus n .

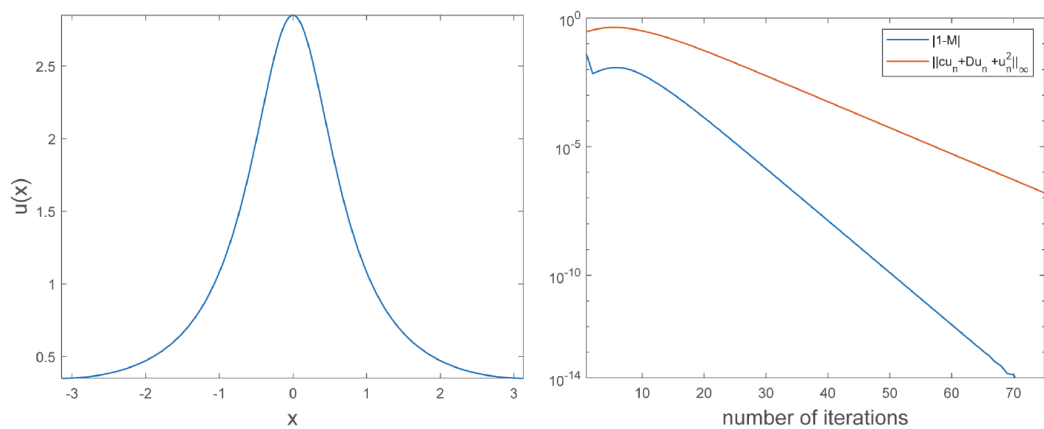


Figure 4.12: Iterations for $c = 1.6$ and $\alpha = 1$. (a) The last iteration versus x . (b) Computational errors versus n .

Chapter 5

Spectral Stability Of Periodic Waves In Fractional KdV Equation

The goal of this chapter is of twofold. First, we want to develop a new variational characterization for the periodic, travelling wave solutions of the fractional KdV equation (1.7) which allows us to determine the conditions with which the periodic solutions can be smoothly continued with respect to the Lagrange multipliers. Second, we wish to study the spectral stability of such waves according to definition 1.2.

Again, we recall the stationary equation of the fractional KdV equation (1.7) when $p = 1$

$$D^\alpha \varphi + c\varphi - \varphi^2 + b = 0, \quad (5.1)$$

where b is another real constant obtained from integrating equation (1.7) in x . If we require that $\varphi(x) : \mathbb{T} \rightarrow \mathbb{R}$ be a periodic function with the zero mean value, then $b = b(c)$ is defined at an admissible solution φ by

$$b(c) := \frac{1}{2\pi} \int_{-\pi}^{\pi} \varphi^2 dx. \quad (5.2)$$

The solution φ also depends on the speed parameter c but we often omit explicit reference to this dependence for notational simplicity. The momentum $F(u)$ (1.11) and mass $M(u)$ (1.10) computed at the solution φ are given by

$$F(\varphi) = \pi b(c), \quad M(\varphi) = 0. \quad (5.3)$$

The relation (5.2) closes the stationary equation (5.1) as the boundary-value problem

$$D^\alpha \varphi + c\varphi = \Pi_0 \varphi^2, \quad \varphi \in H_{\text{per}}^\alpha, \quad (5.4)$$

where $\Pi_0 f := f - \frac{1}{2\pi} \int_{-\pi}^{\pi} f(x) dx$ is the projection operator to the closed subspace X_0 of periodic functions with zero mean

$$X_0 := \left\{ f \in L_{per}^2 : \int_{-\pi}^{\pi} f(x) dx = 0 \right\}.$$

By following the procedure outlined in Section 1.2, spectral stability of the periodic wave φ is determined by the spectrum of the linearized operator $\partial_x \mathcal{H}$ in L_{per}^2 in the sense of Definition 1.2.

5.1 Main Results

The following theorems present the main results of this chapter.

Theorem 5.1. *Fix $\alpha \in (\frac{1}{3}, 2]$. For every $c_0 \in (-1, \infty)$, there exists a solution to the boundary-value problem (5.4) with the even, single-lobe profile φ_0 , which is obtained from a constrained minimizer of the following variational problem:*

$$\inf_{u \in H_{per}^{\frac{\alpha}{2}}(\mathbb{T})} \left\{ \int_{-\pi}^{\pi} [(D^{\frac{\alpha}{2}} u)^2 + c_0 u^2] dx : \int_{-\pi}^{\pi} u^3 dx = 1, \int_{-\pi}^{\pi} u dx = 0 \right\}. \quad (5.5)$$

Remark 5.1. *In [48], the positive single-lobe periodic waves were constructed by minimizing the energy $E(u)$ subject to only one constraint of the fixed momentum $F(u)$. It was shown that for every $\alpha \in (\frac{1}{2}, 2]$ and for every positive value of the fixed momentum each such minimizer is degenerate only up to the translation symmetry and is spectrally stable. Compared to the variational method in [48], our method allows us (i) to construct all single-lobe periodic solutions of the stationary equation (5.1) on the (c, b) parameter plane, (ii) to extend the results for every $\alpha \in (\frac{1}{3}, 2]$, (iii) to filter out the constant solution from the single-lobe periodic solutions, (iv) to find more spectrally stable branches of local minimizers, and (v) to unfold the fold point in Definition 1.3.*

Theorem 5.2. *Fix $\alpha \in (\frac{1}{3}, 2]$. Let φ_0 be the even, single-lobe solution obtained from Theorem 5.1. Assuming that $\text{Ker}(\mathcal{H}|_{X_0}) = \text{span}(\partial_x \varphi_0)$ for the linearized operator \mathcal{H} at φ_0 , there exists a C^1 mapping $c \mapsto \varphi(\cdot, c) \in H_{per}^{\alpha}$ in a local neighborhood of c_0 such that $\varphi(\cdot, c_0) = \varphi_0$ and the spectrum of \mathcal{H} in L_{per}^2 includes*

- a simple negative eigenvalue and a simple zero eigenvalue if $c_0 + 2b'(c_0) > 0$,
- a simple negative eigenvalue and a double zero eigenvalue if $c_0 + 2b'(c_0) = 0$,

- two negative eigenvalues and a simple zero eigenvalue if $c_0 + 2b'(c_0) < 0$.

Theorem 5.3. *Under the same assumption as Theorem 5.2, the periodic wave with profile φ is spectrally stable if $b'(c) \geq 0$ and is spectrally unstable with exactly one unstable (real, positive) eigenvalue of $\partial_x \mathcal{H}$ in L^2_{per} if $b'(c) < 0$.*

Remark 5.2. *Thanks to the correspondence $F(\varphi) = \pi b(c)$ in (5.3), the spectral stability result reproduces the criterion for stability of solitary waves [56, 66, 80, ?bona2]. Note that this scalar criterion, obtained from the new variational characterization of periodic waves in Theorem 5.1, replaces computations of a 2×2 matrix needed to establish if the periodic wave is a constrained minimizer of energy subject to fixed momentum and mass as in [53]. In particular, the sharp criterion based on the sign of $b'(c_0)$ works equally well in the cases when the linearized operator \mathcal{H} has one or two negative eigenvalues, see Remark 5.11.*

Remark 5.3. *If $b'(c_0) > 0$ and the periodic wave with profile φ_0 is spectrally stable, then it is also orbitally stable in $H^{\frac{\alpha}{2}}_{\text{per}}$ according to the standard technique from [9], assuming global well-posedness of the fractional KdV equation (1.7) in H^s_{per} for $s > \frac{\alpha}{2}$. For such results on the orbital stability of the periodic wave, we do not need to use the non-degeneracy assumption on the 2-by-2 matrix of derivatives of momentum $F(\varphi)$ and mass $M(\varphi)$ with respect to parameters c and b stated in Theorem 4.1 in [53].*

5.2 Proof of Theorem 5.1

In this section, we obtain solutions to the boundary-value problem (5.4) for $\alpha > \frac{1}{3}$. These solutions have an even, single-lobe profile φ in the sense of Definition 1.1 for $\alpha \leq 2$. Compared to statement of Theorem 5.1, we use the general notation φ for the profile of the periodic wave satisfying the boundary-value problem (5.4) and c for the (fixed) wave speed. For every fixed $c \in (-1, \infty)$, the assertion of Theorem 5.1 is proven from Theorem 5.4, Corollary 5.1, and Proposition 5.1. First, in Theorem 5.4, we prove the existence of a minimizer of the following minimization problem

$$q_c = \inf_{u \in Y_0} \mathcal{B}_c(u), \quad \mathcal{B}_c(u) := \frac{1}{2} \int_{-\pi}^{\pi} [(D^{\frac{\alpha}{2}} u)^2 + cu^2] dx \quad (5.6)$$

in the constrained set

$$Y_0 := \left\{ u \in H^{\frac{\alpha}{2}}_{\text{per}}(\mathbb{T}) : \int_{-\pi}^{\pi} u^3 dx = 1, \quad \int_{-\pi}^{\pi} u dx = 0 \right\}. \quad (5.7)$$

Second, in Corollary 5.1, we use Lagrange multipliers to show that the Euler–Lagrange equation for (5.6) and (5.7) is equivalent to the stationary equation

(5.1). Third, by using bootstrapping argument similar to the one given in Step 4 of the proof of Theorem 3.3, we conclude that the solution φ of the minimization problem (5.6) is actually smooth in $H_{\text{per}}^\infty(\mathbb{R})$ so that it satisfies the boundary-value problem (5.4).

Theorem 5.4. *Fix $\alpha > \frac{1}{3}$. For every $c > -1$, there exists a ground state of the constrained minimization problem (5.6), that is, there exists $\phi \in Y_0$ satisfying*

$$\mathcal{B}_c(\phi) = \inf_{u \in Y_0} \mathcal{B}_c(u). \quad (5.8)$$

If $\alpha \leq 2$, the ground state has an even, single-lobe profile ϕ in the sense of Definition 1.1.

Proof. It follows that \mathcal{B}_c is a smooth functional bounded on $H_{\text{per}}^{\frac{\alpha}{2}}(\mathbb{T})$. Moreover, \mathcal{B}_c is proportional to the quadratic form of the operator $c + D^\alpha$ with the spectrum in L_{per}^2 given by $\{c + |m|^\alpha, m \in \mathbb{Z}\}$. Thanks to the zero-mass constraint in (5.7), for every $c > -1$, we have

$$\mathcal{B}_c(u) \geq \frac{1}{2}(c+1)\|u\|_{L_{\text{per}}^2}^2, \quad u \in Y_0, \quad (5.9)$$

and by the standard Gårding's inequality, for every $c > -1$ there exists $C > 0$ such that

$$\mathcal{B}_c(u) \geq C\|u\|_{H_{\text{per}}^{\frac{\alpha}{2}}}^2, \quad u \in Y_0.$$

Hence \mathcal{B}_c is equivalent to the squared norm in $H_{\text{per}}^{\frac{\alpha}{2}}(\mathbb{T})$ for functions in Y_0 , yielding $q_c \geq 0$ in (5.6). Let $\{u_n\}_{n \in \mathbb{N}}$ be a minimizing sequence for the constrained minimization problem (5.6), that is, a sequence in Y_0 satisfying

$$\mathcal{B}_c(u_n) \rightarrow q_c \quad \text{as } n \rightarrow \infty.$$

Since $\{u_n\}_{n \in \mathbb{N}}$ is bounded in $H_{\text{per}}^{\frac{\alpha}{2}}(\mathbb{T})$, there exists $\phi \in H_{\text{per}}^{\frac{\alpha}{2}}(\mathbb{T})$ such that, up to a subsequence,

$$u_n \rightharpoonup \phi \quad \text{in } H_{\text{per}}^{\frac{\alpha}{2}}(\mathbb{T}), \quad \text{as } n \rightarrow \infty.$$

For every $\alpha > \frac{1}{3}$, the energy space $H_{\text{per}}^{\frac{\alpha}{2}}(\mathbb{T})$ is compactly embedded in $L_{\text{per}}^3(\mathbb{T})$. Thus,

$$u_n \rightarrow \phi \quad \text{in } L_{\text{per}}^3, \quad \text{as } n \rightarrow \infty.$$

Using the estimate

$$\begin{aligned} \left| \int_{-\pi}^{\pi} (u_n^3 - \phi^3) dx \right| &\leq \int_{-\pi}^{\pi} |u_n^3 - \phi^3| dx \\ &\leq \left(\|\phi\|_{L_{\text{per}}^3}^2 + \|\phi\|_{L_{\text{per}}^3} \|u_n\|_{L_{\text{per}}^3} + \|u_n\|_{L_{\text{per}}^3}^2 \right) \|u_n - \phi\|_{L_{\text{per}}^3}, \end{aligned}$$

it follows that $\int_{-\pi}^{\pi} \phi^3 dx = 1$. By a similar argument, since $H_{\text{per}}^{\frac{\alpha}{2}}(\mathbb{T})$ is also compactly embedded in $L_{\text{per}}^1(\mathbb{T})$, it follows that $\int_{-\pi}^{\pi} \phi dx = 0$. Hence, $\phi \in Y_0$. Thanks to the weak lower semi-continuity of \mathcal{B}_c , we have

$$\mathcal{B}_c(\phi) \leq \liminf_{n \rightarrow \infty} \mathcal{B}(u_n) = q_c.$$

Therefore, $\mathcal{B}_c(\phi) = q_c$.

If $\alpha \in (0, 2]$, the symmetric decreasing rearrangements of u do not increase $\mathcal{B}_c(u)$ while leaving the constraints in Y_0 invariant thanks to the fractional Polya–Szegő inequality, see Lemma A.1 in [30]. As a result, the minimizer $\phi \in Y_0$ of $\mathcal{B}_c(u)$ must decrease away symmetrically from the maximum point. By the translational invariance, the maximum point can be placed at $x = 0$, which yields an even, single-lobe profile for ϕ . \square

Corollary 5.1. *For every $\alpha \in (\frac{1}{3}, 2]$, there exists a solution to the boundary-value problem (5.4) with an even, single-lobe profile φ .*

Proof. By Lagrange’s Multiplier Theorem, the constrained minimizer $\phi \in Y_0$ in Theorem 5.4 satisfies the stationary equation

$$D^\alpha \phi + c\phi = C_1 \phi^2 + C_2, \quad (5.10)$$

for some constants C_1 and C_2 . From the two constraints in Y_0 , we have

$$C_1 = 2\mathcal{B}_c(\phi), \quad C_2 = -\frac{1}{2\pi} \left(\int_{-\pi}^{\pi} \phi^2 dx \right) C_1, \quad (5.11)$$

The scaling transformation $\varphi = C_1 \phi$ maps the stationary equation (5.10) to the form (5.1) with $b = b(c)$ computed from φ by (5.2). \square

The following lemma states that the infimum q_c in (5.6) is continuous in c for $c > -1$ and that $q_c \rightarrow 0$ as $c \rightarrow -1$.

Lemma 5.1. *Let $\phi \in Y_0$ be the ground state of the constrained minimization problem (5.6) in Theorem 5.4 and $q_c = \mathcal{B}_c(\phi)$. Then q_c is continuous in c for $c > -1$ and $q_c \rightarrow 0$ as $c \rightarrow -1$.*

Proof. For a fixed $u \in Y_0$ and for every $c' > c > -1$, we have

$$0 \leq \mathcal{B}_{c'}(u) - \mathcal{B}_c(u) = \frac{1}{2}(c' - c)\|u\|_{L_{\text{per}}^2}^2 \leq \frac{c' - c}{c + 1}\mathcal{B}_c(u),$$

thanks to the bound (5.9). Let $\mathcal{B}_c(\phi) = q_c$ and $\mathcal{B}_{c'}(\phi') = q_{c'}$. Then, we have

$$q_{c'} - q_c = \mathcal{B}_{c'}(\phi') - \mathcal{B}_c(\phi') + \mathcal{B}_c(\phi') - \mathcal{B}_c(\phi) \geq \mathcal{B}_{c'}(\phi') - \mathcal{B}_c(\phi') \geq 0$$

and

$$q_{c'} - q_c = \mathcal{B}_{c'}(\phi') - \mathcal{B}_{c'}(\phi) + \mathcal{B}_{c'}(\phi) - \mathcal{B}_c(\phi) \leq \mathcal{B}_{c'}(\phi) - \mathcal{B}_c(\phi) \leq \frac{c' - c}{c + 1}\mathcal{B}_c(\phi).$$

From here, it is clear that $q_{c'} \rightarrow q_c$ as $c' \rightarrow c$, so that q_c is continuous in c for $c > -1$. It remains to show that $q_c \rightarrow 0$ as $c \rightarrow -1$. Consider the following family of two-mode functions in Y_0 :

$$u_\mu(x) = \mu \cos(x) + \frac{2}{3\pi\mu^2} \cos(2x), \quad \mu > 0,$$

which satisfy the constraints in (5.7). Substituting u_μ into $\mathcal{B}_c(u)$ yields

$$\mathcal{B}_c(u_\mu) = \frac{\pi}{2} \left[\mu^2(1 + c) + \frac{4}{9\pi^2\mu^4}(2^\alpha + c) \right] \geq \frac{3\pi(2^\alpha + c)^{\frac{1}{3}}(1 + c)^{2/3}}{2(3\pi)^{2/3}},$$

where the lower bound is found from the minimization of $\mathcal{B}_c(u_\mu)$ in μ . Therefore, we obtain

$$0 \leq q_c \leq \frac{3\pi(2^\alpha + c)^{\frac{1}{3}}(1 + c)^{2/3}}{2(3\pi)^{2/3}},$$

which shows that $q_c \rightarrow 0$ as $c \rightarrow -1$. \square

The following proposition ensures that φ is smooth in x and hence satisfies the boundary-value problem (5.4).

Proposition 5.1. *Assume that $\varphi \in H_{\text{per}}^{\frac{\alpha}{2}}(\mathbb{T})$ is a solution of the stationary equation (5.1) with $c > -1$ and $b = b(c)$ in the sense of distributions. Then $\varphi \in H_{\text{per}}^\infty(\mathbb{T})$.*

Proof. See Step 4 of the proof of Theorem 3.3 in Section 3.4. \square

We show next that the periodic waves of the boundary-value problem (5.4) with an even, single-lobe profile ψ in the sense of Definition 1.1 are given by the Stokes expansion for c near -1 . Because we reuse the method of Lyapunov–Schmidt reductions from [54], the results on the Stokes expansion of the periodic wave ψ are restricted to the values of $\alpha > \frac{1}{2}$.

The small-amplitude (Stokes) expansion for single-lobe periodic waves of the boundary-value problem (5.4) is constructed in three steps. First, we present *Galilean transformation* between solutions of the stationary equation (5.1). Second, we obtain Stokes expansion of the normalized stationary equation. Third, we transform the Stokes expansion of the normalized stationary equation back to the solutions of the boundary-value problem (5.4)

Proposition 5.2. *Let $\varphi \in H_{\text{per}}^\alpha$ be a solution to the stationary equation (5.1) with some (c, b) . Then,*

$$\psi := \varphi - \frac{1}{2} \left(c - \sqrt{c^2 + 4b} \right) \quad (5.12)$$

is a solution of the stationary equation

$$D^\alpha \psi + \omega \psi - \psi^2 = 0, \quad \psi \in H_{\text{per}}^\alpha, \quad (5.13)$$

with $\omega := \sqrt{c^2 + 4b}$.

Proof. The proof is given by direct substitution. \square

Proposition 5.3. *For every $\alpha > \frac{1}{2}$, there exists $a_0 > 0$ such that for every $a \in (0, a_0)$ there exists a locally unique, even, single-lobe solution φ of the stationary equation (5.13) in the sense of Definition 1.1. The pair $(\omega, \varphi) \in \mathbb{R} \times H_{\text{per}}^\alpha$ is smooth in a and is given by the following Stokes expansion:*

$$\psi(x) = 1 + a \cos(x) + a^2 \psi_2(x) + a^3 \psi_3(x) + \mathcal{O}(a^4), \quad (5.14)$$

and

$$\omega = 1 + \omega_2 a^2 + \mathcal{O}(a^4), \quad (5.15)$$

where the corrections terms are

$$\psi_2(x) = \omega_2 - \frac{1}{2} + \frac{1}{2(2^\alpha - 1)} \cos(2x), \quad (5.16)$$

$$\psi_3(x) = \frac{1}{2(2^\alpha - 1)(3^\alpha - 1)} \cos(3x). \quad (5.17)$$

$$\omega_2 = 1 - \frac{1}{2(2^\alpha - 1)}. \quad (5.18)$$

Proof. The proof is given by algorithmic computations similarly to the proof of Theorem 3.1 in Section 3.2. However, we note that in Theorem 3.1 the parameter b was set to be 0 whereas in this case we consider nonzero b . \square

Corollary 5.2. *For every $\alpha \in (\frac{1}{2}, 2]$, there exists $c_0 \in (-1, \infty)$ such that the solution of the boundary-value problem (5.4) for every $c \in (-1, c_0)$ with an*

even, single-lobe profile φ in Theorem 5.4 and Corollary 5.1 is given by the following Stokes expansion:

$$\varphi = a \cos(x) + \frac{a^2}{2(2^\alpha - 1)} \cos(2x) + \frac{a^3}{2(2^\alpha - 1)(3^\alpha - 1)} \cos(3x) + \mathcal{O}(a^4) \quad (5.19)$$

with parameters

$$c = -1 + \frac{1}{2(2^\alpha - 1)} a^2 + \mathcal{O}(a^4) \quad (5.20)$$

and

$$b(c) = \frac{1}{2} a^2 + \mathcal{O}(a^4). \quad (5.21)$$

Proof. We apply the Galilean transformation (5.12) of Proposition 5.2 to the Stokes expansion (5.14) and (5.15) in Proposition 5.3. Therefore, we define

$$\varphi = \Pi_0 \psi, \quad c = \omega - \frac{1}{\pi} \int_{-\pi}^{\pi} \psi dx, \quad b(c) = \frac{1}{4} (\omega^2 - c^2) \quad (5.22)$$

and obtain the Stokes expansion (5.19), (5.20), and (5.21) for solutions of the boundary-value problem (5.4).

It follows from (5.19) and (5.20) that $\|\varphi\|_{L^2_{\text{per}}} \rightarrow 0$ as $c \rightarrow -1$. Since the Stokes expansion (5.14) for the even, single-lobe solution φ is locally unique by Proposition 5.3 and $\mathcal{B}_c(\phi) \rightarrow 0$ as $c \rightarrow -1$ by Lemma 5.1 implies that $\|\varphi\|_{L^2_{\text{per}}} \rightarrow 0$ as $c \rightarrow -1$, the small-amplitude periodic wave (5.19) with an even, single-lobe profile φ coincides as $c \rightarrow -1$ with the family of minimizers in Theorem 5.4 and Corollary 5.1 given by $\varphi = 2\mathcal{B}_c(\phi)\phi$. \square

Remark 5.4. *It follows from (5.18) that $\omega_2 > 0$ if and only if $\alpha > \alpha_0$, where*

$$\alpha_0 := \frac{\log 3}{\log 2} - 1 \approx 0.585.$$

It follows from the expansions (5.19), (5.20), and (5.21) that the threshold α_0 does not show up in the Stokes expansion of the solution φ to the boundary-value problem (5.4).

5.3 Proof of Theorem 5.2

In order to prove Theorem 5.2, we first characterize the number and multiplicity of negative and zero eigenvalues of the linearized operator \mathcal{H} in L^2_{per} in Corollary 5.3. Because we use the oscillation theory from [53], the results on the smooth continuation of periodic waves with respect to wave speed c are limited to the interval $\alpha \in (\frac{1}{3}, 2]$ and to the periodic waves with an even, single-lobe profile φ .

Next, in Lemma 5.3 we find a sharp condition for the continuation of the zero-mean solution ψ of the boundary-value problem (5.4) as a smooth family with respect to the wave speed c in a local neighborhood of c_0 . Then, for each value of $c_0 \in (-1, \infty)$, for which the family is a C^1 function of c , we show in Lemma 5.4 that the number of negative eigenvalues of \mathcal{H} is characterized by the sign of $c_0 + 2b'(c_0)$. Moreover, \mathcal{H} has a double zero eigenvalue if $c_0 + 2b'(c_0) = 0$ and a simple zero eigenvalue if $c_0 + 2b'(c_0) \neq 0$. The assertion of Theorem 5.2 is proven from Lemma 5.3, Corollary 5.6, and Lemma 5.4.

Let $\varphi \in H_{\text{per}}^\infty$ be a solution to the boundary-value problem (5.4) for some $c \in (-1, \infty)$ obtained with Theorem 5.4, Corollary 5.1, and Proposition 5.1. The solution has an even, single-lobe profile φ in the sense of Definition 1.1. The linearized operator \mathcal{H} at φ is given by (1.15), which we rewrite again as the following self-adjoint operator:

$$\mathcal{H} = D^\alpha + c - 2\varphi : H_{\text{per}}^\alpha \subset L_{\text{per}}^2 \rightarrow L_{\text{per}}^2. \quad (5.23)$$

For continuation of the solution $\varphi \in H_{\text{per}}^\infty$ to the boundary-value problem (5.4) in c , we need to determine the multiplicity of the zero eigenvalue of \mathcal{H} denoted as $z(\mathcal{H})$. For spectral stability of the periodic wave φ , we also need to determine the number of negative eigenvalues of \mathcal{H} with the account of their multiplicities denoted as $n(\mathcal{H})$.

It follows by direct computations from the boundary-value problem (5.4) that

$$\mathcal{H}\varphi = -\varphi^2 - b(c) \quad (5.24)$$

and

$$\mathcal{H}1 = -2\varphi + c. \quad (5.25)$$

By the translational symmetry, we always have $\mathcal{H}\partial_x\varphi = 0$. However, the main question is whether $\text{Ker}(\mathcal{H}) = \text{span}(\partial_x\varphi)$, that is, if $z(\mathcal{H}) = 1$. The following corollary gives the count for zero eigenvalues and negative eigenvalues of operator \mathcal{H} .

Corollary 5.3. *Assume φ be an even, single-lobe periodic wave obtained with Theorem 5.4, Corollary 5.1, and Proposition 5.1 for $\alpha \in (\frac{1}{3}, 2]$ and $c \in (-1, \infty)$. Then, $n(\mathcal{H}) \in \{1, 2\}$ and $z(\mathcal{H}) \in \{1, 2\}$.*

Proof. It follows by (5.24) that

$$\langle \mathcal{H}\varphi, \varphi \rangle = - \int_{-\pi}^{\pi} \varphi^3 dx = -8\mathcal{B}_c(\phi)^3 < 0, \quad (5.26)$$

thanks to (5.7), (5.9), and (5.11). Therefore, $n(\mathcal{H}) \geq 1$. Thanks to the variational formulation (5.6)–(5.7) and Theorem 5.4, $\varphi \in H_{\text{per}}^\infty$ is a minimizer of $G(u)$ in (6.3) for every $c \in (-1, \infty)$ subject to two constraints in (5.7). Since \mathcal{H} is the Hessian operator for $G(u)$ in (1.15), we have

$$\mathcal{H}|_{\{1, \varphi^2\}^\perp} \geq 0. \quad (5.27)$$

By Courant’s Mini-Max Principle, $n(\mathcal{H}) \leq 2$, so that $n(\mathcal{H}) \in \{1, 2\}$ is proven.

Since φ is even, L_{per}^2 is decomposed into an orthogonal sum of an even and odd subspaces. By Proposition A.3, 0 is the lowest eigenvalue of \mathcal{H} in the subspace of odd functions in L_{per}^2 with the eigenfunction $\partial_x \varphi$ with a single node. Hence, $z(\mathcal{H}) \geq 1$. To determine the upper bound for $z(\mathcal{H})$, we rely on Proposition A.1 which concerns Sturm’s oscillation theory for fractional derivative operators developed in [53].

In the subspace of even functions in L_{per}^2 , the number of nodes is even. If $n(\mathcal{H}) = 1$, then 0 is the second eigenvalue of \mathcal{H} . By Proposition A.1, the corresponding even function may have at most two nodes, hence there may be at most one such eigenfunction of \mathcal{H} for the zero eigenvalue in the subspace of even functions in L_{per}^2 . If $n(\mathcal{H}) = 2$, then the second (negative) eigenvalue has an even eigenfunction with exactly two nodes, whereas 0 is the third eigenvalue of \mathcal{H} . According to Proposition A.1, the corresponding even function for the zero eigenvalue may have at most four nodes, hence there may be at most one such eigenfunction of \mathcal{H} in the subspace of even functions in L_{per}^2 . In both cases, $z(\mathcal{H}) \leq 2$, so that $z(\mathcal{H}) \in \{1, 2\}$ is proven. \square

The following lemma characterizes the kernel of $\mathcal{H}|_{X_0} = \Pi_0 \mathcal{H} \Pi_0$, where Π_0 is defined in (5.4) and $X_0 := \left\{ f \in L_{\text{per}}^2 : \int_{-\pi}^{\pi} f(x) dx = 0 \right\}$.

Lemma 5.2. *Assume $\alpha \in (\frac{1}{3}, 2]$ and $\varphi \in H_{\text{per}}^\infty$ be an even, single-lobe periodic wave. If there exists $f \in \text{Ker}(\mathcal{H}|_{X_0})$ such that $\langle f, \partial_x \varphi \rangle = 0$ and $f \neq 0$, then*

$$\text{Ker}(\mathcal{H}) = \text{span}(\partial_x \varphi), \quad \langle f, \varphi \rangle \neq 0, \quad \text{and} \quad \langle f, \varphi^2 \rangle = 0. \quad (5.28)$$

Proof. Since $f \in \text{Ker}(\mathcal{H}|_{X_0})$, then $\langle 1, f \rangle = 0$ and f satisfies

$$0 = \mathcal{H}|_{X_0} f = \mathcal{H}f + \frac{1}{\pi} \int_{-\pi}^{\pi} f \varphi dx. \quad (5.29)$$

Either $\langle f, \varphi \rangle = 0$ or $\langle f, \varphi \rangle \neq 0$.

Assume first that $\langle f, \varphi \rangle = 0$. It follows by (5.29) that $f \in \text{Ker}(\mathcal{H})$ and by equality (5.24), we have $\langle f, \varphi^2 \rangle = 0$. By Corollary 5.3, the kernel of \mathcal{H} can be at most two-dimensional, hence $\text{Ker}(\mathcal{H}) = \text{span}(\partial_x \varphi, f)$ and $\{1, \varphi, \varphi^2\} \in [\text{Ker}(\mathcal{H})]^\perp$. By Fredholm theorem for self-adjoint operator (5.23),

we have $\{1, \varphi, \varphi^2\} \in \text{Range}(\mathcal{H})$ and by Proposition A.2, $\text{Ker}(\mathcal{H}) = \text{span}(\partial_x \varphi)$ in contradiction to the conclusion that $f \in \text{Ker}(\mathcal{H})$. Therefore, assumption $\langle f, \varphi \rangle = 0$ leads to contradiction.

Assume now that $\langle f, \varphi \rangle \neq 0$. It follows by (5.29) that $1 \in \text{Range}(\mathcal{H})$. Then, by (5.24) and (5.25), we have $\varphi^2 \in \text{Range}(\mathcal{H})$ and $\varphi \in \text{Range}(\mathcal{H})$ respectively. In other words, $\{1, \varphi, \varphi^2\} \in \text{Range}(\mathcal{H})$ and by Proposition A.2, $\text{Ker}(\mathcal{H}) = \text{span}(\partial_x \varphi)$. In addition, by (5.24), we have

$$\langle f, \varphi^2 \rangle = -\langle f, \mathcal{H}\varphi \rangle = -\langle \mathcal{H}f, \varphi \rangle = \frac{1}{\pi} \langle f, \varphi \rangle \langle 1, \varphi \rangle = 0.$$

This yields (5.28). \square

Remark 5.5. *Proposition A.2 is Proposition 3.1 in [53] and is proven from the property $\{1, \varphi, \varphi^2\} \in \text{Range}(\mathcal{H})$ claimed in (L3) of Lemma 3.3 in [53]. The proof of (L3) relies on the smoothness of minimizers of energy $E(u)$ subject to fixed momentum $F(u)$ and mass $M(u)$ with respect to Lagrange multipliers c and b . Unfortunately, this smoothness cannot be taken as granted and may be false. Indeed, $\text{Ker}(\mathcal{H}) \neq \text{span}(\partial_x \varphi)$ for some periodic waves satisfying the stationary equation (5.1) for $\alpha < \alpha_0$ (see Corollary 5.6, Remark 5.9, and Remark 5.10).*

Corollary 5.4. *If f exists in Lemma 5.2, then $\text{Ker}(\mathcal{H}|_{X_0}) = \text{span}(\partial_x \varphi, f)$.*

Proof. Assume two orthogonal vectors $f_1, f_2 \in \text{Ker}(\mathcal{H}|_{X_0})$ such that $\langle f_{1,2}, \partial_x \varphi \rangle = 0$ and $f_{1,2} \neq 0$. Since $\langle f_{1,2}, \varphi \rangle \neq 0$, there exists a linear combination of f_1 and f_2 in $\text{Ker}(\mathcal{H})$ in contradiction with $\text{Ker}(\mathcal{H}) = \text{span}(\partial_x \varphi)$ in (5.28). \square

Corollary 5.5. $\text{Ker}(\mathcal{H}|_{X_0}) = \text{Ker}(\mathcal{H}|_{\{1, \varphi^2\}^\perp})$.

Proof. By using orthogonal projections, we write

$$\mathcal{H}|_{\{1, \varphi^2\}^\perp} f = \mathcal{H}f + \frac{1}{\pi} \int_{-\pi}^{\pi} f \varphi dx - \alpha \Pi_0 \varphi^2, \quad \alpha = \frac{\langle \mathcal{H}f, \Pi_0 \varphi^2 \rangle}{\langle \varphi^2, \Pi_0 \varphi^2 \rangle}, \quad (5.30)$$

where $\langle \varphi^2, \Pi_0 \varphi^2 \rangle = \|\varphi\|_{L^4}^4 - \frac{1}{2\pi} \|\varphi\|_{L^2}^2 > 0$ for every non-constant (single-lobe) φ .

By Lemma 5.2, if $f \in \text{Ker}(\mathcal{H}|_{X_0})$, then $\langle f, \varphi^2 \rangle = 0$. Since $\langle 1, \Pi_0 \varphi^2 \rangle = 0$, it follows from (5.29) and (5.30) that $f \in \text{Ker}(\mathcal{H}|_{\{1, \varphi^2\}^\perp})$.

In the opposite direction, assume that $f \in \text{Ker}(\mathcal{H}|_{\{1, \varphi^2\}^\perp})$, $\langle f, \partial_x \varphi \rangle = 0$, and $f \neq 0$. Since $\langle f, 1 \rangle = \langle f, \varphi^2 \rangle = 0$, we have by (5.24) that $0 = \langle f, \mathcal{H}\varphi \rangle = \langle \mathcal{H}f, \varphi \rangle = \alpha \langle \Pi_0 \varphi^2, \varphi \rangle$. Since $\langle \Pi_0 \varphi^2, \varphi \rangle = \langle \varphi^2, \varphi \rangle > 0$, thanks to (5.7), (5.9), and (5.11), we obtain $\alpha = 0$ which implies that $f \in \text{Ker}(\mathcal{H}|_{X_0})$. \square

The following lemma provides a sharp condition for a smooth continuation of the periodic wave with profile φ with respect to the wave speed c .

Lemma 5.3. *Assume $\alpha \in (\frac{1}{3}, 2]$ and φ_0 be an even, single-lobe solution of the boundary-value problem (5.4) for a fixed $c_0 \in (-1, \infty)$ obtained with Theorem 5.4, Corollary 5.1, and Proposition 5.1. Assume $\text{Ker}(\mathcal{H}|_{X_0}) = \text{span}(\partial_x \varphi_0)$. Then, there exists a unique continuation of even solutions of the boundary-value problem (5.4) in an open interval $\mathcal{I}_c \subset (-1, \infty)$ containing c_0 such that the mapping*

$$\mathcal{I}_c \ni c \mapsto \varphi(\cdot, c) \in H_{\text{per}}^\alpha(\mathbb{T}) \cap X_0 \quad (5.31)$$

is C^1 and $\varphi(\cdot, c_0) = \varphi_0$.

Proof. Let $\varphi_0 \in H_{\text{per}}^\alpha \cap X_0$ be an even, single-lobe solution of the boundary-value problem (5.4) for $c_0 \in (-1, \infty)$. Let $\varphi \in H_{\text{per}}^\alpha \cap X_0$ be a solution of the boundary-value problem (5.4) for $c \in (-1, \infty)$ to be constructed from φ_0 for c near c_0 . Then, $\tilde{\varphi} := \varphi - \varphi_0 \in H_{\text{per}}^\alpha \cap X_0$ satisfies the following equation:

$$\mathcal{H}_0|_{X_0} \tilde{\varphi} = -(c - c_0)(\varphi_0 + \tilde{\varphi}) + \Pi_0 \tilde{\varphi}^2, \quad (5.32)$$

where \mathcal{H}_0 is obtained from \mathcal{H} in (5.23) at $c = c_0$ and $\varphi = \varphi_0$, whereas $\mathcal{H}_0|_{X_0}$ acts on $\tilde{\varphi}$ by the same expressions as in (5.29).

Assume $\text{Ker}(\mathcal{H}_0|_{X_0}) = \text{span}(\partial_x \varphi_0)$ and consider the subspace of even functions for which φ_0 belongs. Then, $\mathcal{H}_0|_{X_0}$ is invertible on the subspace of even functions in $H_{\text{per}}^\alpha \cap X_0$ so that we can rewrite (5.32) as the fixed-point equation:

$$\tilde{\varphi} = -(c - c_0) (\mathcal{H}_0|_{X_0})^{-1} (\varphi_0 + \tilde{\varphi}) + (\mathcal{H}_0|_{X_0})^{-1} \Pi_0 \tilde{\varphi}^2. \quad (5.33)$$

By the Implicit Function Theorem, there exist an open interval containing c_0 , an open ball $B_r \in H_{\text{per}}^\alpha \cap X_0$ of radius $r > 0$ centered at 0, and a unique C^1 mapping $\mathcal{I}_c \ni c \mapsto \tilde{\varphi}(\cdot, c) \in B_r$ such that $\tilde{\varphi}(\cdot, c)$ is an even solution to the fixed-point equation (5.33) for every $c \in \mathcal{I}_c$ and $\tilde{\varphi}(\cdot, c_0) = 0$. In particular, we find that

$$\partial_c \varphi(\cdot, c_0) := \lim_{c \rightarrow c_0} \frac{\varphi - \varphi_0}{c - c_0} = -(\mathcal{H}_0|_{X_0})^{-1} \varphi_0. \quad (5.34)$$

Hence, $\varphi(\cdot, c)$ is an even solution of the boundary-value problem (5.4) for every $c \in \mathcal{I}_c$. \square

Remark 5.6. *Although the solution φ_0 is obtained from a global minimizer of the variational problem (5.6)–(5.7), the solution $\varphi(\cdot, c)$ in Lemma 5.3 is continued from the Euler–Lagrange equation (5.4). Therefore, even if the solution $\varphi(\cdot, c)$ is C^1 with respect to c in \mathcal{I}_c as in Lemma 5.3, this solution may not coincide with the global minimizer of \mathcal{B}_c in Y_0 for $c \neq c_0$, the existence of which is guaranteed by Theorem 5.4 for every $c \in (-1, \infty)$. For example, the solution may only be a local minimizer of \mathcal{B}_c in Y_0 for $c \neq c_0$ in \mathcal{I}_c . Similarly, we cannot guarantee that the solution $\varphi(\cdot, c)$ has a single-lobe profile for $c \neq c_0$.*

Remark 5.7. *In what follows, we again use the general notation φ for the*

solution to the boundary-value problem (5.4) and c for the (fixed) wave speed.

Corollary 5.6. *For every $c \in (-1, \infty)$ for which $\text{Ker}(\mathcal{H}|_{X_0}) = \text{span}(\partial_x \varphi)$, we have*

$$\mathcal{H}\partial_c \varphi = -\varphi - b'(c), \quad (5.35)$$

where $b'(c) = \frac{1}{\pi} \int_{-\pi}^{\pi} \varphi \partial_c \varphi dx$. If $c + 2b'(c) \neq 0$, then $\text{Ker}(\mathcal{H}) = \text{span}(\partial_x \varphi)$, whereas if $c + 2b'(c) = 0$, then $\text{Ker}(\mathcal{H}) = \text{span}(\partial_x \varphi, 1 - 2\partial_c \varphi)$.

Proof. By Lemma 5.3, equation (5.35) follows from (5.34) and the definition of $\mathcal{H}|_{X_0}$ in (5.29). The same equation can also be obtained by formal differentiation of the boundary-value problem (5.4) in c since φ and b are C^1 with respect to c . It follows from (5.25) and (5.35) that

$$\mathcal{H}(1 - 2\partial_c \varphi) = c + 2b'(c), \quad (5.36)$$

If $c + 2b'(c) = 0$, then $\text{Ker}(\mathcal{H}) = \text{span}(\partial_x \varphi, 1 - 2\partial_c \varphi)$ by Corollary 5.3. If $c + 2b'(c) \neq 0$, then $\{1, \varphi, \varphi^2\} \in \text{Range}(\mathcal{H})$ by (5.24), (5.25), and (5.35), so that $\text{Ker}(\mathcal{H}) = \text{span}(\partial_x \varphi)$ by Proposition A.2. \square

Remark 5.8. *It follows from (5.24) and (5.35) that*

$$-2\pi b(c) \langle \mathcal{H}\partial_c \varphi, \varphi \rangle = \langle \partial_c \varphi, \mathcal{H}\varphi \rangle = -\frac{2\pi}{3} \gamma'(c),$$

so that $\gamma'(c) = 3b(c) > 0$, where $\gamma(c) := \frac{1}{2\pi} \int_{-\pi}^{\pi} \varphi^3 dx$.

Remark 5.9. *If $c_0 + 2b'(c_0) = 0$ for some $c_0 \in (-1, \infty)$, then ψ and ω , which satisfy the stationary equation (5.13) after the Galilean transformation (5.12), are C^1 functions of c in \mathcal{I}_c but not C^1 functions of ω at $\omega_0 := \sqrt{c_0^2 + 4b(c_0)}$. Indeed, differentiating the relation $\omega^2 = c^2 + 4b(c)$ in c yields*

$$\omega \frac{d\omega}{dc} = c + 2b'(c),$$

so that $\frac{d\omega}{dc}|_{c=c_0} = 0$ and the C^1 mapping $\mathcal{I}_c \ni c \rightarrow \omega(c) \in \mathcal{I}_\omega$ is not invertible. Since the kernel of \mathcal{H} at φ_0 is two-dimensional, the solution φ_0 is at the fold point according to Definition 1.3. The fold point yields the fold bifurcation of the solution ψ with respect to parameter ω at ω_0 .

The following lemma provides the explicit count of the number of negative eigenvalues $n(\mathcal{H})$ and the multiplicity of the zero eigenvalue $z(\mathcal{H})$ for the linearized operator \mathcal{H} in (5.23).

Lemma 5.4. *Assume $\alpha \in (\frac{1}{3}, 2]$ and $\varphi \in H_{\text{per}}^\infty$ be an even, single-lobe periodic wave for $c \in (-1, \infty)$ in Lemma 5.3 with $\text{Ker}(\mathcal{H}|_{X_0}) = \text{span}(\partial_x \varphi)$. Then, we have*

$$z(\mathcal{H}) = \begin{cases} 1, & c + 2b'(c) \neq 0, \\ 2, & c + 2b'(c) = 0, \end{cases} \quad (5.37)$$

and

$$n(\mathcal{H}) = \begin{cases} 1, & c + 2b'(c) \geq 0, \\ 2, & c + 2b'(c) < 0. \end{cases} \quad (5.38)$$

Proof. Thanks to (5.27), we have $n(\mathcal{H}|_{\{1, \varphi^2\}^\perp}) = 0$. By Corollary 5.5 and the assumption $\text{Ker}(\mathcal{H}|_{X_0}) = \text{span}(\partial_x \varphi)$, we have $z(\mathcal{H}|_{\{1, \varphi^2\}^\perp}) = 1$. By Theorem 5.3.2 in [55] or Theorem A.3, we construct the following symmetric 2-by-2 matrix related to the two constraints in (5.27):

$$P(\lambda) := \begin{bmatrix} \langle (\mathcal{H} - \lambda I)^{-1} \varphi^2, \varphi^2 \rangle & \langle (\mathcal{H} - \lambda I)^{-1} \varphi^2, 1 \rangle \\ \langle (\mathcal{H} - \lambda I)^{-1} 1, \varphi^2 \rangle & \langle (\mathcal{H} - \lambda I)^{-1} 1, 1 \rangle \end{bmatrix}, \quad \lambda \notin \sigma(\mathcal{H}).$$

By Corollary 5.6, we can use equation (5.35) in addition to equations (5.24) and (5.25). Assuming $c + 2b'(c) \neq 0$, we compute at $\lambda = 0$:

$$\begin{aligned} \langle \mathcal{H}^{-1} 1, 1 \rangle &= \frac{\langle 1 - 2\partial_c \varphi, 1 \rangle}{c + 2b'(c)} = \frac{2\pi}{c + 2b'(c)}, \\ \langle \mathcal{H}^{-1} 1, \varphi^2 \rangle &= \frac{\langle 1 - 2\partial_c \varphi, \varphi^2 \rangle}{c + 2b'(c)} = \frac{2\pi}{c + 2b'(c)} \left[b(c) - \frac{2}{3} \gamma'(c) \right], \\ \langle \mathcal{H}^{-1} \varphi^2, 1 \rangle &= -\langle \varphi, 1 \rangle - b(c) \frac{\langle 1 - 2\partial_c \varphi, 1 \rangle}{c + 2b'(c)} = -\frac{2\pi b(c)}{c + 2b'(c)}, \\ \langle \mathcal{H}^{-1} \varphi^2, \varphi^2 \rangle &= -\langle \varphi, \varphi^2 \rangle - b(c) \frac{\langle 1 - 2\partial_c \varphi, \varphi^2 \rangle}{c + 2b'(c)} = -2\pi \gamma(c) - \frac{2\pi b(c)}{c + 2b'(c)} \left[b(c) - \frac{2}{3} \gamma'(c) \right], \end{aligned}$$

where $\gamma'(c) = 3b(c)$ holds by Remark 5.8. Therefore, the determinant of $P(0)$ for $c + 2b'(c) \neq 0$ is computed as follows:

$$\det P(0) = -\frac{4\pi^2 \gamma(c)}{c + 2b'(c)}. \quad (5.39)$$

Denote the number of negative and zero eigenvalues of $P(0)$ by n_0 and z_0 respectively. If $c + 2b'(c) = 0$, then $P(0)$ is singular, in which case denote the number of diverging eigenvalues of $P(\lambda)$ as $\lambda \rightarrow 0$ by z_∞ . By Theorem 4.1 in [79], we have the following identities:

$$\begin{cases} n(\mathcal{H}|_{\{1, \varphi^2\}^\perp}) = n(\mathcal{H}) - n_0 - z_0, \\ z(\mathcal{H}|_{\{1, \varphi^2\}^\perp}) = z(\mathcal{H}) + z_0 - z_\infty. \end{cases} \quad (5.40)$$

Since $\gamma(c) > 0$, it follows that $z_0 = 0$. Since $n(\mathcal{H}|_{\{1, \varphi^2\}^\perp}) = 0$ we have $n(\mathcal{H}) = n_0$ by (5.40). It follows from the determinant (5.39) that $n_0 = 1$ if $c + 2b'(c) > 0$ and $n_0 = 2$ if $c + 2b'(c) < 0$. This yields (5.38) for $c + 2b'(c) \neq 0$.

Since $z(\mathcal{H}|_{\{1, \varphi^2\}^\perp}) = 1$, we have $z(\mathcal{H}) = 1 + z_\infty$ by (5.40). If $c + 2b'(c) \neq 0$, then $z_\infty = 0$ so that $z(\mathcal{H}) = 1$. The determinant (5.39) implies that one eigenvalue of $P(\lambda)$ remains negative as $\lambda \rightarrow 0$, whereas the other eigenvalue of $P(\lambda)$ in the limit $\lambda \rightarrow 0$ jumps from positive side for $c + 2b'(c) > 0$ to the negative side for $c + 2b'(c) < 0$ through infinity at $c + 2b'(c) = 0$. Therefore, if $c + 2b'(c) = 0$, then $n_0 = 1$ and $z_\infty = 1$ so that $n(\mathcal{H}) = 1$ and $z(\mathcal{H}) = 2$. This yields (5.37) and (5.38) for $c + 2b'(c) = 0$. \square

Remark 5.10. *By Proposition 5.2, we have invariance of the linearized operator \mathcal{H} under the Galilean transformation (5.12):*

$$\mathcal{H} = D^\alpha + c - 2\varphi = D^\alpha + \omega - 2\psi. \quad (5.41)$$

By using (5.20) and (5.21), we compute the small-amplitude expansion

$$c + 2b'(c) = 2^{\alpha+1} - 3 + \mathcal{O}(a^2).$$

Hence, for $\alpha > \alpha_0$ and small $a \in (0, a_0)$, we have $c + 2b'(c) > 0$ so that $n(\mathcal{H}) = 1$ in agreement with Lemma 2.2 in [64], whereas for $\alpha < \alpha_0$ and small $a \in (0, a_0)$, we have $c + 2b'(c) < 0$ so that $n(\mathcal{H}) = 2$. In the continuation of the solution φ in a for $\alpha < \alpha_0$ by Corollary 5.2, there exists a fold point in the sense of Definition 1.3 for which $c + 2b'(c) = 0$, see Corollary 5.6 and Remark 5.9.

5.4 Proof of Theorem 5.3

Here we consider the spectral stability problem (1.18). We assume that $\varphi \in H_{\text{per}}^\infty$ is an even, single-lobe solution to the boundary-value problem (5.4) for some $c \in (-1, \infty)$ obtained with Theorem 5.4, Corollary 5.1, and Proposition 5.1. Since φ is smooth, the domain of $\partial_x \mathcal{H}$ in L_{per}^2 is $H_{\text{per}}^{1+\alpha}$.

If $\text{Ker}(\mathcal{H}|_{X_0}) = \text{span}(\partial_x \varphi)$, then $\varphi(\cdot, c)$ and $b(c)$ are C^1 functions in c by Lemma 5.3. Therefore, we can use the three equations (5.24), (5.25), and (5.35) for the range of \mathcal{H} . We can also use the count of $n(\mathcal{H})$ and $z(\mathcal{H})$ in Lemma 5.4.

It was shown in [36, 50] that the periodic wave φ is spectrally stable if it is a constrained minimizer of energy (1.12) under fixed momentum (1.11) and mass (1.10). Since \mathcal{H} is the Hessian operator for the action functional $G(u)$ in (1.15), the spectral stability holds if

$$\mathcal{H}|_{\{1, \varphi\}^\perp} \geq 0. \quad (5.42)$$

On the other hand, the periodic wave φ is spectrally unstable with exactly one unstable (real, positive) eigenvalue of $\partial_x \mathcal{H}$ in L^2_{per} if $n(\mathcal{H}|_{\{1, \varphi\}^\perp}) = 1$.

By Theorem 5.3.2 in [55] or Theorem 4.1 in [79], we construct the following symmetric 2-by-2 matrix related to the two constraints in (5.42):

$$D(\lambda) := \begin{bmatrix} \langle (\mathcal{H} - \lambda I)^{-1} \varphi, \varphi \rangle & \langle (\mathcal{H} - \lambda I)^{-1} \varphi, 1 \rangle \\ \langle (\mathcal{H} - \lambda I)^{-1} 1, \varphi \rangle & \langle (\mathcal{H} - \lambda I)^{-1} 1, 1 \rangle \end{bmatrix}, \quad \lambda \notin \sigma(\mathcal{H}).$$

Assuming $c + 2b'(c) \neq 0$, we compute at $\lambda = 0$:

$$\begin{aligned} \langle \mathcal{H}^{-1} 1, 1 \rangle &= \frac{2\pi}{c + 2b'(c)}, \\ \langle \mathcal{H}^{-1} 1, \varphi \rangle &= -\frac{2\pi b'(c)}{c + 2b'(c)}, \\ \langle \mathcal{H}^{-1} \varphi, 1 \rangle &= -\frac{2\pi b'(c)}{c + 2b'(c)}, \\ \langle \mathcal{H}^{-1} \varphi, \varphi \rangle &= -\pi b'(c) + \frac{2\pi [b'(c)]^2}{c + 2b'(c)}. \end{aligned}$$

Therefore, the determinant of $D(0)$ for $c + 2b'(c) \neq 0$ is computed as follows:

$$\det D(0) = -\frac{2\pi^2 b'(c)}{c + 2b'(c)}. \quad (5.43)$$

Denote the number of negative and zero eigenvalues of $D(0)$ by n_0 and z_0 respectively. If $c + 2b'(c) = 0$, then $D(0)$ is singular, in which case denote the number of diverging eigenvalues of $D(\lambda)$ as $\lambda \rightarrow 0$ by z_∞ . By Theorem 4.1 in [79], we have the following identities:

$$\begin{cases} n(\mathcal{H}|_{\{1, \varphi\}^\perp}) = n(\mathcal{H}) - n_0 - z_0, \\ z(\mathcal{H}|_{\{1, \varphi\}^\perp}) = z(\mathcal{H}) + z_0 - z_\infty. \end{cases} \quad (5.44)$$

By Lemma 5.4, $n(\mathcal{H}) = 1$ if $c + 2b'(c) \geq 0$ and $n(\mathcal{H}) = 2$ if $c + 2b'(c) < 0$, whereas $z(\mathcal{H}) = 1$ if $c + 2b'(c) \neq 0$ and $z(\mathcal{H}) = 2$ if $c + 2b'(c) = 0$.

Assume first that $c + 2b'(c) \neq 0$ so that $z_\infty = 0$. If $b'(c) > 0$, then $z_0 = 0$ whereas $n_0 = 1$ if $c + 2b'(c) > 0$ and $n_0 = 2$ if $c + 2b'(c) < 0$. In both cases, it follows from (5.44) that $n(\mathcal{H}|_{\{1, \varphi\}^\perp}) = 0$ and $z(\mathcal{H}|_{\{1, \varphi\}^\perp}) = 1$ which implies spectral stability of φ .

If $b'(c) = 0$, then $z_0 = 1$ whereas $n_0 = 0$ if $c + 2b'(c) > 0$ and $n_0 = 1$ if $c + 2b'(c) < 0$. In both cases, it follows from (5.44) that $n(\mathcal{H}|_{\{1, \varphi\}^\perp}) = 0$ and $z(\mathcal{H}|_{\{1, \varphi\}^\perp}) = 2$, which still implies spectral stability of φ .

If $b'(c) < 0$, then $z_0 = 0$ whereas $n_0 = 0$ if $c + 2b'(c) > 0$ and $n_0 = 1$ if

$c + 2b'(c) < 0$. In both cases, it follows from (5.44) that $n(\mathcal{H}|_{\{1,\varphi\}^\perp}) = 1$ and $z(\mathcal{H}|_{\{1,\varphi\}^\perp}) = 1$, which implies spectral instability of φ .

If $c + 2b'(c) = 0$, then $z_\infty = 1$ and $z(\mathcal{H}) = 2$. Therefore, there is no change in the count compared to the previous cases.

Remark 5.11. *By using (5.20) and (5.21), we compute*

$$b'(c) = 2^\alpha - 1 + \mathcal{O}(a^2),$$

which shows that the small-amplitude periodic waves are spectrally stable for small a and $\alpha > 0$ thanks to Lemma 5.3. Since the fold point in the sense of Definition 1.3 exists for $\alpha < \alpha_0$, see Remark 5.10, the result of Lemma 5.3 shows spectral stability of the periodic waves across the fold point as long as $b'(c) > 0$.

5.5 Numerical Illustrations

Here, we illustrate the theoretical results by approximating the existence curve for the single-lobe periodic solutions of the boundary-value problem (5.4) on the parameter plane (c, b) for $\alpha \in (\frac{1}{3}, 2]$.

For the integrable BO equation ($\alpha = 1$), the single-lobe periodic solution to the boundary-value problem (5.13) is known in the exact form:

$$\omega = \coth \gamma, \quad \psi(x) = \frac{\sinh \gamma}{\cosh \gamma - \cos x}, \quad (5.45)$$

where $\gamma \in (0, \infty)$ is a free parameter of the solution. Since $\int_0^\pi \psi(x) dx = \pi$, we compute explicitly $c = \omega - 2$ and $b = \frac{1}{4}(\omega^2 - c^2) = \omega - 1$. Eliminating $\omega \in (1, \infty)$ yields $b(c) = c + 1$, shown on the left panel of Fig. 5.1.

In the right panel of Fig 5.1 we reproduce the existence curve but on the parameter plane (ω, μ) , where ω is the Lagrange multiplier in the boundary-value problem (5.13) and $\mu := \frac{1}{2\pi} \int_{-\pi}^\pi \psi^2 dx$ is the period-normalized momentum computed at the periodic wave ψ . The parameter (ω, μ) corresponds to the minimization of the energy $E(u)$ subject to the fixed momentum $F(u)$ with $a = 0$ used in [48].

There exists a constrained minimizer of energy for every $\mu > 0$ as in Theorem 1 in [48], however, it is given by the constant solution for $\mu \in (0, 1)$ and $\omega \in (0, 1)$ with the exact relation $\mu = \omega^2$ (solid black curve) and by the single-lobe periodic solution for $\mu \in (1, \infty)$ and $\omega \in (1, \infty)$ with the exact relation $\mu = \omega$ (solid blue curve).

As shown in Chapter 3 (see Remark 3.8), the constant solution is a saddle point of energy for $\mu \in (1, \infty)$ (dotted black curve). As a result, the family of

constrained minimizers of energy is piecewise smooth and a transition between the two minimizers occur at $\mu = 1$. Moreover, the slope of μ along the branch for single-lobe periodic waves at $\omega = \mu = 1$ can be found directly from the Stokes expansion (5.14) and (5.20) as

$$\lim_{\omega \searrow 1} \mu'(\omega) = 2 - \frac{1}{2\omega_2} = \frac{3 \cdot 2^\alpha - 5}{2 \cdot 2^\alpha - 3}.$$

The slope becomes horizontal at $\alpha = \alpha_* = \frac{\log 5 - \log 3}{\log 2} \approx 0.737$, negative for $\alpha \in (\alpha_0, \alpha_*)$, vertical at $\alpha = \alpha_0 = \frac{\log 3}{\log 2} - 1 \approx 0.585$, and positive for $\alpha < \alpha_0$. By comparing the left and right panels of Fig. 5.1, we highlight the differences in the outcomes of our variational method to the method of [48] as mentioned in Remark 5.1.

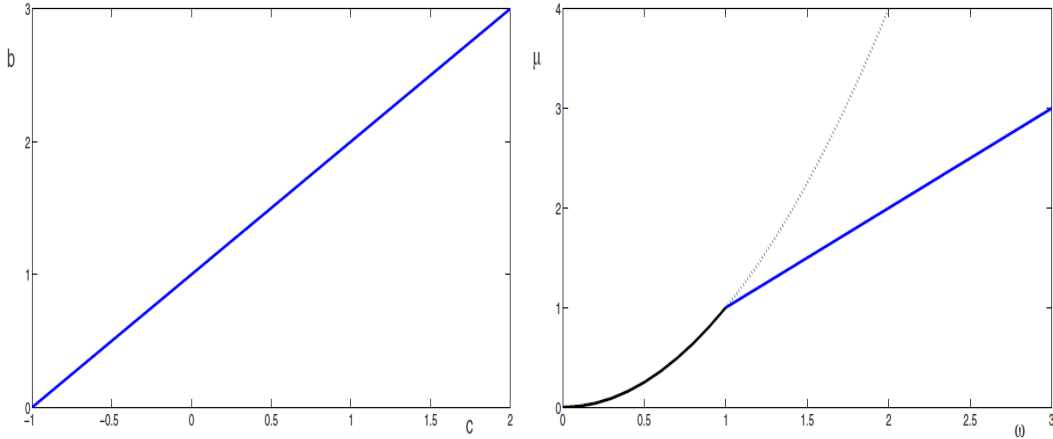


Figure 5.1: The dependence of b versus c (left) and μ versus ω (right) for $\alpha = 1$.

For the integrable KdV equation ($\alpha = 2$), the single-lobe periodic solution to the boundary-value problem (5.13) is known in the exact form:

$$\omega = \frac{4K(k)^2}{\pi^2} \sqrt{1 - k^2 + k^4} \tag{5.46}$$

and

$$\psi(x) = \frac{2K(k)^2}{\pi^2} \left[\sqrt{1 - k^2 + k^4} + 1 - 2k^2 + 3k^2 \operatorname{cn}^2 \left(\frac{K(k)}{\pi} x; k \right) \right], \tag{5.47}$$

where the elliptic modulus $k \in (0, 1)$ is a free parameter of the solution. Since

$$\int_0^\pi \psi(x) dx = \frac{2K(k)^2}{\pi} \left[\sqrt{1 - k^2 + k^4} + 1 - 2k^2 \right] + \frac{6K(k)}{\pi} [E(k) + (k^2 - 1)K(k)],$$

where $K(k)$ and $E(k)$ are complete elliptic integrals of the first and second kinds, respectively, we compute explicitly

$$c = \frac{4K(k)^2}{\pi^2} \left[2 - k^2 - \frac{3E(k)}{K(k)} \right] \tag{5.48}$$

and

$$b = \frac{4K(k)^4}{\pi^4} \left[-3(1 - k^2) + (2 - k^2) \frac{6E(k)}{K(k)} - \frac{9E(k)^2}{K(k)^2} \right]. \tag{5.49}$$

Fig.5.2 (left) shows the existence curve (5.48) and (5.49) on the parameter plane (c, b) . It follows that the function $b(c)$ is monotonically increasing in c . In the limit $k \rightarrow 1$, for which $K(k) \rightarrow \infty$ and $E(k) \rightarrow 1$, we compute from (5.48) and (5.49) the asymptotic behavior

$$b(c) \sim \frac{3}{\pi} c^{3/2} \quad \text{as } c \rightarrow \infty,$$

which coincides with the behavior of KdV solitons.

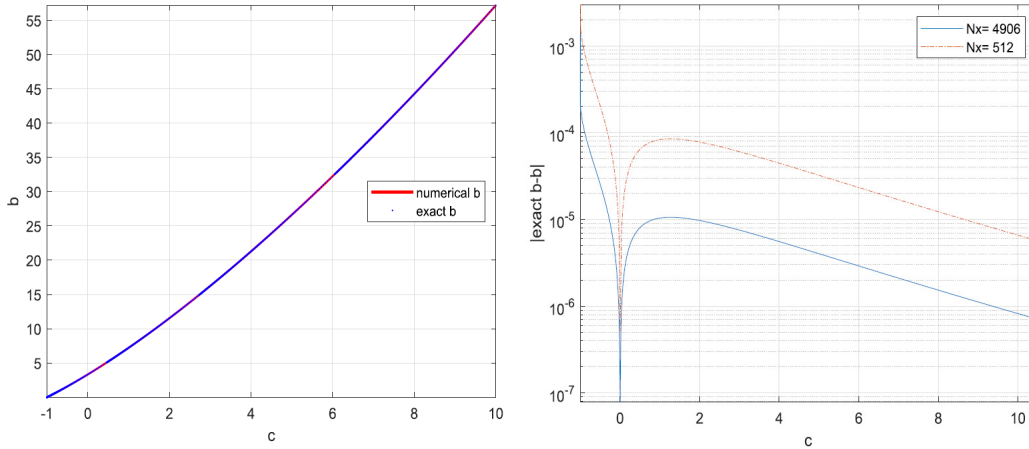


Figure 5.2: Left: the dependence of b versus c for $\alpha = 2$. Right: the difference between the numerical and exact values of b versus c .

The existence curve on the (c, b) plane is also computed numerically by using the Petviashvili method (see Chapter 4) for the stationary equation (5.13) with $\omega \in (1, \infty)$ and applying the transformation formula (5.22). Fig.5.2 (left) also shows the numerically obtained existence curve (invisible from the theoretical curve). The right panel of Fig.5.2 shows the error between the numerical and exact curves for two computations different by the number N of Fourier modes in the approximation of periodic solutions (for $N = 512$ by red curve and $N = 4906$ by blue curve). The more Fourier modes are included, the smaller is the error.

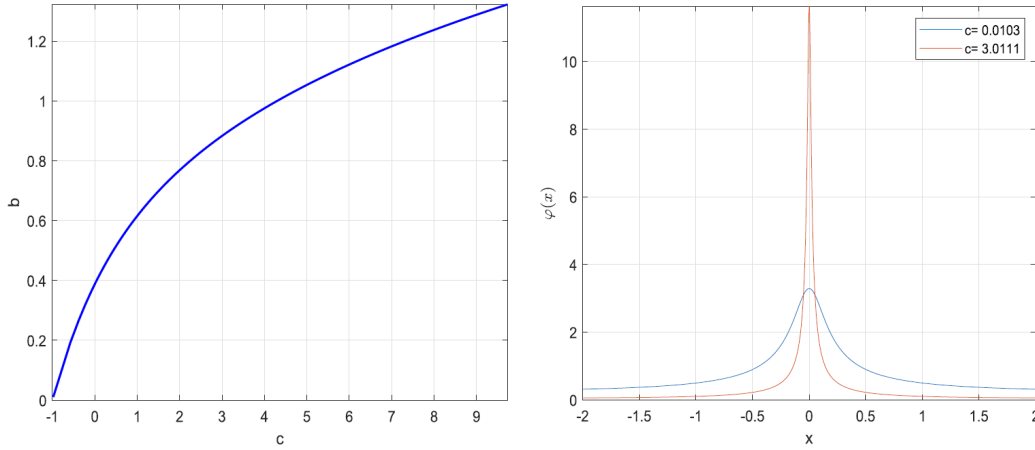


Figure 5.3: Left: the dependence of b versus c for $\alpha = 0.6$ obtained with the Petviashvili method. Right: Profiles of ψ for two values of c .

For other values of α in $(\frac{1}{3}, 1)$, we only compute the existence curve numerically. Fig.5.3 shows the existence curve (left) and two profiles of the numerically computed ψ in the stationary equation (5.13) (right) in the case $\alpha = 0.6 > \alpha_0$. The function $b(c)$ is still monotonically increasing in c and the values of $c \in (-1, \infty)$ are obtained monotonically from the values of $\omega \in (1, \infty)$ in the stationary equation (5.13). We also note that the greater is the wave speed c , the larger is the amplitude of the periodic wave and the smaller is its characteristic width.

Fig.5.4 (left) shows the existence curve in the case $\alpha = 0.55 < \alpha_0$ computed numerically (blue curve) and by using Stokes expansions (5.20) and (5.21) (red curve). The insert displays the mismatch between the red and blue curves with a small gap. The reason for mismatch is the lack of numerical data for $c \in (-1, -0.6)$ due to the fold point discussed in Remarks 5.4, 5.9, and 5.10. The function $\omega(c)$ is not monotonically increasing near the fold point and there exist two single-humped solutions for $\omega < 1$. Only the solution with $n(\mathcal{H}) = 1$ can be approximated with the Petviashvili method (see Chapter 4), whereas the other solution with $n(\mathcal{H}) = 2$ is unstable in the iterations of the Petviashvili method which then converge to a constant solution instead of the single-lobe solution. This is why we augmented the existence curve on Fig. 5.4 (left) with the Stokes expansion given by (5.20) and (5.21).

The right panel of Fig.5.4 shows the number of Fourier modes used in our numerical computations as the wave speed c increases. We have to increase the number of Fourier modes in order to control the accuracy of the numerical approximations and to ensure that the strongly compressed solution with the wave profile ψ is properly resolved. It follows from the Heisenberg's uncertainty principle that the narrower is the characteristic width of the wave profile, the

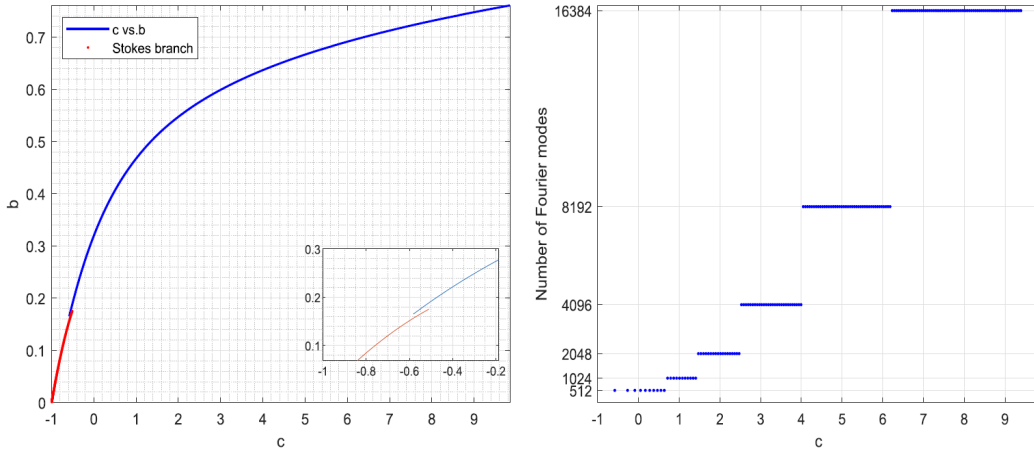


Figure 5.4: Left: the dependence of b versus c for $\alpha = 0.55$ obtained with the Petviashvili method. Right: The number of Fourier modes versus c .

weaker is the decay of the Fourier transform at infinity. We compute the maximum of the Fourier transform at the last ten Fourier modes and increase the number of Fourier modes every time the maximum becomes bigger than a certain tolerance level of the size 10^{-8} . The computational time becomes longer for larger values of the wave speed, nevertheless, it is clear that the function $b(c)$ is still monotonically increasing in c .

In order to overcome the computational problem seen on Fig.5.4 (left), we have developed the Newton’s method for the solutions ψ to the stationary equation (5.13) near the fold point that exists for $\alpha < \alpha_0$. With the initial guess from the Stokes expansion in (5.14) and (5.15), we were able to find the branch of solutions with $n(\mathcal{H}) = 2$ and connect it with the branch of solutions with $n(\mathcal{H}) = 1$. As a result, the mismatch seen on the insert of Fig.5.4 for $\alpha = 0.55$ has been eliminated by using the Newton’s method (not shown).

Fig.5.5 shows the existence curve on the parameter plane (c, b) in the cases $\alpha = 0.5$ (left) and $\alpha = 0.45$ (right) obtained with Newton’s method. It is obvious that the function $b(c)$ is monotonically increasing in c for $\alpha = 0.5$ and approaches to the horizontal asymptote as $c \rightarrow \infty$, whereas the function $b(c)$ is not monotone in c for $\alpha = 0.45$ and is decreasing for large values of c . This coincides with the conclusion of [13] on the solitary waves which correspond to the limit of $c \rightarrow \infty$.

By the stability result of Theorem 5.2, we conjecture based on our numerical results that the single-lobe periodic waves are spectrally stable for $\alpha \in [\frac{1}{2}, 2]$ since $b'(c) > 0$ for every $c \in (-1, \infty)$. On the other hand, for $\alpha \in (\frac{1}{3}, \frac{1}{2})$, there exists $c_* \in (-1, \infty)$ such that $b'(c) > 0$ for $c \in (-1, c_*)$ and $b'(c) < 0$ for $c \in (c_*, \infty)$, hence the periodic waves are spectrally stable for $c \in (-1, c_*)$ and spectrally unstable for $c \in (c_*, \infty)$.

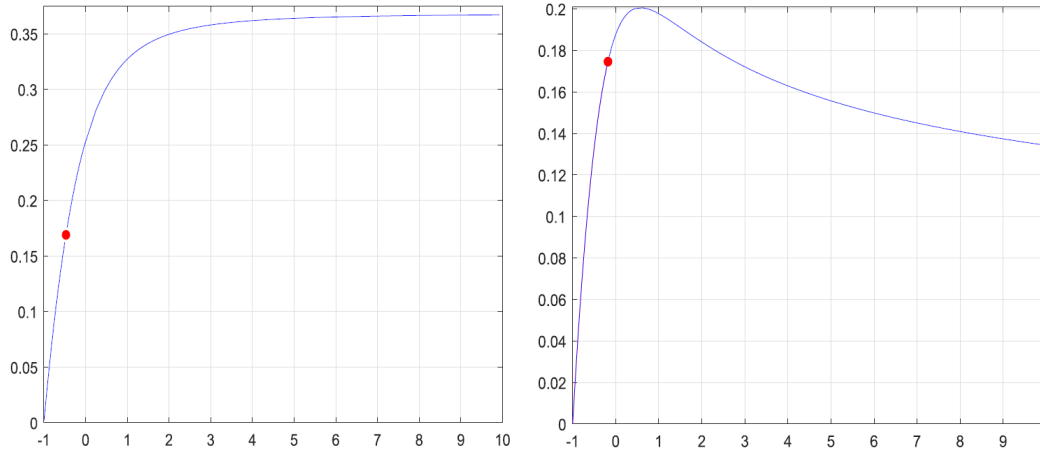


Figure 5.5: The dependence of b versus c for $\alpha = 0.5$ (left) and $\alpha = 0.45$ (right) obtained with the Newton’s method.

Fig.5.6 shows the bifurcation diagram on the parameter plane (ω, μ) for $\alpha = 0.6$ (left) and $\alpha = 0.5$ (right).

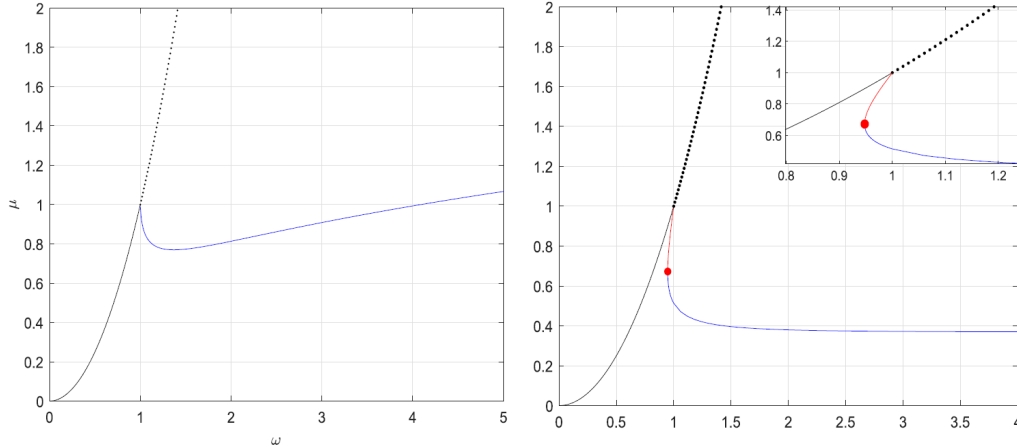


Figure 5.6: The dependence of μ versus ω for $\alpha = 0.6$ (left) and $\alpha = 0.5$ (right) obtained with the Newton’s method.

For $\alpha = 0.6$, see Fig. 5.6 (left), two single-lobe periodic waves (blue curve) coexist for the same value of μ below 1. The right branch is a local minimizer of energy $E(u)$ subject to fixed momentum $F(u)$, whereas the left branch is a saddle point of energy subject to fixed momentum and is a local minimizer of energy $E(u)$ subject to two constraints of momentum $F(u)$ and mass $M(u)$. This folded picture is unfolded on Fig. 5.3 (left), which contains all the single-lobe periodic waves and none of the constant solutions.

For $\alpha = 0.5$, see Fig. 5.6 (right), the folded diagram on the (ω, μ) plane

becomes more complicated because two single-lobe periodic waves coexist for ω below 1 (red and blue curves) and two periodic waves coexist for μ below 1. The red (blue) curve on Fig. 5.6 (right) corresponds to the part of the curve on Fig. 5.5 (left) below (above) the red point. Both branches are resolved well by using the Newton's method. The branch shown by the red curve corresponds to $n(\mathcal{H}) = 2$, nevertheless, it is a local minimizer of energy $E(u)$ subject to two constraints of momentum $F(u)$ and mass $M(u)$. At the fold point $\omega_0 \in (0, 1)$, the linearized operator \mathcal{H} is degenerate with $z(\mathcal{H}) = 2$. The branch is continued below the fold point and then to the right with $n(\mathcal{H}) = 1$. The decreasing and increasing parts of the branch have the same variational characterization as those on Fig. 5.6 (left). The folded picture is again unfolded on Fig. 5.5 (left) on the parameter plane (c, b) , where the scalar condition $b'(c) > 0$ for spectral stability of the single-lobe periodic waves implies that every point on the folded bifurcation diagram on the (ω, μ) parameter plane correspond to spectrally stable periodic waves. The fold point on Fig. 5.6 (right), where the linearized operator \mathcal{H} is degenerate and the momentum and mass are not smooth with respect to Lagrange multipliers, appears to be an internal point on the branch on Fig. 5.5 (left) which remains smooth with respect to the only parameter of the wave speed c .

Thus, we conclude that the new variational characterization of the zero-mean single-lobe periodic waves in the fractional KdV equation (1.7) allows us to unfold all the solution branches on the parameter plane (c, b) and to identify the stable periodic waves using the scalar criterion $b'(c) > 0$.

Chapter 6

Periodic Waves In Fractional Modified KdV Equation

In this chapter, our goal is to extend the variational framework outlined in Chapter 5 to study existence, variational characterization, bifurcations and spectral stability of periodic solutions of the fractional mKdV equation

$$u_t + 6u^2u_x - (D^\alpha u)_x = 0, \quad (6.1)$$

with $u(t, x) : \mathbb{R} \times \mathbb{T} \mapsto \mathbb{R}$. A travelling wave solution to the mKdV equation (6.1) satisfies the stationary equation

$$D^\alpha \psi + c\psi + b = 2\psi^3, \quad (6.2)$$

where the wave $\psi(x) : \mathbb{T} \mapsto \mathbb{R}$ has single-lobe profile defined accordingly to Definition 1.1, (c, b) are real parameters, and D^α is the fractional Laplacian operator on \mathbb{T} as defined in (1.6).

The fractional mKdV equation (6.1) admits the following conserved quantities:

$$\begin{aligned} M(u) &= \int_{-\pi}^{\pi} u dx, \\ F(u) &= \frac{1}{2} \int_{-\pi}^{\pi} u^2 dx, \\ E(u) &= \frac{1}{2} \int_{-\pi}^{\pi} \left((D^{\frac{\alpha}{2}} u)^2 - u^4 \right) dx, \end{aligned}$$

which stand for mass, momentum and energy respectively. The stationary equation (6.2) is the Euler–Lagrange equation for the action functional,

$$G(u) = E(u) + cF(u) + bM(u), \quad (6.3)$$

so that $G'(\psi) = 0$. The Hessian operator from the action functional (6.3) yields the linearized operator around the wave ψ in the form:

$$\mathcal{H} := G''(\psi) = D^\alpha + c - 6\psi^2. \quad (6.4)$$

Global well-posedness results for the initial data in $H^s(\mathbb{R})$ with $s > \frac{1}{4}$ and in $H^s(\mathbb{T})$ with $s \geq \frac{1}{2}$ were obtained for $\alpha = 2$ in [33]. Local well-posedness results for initial data in $H^s(\mathbb{R})$ with $s \geq \frac{1}{2}$ were obtained for $\alpha = 1$ in [59]. Energy and momentum are conserved in the time evolution of such solutions. Local solutions with sufficiently large initial data in $H^{\frac{1}{2}}(\mathbb{R})$ blow up in a finite time [58, 70].

In the case of the fractional KdV, we saw that the variational approach in Chapter 5 combining with the Galilean transformation allow us to represent all possible periodic waves of the single-lobe profile ψ and to derive a simple stability criterion from the derivative of the momentum $F(\psi)$ with respect to the wave speed c . However, when these ideas are extended to the cubic nonlinearity in the framework of the stationary equation (6.2), we face the difficulty that the Galilean transformation generates a quadratic nonlinear term and connects solutions of the fractional mKdV equation to solutions of the fractional Gardner equation. As a result, we are not able yet to characterize all possible periodic waves of the single-lobe profile in the stationary equation (6.2). Instead, we shall study the two particular families of solutions which correspond to $b = 0$ and generalize the sign-definite dnoidal and sign-indefinite cnoidal elliptic solutions of the local case $\alpha = 2$. Both families are obtained as minimizers of the quadratic part of the action functional $G(u)$ subject to the fixed quartic part of the energy, but one family is obtained in the subspace of even functions which we refer to as *the even periodic waves*, and the other family is obtained in the subspace of odd function and to be referred to as *the odd periodic waves*.

The chapter is organized as follows. The main results are stated in Section 6.1 followed by their proofs in Sections 6.2 and 6.3. Lastly, the numerical illustrations are collected in Section 6.4.

6.1 Main Results

The following two theorems describe the variational characterization and criteria for spectral stability for the *even periodic waves* and the *odd periodic waves* the stationary equation (6.2) when $b = 0$. The subspace of odd (even) functions in L^2 is denoted by L^2_{odd} (L^2_{even}). Similarly, the subspace of odd (even) periodic functions in H^s_{per} is denoted by $H^s_{\text{per,odd}}$ ($H^s_{\text{per,even}}$).

Theorem 6.1 (Odd periodic wave). *Fix $\alpha \in (\frac{1}{2}, 2]$. For every $c_0 \in (-1, \infty)$,*

there exists a solution to the stationary equation (6.2) with $b = 0$ and the odd, single-lobe profile ψ_0 , which is obtained from a constrained minimizer of the following variational problem:

$$\inf_{u \in H_{\text{per,odd}}^{\frac{\alpha}{2}}} \left\{ \int_{-\pi}^{\pi} [(D^{\frac{\alpha}{2}} u)^2 + c_0 u^2] dx : \int_{-\pi}^{\pi} u^4 dx = 1 \right\}. \quad (6.5)$$

There exists a C^1 mapping $c \mapsto \psi(\cdot, c) \in H_{\text{per,odd}}^{\alpha}$ in a local neighborhood of c_0 such that $\psi(\cdot, c_0) = \psi_0$. The spectrum of \mathcal{H} in $L^2(\mathbb{T})$ has exactly two negative eigenvalues and if $1 \in \text{Range}(\mathcal{H})$, a simple zero eigenvalue. Assuming $1 \in \text{Range}(\mathcal{H})$ and setting $\sigma_0 := \langle \mathcal{H}^{-1}1, 1 \rangle$, the periodic wave with the profile ψ_0 is spectrally stable if

$$\sigma_0 \leq 0, \quad \frac{d}{dc} \|\psi\|_{L^2}^2 \geq 0 \quad (6.6)$$

and is spectrally unstable with exactly one real, positive eigenvalue of $\partial_x \mathcal{H}$ in $L^2(\mathbb{T})$ if

$$\text{either } \sigma_0 \frac{d}{dc} \|\psi\|_{L^2}^2 > 0 \quad \text{or } \sigma_0 = 0, \quad \frac{d}{dc} \|\psi\|_{L^2}^2 < 0, \quad \text{or } \sigma_0 > 0, \quad \frac{d}{dc} \|\psi\|_{L^2}^2 = 0. \quad (6.7)$$

If $1 \notin \text{Range}(\mathcal{H})$, then the periodic wave is spectrally unstable with exactly one real positive eigenvalue of $\partial_x \mathcal{H}$ in $L^2(\mathbb{T})$ if

$$\frac{d}{dc} \|\psi\|_{L^2}^2 \geq 0. \quad (6.8)$$

Remark 6.1. If $\sigma_0 = 0$, the odd periodic wave of Theorem 6.1 undertakes the stability bifurcation, which also results in the bifurcation of new solutions in the stationary equation (6.2) with $b \neq 0$. The stability bifurcation was first discovered in [36] for $\alpha = 2$. We show numerically that this bifurcation is generic for every $\alpha \in (\frac{1}{2}, 2)$.

Remark 6.2. Based on numerical studies, see Section 6.4, we conjecture that the case $1 \notin \text{Range}(\mathcal{H})$ is impossible for the odd periodic wave in Theorem 6.1 for every $\alpha \in (\frac{1}{2}, 2]$ and every $c \in (-1, \infty)$. Nevertheless, the case $1 \notin \text{Range}(\mathcal{H})$ is observed for the new solutions bifurcating from the odd periodic wave in Theorem 6.1.

Remark 6.3. Although the solution ψ_0 is obtained as a global minimizer of the variational problem (6.5), the solution $\psi(\cdot, c) \in H_{\text{per,odd}}^{\alpha}$ in a local neighborhood of c_0 is continued from the Euler–Lagrange equation. Therefore, even if the solution $\psi(\cdot, c) \in H_{\text{per,odd}}^{\alpha}$ is C^1 with respect to c , it may not coincide with the global minimizer of (6.5) for $c \neq c_0$ because uniqueness of minimizers of

the variational problem (6.5) is not proven. Nevertheless, the spectral stability conclusions of Theorem 6.1 apply to every global minimizer of the variational problem (6.5) for every $c_0 \in (-1, \infty)$.

Theorem 6.2 (Even periodic wave). *Fix $\alpha \in (\frac{1}{2}, 2]$. For every $c_0 \in (\frac{1}{2}, \infty)$, there exists a solution to the stationary equation (6.2) with $b = 0$ and the even, single-lobe profile ψ_0 , which is obtained from a constrained minimizer of the following variational problem:*

$$\inf_{u \in H_{\text{per,even}}^{\frac{\alpha}{2}}} \left\{ \int_{-\pi}^{\pi} [(D^{\frac{\alpha}{2}} u)^2 + c_0 u^2] dx : \int_{-\pi}^{\pi} u^4 dx = 1 \right\}. \quad (6.9)$$

The spectrum of \mathcal{H} in $L^2(\mathbb{T})$ has exactly one simple negative eigenvalue and if $1 \in \text{Range}(\mathcal{H})$, a simple zero eigenvalue. With the transformation,

$$\psi_0(x) = a_0 + \phi_0(x), \quad a_0 := \frac{1}{2\pi} \int_{-\pi}^{\pi} \psi_0(x) dx, \quad \omega_0 := c_0 - 6a_0^2, \quad (6.10)$$

assuming $\omega_0 \in (-1, \infty)$, there exists a C^1 mapping $(\omega, a) \mapsto \phi(\cdot, \omega, a) \in H_{\text{per,even}}^{\alpha}$ in a local neighborhood of (ω_0, a_0) such that $\phi(\cdot, \omega_0, a_0) = \phi_0$ and the mean value of ϕ is zero. The periodic wave ψ_0 is spectrally stable if

$$\frac{\partial}{\partial \omega} \|\phi\|_{L^2}^2 \geq 0 \quad (6.11)$$

and is spectrally unstable with exactly one real, positive eigenvalue of $\partial_x \mathcal{H}$ in $L^2(\mathbb{T})$ if

$$\frac{\partial}{\partial \omega} \|\phi\|_{L^2}^2 < 0. \quad (6.12)$$

Remark 6.4. We derive the criterion for $1 \notin \text{Range}(\mathcal{H})$, in which case \mathcal{H} has the double zero eigenvalue and the even periodic wave of Theorem 6.2 undertakes the fold bifurcation. Two solutions of the stationary equation (6.2) with $b = 0$ coexist for the same value of c near the fold bifurcation. We show numerically that the fold bifurcation is generic for every $\alpha \in (\frac{1}{2}, \alpha_0)$, where

$$\alpha_0 := \frac{\log 8 - \log 5}{\log 2} \approx 0.6781.$$

If $\alpha \in (\frac{1}{2}, \alpha_0)$, two solutions with the even, single-lobe profile exist for the same value of $c \in (c_0, \frac{1}{2})$ with $c_0 \in (0, \frac{1}{2})$ beyond the admissible range of values of c in Theorem 6.2.

Remark 6.5. Based on numerical evidences, we conjecture that $\omega \in (-1, \infty)$ is always satisfied for the even periodic wave in Theorem 6.2.

Remark 6.6. *Similarly to Remark 6.3, the smooth continuation of the solution $\psi(\cdot, \omega, a) = a + \phi(x, \omega, a)$ with $\phi(\cdot, c, a) \in H_{\text{per,even}}^\alpha$ is obtained from the Euler–Lagrange equation and the solution $\psi(\cdot, \omega, a)$ may not coincide with the global minimizer of (6.9) for $c(\omega, a) \neq c_0$. Nevertheless, under the assumption $\omega_0 \in (-1, \infty)$, the spectral stability conclusions of Theorem 6.2 apply to every global minimizer of the variational problem (6.9) for every $c_0 \in (\frac{1}{2}, \infty)$.*

6.2 Odd Periodic Waves

Here, we study the odd periodic waves and provide the proof of Theorem 6.1. First, in Theorem 6.3 and Corollary 6.1, we obtain the variational characterization of the odd periodic waves. Next, Lemma 6.2 provides a smooth continuation of the odd periodic waves with respect to the speed parameter c . Finally, we obtain the spectral stability conclusions in Lemma 6.5 and Theorem 6.4.

6.2.1 Variational Characterization

If $\psi \in H_{\text{per}}^\alpha$ is a solution to the stationary equation (6.2) with $b = \frac{1}{\pi} \int_{-\pi}^{\pi} \psi^3 dx$, then ψ satisfies the zero-mean constraint and the boundary-value problem:

$$D^\alpha \psi + c\psi = 2\Pi_0\psi^3, \tag{6.13}$$

where $\Pi_0 f := f - \frac{1}{2\pi} \int_{-\pi}^{\pi} f(x) dx$ is the projection operator reducing the mean value of 2π -periodic functions to zero. Since we use variational methods, we consider weak solutions of the boundary-value problem (6.13) in $H_{\text{per}}^{\frac{\alpha}{2}}$. By the same bootstrapping argument as in Proposition 5.1, if $\psi \in H_{\text{per}}^{\frac{\alpha}{2}}$ is a weak solution of the boundary-value problem (6.13), then $\psi \in H_{\text{per}}^\infty$ and, in particular, it is a strong solution to the boundary-value problem (6.13) in H_{per}^α .

The following theorem and its corollary give the construction and properties of the periodic waves in a subspace of odd functions which satisfy the boundary-value problem (6.13).

Theorem 6.3. *Fix $\alpha > \frac{1}{2}$. For every $c > -1$, there exists the ground state (minimizer) $\chi \in H_{\text{per,odd}}^{\frac{\alpha}{2}}$ of the following constrained minimization problem:*

$$q_{c,\text{odd}} := \inf_{u \in H_{\text{per,odd}}^{\frac{\alpha}{2}}} \left\{ \mathcal{B}_c(u) : \int_{-\pi}^{\pi} u^4 dx = 1 \right\}, \tag{6.14}$$

where

$$\mathcal{B}_c(u) := \frac{1}{2} \int_{-\pi}^{\pi} [(D^{\frac{\alpha}{2}} u)^2 + cu^2] dx. \tag{6.15}$$

If $\alpha \leq 2$, the ground state has the single-lobe profile, which is even with respect to the points at $x = \pm\pi/2$.

Proof. The proof follows from the proof of Theorem 5.4, mutatis mutandis. We note that the symmetric rearrangement of the ground state yields the single-lobe profile with the maximum points located at $x = \pm\pi/2$ as opposed to at $x = 0$ in the proof of Theorem 5.4. \square

Corollary 6.1. *Let χ be the ground state of Theorem 6.3. There exists $C > 0$ such that $\psi(x) = C\chi(x)$ satisfies the stationary equation (6.2) with $b = 0$.*

Proof. By Lagrange's Multiplier Theorem, the constrained minimizer $\chi \in H_{\text{per,odd}}^{\frac{\alpha}{2}}$ satisfies the stationary equation

$$D^\alpha \chi + c\chi = \mu\chi^3, \quad (6.16)$$

where $\mu = 2\mathcal{B}_c(\chi)$ is the Lagrange multiplier found from the constraint $\int_{-\pi}^{\pi} \chi^4 dx = 1$. Since $\mathcal{B}_c(\chi) > 0$, the scaling transformation $\psi = C\chi$ with $C := \sqrt{\mathcal{B}_c(\chi)}$ maps the stationary equation (6.16) to the form (6.2) with $b = 0$. \square

Lemma 6.1. *Let χ be the ground state of Theorem 6.3 and $q_{c,\text{odd}} = \mathcal{B}_c(\chi)$. Then $q_{c,\text{odd}}$ is continuous in c for $c > -1$ and $q_{c,\text{odd}} \rightarrow 0$ as $c \rightarrow -1$.*

Proof. The proof of continuity of $q_{c,\text{odd}}$ follows the proof of Lemma 5.1 verbatim. In order to show that $q_{c,\text{odd}} \rightarrow 0$ as $c \rightarrow -1$, we consider the following function

$$u(x) = A \sin(x),$$

which satisfy the constraint in (6.14) for $A := \left(\frac{4}{3\pi}\right)^{1/4}$. Substituting u into $\mathcal{B}_c(u)$ yields

$$\mathcal{B}_c(u) = \frac{\pi}{2} A^2 (1+c) = \frac{\sqrt{\pi}}{\sqrt{3}} (1+c).$$

Since

$$0 \leq q_{c,\text{odd}} \leq \mathcal{B}_c(u),$$

it follows that $q_{c,\text{odd}} \rightarrow 0$ as $c \rightarrow -1$. \square

6.2.2 Smooth continuation

Let $\psi \in H_{\text{per,odd}}^\alpha$ be a solution to the boundary-value problem (6.13) for some $c \in (-1, \infty)$ obtained by Theorem 6.3 and Corollary 6.1. Let \mathcal{H} be the linearized operator around the wave ψ given by (6.4) and

$$\mathcal{H} : H_{\text{per}}^\alpha \subset L^2(\mathbb{T}) \rightarrow L^2(\mathbb{T}). \quad (6.17)$$

In what follows, we determine the multiplicity of the zero eigenvalue of \mathcal{H} denoted as $z(\mathcal{H})$ and the number of negative eigenvalues of \mathcal{H} with the account of their multiplicities denoted as $n(\mathcal{H})$. It follows from the stationary equation (6.2) with $b = 0$ that

$$\mathcal{H}1 = c - 6\psi^2 \quad (6.18)$$

and

$$\mathcal{H}\psi = -4\psi^3. \quad (6.19)$$

Due to the translational symmetry, we always have $\mathcal{H}\partial_x\psi = 0$.

By an elementary application of the implicit function theorem (similarly to Lemma 5.3), we obtain the smooth continuation of the solution to the boundary value problem (6.13) with respect to parameter c .

Lemma 6.2. *Assume $\alpha \in (\frac{1}{2}, 2]$ and $\psi_0 \in H_{\text{per,odd}}^\alpha$ be a solution obtained in Theorem 6.3 and Corollary 6.1 for $c = c_0$. Assume $\text{Ker}(\mathcal{H}|_{L_{\text{odd}}^2})$ is trivial. Then, there exists a C^1 mapping in an open subset of c_0 denoted by $\mathcal{I} \subset \mathbb{R}$:*

$$\mathcal{I} \ni c \mapsto \psi(\cdot; c) \in H_{\text{per,odd}}^\alpha \quad (6.20)$$

such that $\psi(\cdot; c_0) = \psi_0$ and $\mathcal{H}\partial_c\psi(\cdot; c_0) = -\psi_0$.

Proof. Let $\Upsilon : (-1, \infty) \times H_{\text{per,odd}}^\alpha \rightarrow L_{\text{odd}}^2(\mathbb{T})$ be defined by $\Upsilon(c, f) := D^\alpha f + cf - 2f^3$. By hypothesis of the lemma, we have $\Upsilon(c_0, \psi_0) = 0$. Moreover, Υ is smooth and its Fréchet derivative with respect to f evaluated at (c_0, ψ_0) is given by \mathcal{H} computed at ψ_0 . Since $\text{Ker}(\mathcal{H}|_{L_{\text{odd}}^2})$ is empty by the assumption, we conclude that \mathcal{H} is one-to-one. It is also onto since its spectrum consists of nonzero isolated eigenvalues with finite algebraic multiplicities because $H_{\text{per,odd}}^\alpha$ is compactly embedded in $L_{\text{odd}}^2(\mathbb{T})$ if $\alpha > 1/2$ and because \mathcal{H} is a self-adjoint operator. Hence, \mathcal{H} is a bounded linear operator with a bounded inverse. Thus, since Υ and its derivative with respect to f are smooth maps on their domains, the result follows from the implicit function theorem. \square

Since ψ is the single-lobe profile of the periodic wave in the sense of Definition 1.1 and since ψ is even with respect to the points at $x = \pm\pi/2$, then we can place the unique maximum of ψ at $x = \pi/2$ and adopt several results in Propositions A.1, A.2, A.3 after translating $x \mapsto x - \pi/2$. We compute $n(\mathcal{H})$ and $z(\mathcal{H})$ in the following lemma.

Lemma 6.3. *Let $\alpha \in (\frac{1}{2}, 2]$ and $\psi \in H_{\text{per,odd}}^\alpha$ be a solution obtained in Theorem 6.3 and Corollary 6.1. Then, $n(\mathcal{H}) = 2$ and*

$$z(\mathcal{H}) = \begin{cases} 1, & \text{if } 1 \in \text{Range}(\mathcal{H}), \\ 2, & \text{if } 1 \notin \text{Range}(\mathcal{H}). \end{cases}$$

Proof. Since $\psi \in H_{\text{per,odd}}^\alpha$ is a minimizer of the constrained variational problem (6.14) with only one constraint, we have $n(\mathcal{H}|_{L^2_{\text{odd}}}) \leq 1$. On the other hand, we have

$$\langle \mathcal{H}\psi, \psi \rangle_{L^2} = -4\|\psi\|_{L^4}^4 < 0,$$

with odd ψ , hence $n(\mathcal{H}|_{L^2_{\text{odd}}}) \geq 1$, so that $n(\mathcal{H}|_{L^2_{\text{odd}}}) = 1$.

Thanks to Proposition A.1, which states that an eigenfunction corresponding to the n -th eigenvalue of \mathcal{H} can change signs at most $2(n-1)$ times over \mathbb{T} , we see that 0 is not the first eigenvalue of $\mathcal{H}|_{L^2_{\text{even}}}$ because $\partial_x \psi \in \text{Ker}(\mathcal{H})$ and $\partial_x \psi$ is even with two nodes on \mathbb{T} . Hence, $n(\mathcal{H}|_{L^2_{\text{even}}}) \geq 1$. However, another negative eigenvalue of $\mathcal{H}|_{L^2_{\text{even}}}$ is impossible since the eigenfunction for the second eigenvalue of $\mathcal{H}|_{L^2_{\text{even}}}$ must have two nodes by Proposition A.1 and the nodes are located at the symmetry points $x = \pm\pi/2$, hence this eigenfunction is not orthogonal to $\partial_x \psi \in \text{Ker}(\mathcal{H})$. Therefore, 0 is the second eigenvalue of $\mathcal{H}|_{L^2_{\text{even}}}$, which yields $n(\mathcal{H}|_{L^2_{\text{even}}}) = 1$ and

$$n(\mathcal{H}) = n(\mathcal{H}|_{L^2_{\text{odd}}}) + n(\mathcal{H}|_{L^2_{\text{even}}}) = 2.$$

It remains to consider $z(\mathcal{H}) \geq 1$. For illustration purposes, we give the first five eigenfunctions of the operator \mathcal{H} in $L^2(\mathbb{T})$ for $\alpha = 2$ on Figure 6.1.

By the symmetry of ψ and ψ^2 , the operator \mathcal{H} in (6.4) and (6.17) has a π -periodic potential, which is even with respect to both $x = 0$ and $x = \pi/2$. The negative eigenvalue of \mathcal{H} in L^2_{even} , which is the lowest eigenvalue of \mathcal{H} in $L^2(\mathbb{T})$, corresponds to the sign-definite π -periodic function, which is even with respect to both $x = 0$ and $x = \pi/2$. The negative eigenvalue in L^2_{odd} , which is the second eigenvalue of \mathcal{H} in $L^2(\mathbb{T})$, corresponds to the eigenfunction with two nodes on \mathbb{T} , which is even with respect to $x = \pi/2$. The eigenfunction $\partial_x \psi$ for the zero eigenvalue in L^2_{even} , which is the third eigenvalue of \mathcal{H} in $L^2(\mathbb{T})$, has two nodes and is odd with respect to $x = \pi/2$. By Proposition A.3, the zero eigenvalue is the lowest eigenvalue for the eigenfunctions that are odd with respect to $x = \pi/2$.

Finally, we consider the eigenfunctions with four nodes on \mathbb{T} since 0 is the third eigenvalue of \mathcal{H} . These eigenfunctions have the same parity with respect to $x = 0$ and $x = \pi/2$, hence odd functions in L^2_{odd} are also odd with respect to $x = \pi/2$. Since the zero eigenvalue is the lowest eigenvalue for the eigenfunctions that are odd with respect to $x = \pi/2$, the odd eigenfunction of \mathcal{H} in L^2_{odd} with four nodes corresponds to the positive eigenvalue of \mathcal{H} . Therefore, $z(\mathcal{H}|_{L^2_{\text{odd}}}) = 0$ and by Lemma 6.2, the mapping $c \mapsto \psi(\cdot; c)$ is C^1 in c with $\mathcal{H}\partial_c \psi = -\psi$, so that $\psi \in \text{Range}(\mathcal{H})$.

Assume that the even eigenfunction of \mathcal{H} in L^2_{even} with four nodes (call it f) belongs to $\text{Ker}(\mathcal{H})$, hence $\text{Ker}(\mathcal{H}) = \text{span}(\partial_x \psi, f)$. Either $\langle 1, f \rangle_{L^2} = 0$ or $\langle 1, f \rangle_{L^2} \neq 0$. If $\langle 1, f \rangle_{L^2} = 0$, then $1 \in \text{Range}(\mathcal{H})$. It follows from (6.18) that if $1 \in \text{Range}(\mathcal{H})$, then $\psi^2 \in \text{Range}(\mathcal{H})$. Therefore, $\{1, \psi, \psi^2\} \in \text{Range}(\mathcal{H})$ and

by Proposition A.2, $\text{Ker}(\mathcal{H}) = \text{span}(\partial_x \psi)$, so that the existence of $f \in \text{Ker}(\mathcal{H})$ leads to a contradiction. Hence, $z(\mathcal{H}) = 1$ if $1 \in \text{Range}(\mathcal{H})$. If $\langle 1, f \rangle_{L^2} \neq 0$, then $1 \notin \text{Range}(\mathcal{H})$ because $\text{Range}(\mathcal{H})$ is orthogonal to $\text{Ker}(\mathcal{H})$. Hence, $z(\mathcal{H}) = 2$ if and only if $1 \notin \text{Range}(\mathcal{H})$. \square

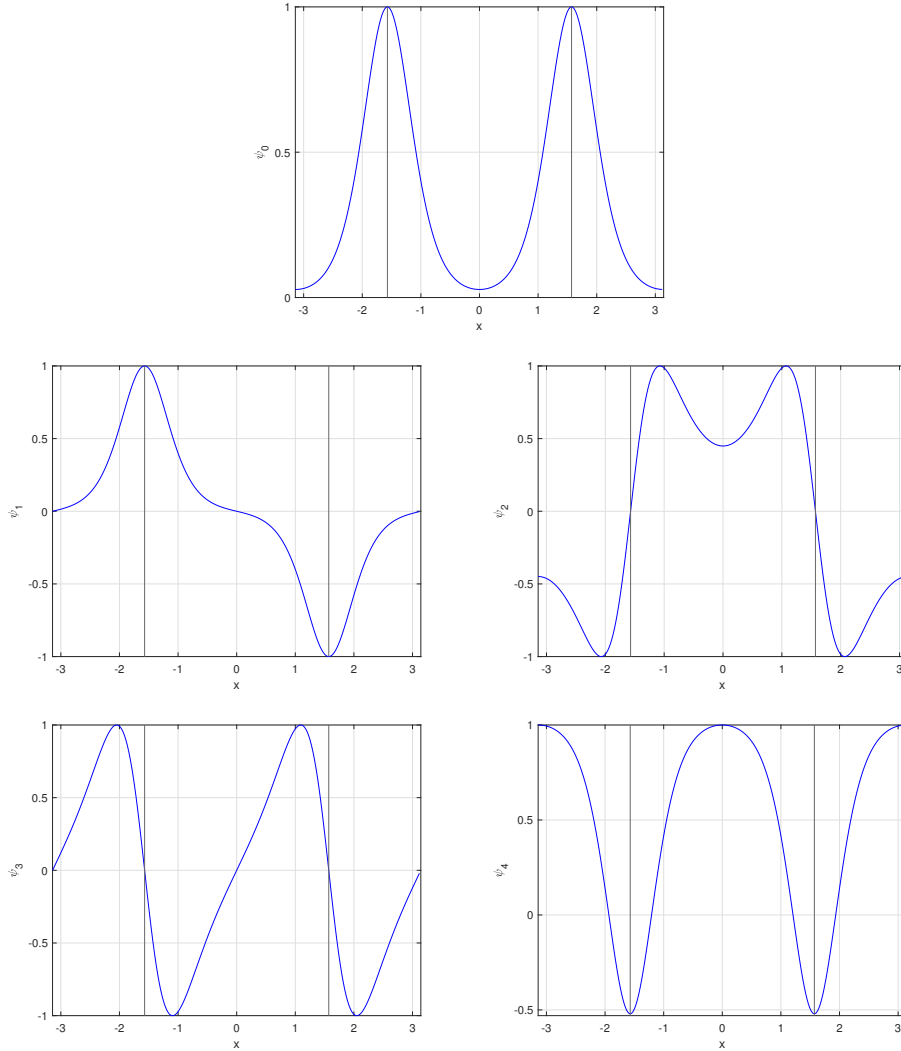


Figure 6.1: Normalized eigenfunctions of \mathcal{H} on \mathbb{T} for $\alpha = 2$ computed from the exact expression of equations (6.71)–(6.73) and (6.75)–(6.76)

Next, we recall the subspace of L^2 with zero mean X_0 defined in (1.19):

$$X_0 := \left\{ f \in L^2(\mathbb{T}) : \int_{-\pi}^{\pi} f(x) dx = 0 \right\}. \tag{6.21}$$

Denote $\Pi_0 \mathcal{H} \Pi_0$ by $\mathcal{H}|_{X_0}$. By an explicit computation, it follows that if $f \in$

$H_{\text{per}}^\alpha \cap X_0$, then

$$\mathcal{H}|_{X_0} f := \mathcal{H}f + \frac{3}{\pi} \langle f, \psi^2 \rangle. \quad (6.22)$$

The following result is similar to Lemma 5.2.

Lemma 6.4. *Let $\alpha \in (\frac{1}{2}, 2]$ and $\psi \in H_{\text{per,odd}}^\alpha$ be a solution obtained in Theorem 6.3 and Corollary 6.1. If there exists a nonzero $f \in \text{Ker}(\mathcal{H}|_{X_0})$ such that $\langle f, \partial_x \psi \rangle = 0$, then*

$$z(\mathcal{H}) = 1, \quad \text{and} \quad \langle f, \psi^2 \rangle \neq 0. \quad (6.23)$$

Proof. Since $f \in \text{Ker}(\mathcal{H}|_{X_0})$, then $\langle 1, f \rangle = 0$ and f satisfies

$$\mathcal{H}f = -\frac{3}{\pi} \langle f, \psi^2 \rangle. \quad (6.24)$$

Either $\langle f, \psi^2 \rangle = 0$ or $\langle f, \psi^2 \rangle \neq 0$.

If $\langle f, \psi^2 \rangle = 0$, then $f \in \text{Ker}(\mathcal{H})$ so that $z(\mathcal{H}) = 2$ and $1 \notin \text{Range}(\mathcal{H})$ by Lemma 6.3. However, $1 \perp \text{span}(\partial_x \psi, f) = \text{Ker}(\mathcal{H})$ implies $1 \in \text{Range}(\mathcal{H})$, which is a contradiction.

If $\langle f, \psi^2 \rangle \neq 0$, then it follows from (6.24) that $1 \in \text{Range}(\mathcal{H})$ and hence $z(\mathcal{H}) = 1$ by Lemma 6.3. This yields (6.23). \square

Remark 6.7. *Assuming $1 \in \text{Range}(\mathcal{H})$, let us define $\sigma_0 := \langle \mathcal{H}^{-1}1, 1 \rangle$. Then, $z(\mathcal{H}|_{X_0}) = 2$ if and only if $\sigma_0 = 0$. On the other hand, $z(\mathcal{H}) = 2$ if and only if σ_0 is unbounded.*

6.2.3 Spectral Stability

Next, we study the condition for which the ground state of the variational problem (6.14) with a single constraint is a local minimizer of the following variational problem with two constraints:

$$r_c := \inf_{u \in H_{\text{per}}^{\frac{\alpha}{2}}} \left\{ \mathcal{B}_c(u) : \int_{-\pi}^{\pi} u^4 dx = 1, \quad \int_{-\pi}^{\pi} u dx = 0 \right\}. \quad (6.25)$$

It is clear that $r_c \leq q_{c,\text{odd}}$ and therefore, minimizers of (6.14) could be saddle points of (6.25).

The following lemma provides the count of the negative and zero eigenvalues of the operator \mathcal{H} in the constrained space related to the variational problem (6.25).

Lemma 6.5. *Let $\alpha \in (\frac{1}{2}, 2]$ and $\psi \in H_{\text{per,odd}}^\alpha$ be a solution obtained in Theorem 6.3 and Corollary 6.1. If $1 \in \text{Range}(\mathcal{H})$, then*

$$n(\mathcal{H}|_{\{1, \psi^3\}^\perp}) = \begin{cases} 0, & \sigma_0 \leq 0, \\ 1, & \sigma_0 > 0, \end{cases} \quad z(\mathcal{H}|_{\{1, \psi^3\}^\perp}) = \begin{cases} 1, & \sigma_0 \neq 0, \\ 2, & \sigma_0 = 0, \end{cases} \quad (6.26)$$

where $\sigma_0 := \langle \mathcal{H}^{-1}1, 1 \rangle$. If $1 \notin \text{Range}(\mathcal{H})$, then

$$n(\mathcal{H}|_{\{1, \psi^3\}^\perp}) = 1, \quad z(\mathcal{H}|_{\{1, \psi^3\}^\perp}) = 1. \quad (6.27)$$

Proof. By using the result of Theorem A.3, we construct the following symmetric 2-by-2 matrix related to the two constraints in (6.25):

$$P(\lambda) := \begin{bmatrix} \langle (\mathcal{H} - \lambda I)^{-1} \psi^3, \psi^3 \rangle & \langle (\mathcal{H} - \lambda I)^{-1} \psi^3, 1 \rangle \\ \langle (\mathcal{H} - \lambda I)^{-1} 1, \psi^3 \rangle & \langle (\mathcal{H} - \lambda I)^{-1} 1, 1 \rangle \end{bmatrix}, \quad \lambda \notin \sigma(\mathcal{H}).$$

If $1 \in \text{Range}(\mathcal{H})$, then

$$\langle \mathcal{H}^{-1}1, 1 \rangle = \sigma_0, \quad \langle \mathcal{H}^{-1}1, \psi^3 \rangle = \langle \mathcal{H}^{-1}\psi^3, 1 \rangle = 0, \quad \langle \mathcal{H}^{-1}\psi^3, \psi^3 \rangle = -\frac{1}{4} \int_{-\pi}^{\pi} \psi^4 dx \quad (6.28)$$

thanks to equation (6.19). By Theorem A.3, we have the following identities:

$$\begin{cases} n(\mathcal{H}|_{\{1, \psi^3\}^\perp}) = n(\mathcal{H}) - n_0 - z_0, \\ z(\mathcal{H}|_{\{1, \psi^3\}^\perp}) = z(\mathcal{H}) + z_0, \end{cases} \quad (6.29)$$

where n_0 and z_0 are the numbers of negative and zero eigenvalues of $P(0)$. Since $n(\mathcal{H}) = 2$ and $z(\mathcal{H}) = 1$ by Lemma 6.3, the count (6.29) yields (6.26) due to (6.28).

If $1 \notin \text{Range}(\mathcal{H})$, then $z(\mathcal{H}) = 2$ but $z(\mathcal{H}|_{X_0}) = 1$ by Lemma 6.4. By Theorem A.3, the count (6.29) must be replaced by

$$\begin{cases} n(\mathcal{H}|_{\{1, \psi^3\}^\perp}) = n(\mathcal{H}) - n_0 - z_0, \\ z(\mathcal{H}|_{\{1, \psi^3\}^\perp}) = z(\mathcal{H}) + z_0 - z_\infty, \end{cases} \quad (6.30)$$

where $z_\infty = 1$, $z_0 = 0$, and $n_0 = 1$. The count (6.30) yields (6.27). \square

It follows by Lemma 6.5 that the ground state of the variational problem (6.14) is a local minimizer of the variational problem (6.25) if $\sigma_0 \leq 0$, which is only degenerate by the translational symmetry if $\sigma_0 \neq 0$, whereas it is the saddle point of the variational problem (6.25) if $\sigma_0 > 0$ or if $1 \notin \text{Range}(\mathcal{H})$, in which case σ_0 is unbounded.

Equipped with the variational characterization of Lemma 6.5, we can clarify the spectral stability of the odd periodic waves. The following theorem gives the relevant result.

Theorem 6.4. *Let $\alpha \in (\frac{1}{2}, 2]$ and $\psi \in H_{\text{per, odd}}^\alpha$ be a solution obtained in Theorem 6.3 and Corollary 6.1. If $1 \in \text{Range}(\mathcal{H})$, then the periodic wave is spectrally stable if*

$$\sigma_0 \leq 0, \quad \frac{d}{dc} \|\psi\|_{L^2}^2 \geq 0, \quad (6.31)$$

and is spectrally unstable with exactly one real positive eigenvalue of $\partial_x \mathcal{H}$ in $L^2(\mathbb{T})$ if

$$\text{either } \sigma_0 \frac{d}{dc} \|\psi\|_{L^2}^2 > 0 \quad \text{or } \sigma_0 = 0, \quad \frac{d}{dc} \|\psi\|_{L^2}^2 < 0, \quad \text{or } \sigma_0 > 0, \quad \frac{d}{dc} \|\psi\|_{L^2}^2 = 0, \quad (6.32)$$

where $\sigma_0 := \langle \mathcal{H}^{-1}1, 1 \rangle$. If $1 \notin \text{Range}(\mathcal{H})$, then the periodic wave is spectrally unstable with exactly one real positive eigenvalue of $\partial_x \mathcal{H}$ in $L^2(\mathbb{T})$ if

$$\frac{d}{dc} \|\psi\|_{L^2}^2 \geq 0. \quad (6.33)$$

Proof. It is well-known [50] that the periodic wave ψ is spectrally stable if it is a constrained minimizer of energy (1.13) under fixed momentum (1.11) and mass (1.10). Since \mathcal{H} is the Hessian operator for $G(u)$ in (6.4), the spectral stability holds if

$$\mathcal{H}|_{\{1, \psi\}^\perp} \geq 0. \quad (6.34)$$

On the other hand, the periodic wave ψ is spectrally unstable with exactly one real positive eigenvalue if $n(\mathcal{H}|_{\{1, \psi\}^\perp}) = 1$, whereas the case $n(\mathcal{H}|_{\{1, \psi\}^\perp}) = 2$ is inconclusive (see [80]).

Similarly to the proof of Lemma 6.5, we construct the following symmetric 2-by-2 matrix related to the two constraints in (6.34):

$$D(\lambda) := \begin{bmatrix} \langle (\mathcal{H} - \lambda I)^{-1} \psi, \psi \rangle & \langle (\mathcal{H} - \lambda I)^{-1} \psi, 1 \rangle \\ \langle (\mathcal{H} - \lambda I)^{-1} 1, \psi \rangle & \langle (\mathcal{H} - \lambda I)^{-1} 1, 1 \rangle \end{bmatrix}.$$

If $1 \in \text{Range}(\mathcal{H})$, then

$$\langle \mathcal{H}^{-1}1, 1 \rangle = \sigma_0, \quad \langle \mathcal{H}^{-1}1, \psi \rangle = \langle \mathcal{H}^{-1}\psi, 1 \rangle = 0, \quad \langle \mathcal{H}^{-1}\psi, \psi \rangle = -\frac{1}{2} \frac{d}{dc} \|\psi\|_{L^2}^2 \quad (6.35)$$

where we have used $\mathcal{H}\partial_c \psi = -\psi$ from Lemma 6.2, which can be applied since $z(\mathcal{H}|_{L^2_{\text{odd}}}) = 0$ follows from the proof of Lemma 6.3. By Theorem A.3, we have the following identities:

$$\begin{cases} n(\mathcal{H}|_{\{1, \psi\}^\perp}) = n(\mathcal{H}) - n_0 - z_0, \\ z(\mathcal{H}|_{\{1, \psi\}^\perp}) = z(\mathcal{H}) + z_0, \end{cases} \quad (6.36)$$

where n_0 and z_0 are the numbers of negative and zero eigenvalues of $D(0)$. Since $n(\mathcal{H}) = 2$ and $z(\mathcal{H}) = 1$ by Lemma 6.3, the count (6.36) implies $n(\mathcal{H}|_{\{1, \psi\}^\perp}) = 0$ due to (6.35) if the conditions (6.31) are satisfied and $n(\mathcal{H}|_{\{1, \psi\}^\perp}) = 1$ if the condition (6.32) is satisfied.

If $1 \notin \text{Range}(\mathcal{H})$, then $z(\mathcal{H}) = 2$ but $z(\mathcal{H}|_{X_0}) = 1$ by Lemma 6.4. By

Theorem A.3, the count (6.36) must be replaced by

$$\begin{cases} n(\mathcal{H}|_{\{1,\psi\}^\perp}) = n(\mathcal{H}) - n_0 - z_0, \\ z(\mathcal{H}|_{\{1,\psi\}^\perp}) = z(\mathcal{H}) + z_0 - z_\infty, \end{cases} \quad (6.37)$$

where $z_\infty = 1$ and $n_0 + z_0 = 1$ if the condition (6.33) is satisfied. In this case, $n(\mathcal{H}|_{\{1,\psi\}^\perp}) = 1$ and the periodic wave is spectrally unstable. \square

Remark 6.8. *If $1 \in \text{Range}(\mathcal{H})$, the case $\sigma_0 > 0$ and $\frac{d}{dc}\|\psi\|_{L^2}^2 < 0$ is inconclusive because $n(\mathcal{H}|_{\{1,\psi\}^\perp}) = 2$. In this case, one needs to find if the spectral stability problem has eigenvalues $\lambda \in i\mathbb{R}$ with so-called negative Krein signature, see [80] for further details. The same is true if $1 \notin \text{Range}(\mathcal{H})$ and $\frac{d}{dc}\|\psi\|_{L^2}^2 < 0$.*

6.3 Even Periodic Waves

Here, we consider the even periodic waves and provide the proof of Theorem 6.2. The structure is similar to that of Section 6.2. First, in Theorem 6.5, we obtain the variational characterization of the even periodic waves. Next, a smooth continuation of the even periodic waves is provided in Lemma 6.8. Finally, we prove criteria for the spectral stability in Theorem 6.6.

6.3.1 Variational characterization

The odd periodic wave constructed in Theorem 6.3 and Corollary 6.1 is even after translation $x \mapsto x - \pi/2$. However, since $n(\mathcal{H}) = 2$ by Lemma 6.3 and the eigenfunctions corresponding to the negative eigenvalues are both even after the translation $x \mapsto x - \pi/2$ Figure 6.1, the odd periodic wave translated into an even function cannot be a solution of the constrained minimization problem with a single constraint. Therefore, the same constrained minimization problem (6.14) in a subspace of even functions yields a different branch of periodic waves. The following theorem gives the construction and properties of the even periodic waves.

Theorem 6.5. *Let $\alpha > \frac{1}{2}$ be fixed. For every $c > 0$, there exists the ground state (minimizer) $\chi \in H_{\text{per,even}}^{\frac{\alpha}{2}}$ of the following constrained minimization problem:*

$$q_{c,\text{even}} := \inf_{u \in H_{\text{per,even}}^{\frac{\alpha}{2}}} \left\{ \mathcal{B}_c(u) : \int_{-\pi}^{\pi} u^4 dx = 1 \right\}, \quad (6.38)$$

with the same $\mathcal{B}_c(u)$ as in (6.15). There exists $C > 0$ such that $\psi(x) = C\chi(x)$ satisfies the stationary equation (6.2) with $b = 0$. If $\alpha \leq 2$, the ground state

is the constant solution for $c \in (0, \frac{1}{2}]$ and has the single-lobe profile for $c \in (\frac{1}{2}, \infty)$.

Proof. The proof follows from the proof of Theorem 5.4, mutatis mutandis. Here, we note that in order to ensure that the minimizer has the single-lobe profile, we need to eliminate the constant solution in $H_{\text{per,even}}^{\frac{\alpha}{2}}$. By Lagrange’s Multiplier Theorem, the constrained minimizer $\chi \in H_{\text{per,even}}^{\frac{\alpha}{2}}$ satisfies the stationary equation

$$D^\alpha \chi + c\chi = \mu\chi^3, \tag{6.39}$$

where $\mu = 2\mathcal{B}_c(\chi)$ due to the normalization in (6.38). Since $\mathcal{B}_c(\chi) > 0$, the scaling transformation $\psi = C\chi$ with $C := \sqrt{\mathcal{B}_c(\chi)}$ maps the stationary equation (6.39) to the form (6.2) with $b = 0$. The nonzero constant solution to the stationary equation (6.2) with $b = 0$ is given by $\psi(x) = \sqrt{c/2}$ up to a sign choice. The linearization operator \mathcal{H} in (6.4) evaluated at the constant solution is given by

$$\mathcal{H} = D^\alpha + c - 6\psi^2 = D^\alpha - 2c.$$

Since $n(\mathcal{H}) = 1$ if and only if $c \in (0, \frac{1}{2}]$, the constant wave is a constrained minimizer of (6.38) for $c \in (0, \frac{1}{2}]$ and a saddle point of (6.38) for $c \in (\frac{1}{2}, \infty)$. By the symmetric rearrangements, the global minimizer is given by the constant solution in the former case and by a non-constant solution with the single-lobe profile in the latter case. \square

6.3.2 Smooth continuation

Let $\psi \in H_{\text{per,even}}^\alpha$ be a solution to the stationary equation (6.2) with $b = 0$ for $c \in (\frac{1}{2}, \infty)$ obtained by Theorem 6.5. We introduce again the linearized operator \mathcal{H} by (6.4) and (6.17). Equalities (6.18) and (6.19) hold true for the even periodic wave and.

The following lemma presents the count of $n(\mathcal{H})$ and $z(\mathcal{H})$ for the even periodic wave.

Lemma 6.6. *Let $\alpha \in (\frac{1}{2}, 2]$ and $\psi \in H_{\text{per,even}}^\alpha$ be a solution obtained in Theorem 6.5. Then, $n(\mathcal{H}) = 1$ and*

$$z(\mathcal{H}) = \begin{cases} 1, & \text{if } 1 \in \text{Range}(\mathcal{H}), \\ 2, & \text{if } 1 \notin \text{Range}(\mathcal{H}). \end{cases}$$

Proof. Since $\psi \in H_{\text{per,even}}^\alpha$ is a minimizer of the constrained variational problem (6.38) with only one constraint, we have $n(\mathcal{H}|_{L^2_{\text{even}}}) \leq 1$. On the other hand, we have

$$\langle \mathcal{H}\psi, \psi \rangle_{L^2} = -4\|\psi\|_{L^4}^4 < 0,$$

with even ψ , hence $n(\mathcal{H}|_{L^2_{\text{even}}}) \geq 1$, so that $n(\mathcal{H}|_{L^2_{\text{even}}}) = 1$. By Proposition A.3 (without translation), $n(\mathcal{H}|_{L^2_{\text{odd}}}) = 0$ and $z(\mathcal{H}|_{L^2_{\text{odd}}}) = 1$. Hence, $n(\mathcal{H}) = 1$.

It remains to consider $z(\mathcal{H}) \geq 1$. Since 0 is the second eigenvalue of \mathcal{H} , Proposition A.1 suggests that if $z(\mathcal{H}) = 2$, then the even eigenfunction of $\text{Ker}(\mathcal{H})$ has at most two symmetric nodes on \mathbb{T} . If the periodic wave has the single-lobe profile ψ , then ψ^3 has also the single-lobe profile. By using the same argument as in the proof of Proposition 3.1 in [53], it follows that $z(\mathcal{H}) = 1$ if and only if $\{1, \psi^3\} \in \text{Range}(\mathcal{H})$.

Indeed, if $h \in \text{Ker}(\mathcal{H})$ is an even eigenfunction in the case $z(\mathcal{H}) = 2$ and $\{1, \psi^3\} \in \text{Range}(\mathcal{H})$, then $\langle h, 1 \rangle = 0$ and $\langle h, \psi^3 \rangle = 0$. The first condition suggests that h is sign-indefinite with exactly two symmetric nodes at $\pm x_0$ with $x_0 \in (0, \pi)$, but then $\langle h, \psi^3 - \psi^3(x_0) \rangle$ is sign-definite and cannot be zero, so that no $h \in \text{Ker}(\mathcal{H})$ exists.

Since $\psi^3 \in \text{Range}(\mathcal{H})$ due to equation (5.25), it follows that $z(\mathcal{H}) = 1$ if and only if $1 \in \text{Range}(\mathcal{H})$. \square

The definition of $\mathcal{H}|_{X_0}$, where $X_0 \subset L^2(\mathbb{T})$ is defined by (6.21), is the same as in (6.22). The result of Lemma 6.4 holds true for the even periodic wave $\psi \in H^{\alpha}_{\text{per,even}}$. In order to count the indices $n(\mathcal{H}|_{X_0})$ and $z(\mathcal{H}|_{X_0})$, we shall re-parameterize the even periodic wave to the zero-mean periodic waves.

The even periodic wave with profile ψ has generally nonzero mean value and does not satisfy the boundary-value problem (6.13). Let us define $\psi(x) = a + \phi(x)$, where $a := \frac{1}{2\pi} \int_{-\pi}^{\pi} \psi(x) dx$. Then, $\phi \in H^{\alpha}_{\text{per,even}} \cap X_0$ is a solution of the stationary equation:

$$D^{\alpha} \phi + \omega \phi + \beta = 2(\phi^3 + 3a\phi^2), \quad (6.40)$$

where $\omega := c - 6a^2$ and $\beta := ca - 2a^3$. Since ϕ has zero mean, β can be equivalently written as

$$\beta := \frac{1}{\pi} \int_{-\pi}^{\pi} (\phi^3 + 3a\phi^2) dx, \quad (6.41)$$

so that the stationary equation (6.40) can be rewritten as the boundary-value problem:

$$D^{\alpha} \phi + \omega \phi = 2\Pi_0(\phi^3 + 3a\phi^2). \quad (6.42)$$

The following lemma presents the computation of $n(\mathcal{H}|_{X_0})$ and $z(\mathcal{H}|_{X_0})$.

Lemma 6.7. *Let $\alpha \in (\frac{1}{2}, 2]$ and $\psi \in H^{\alpha}_{\text{per,even}}$ be a solution obtained in Theorem 6.5. Assume that $\omega \in (-1, \infty)$ after the transformation to the stationary equation (6.40). Then, $n(\mathcal{H}|_{X_0}) = 1$ and $z(\mathcal{H}|_{X_0}) = 1$.*

Proof. Transformation $\psi = a + \phi$ and $\omega = c - 6a^2$ changes \mathcal{H} given by (6.4)

into the equivalent form:

$$\mathcal{H} = D^\alpha + c - 6\psi^2 = D^\alpha + \omega - 6\phi^2 - 12a\phi =: \tilde{\mathcal{H}}. \quad (6.43)$$

Then, it follows directly that

$$\langle \mathcal{H}|_{X_0} \phi, \phi \rangle = -4 \int_{-\pi}^{\pi} \phi^4 dx - 6a \int_{-\pi}^{\pi} \phi^3 dx. \quad (6.44)$$

Taking an inner product of the stationary equation (6.40) with ϕ yields the Pohozaev-type identity

$$B_\omega(\phi) = \int_{-\pi}^{\pi} \phi^4 dx + 3a \int_{-\pi}^{\pi} \phi^3 dx. \quad (6.45)$$

where $B_\omega(\phi)$ is defined by (6.15). Since $\omega \in (-1, \infty)$ and $\phi \in H_{\text{per,even}}^\alpha \cap X_0$, we have $B_\omega(\phi) \geq 0$, so that the equality (6.44) can be estimated by

$$\langle \mathcal{H}|_{X_0} \phi, \phi \rangle \leq -2 \int_{-\pi}^{\pi} \phi^4 dx < 0. \quad (6.46)$$

Hence $n(\mathcal{H}|_{X_0}) \geq 1$ and since $n(\mathcal{H}) = 1$ by Lemma 6.6, we have $n(\mathcal{H}|_{X_0}) = 1$. By Theorem A.3, we have the following identities:

$$\begin{cases} n(\mathcal{H}|_{X_0}) = n(\mathcal{H}) - n_0 - z_0, \\ z(\mathcal{H}|_{X_0}) = z(\mathcal{H}) + z_0 - z_\infty, \end{cases} \quad (6.47)$$

where $z_\infty = 1$ if $1 \notin \text{Range}(\mathcal{H})$. It follows from the first equality in (6.47) that $n_0 = z_0 = 0$ since $n(\mathcal{H}) = n(\mathcal{H}|_{X_0}) = 1$. Then, the second equality yields $z(\mathcal{H}|_{X_0}) = z(\mathcal{H}) - z_\infty$. If $z(\mathcal{H}|_{X_0}) = 2$, then $z(\mathcal{H}) \geq 2$, which is in contradiction with Lemma 5.2 extended to the even periodic wave $\psi \in H_{\text{per,even}}^\alpha$. Hence, $z(\mathcal{H}|_{X_0}) = 1$, in which case $z(\mathcal{H}) = 1 + z_\infty$ in agreement with Lemma 6.6. \square

Remark 6.9. *It follows from the proof of Lemma 6.7 that $\sigma_0 > 0$ if $1 \in \text{Range}(\mathcal{H})$, where $\sigma_0 := \langle \mathcal{H}^{-1}1, 1 \rangle$.*

In order to derive the spectral stability result, we shall now extend solutions to the stationary equation (6.40) with respect to two independent parameters (ω, a) with β being a C^1 function of (ω, a) . Since the periodic waves satisfy the stationary equation (6.2) with $b = 0$, where c is the only parameter, parameters ω, a , and β in the stationary equation (6.40) are parameterized by c , hence a is not independent of ω . The following lemma allows us to extend zero-mean solutions to the boundary-value problem (6.42) with respect to independent parameters (ω, a) near each uniquely defined point (ω_0, a_0) .

Lemma 6.8. *Assume $\alpha \in (\frac{1}{2}, 2]$ and $\phi_0 \in H_{\text{per,even}}^\alpha \cap X_0$ be a solution to the boundary-value problem (6.42) with $\omega = \omega_0 \in (-1, \infty)$ and $a = a_0 \in \mathbb{R}$. Then, there exists a C^1 mapping in an open subset of (ω_0, a_0) denoted by $\mathcal{O} \subset \mathbb{R}^2$:*

$$\mathcal{O} \ni (\omega, a) \mapsto \phi(\cdot; \omega, a) \in H_{\text{per,even}}^\alpha \cap X_0, \quad (6.48)$$

such that $\phi(\cdot; \omega_0, a_0) = \phi_0$.

Proof. The proof repeats the arguments in the proof of Lemma 6.2. Let $\Upsilon : (-1, \infty) \times \mathbb{R} \times H_{\text{per,even}}^\alpha \cap X_0 \rightarrow L_{\text{even}}^2(\mathbb{T}) \cap X_0$ be defined by

$$\Upsilon(\omega, a, g) := D^\alpha g + \omega g - 2\Pi_0 (g^3 + 3ag^2). \quad (6.49)$$

By hypothesis we have $\Upsilon(\omega_0, a_0, \phi_0) = 0$. Moreover, since Υ is smooth, its Fréchet derivative with respect to g evaluated at (ω_0, a_0, ϕ_0) is given by

$$D_g \Upsilon(\omega_0, a_0, \phi_0) = D^\alpha + \omega_0 - 6\Pi_0 (\phi_0^2 + 2a_0 \phi_0) = D^\alpha + c_0 - 6\Pi_0 \psi_0^2 = \mathcal{H}|_{X_0}, \quad (6.50)$$

where we have unfolded the previous transformation $\psi_0 = a_0 + \phi_0$ and $\omega_0 = c_0 - 6a_0^2$ and used the same operator as in (6.22) computed at ψ_0 .

Since $z(\mathcal{H}|_{X_0}) = 1$ by Lemma 6.7 and $\text{Ker}(\mathcal{H}|_{X_0}) = \text{span}\{\partial_x \phi_0\}$ with $\partial_x \phi_0 \notin H_{\text{per,even}}^\alpha \cap X_0$, we conclude that $D_g \Upsilon(\omega_0, a_0, \phi_0)$ is one-to-one. Next, we show that $D_g \Upsilon(\omega_0, a_0, \phi_0)$ is onto. Since $H_{\text{per,even}}^\alpha \cap X_0$ is compactly embedded in $L_{\text{even}}^2(\mathbb{T}) \cap X_0$ if $\alpha > 1/2$, the operator $\mathcal{H}|_{X_0}$ has compact resolvent. In addition, $\mathcal{H}|_{X_0}$ is a self-adjoint operator, hence its spectrum $\sigma(\mathcal{H}|_{X_0})$ consists of isolated eigenvalues with finite algebraic multiplicities. Since $D_g \Upsilon(\omega_0, a_0, \phi_0)$ is one-to-one, it follows that 0 is not in the spectrum of $D_g \Upsilon(\omega_0, a_0, \phi_0)$, so that it is onto. Hence, $D_g \Upsilon(\omega_0, a_0, \phi_0)$ is a bounded linear operator with a bounded inverse. Thus, since Υ and its derivative with respect to g are smooth maps on their domains, the result follows from the implicit function theorem. \square

Recall that $\mathcal{H} = \tilde{\mathcal{H}}$ in (6.43). Extension of relations (6.18) and (6.19) yields

$$\tilde{\mathcal{H}}1 = \omega - 12a\phi - 6\phi^2 \quad (6.51)$$

and

$$\tilde{\mathcal{H}}\phi = -\beta - 6a\phi^2 - 4\phi^3, \quad (6.52)$$

where $\beta = \beta(\omega, a)$ is a C^1 function by Lemma 6.8 and the representation (6.41). Therefore, we also obtain two more relations:

$$\tilde{\mathcal{H}}\partial_\omega \phi = -\partial_\omega \beta - \phi, \quad (6.53)$$

and

$$\tilde{\mathcal{H}}\partial_a\phi = -\partial_a\beta + 6\phi^2. \quad (6.54)$$

These relations allow us to completely characterize $\text{Ker}(\mathcal{H})$, which can be two-dimensional if $1 \notin \text{Range}(\mathcal{H})$ by Lemma 6.6.

Lemma 6.9. *Assume $\alpha \in (\frac{1}{2}, 2]$ and $\phi \in H_{\text{per,even}}^\alpha \cap X_0$ be a single-lobe solution to the boundary-value problem (6.42) with $\omega \in (-1, \infty)$ and $a \in \mathbb{R}$. Then, $z(\mathcal{H}) = 1$ if and only if $s_0 := \omega - \partial_a\beta + 12a\partial_\omega\beta \neq 0$.*

Proof. Eliminating ϕ and ϕ^2 from (6.51), (6.53), and (6.54) yields

$$\tilde{\mathcal{H}}(1 + \partial_a\phi - 12a\partial_\omega\phi) = \omega - \partial_a\beta + 12a\partial_\omega\beta =: s_0. \quad (6.55)$$

Recall that $\tilde{\mathcal{H}} = \mathcal{H}$ in (6.43). If $s_0 \neq 0$, then $1 \in \text{Range}(\mathcal{H})$, so that $z(\mathcal{H}) = 1$ holds by Lemma 6.6. If $s_0 = 0$, then $1 + \partial_a\phi - 12a\partial_\omega\phi \in \text{Ker}(\mathcal{H})$ in addition to $\partial_x\phi \in \text{Ker}(\mathcal{H})$. \square

6.3.3 Spectral stability of even periodic waves

We are now ready to provide the criterion for spectral stability of the even periodic waves. This result is given by the following theorem.

Theorem 6.6. *Assume $\alpha \in (\frac{1}{2}, 2]$ and $\phi \in H_{\text{per,even}}^\alpha \cap X_0$ be a single-lobe solution to the boundary-value problem (6.42) with $\omega \in (-1, \infty)$ and $a \in \mathbb{R}$. The periodic wave is spectrally stable if and only if*

$$\frac{\partial}{\partial\omega} \|\phi\|_{L^2}^2 \geq 0, \quad (6.56)$$

independently of either $z(\mathcal{H}) = 1$ or $z(\mathcal{H}) = 2$.

Proof. We proceed similarly to the proof of Theorem 6.4. If $1 \in \text{Range}(\mathcal{H})$, we use (6.55) and compute

$$\sigma_0 := \langle \mathcal{H}^{-1}1, 1 \rangle = \frac{2\pi}{s_0},$$

where $s_0 \neq 0$ by Lemma 6.9. For the even periodic wave, we have $\sigma_0 > 0$ (see Remark 6.9), so that $s_0 > 0$. Eliminating constant term from (6.53) and (6.55) yields

$$\tilde{\mathcal{H}} [\partial_\omega\phi + s_0^{-1}\partial_\omega\beta(1 + \partial_a\phi - 12a\partial_\omega\phi)] = -\phi, \quad (6.57)$$

By projecting (6.53) to $\partial_a\phi$ and (6.54) to $\partial_\omega\phi$, it is easy to verify that

$$6\langle \phi^2, \partial_\omega\phi \rangle + \langle \phi, \partial_a\phi \rangle = 0. \quad (6.58)$$

Using (6.57) yields

$$\langle \mathcal{H}^{-1}1, \phi \rangle = \langle \mathcal{H}^{-1}\phi, 1 \rangle = -\sigma_0 \partial_\omega \beta,$$

where we have used that

$$2\pi \partial_\omega \beta = 6\langle \phi^2, \partial_\omega \phi \rangle + 12a\langle \phi, \partial_\omega \phi \rangle = -\langle \phi, \partial_a \phi \rangle + 12a\langle \phi, \partial_\omega \phi \rangle,$$

which follows from (6.41) and (6.58). Finally, we obtain from (6.57) and (6.58) that

$$\langle \mathcal{H}^{-1}\phi, \phi \rangle = -\langle \phi, \partial_\omega \phi \rangle + \sigma_0 (\partial_\omega \beta)^2.$$

Theorem A.3, we have the following identities:

$$\begin{cases} n(\mathcal{H}|_{\{1, \psi\}^\perp}) = n(\mathcal{H}) - n_0 - z_0, \\ z(\mathcal{H}|_{\{1, \psi\}^\perp}) = z(\mathcal{H}) + z_0, \end{cases} \quad (6.59)$$

where n_0 and z_0 are the numbers of negative and zero eigenvalues of $D(0)$ in the proof of Theorem 6.4. Since

$$\det D(0) = -\sigma_0 \langle \phi, \partial_\omega \phi \rangle.$$

and $\sigma_0 > 0$, we have $n_0 + z_0 = 1$ if the condition (6.56) is satisfied and $n_0 + z_0 = 0$ if it is not satisfied. Since $n(\mathcal{H}) = 1$ and $z(\mathcal{H}) = 1$ by Lemmas 6.6 and 6.9, the count (6.59) implies $n(\mathcal{H}|_{\{1, \psi\}^\perp}) = 0$ if the condition (6.56) is satisfied and $n(\mathcal{H}|_{\{1, \psi\}^\perp}) = 1$ if it is not satisfied. This gives the assertion of the theorem if $1 \in \text{Range}(\mathcal{H})$.

If $1 \notin \text{Range}(\mathcal{H})$, then $z(\mathcal{H}) = 2$ and $s_0 = 0$. In this case, the count (6.59) should be adjusted as

$$\begin{cases} n(\mathcal{H}|_{\{1, \psi\}^\perp}) = n(\mathcal{H}) - n_0 - z_0, \\ z(\mathcal{H}|_{\{1, \psi\}^\perp}) = z(\mathcal{H}) + z_0 - z_\infty, \end{cases} \quad (6.60)$$

where $z_\infty = 1$. At the same time, $n_0 + z_0 = 1$ if and only if the same condition (6.56) is satisfied and $n_0 + z_0 = 0$ if it is not satisfied. Hence the stability conclusion remains unchanged if $1 \notin \text{Range}(\mathcal{H})$. \square

Remark 6.10. *The momentum (1.11) computed at the even periodic wave with the profile ψ and the decomposition $\psi = a + \phi$ is given by*

$$F(\psi) = F(\phi) + \pi a^2.$$

If ω and a are independent parameters, it is true that

$$\frac{\partial}{\partial \omega} F(\phi) = \frac{\partial}{\partial \omega} F(\psi), \quad (6.61)$$

however, this quantity is not defined by the dependence of the momentum $F(\psi)$ on the original wave speed c . In addition, if ψ satisfies the stationary equation (6.2) with $b = 0$, then a depends on ω , therefore, the dependence of $F(\psi)$ versus ω does not generally provide information about the slope condition (6.61). See also numerical approximations in the next section.

6.4 Examples and Numerical Illustrations

Here, we provide examples for the odd and even periodic waves.

6.4.1 Stokes Expansion for Odd Waves

Stokes expansions of small-amplitude periodic waves near the bifurcation point $c = -1$ are rather standard in getting precise results on the existence and stability of periodic waves. The following proposition describes the properties of the small-amplitude periodic waves.

Proposition 6.1. *For each $\alpha \in (\frac{1}{2}, 2]$, there exists $c_0 \in (-1, \infty)$ such that the odd periodic wave exists for $c \in (-1, c_0)$ with $n(\mathcal{H}) = 2$, $z(\mathcal{H}) = 1$ and is spectrally stable.*

Proof. We solve the stationary equation (6.2) with $b = 0$ in the space of odd functions by using Stokes expansions in terms of small amplitude A :

$$\psi(x) = A\psi_1(x) + A^3\psi_3(x) + \mathcal{O}(A^5) \quad (6.62)$$

and

$$c = -1 + A^2c_2 + \mathcal{O}(A^4). \quad (6.63)$$

We obtain recursively: $\psi_1(x) = \sin(x)$,

$$\psi_3(x) = \frac{1}{2(1 - 3^\alpha)} \sin(3x),$$

and $c_2 = \frac{3}{2}$ uniformly in α .

Since $\mathcal{H} = D^\alpha - 1 + \mathcal{O}(A^2)$, then $1 \in \text{Range}(\mathcal{H})$ for small A , so that $n(\mathcal{H}) = 2$ and $z(\mathcal{H}) = 1$ for any $\alpha \in (\frac{1}{2}, 2]$ by Lemma 6.3.

Furthermore, $\mathcal{H}^{-1}1 = -1 + \mathcal{O}(A^2)$, so that $\sigma_0 = \langle \mathcal{H}^{-1}1, 1 \rangle = -2\pi + \mathcal{O}(A^2) < 0$, which implies $n(\mathcal{H}|_{\{1, \psi^3\}^\perp}) = 0$ and $z(\mathcal{H}|_{\{1, \psi^3\}^\perp}) = 1$ by Lemma 6.5. Hence, the odd periodic wave for small amplitude A represents a local

minimizer of the variational problem (6.25) with two constraints for any $\alpha \in (\frac{1}{2}, 2]$.

Finally, we obtain $\|\psi\|_{L^2}^2 = \pi A^2 + \mathcal{O}(A^4)$ so that

$$\frac{d}{dc} \|\psi\|_{L^2}^2 = \frac{2\pi}{3} [1 + \mathcal{O}(A^2)] > 0.$$

By Theorem 6.4, the Stokes wave (6.62) for small A is spectrally stable since the criterion (6.31) is satisfied. \square

Remark 6.11. *For c near -1 , the small-amplitude wave of Proposition 6.1 coincides with the odd periodic wave obtained in Theorem 6.3 and Corollary 6.1. This follows from local uniqueness of the small-amplitude wave in the neighborhood of $(0, -1)$ in $H_{\text{per,odd}}^{\frac{\alpha}{2}} \times \mathbb{R} \ni (\psi, c)$ and the result of Lemma 6.1 which guarantees that $\psi \rightarrow 0$ in $H_{\text{per,odd}}^{\frac{\alpha}{2}}$ as $c \rightarrow -1$.*

6.4.2 Exact Solutions for Odd Wave with $\alpha = 2$

In the case of the modified KdV equation ($\alpha = 2$), the stationary equation (6.2) with $b = 0$ can be solved in the space of odd functions by using the Jacobian cnoidal function [15, 36].

Let us recall the normalized second-order equation

$$\psi_0''(z) + (1 - 2k^2)\psi_0(z) + 2\psi_0(z)^3 = 0, \quad (6.64)$$

which admits the periodic solution $\psi_0(z) = k \text{cn}(z; k)$ with the period $4K(k)$, where $K(k)$ is the complete elliptic integral of the first kind and $k \in (0, 1)$. The periodic solution also satisfies the first-order invariant given by

$$(\psi_0')^2 + (1 - 2k^2)\psi_0^2 + \psi_0^4 = k^2(1 - k^2). \quad (6.65)$$

By adopting a scaling transformation and a translation of the even function $\text{cn}(z; k)$ by a quarter-period, we obtain the exact solution for the odd periodic wave in the form:

$$\begin{aligned} \psi(x) &= \frac{2}{\pi} k K(k) \text{cn} \left[\frac{2}{\pi} K(k)x - K(k); k \right] \\ &= \frac{2}{\pi} k \sqrt{1 - k^2} K(k) \frac{\text{sn} \left[\frac{2}{\pi} K(k)x; k \right]}{\text{dn} \left[\frac{2}{\pi} K(k)x; k \right]} \end{aligned} \quad (6.66)$$

with

$$c = \frac{4}{\pi^2} K(k)^2 (2k^2 - 1). \quad (6.67)$$

We recall some properties of complete elliptic integrals $K(k)$ and $E(k)$ of the

first and second kinds, respectively:

$$\begin{aligned} \text{(a)} \quad & E(0) = K(0) = \frac{\pi}{2}, \\ \text{(b)} \quad & E(k) \rightarrow 1, \quad K(k) \rightarrow \infty, \quad \text{as } k \rightarrow 1, \end{aligned}$$

and

$$\text{(c)} \quad \frac{d}{dk}E(k) = \frac{E(k) - K(k)}{k} < 0, \quad \frac{d}{dk}K(k) = \frac{E(k)}{k(1-k^2)} - \frac{K(k)}{k} > 0.$$

It follows from (a) and (c) that

$$(1 - k^2)K(k) < E(k) < K(k), \quad k \in (0, 1). \quad (6.68)$$

The following proposition summarizes properties of the odd periodic waves for $\alpha = 2$. These properties were also studied in [36] and [15].

Proposition 6.2. *Fix $\alpha = 2$. The odd periodic wave (6.66) exists for every $c \in (-1, \infty)$ with $n(\mathcal{H}) = 2$ and $z(\mathcal{H}) = 1$. There exists $c_* \in (-1, \infty)$ such that the odd periodic wave is spectrally stable for $c \in (-1, c_*]$ and is spectrally unstable with one real positive eigenvalue for $c \in (c_*, \infty)$.*

Proof. The mapping $(0, 1) \ni k \mapsto c(k) \in (-1, \infty)$ is one-to-one and onto. This follows from

$$\frac{\pi^2}{8} \frac{dc}{dk} = \frac{K(k)}{k(1-k^2)} [(1-k^2)[K(k) - E(k)] + k^2 E(k)] > 0,$$

where property (6.68) has been used. Hence, the odd periodic wave parameterized by $k \in (0, 1)$ in (6.66) and (6.67) exists for every $c \in (-1, \infty)$.

The first five eigenvalues and eigenfunctions of the normalized linearized operator

$$\mathcal{H}_0 = -\partial_z^2 + 2k^2 - 1 - 6k^2 \text{cn}(z; k)^2 \quad (6.69)$$

are known in space $L^2(-2K(k), 2K(k))$ in the explicit form [12, 36]. The two negative eigenvalues and a simple zero eigenvalue with the corresponding eigenfunctions are given by

$$\lambda_0 = 1 - 2k^2 - 2\sqrt{1 - k^2 + k^4}, \quad \lambda_1 = -3k^2, \quad \lambda_2 = 0, \quad (6.70)$$

$$\varphi_0(z) = 1 + k^2 + \sqrt{1 - k^2 + k^4} - 3k^2 \text{sn}(z; k)^2, \quad (6.71)$$

$$\varphi_1(z) = \text{cn}(z; k) \text{dn}(z; k), \quad (6.72)$$

$$\varphi_2(z) = \text{sn}(z; k) \text{dn}(z; k). \quad (6.73)$$

The next two positive eigenvalues with the corresponding eigenfunctions are

given by

$$\lambda_3 = 3(1 - k^2), \quad \lambda_4 = 1 - 2k^2 + 2\sqrt{1 - k^2 + k^4}, \quad (6.74)$$

$$\varphi_3(z) = \operatorname{sn}(z; k)\operatorname{cn}(z; k), \quad (6.75)$$

$$\varphi_4(z) = 1 + k^2 - \sqrt{1 - k^2 + k^4} - 3k^2\operatorname{sn}(z; k)^2. \quad (6.76)$$

Eigenvalues and eigenvectors of the linearized operator \mathcal{H} are obtained after the same scaling and translational transformation as in (6.66), see Figure 6.1. In agreement with Lemma 6.3, we have $n(\mathcal{H}) = 2$, $z(\mathcal{H}) = 1$, and $1 \in \operatorname{Range}(\mathcal{H})$ for every $c \in (-1, \infty)$. Moreover, we compute

$$\frac{1}{2\sqrt{1 - k^2 + k^4}}\mathcal{H}_0 \left[\frac{\lambda_4\varphi_0 - \lambda_0\varphi_4}{\lambda_0\lambda_4} \right] = 1 \quad \text{and} \quad \frac{1}{2\sqrt{1 - k^2 + k^4}}[\varphi_0 - \varphi_4] = 1,$$

from which it follows that

$$\langle \mathcal{H}_0^{-1}1, 1 \rangle = \frac{\lambda_4\langle \varphi_0, 1 \rangle - \lambda_0\langle \varphi_4, 1 \rangle}{2\sqrt{1 - k^2 + k^4}\lambda_0\lambda_4} = -4[2E(k) - K(k)].$$

Since

$$\frac{d}{dk}kE(k) = 2E(k) - K(k), \quad (6.77)$$

$$\frac{d^2}{dk^2}kE(k) = \frac{(1 - k^2)[E(k) - K(k)] - k^2E(k)}{k(1 - k^2)} < 0, \quad (6.78)$$

in addition to (b), there exists exactly one value of k , labeled as $k^* \approx 0.909$ in [36], such that $\langle \mathcal{H}_0^{-1}1, 1 \rangle < 0$ for $k \in (0, k^*)$ and $\langle \mathcal{H}_0^{-1}1, 1 \rangle > 0$ for $k \in (k^*, 1)$. Up to a positive scaling factor, $\langle \mathcal{H}_0^{-1}1, 1 \rangle$ gives the value of $\sigma_0 = \langle \mathcal{H}^{-1}1, 1 \rangle$. By Lemma 6.5, this implies that $n(\mathcal{H}|_{\{1, \psi^3\}^\perp}) = 0$ for $k \in (0, k^*]$ and $n(\mathcal{H}|_{\{1, \psi^3\}^\perp}) = 1$ for $k \in (k^*, 1)$. Therefore, there exists a bifurcation at $k = k^*$ such that the odd periodic wave (6.66) is a local minimizer of the variational problem (6.25) with two constraints for $k \in (0, k^*)$ and a saddle point for $k \in (k^*, 1)$. The value of k^* defines uniquely a value $c^* \approx 1.425$ by (6.67).

Finally, we obtain

$$\|\psi\|_{L^2}^2 = \frac{8}{\pi}K(k) [E(k) - (1 - k^2)K(k)] > 0$$

and

$$\frac{\pi}{9} \frac{d}{dk} \|\psi\|_{L^2}^2 = \frac{1}{k(1-k^2)} [(1-k^2)K(k)[K(k) - E(k)] + E(k)[E(k) - (1-k^2)K(k)]] > 0,$$

for every $k \in (0, 1)$, where the property (6.68) has been used. By Theorem 6.4 due to the stability and instability criteria (6.31) and (6.32), the odd periodic wave (6.66) with the speed (6.67) is spectrally stable for $c \in (-1, c^*]$ and is spectrally unstable with exactly one real positive eigenvalue if $c \in (c^*, \infty)$. \square

Remark 6.12. *The cnoidal wave of Proposition 6.2 coincides with the odd periodic wave obtained in Theorem 6.3 and Corollary 6.1 for $\alpha = 2$. This follows from uniqueness of smooth, odd, and 2π -periodic solutions of the differential equation*

$$-\psi'' + c\psi = 2\psi^3, \quad (6.79)$$

with $c \in (-1, \infty)$, where the second-order equation (6.79) is the Euler–Lagrange equation for the variational problem in Theorem 6.3 and Corollary 6.1.

The claim in Remark 6.12 is based on the following proposition. Since the previous results in [45, 89] are not sufficient for the proof of this proposition, we provide a simple proof based on explicit computations.

Proposition 6.3. *For every $c \in \mathbb{R}$, there exists a family of L -periodic, sign-indefinite solutions of the differential equation (6.79), which can be parameterized by the value \mathcal{I} of the first-order invariant*

$$\mathcal{I} = (\psi')^2 - c\psi^2 + \psi^4. \quad (6.80)$$

The mapping $\mathcal{I} \mapsto L$ is monotonically decreasing for every $c \in \mathbb{R}$ with $L \in (0, 2\pi|c|^{-1/2})$ for $c < 0$ and $L \in (0, \infty)$ for $c \geq 0$. Consequently, the odd, 2π -periodic solution of the differential equation (6.79) for $c \in (-1, \infty)$ is unique.

Proof. Elementary phase-plane analysis (see [45, 89]) shows the existence of the L -periodic, sign-indefinite solutions of the differential equation (6.79) integrable with the first-order invariant (6.80). By using the scaling transformation, the L -periodic sign-indefinite solution is obtained from the periodic solution $\psi_0(z) = k \operatorname{cn}(z; k)$ of the normalized equations (6.64) and (6.65) in the form:

$$\psi(x) = k \alpha \operatorname{cn}(\alpha x; k), \quad \alpha := \left(\frac{c}{2k^2 - 1} \right)^{1/2}, \quad (6.81)$$

where $k \in (0, \frac{1}{\sqrt{2}})$ if $c < 0$ and $k \in (\frac{1}{\sqrt{2}}, 1)$ if $c > 0$. For $c = 0$, the choice $k = \frac{1}{\sqrt{2}}$ is unique but parameter α is arbitrary.

It follows from (6.81) that period L and parameter \mathcal{I} are expressed uniquely by

$$L = 4\alpha^{-1}K(k), \quad \mathcal{I} = \alpha^4 k^2(1 - k^2), \quad (6.82)$$

where α depends on k if $c \neq 0$. Computing derivatives in k yields

$$\frac{d\mathcal{I}}{dk} = -\frac{2kc}{(1 - 2k^2)^3}, \quad \frac{dL}{dk} = \frac{4}{\sqrt{c(2k^2 - 1)}} \left[(1 - 2k^2) \frac{d}{dk} K(k) - 2kK(k) \right].$$

If $c > 0$ and $k \in (\frac{1}{\sqrt{2}}, 1)$, then $\frac{d\mathcal{I}}{dk} > 0$ and $\frac{dL}{dk} < 0$ so that the mapping $\mathcal{I} \mapsto L$ is monotonically decreasing. As $k \rightarrow \frac{1}{\sqrt{2}}$, $\alpha \rightarrow \infty$ and $L \rightarrow 0$. As $k \rightarrow 1$, $K(k) \rightarrow \infty$ and $L \rightarrow \infty$.

If $c < 0$ and $k \in (0, \frac{1}{\sqrt{2}})$, then $\frac{d\mathcal{I}}{dk} < 0$ and $\frac{dL}{dk} < 0$ due to (6.68) and

$$\frac{dL}{dk} = \frac{4}{\sqrt{c(2k^2 - 1)}k(1 - k^2)} \left[(1 - k^2)(E(k) - K(k)) - k^2K(k) \right] < 0,$$

so that the mapping $\mathcal{I} \mapsto L$ is also monotonically decreasing. As $k \rightarrow \frac{1}{\sqrt{2}}$, $\alpha \rightarrow \infty$ and $L \rightarrow 0$. As $k \rightarrow 0$, $K(k) \rightarrow \frac{\pi}{2}$ and $L \rightarrow 2\pi|c|^{-1/2}$.

If $c = 0$ and $k = \frac{1}{\sqrt{2}}$, then the parameter $\alpha \in \mathbb{R}$ is arbitrary and it follows from (6.81) that $\mathcal{I} = C/L^4$ for some $C > 0$ so that the mapping $\mathcal{I} \mapsto L$ is also monotonically decreasing and $L \in (0, \infty)$.

Since the period function $L = L(\mathcal{I})$ is monotonically decreasing in \mathcal{I} , there exists exactly one odd, 2π -periodic solution for every $c \in (-1, \infty)$ and by uniqueness of solutions to differential equations, this unique solution is given by the cnoidal wave (6.66) and (6.67). \square

6.4.3 Numerical Approximations for Odd Waves

Here, we numerically compute solutions of the stationary equation (6.2) using Newton's method in the Fourier space. For better performance, the odd periodic wave with profile ψ in Theorem 6.3 is translated by a quarter period $\pi/2$ to an even function of x . The starting iteration is generated from the Stokes expansion (6.62) after the translation and this solution is uniquely continued in c for all $c \in (-1, \infty)$. This family of solutions correspond to $b = 0$ in the stationary equation (6.2).

Additionally, we add a perturbation to the profile ψ to preserve the even symmetry but to break the odd symmetry after the translation. Numerical iterations converge back to the same family of solutions with $b = 0$ for $c < c_*$, where $c_* \in (-1, \infty)$ is the bifurcation point for which a nontrivial solution in Lemma 6.4 exists. The value of c_* exists for all $\alpha \in (\frac{1}{2}, 2]$. When $c > c_*$, numerical iterations converge to a new family of solutions to the stationary

equation (6.2) with $b \neq 0$, which is then continued with respect to c . Convergence of numerical iterations is measured by the L^2 norm of the residue for the stationary equation (6.2), with the tolerance equals to 10^{-10} .

Figure 6.2 presents the periodic wave solutions to the stationary equation (6.2) for $\alpha = 2$. The top left panel shows the profiles of ψ of the family with $b = 0$ for three different values of c : near the Stokes wave limit (blue curve), near the bifurcation point c_* (black curve) and when c is away from the bifurcation point c_* (red curve). The top right panel shows the profiles of ψ of the bifurcating family with $b \neq 0$ near the bifurcation point c_* (black curve) and increasingly away from the bifurcation point (blue and red curves). The vertical lines show the symmetry points at $x = \pm\pi/2$. The family with $b = 0$ has odd symmetry with respect to these points, whereas the family with $b \neq 0$ does not have this symmetry; both families are even at $x = 0$ and $x = \pm\pi$.

The middle left panel of Figure 6.2 shows the dependence of b in the stationary equation (6.2) versus speed c . The pitchfork bifurcation point is located at $c_* \approx 1.425$. The two symmetric branches of solutions with $b > 0$ and $b < 0$ are obtained by using the positive and negative perturbations to the family of solutions with $b = 0$.

The middle right panel of Figure 6.2 shows the momentum $F(\psi)$ versus c . The bottom left panel shows the dependence of σ_0 versus c . The bottom right panel displays the lowest eigenvalues of \mathcal{H} versus c . The blue curve shows the family of solutions with $b = 0$, whereas the red curve shows the family of solutions with $b \neq 0$.

As shown on the middle right panel of Figure 6.2, the momentum $F(\psi)$ is increasing function of c for both the families. In agreement with the theory, σ_0 for the family with $b = 0$ changes sign from negative to positive when c passes through the bifurcation point c_* , see the bottom left panel of Figure 6.2. By Theorem 6.4, it follows that the family of solutions with $b = 0$ is spectrally stable for $c < c_*$ and spectrally unstable for $c > c_*$.

On the other hand, the bifurcating family with $b \neq 0$ has $\sigma_0 < 0$ near the bifurcation point but there exists another point $\hat{c}_* > c_*$ such that σ_0 diverges at $c = \hat{c}_*$ and becomes positive for $c > \hat{c}_*$. This agrees with the behavior of the lowest eigenvalues of \mathcal{H} shown on the bottom right panel of Figure 6.2 since $z(\mathcal{H}) = 2$ at $c = \hat{c}_*$, $n(\mathcal{H}) = 2$ for $c < \hat{c}_*$ and $n(\mathcal{H}) = 1$ for $c > \hat{c}_*$. Lemma 6.5 and Theorem 6.4 are trivially extended to the family with $b \neq 0$ and they confirm that for both cases of $c < \hat{c}_*$ and $c > \hat{c}_*$, the periodic waves of the family with $b \neq 0$ correspond to minimizers of the constrained variational problem (5.6) and they are spectrally stable for $c > c_*$.

Figure 6.3 presents similar results for the periodic wave solutions to the stationary equation (6.2) for $\alpha = 1$. Note that bifurcation point c_* moves to the left and becomes $c_* \approx -0.310$. The existence and stability of the family of solutions with $b = 0$ is very similar with the only difference that the dependence

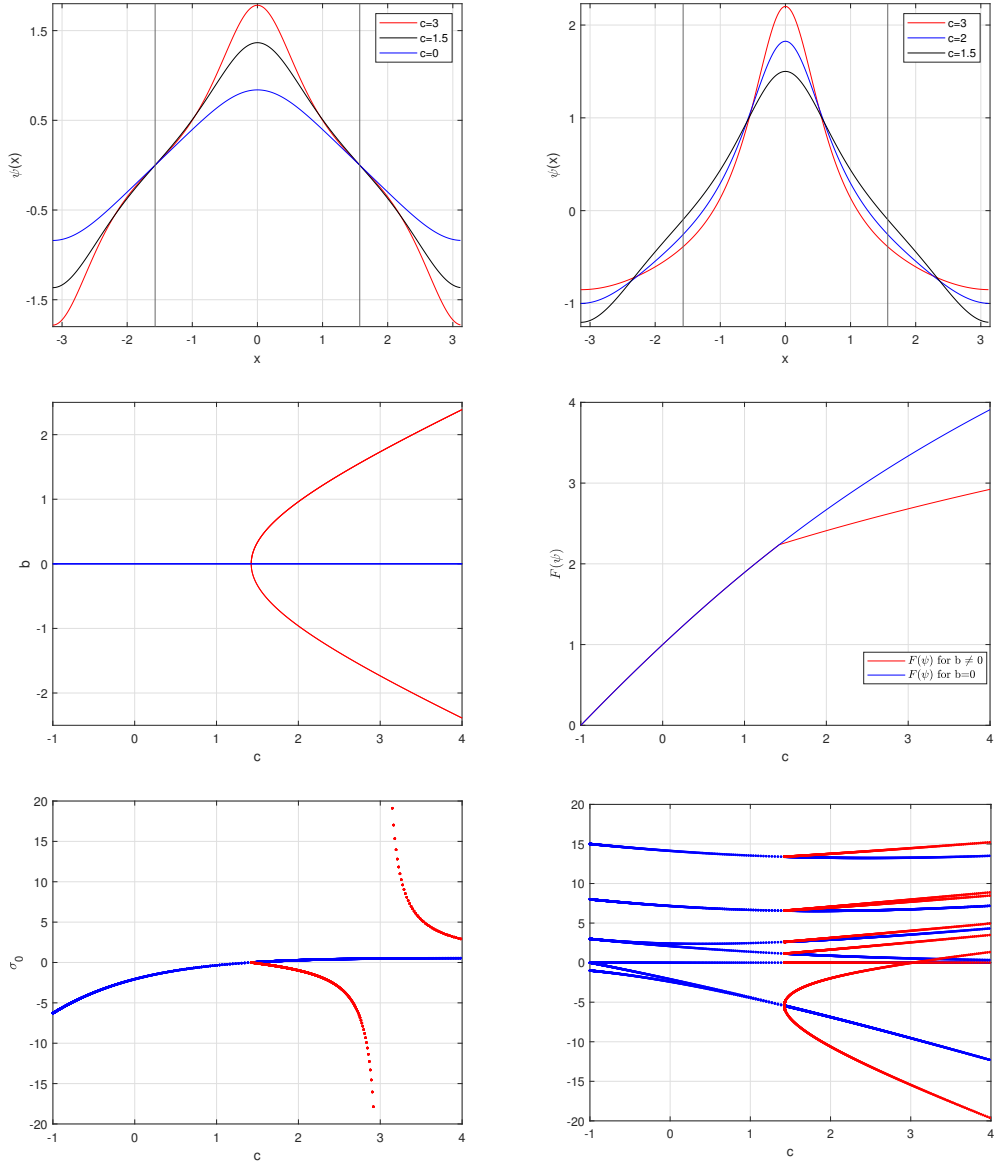


Figure 6.2: Periodic waves for $\alpha = 2$. Top left: Profiles of ψ with $b = 0$ for three different values of c . Top right: Profiles of ψ with $b \neq 0$ for three values of c . Middle left: Dependence of b versus c showing the pitchfork bifurcation point c_* . Middle right: Dependence of the momentum $F(\psi)$ versus c . Bottom left: Dependence of σ_0 versus c . Bottom right: The lowest eigenvalues of \mathcal{H} versus c . The blue (red) line corresponds to the family with $b = 0$ ($b \neq 0$).

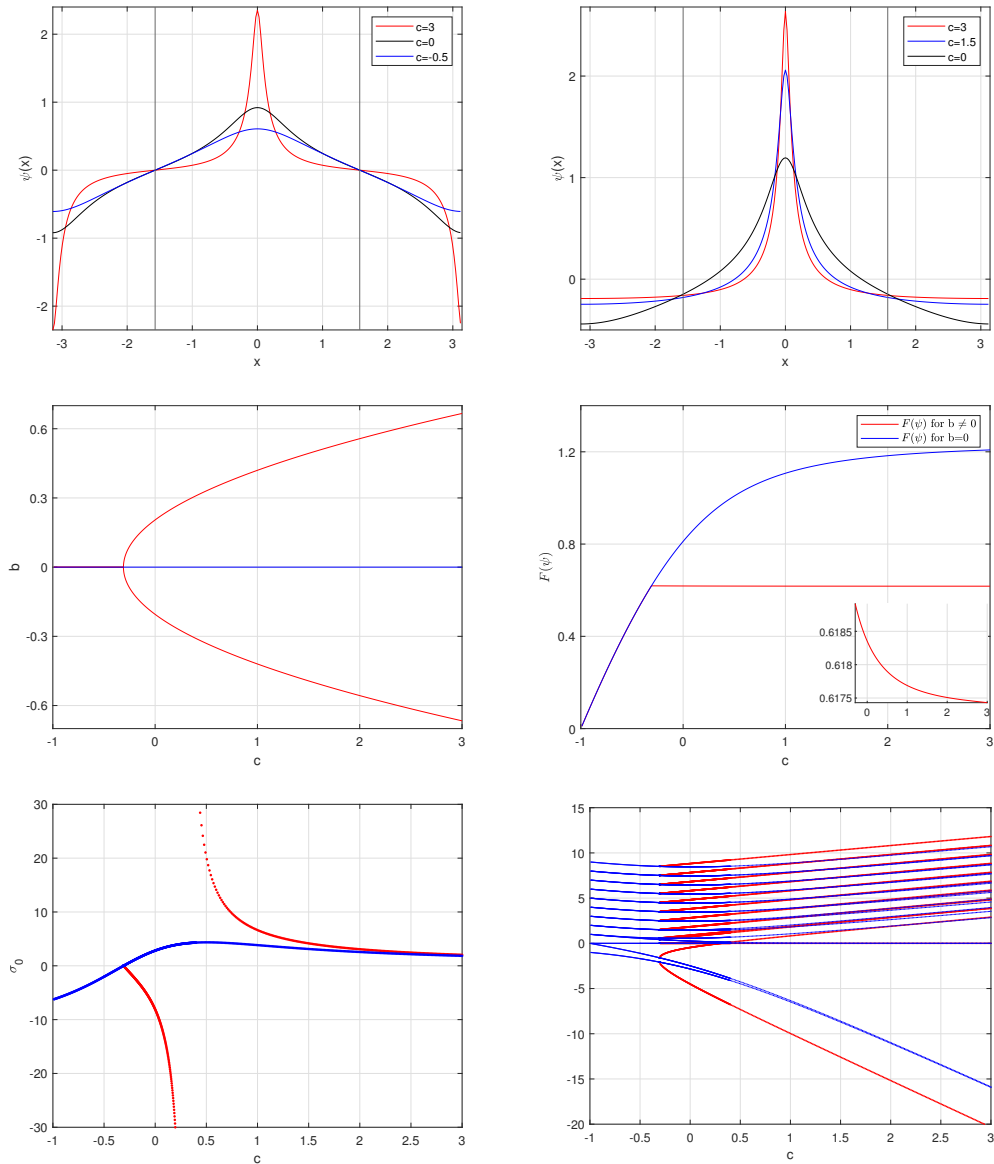


Figure 6.3: The same as Figure 6.2 but for $\alpha = 1$.

of the momentum $F(\psi)$ versus speed c approaches the horizontal asymptote as $c \rightarrow \infty$ since $\alpha = 1$ is the L^2 -critical modified Benjamin–Ono equation [20, 58, 70] and the periodic waves with the single-lobe profile converge to the solitary waves in the limit $c \rightarrow \infty$.

The stability of the family of solutions with $b \neq 0$ is however different. The momentum $F(\psi)$ is a decreasing function of the speed c , as the insert shows, hence the family of solutions is spectrally unstable for all $c > c_*$. It also approaches to the horizontal asymptote as $c \rightarrow \infty$. Profiles of both the families in the limit of large c approach the soliton profile, but the family with $b = 0$ contains two solitons on the period, whereas the family with $b \neq 0$ contains a single soliton on the period. Hence the momentum $F(\psi)$ of the family with $b = 0$ approaches the double horizontal asymptote as $c \rightarrow \infty$ compared to the momentum $F(\psi)$ of the family with $b \neq 0$.

We have checked again that σ_0 along the family with $b = 0$ changes sign from negative to positive at the bifurcation point $c = c_*$, whereas σ_0 along the family with $b \neq 0$ is negative for $c \in (c_*, \hat{c}_*)$ and positive for $c \in (\hat{c}_*, \infty)$, where \hat{c}_* is the point where $z(\mathcal{H}) = 2$ along the family with $b \neq 0$.

6.4.4 Stokes Expansion for Even Waves

Stokes expansion gives again a direct way to illustrate small-amplitude periodic waves bifurcating from the constant solutions at $c = \frac{1}{2}$. In order to eliminate the constant wave, we set

$$\psi(x) = \frac{\sqrt{c}}{\sqrt{2}} + \varphi(x), \quad (6.83)$$

where φ is not required to satisfy the zero-mean property. The stationary equation (6.2) with $b = 0$ is written in the equivalent form:

$$D^\alpha \varphi - 2c\varphi = 2\varphi^3 + 3\sqrt{2c}\varphi^2. \quad (6.84)$$

By using the Stokes expansion in terms of small amplitude A :

$$\begin{cases} \varphi(x) = A\varphi_1(x) + A^2\varphi_2(x) + A^3\varphi_3(x) + \mathcal{O}(A^4), \\ 2c = 1 + A^2\gamma_2 + \mathcal{O}(A^4), \end{cases}, \quad (6.85)$$

we obtain recursively: $\varphi_1(x) = \cos(x)$,

$$\varphi_2(x) = -\frac{3}{2} + \frac{3}{2(2^\alpha - 1)} \cos(2x),$$

$$\varphi_3(x) = \frac{1}{2(3^\alpha - 1)} \left[1 + \frac{9}{2^\alpha - 1} \right] \cos(3x),$$

and

$$\gamma_2 = \frac{15}{2} - \frac{9}{2(2^\alpha - 1)}.$$

It follows that $\gamma_2 = 0$ if and only if $2^\alpha = \frac{8}{5}$, which is true at

$$\alpha_0 := \frac{\log 8 - \log 5}{\log 2} \approx 0.6781. \quad (6.86)$$

The following proposition summarizes properties of the small-amplitude periodic waves.

Proposition 6.4. *Let α_0 be given by (6.86). For each $\alpha \in (\alpha_0, 2]$, there exists $c_0 > \frac{1}{2}$ such that the even periodic wave exists for $c \in (\frac{1}{2}, c_0)$ with $n(\mathcal{H}) = 1$, $z(\mathcal{H}) = 1$ and is spectrally stable. For each $\alpha \in (\frac{1}{2}, \alpha_0)$, there exists $c_0 < \frac{1}{2}$ such that the even periodic wave exists for $c \in (c_0, \frac{1}{2})$ with $n(\mathcal{H}) = 2$, $z(\mathcal{H}) = 1$, and is spectrally stable.*

Proof. The existence statement follows from the Stokes expansion (6.85) with small wave amplitude A since $\gamma_2 > 0$ for $\alpha > \alpha_0$ and $\gamma_2 < 0$ for $\alpha < \alpha_0$.

In order to compute $n(\mathcal{H})$ and $z(\mathcal{H})$, we substitute (6.83) and (6.85) into (6.4) and obtain

$$\mathcal{H} = D^\alpha - 1 - A \cos(x) - A^2 [\gamma_2 + 6\varphi_2(x) - 6 \cos^2(x)] + \mathcal{O}(A^3).$$

We solve the spectral problem $\mathcal{H}v = \lambda v$ perturbatively near the eigenvalue $\lambda = 0$ associated with the subspace of even functions in $L^2(\mathbb{T})$. Hence, we expand

$$u = \cos(x) + Au_1(x) + A^2u_2(x) + \mathcal{O}(A^3), \quad \lambda = A^2\lambda_2 + \mathcal{O}(A^4),$$

and obtain recursively: $u_1(x) = 2\varphi_2(x)$ and $\lambda_2 = 2\gamma_2$. Hence, $\lambda > 0$ if $\gamma_2 > 0$ and $\lambda < 0$ if $\gamma_2 < 0$. The zero eigenvalue associated with the subspace of odd functions in $L^2(\mathbb{T})$ is preserved at zero for every A due to $\partial_x \psi \in \text{Ker}(\mathcal{H})$. In addition, there exists a negative eigenvalue of \mathcal{H} associated with the constant functions at $A = 0$. Hence, we confirm that $n(\mathcal{H}) = 1$ for $\alpha > \alpha_0$ and $n(\mathcal{H}) = 2$ for $\alpha < \alpha_0$, whereas $z(\mathcal{H}) = 1$ for both $\alpha > \alpha_0$ and $\alpha < \alpha_0$.

In order to deduce the spectral stability conclusion, we use transformation $\psi(x) = a + \phi(x)$, where the zero-mean function ϕ satisfies the boundary-value problem (6.42). Computing the mean value

$$a := \frac{1}{2\pi} \int_{-\infty}^{\infty} \psi(x) dx = \frac{1}{2} + \frac{3}{8} \left[1 - \frac{3}{2^\alpha - 1} \right] A^2 + \mathcal{O}(A^4)$$

we obtain

$$\omega := c - 6a^2 = -1 + \frac{3}{2} \left[1 + \frac{3}{2^\alpha - 1} \right] A^2 + \mathcal{O}(A^2)$$

and

$$\beta := ca - 2a^3 = \frac{3}{2} A^2 + \mathcal{O}(A^4).$$

No fold point occurs in the expansion of ω with respect to the Stokes amplitude A , in particular,

$$\frac{d\omega}{dA^2} = \frac{3}{2} \left[1 + \frac{3}{2^\alpha - 1} \right] + \mathcal{O}(A^2) > 0.$$

Since $\|\phi\|_{L^2}^2 = \pi A^2 + \mathcal{O}(A^4)$, we have

$$\frac{d}{d\omega} \|\phi\|_{L^2}^2 = \frac{2\pi}{3} \frac{2^\alpha - 1}{2^\alpha + 2} + \mathcal{O}(A^2) > 0, \quad (6.87)$$

and

$$\frac{\partial}{\partial \omega} \|\phi\|_{L^2}^2 = \frac{d}{d\omega} \|\phi\|_{L^2}^2 + \mathcal{O}(A^2) > 0.$$

By Theorem 6.6, the periodic waves are spectrally stable for small A both for $\alpha > \alpha_0$ and $\alpha < \alpha_0$. \square

Remark 6.13. For $\alpha > \alpha_0$, the small-amplitude periodic wave in Proposition 6.4 have the same properties $n(\mathcal{H}) = 1$, $z(\mathcal{H}) = 1$, and $\sigma_0 > 0$ as the even periodic wave in Theorem 6.5. However, for $\alpha < \alpha_0$, the small-amplitude periodic wave in Proposition 6.4 cannot be a minimizer of the constrained variational problem (6.38) in Theorem 6.5 because it exists for $c < \frac{1}{2}$ and has $n(\mathcal{H}) = 2$ and $\sigma_0 < 0$. Spectral stability of the periodic wave with $n(\mathcal{H}) = 2$, $\sigma_0 < 0$, and the slope condition (6.56) follows from the same computation as in the proof of Theorem 6.6.

6.4.5 Exact Solutions for Even Wave with $\alpha = 2$

In the case of the modified KdV equation ($\alpha = 2$), the stationary equation (6.2) with $b = 0$ can be solved in the space of even functions by using the Jacobian dnoidal function [12, 36].

Let us recall the normalized second-order equation

$$\psi_0''(z) + (k^2 - 2)\psi_0(z) + 2\psi_0(z)^3 = 0, \quad (6.88)$$

which admits the periodic solution $\psi_0(z) = \text{dn}(z; k)$ with the period $2K(k)$, where $K(k)$ is the complete elliptic integral of the first kind. Adopting an

elementary scaling transformation yields the exact solution in the form:

$$\psi(x) = \frac{1}{\pi} K(k) \operatorname{dn} \left[\frac{1}{\pi} K(k)x; k \right] \quad (6.89)$$

with

$$c = \frac{1}{\pi^2} K(k)^2 (2 - k^2). \quad (6.90)$$

The following proposition summarizes properties of the even periodic waves for $\alpha = 2$. These properties were studied in [12, 36].

Proposition 6.5. *Fix $\alpha = 2$. The even periodic wave (6.89) exists and is spectrally stable for every $c \in (\frac{1}{2}, \infty)$. Moreover, $n(\mathcal{H}) = 1$, $z(\mathcal{H}) = 1$, and $\sigma_0 > 0$ for every $c \in (\frac{1}{2}, \infty)$.*

Proof. The mapping $(0, 1) \ni k \mapsto c(k) \in (\frac{1}{2}, \infty)$ is one-to-one and onto. This follows from

$$\frac{\pi^2}{2} \frac{dc}{dk} = \frac{K(k)}{k(1-k^2)} [(2-k^2)E(k) - 2(1-k^2)K(k)] > 0, \quad (6.91)$$

where the latter inequality was proved in [12] (see also [36]). Indeed, if

$$f(k) := (2 - k^2)E(k) - 2(1 - k^2)K(k),$$

then $f(0) = 0$, whereas $f'(k) = 3k[K(k) - E(k)] > 0$ so that $f(k) > 0$ for $k \in (0, 1)$.

The mean value of the periodic wave in (6.89) is computed explicitly by

$$a := \frac{1}{2\pi} \int_{-\pi}^{\pi} \psi(x) dx = \frac{1}{\pi} \int_0^{K(k)} \operatorname{dn}(z; k) dz = \frac{1}{2}.$$

Hence, the zero-mean function $\phi(x) := \psi(x) - a$ is a solution to the boundary-value problem (6.42) with

$$\omega = c - \frac{3}{2}, \quad \beta = \frac{1}{2} \left(c - \frac{1}{2} \right).$$

This gives the straight line dependence $\beta = \frac{1}{2}(\omega + 1)$ for the periodic waves with the single-lobe profile. Furthermore, we can compute

$$\|\phi\|_{L^2}^2 = \frac{2}{\pi} K(k)E(k) - \frac{\pi}{2},$$

from which we verify that

$$\langle \phi, \partial_k \phi \rangle = -\frac{1}{\pi k(1-k^2)} [K(k)^2(1-k^2) - E(k)^2] > 0.$$

The latter inequality is also proven directly by setting

$$f(k) := K(k)^2(1-k^2) - E(k)^2$$

such that $f(0) = 0$ and $f'(k) = -2k^{-1}[K(k) - E(k)]^2 < 0$ so that $f(k) < 0$ for $k \in (0, 1)$. By Theorem 6.6, the even periodic wave (6.89) with the speed (6.90) satisfying (6.91) is spectrally stable for $c \in (\frac{1}{2}, \infty)$.

Other properties such as $1 \in \text{Range}(\mathcal{H})$, $\sigma_0 > 0$, and $n(\mathcal{H}) = 1$ for every $k \in (0, 1)$ can be confirmed by explicit computations. The normalized linearized operator is given by

$$\mathcal{H}_0 = -\partial_z^2 - 4 + 5k^2 - 6k^2 \text{cn}(z; k)^2. \quad (6.92)$$

Eigenvalues of \mathcal{H}_0 in (6.92) are given by subtracting $3(1-k^2)$ from eigenvalues of \mathcal{H}_0 in (6.69). However, \mathcal{H}_0 in (6.92) is considered in space $L^2(-K(k), K(k))$ so that the eigenvalues λ_1 and λ_2 given below (6.92) with the eigenfunctions in $L^2(-2K(k), 2K(k))$ are not relevant. Hence, the first three eigenvalues of \mathcal{H}_0 in (6.92) are given by

$$\begin{aligned} \lambda_0 &= -2 + k^2 - 2\sqrt{1-k^2+k^4}, & \varphi_0(z) &= 1 + k^2 + \sqrt{1-k^2+k^4} - 3k^2 \text{sn}(z; k)^2, \\ \lambda_1 &= 0, & \varphi_1(z) &= \text{sn}(z; k) \text{cn}(z; k), \\ \lambda_2 &= -2 + k^2 + 2\sqrt{1-k^2+k^4}, & \varphi_2(z) &= 1 + k^2 - \sqrt{1-k^2+k^4} - 3k^2 \text{sn}(z; k)^2. \end{aligned}$$

Eigenvalues and eigenvectors of the linearized operator \mathcal{H} are obtained after the same scaling transformation as in (6.89). In agreement with Lemma 6.6, we have $n(\mathcal{H}) = 1$ and $z(\mathcal{H}) = 1$. The property $1 \in \text{Range}(\mathcal{H})$ follows from the representation

$$\frac{1}{2\sqrt{1-k^2+k^4}} \mathcal{H}_0 \left[\frac{\lambda_2 \varphi_0 - \lambda_0 \varphi_2}{\lambda_0 \lambda_2} \right] = 1 \quad \text{and} \quad \frac{1}{2\sqrt{1-k^2+k^4}} [\varphi_0 - \varphi_2] = 1.$$

Direct computations yield

$$\langle \mathcal{H}_0^{-1} 1, 1 \rangle = \frac{\lambda_2 \langle \varphi_0, 1 \rangle - \lambda_0 \langle \varphi_2, 1 \rangle}{2\sqrt{1-k^2+k^4} \lambda_0 \lambda_2} = \frac{2}{k^4} [(2-k^2)K(k) - 2E(k)] > 0,$$

where the latter inequality is justified by assigning

$$f(k) := (2-k^2)K(k) - 2E(k)$$

with $f(0) = 0$ and $f'(k) = k(1 - k^2)^{-1}[E(k) - (1 - k^2)K(k)] > 0$ so that $f(k) > 0$ for $k \in (0, 1)$. \square

Remark 6.14. *Explicit computations in the proof of Proposition 6.5 repeat computations in [36], however, the expression for $\langle \mathcal{H}_0^{-1}1, 1 \rangle$ was typed incorrectly in [36].*

Remark 6.15. *The dnoidal wave of Proposition 6.5 coincides with the even periodic wave obtained in Theorem 6.5 for $\alpha = 2$. Similarly to Remark 6.12, this follows from uniqueness of smooth, positive, and 2π -periodic solutions of the differential equation (6.79) with $c \in (\frac{1}{2}, \infty)$, where the second-order equation (6.79) is the Euler–Lagrange equation for the variational problem in Theorem 6.5. Compared to Proposition 6.3, it is well-known (see, e.g., [?Yaga]) that the mapping $\mathcal{I} \mapsto L$ is monotonically increasing for the L -periodic, positive solutions of the differential equation (6.79) with the first-order invariant (6.80) for $c > 0$ such that $L \in (2\pi(2c)^{-1/2}, \infty)$. Therefore, there exists exactly one even, positive, 2π -periodic solution for every $c \in (\frac{1}{2}, \infty)$ and by uniqueness of solutions to differential equations, this unique solution is given by the dnoidal wave (6.89) and (6.90).*

6.4.6 Numerical Approximations

Here we numerically compute solutions of the stationary equation (6.2) with $b = 0$ using Newton’s method in the Fourier space. The starting iteration is generated from the Stokes expansion (6.85) and this solution is uniquely continued in c for all $c \in (\frac{1}{2}, \infty)$ if $\alpha > \alpha_0$.

Figure 6.4 presents the periodic wave solutions for $\alpha = 2$. The top panel shows the profiles of ψ for three different values of c . The bottom panels show the dependence of $F(\psi)$ versus c (left) and the dependence of $F(\phi)$ versus ω (right), where ϕ and ω was computed from the transformation $\phi(x) = \psi(x) - a$ and $\omega = c - 6a^2$ with $a := \frac{1}{2\pi} \int_{-\pi}^{\pi} \psi(x) dx$. The even periodic wave with the single-lobe profile ψ (red line) bifurcates at $c = \frac{1}{2}$ from the constant wave (grey line) shown on the bottom left. Since $F(\phi)$ is increasing in ω and $a = \frac{1}{2}$ is independent of ω , the even periodic wave is stable by Theorem 6.6.

Figure 6.5 presents similar results but for $\alpha = 1$. The periodic wave (red line on the top right panel) still bifurcates from the constant wave (grey line on the top right panel) to the right of the bifurcation point at $c = \frac{1}{2}$. However, a depends on ω for the even periodic wave, hence

$$\frac{d}{d\omega} F(\phi) = \frac{\partial}{\partial \omega} F(\phi) + \frac{da}{d\omega} \frac{\partial}{\partial a} F(\phi)$$

by the chain rule. In the Stokes limit, we have shown in Appendix A that

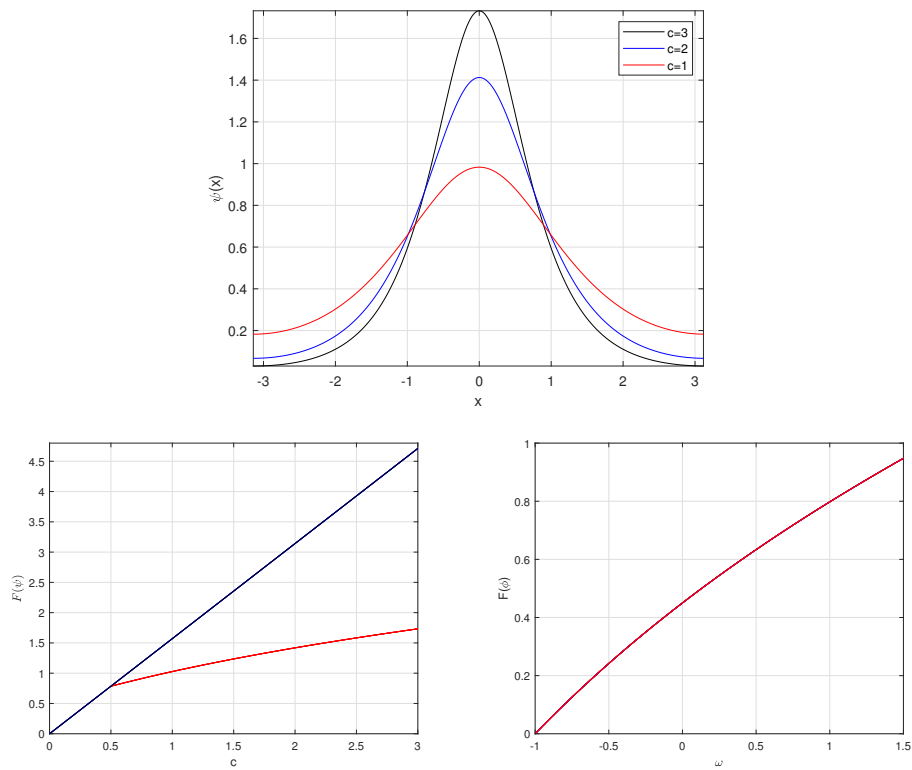


Figure 6.4: Periodic waves for $\alpha = 2$. Top: Profiles of ψ for three different values of c . Bottom: Dependence of the momentum $F(\psi)$ versus c (left) and $F(\phi)$ versus ω (right).

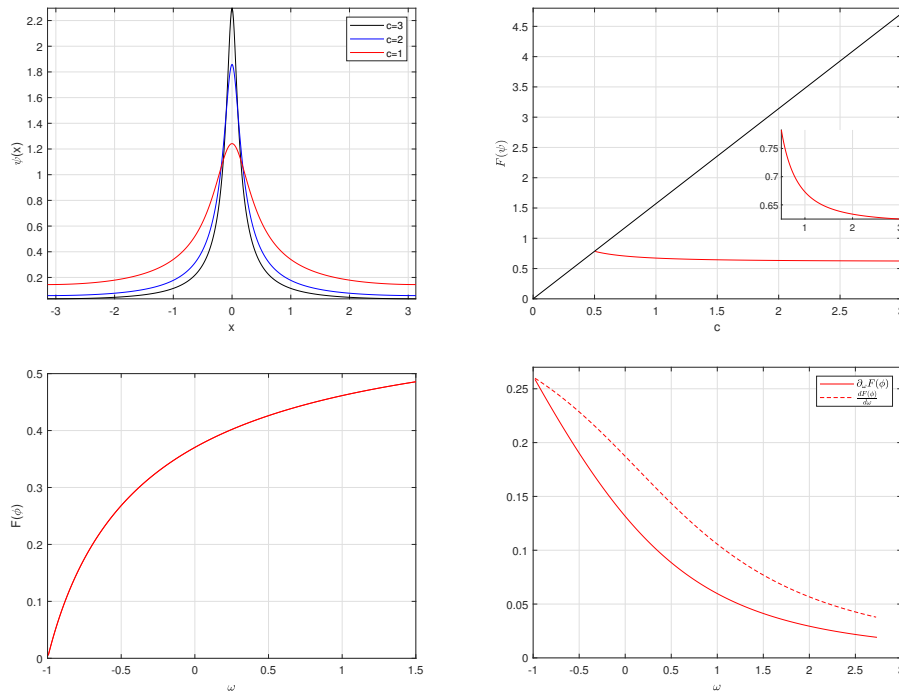


Figure 6.5: Periodic waves for $\alpha = 1$. Top: Profiles of ψ for three different values of c (left). Dependence of the momentum $F(\psi)$ versus c (right). Bottom: Dependence of $F(\phi)$ versus ω (left). and derivatives of $F(\phi)$ in ω (right). The solid (dashed) line shows the partial (ordinary) derivative in ω .

$\frac{\partial}{\partial \alpha} F(\phi) = \mathcal{O}(A^2)$ for small A so that

$$\frac{\partial}{\partial \omega} F(\phi) = \frac{d}{d\omega} F(\phi) + \mathcal{O}(A^2) > 0.$$

However, a discrepancy between partial and ordinary derivatives of $F(\phi)$ in ω exists away from the Stokes limit. The additional bottom right panel on Fig. 6.5 (compared to Fig. 6.4) shows the partial and ordinary derivatives on the same graph by the solid and dashed lines respectively. Since $\frac{\partial}{\partial \omega} F(\phi)$ remains positive, the even periodic wave is stable by Theorem 6.6. Since $F(\psi)$ for the even periodic wave is decreasing in c towards the horizontal asymptote as $c \rightarrow \infty$, it is clear that the stability conclusion does not follow from the dependence of the momentum $F(\psi)$ versus the wave speed c (see Remark 6.10).

Figure 6.6 presents similar results but for $\alpha = 0.6 < \alpha_0$. The periodic wave with the single-lobe profile ψ bifurcates to the left of the bifurcation point at $c = \frac{1}{2}$. There exists a fold point $c = c_0 \approx 0.4722$, where the branch turns and extends to all values of $c > c_0$. The upper branch (shown in red line on the top right panel) in $c \in (c_0, \frac{1}{2})$ has $n(\mathcal{H}) = 2$, whereas the lower branch (shown in blue line on the top right panel) has $n(\mathcal{H}) = 1$. The two branches were found iteratively from different initial approximations: the Stokes expansion was used for the upper branch and the periodic wave with larger $c > \frac{1}{2}$ was used for the lower branch, then the two branches were continued in either direction. The grey line on the top right panel shows the momentum $F(\psi)$ of the constant solution.

It follows from the graph of $F(\phi)$ versus ω and its derivatives (bottom panels) that the periodic wave is stable near the bifurcation point before and after the fold point but there exists $c_* \approx 0.4774$ such that the even periodic wave is stable for $c < c_*$ and unstable for $c > c_*$. By comparing the partial and ordinary derivatives of $F(\phi)$ with respect to ω (solid and dashed lines, respectively), we can see that the partial derivative becomes zero for a smaller value of ω , which gives the correct transition from stability to instability at $c = c_*$ by Theorem 6.6.

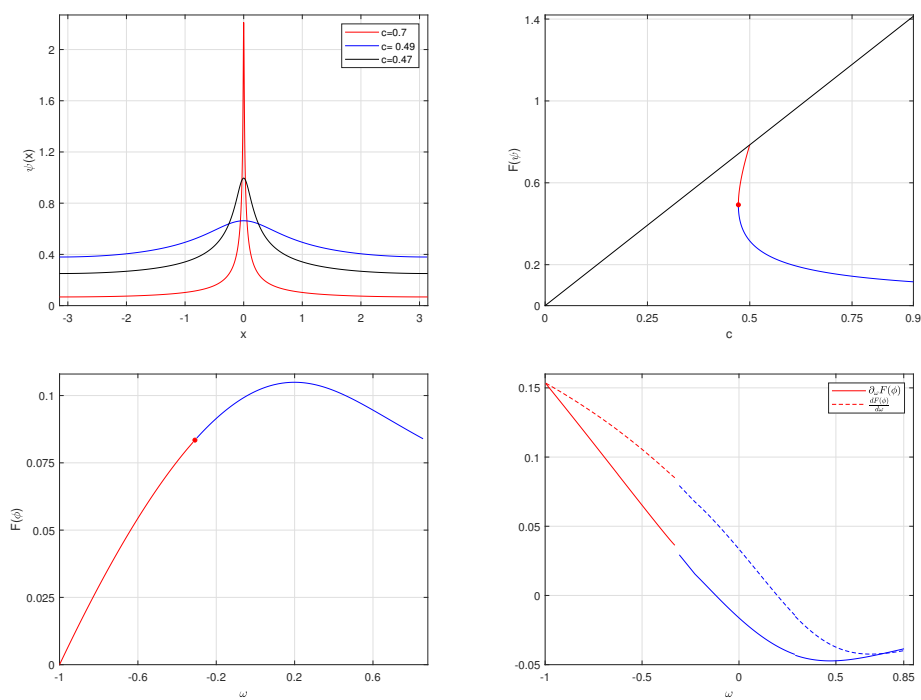


Figure 6.6: The same as Figure 6.5 but for $\alpha = 0.6$.

Appendix A

Preliminary Results

Here, we list a few basic definitions and results which are referred to throughout the thesis.

Definition A.1 (Resolvent and Spectrum set).

Let H be a Hilbert space with the inner product $\langle \cdot, \cdot \rangle_H$ and L be a densely defined operator on H with the domain $\text{Dom}(L) \subseteq H$. The resolvent set of L , denoted $\rho(L)$ is the set of $\lambda \in \mathbb{C}$ such that $(L - \lambda I)^{-1}$ exists, bounded and $\text{Ran}(L - \lambda I)$ is dense in H .

The spectrum of L , denoted $\sigma(L)$, is the complement of the resolvent set of L , that is, $\sigma(L) = \mathbb{C} \setminus \rho(L)$. Moreover, spectrum of L comprises of three disjoint sets:

- The point spectrum $\sigma_p(L)$ is the set of $\lambda \in \sigma(L)$ such that $\text{Ker}(L - \lambda I) \neq \{0\}$,
- The residual spectrum $\sigma_r(L)$ is set of $\lambda \in \sigma(L)$ such that $(L - \lambda I)^{-1}$ exists and $\text{Ran}(L - \lambda I)$ is not dense in H ,
- The continuous spectrum $\sigma_c(L)$ is the set of $\lambda \in \sigma(L)$ such that $(L - \lambda I)^{-1}$, $\text{Ran}(L - \lambda I)$ is dense in H but the operator $(L - \lambda I)^{-1}$ is not bounded.

Definition A.2 (Adjoint operator).

Let H be a Hilbert space with the inner product $\langle \cdot, \cdot \rangle_H$ and L be a densely defined operator on H with the domain $\text{Dom}(L) \subseteq H$. The adjoint operator L^* with the domain $\text{Dom}(L^*) \subseteq H$ is defined by

$$\forall u \in \text{Dom}(L), v \in \text{Dom}(L^*) : \quad \langle Lu, v \rangle = \langle u, L^*v \rangle$$

We say L is self-adjoint if $L = L^*$.

Definition A.3 (Fredholm operator).

We say a linear operator $L : \text{Dom}(L) \subset H \rightarrow H$ is a Fredholm operator of index zero if

$$\dim(\ker(L)) = \dim(\ker(L^*)) < \infty$$

and $\text{Ran}(L)$ is closed.

Theorem A.1 (Orthogonal decomposition of H).

Let L be a Fredholm operator of index zero. Then

$$H = \text{Ker}(L^*) \oplus \text{Ran}(L), \quad H = \text{Ker}(L) \oplus \text{Ran}(L^*).$$

Theorem A.2 (Fredholm Alternative).

Let $L : \text{Dom}(L) \subset H \rightarrow H$ is a Fredholm operator of index zero. There exists a solution $u \in \text{Dom}(L)$ of the inhomogeneous equation $Lu = f$ for a given $f \in H$ if and only if $\langle f, v_0 \rangle = 0$ for all $v_0 \in \text{Ker}(L^*)$. Moreover, the solution u is unique under the constraint $\langle u, w_0 \rangle = 0$ for all $w_0 \in \text{Ker}(L)$.

Theorem A.3 (Eigenvalue Count in Constrained L^2 space). [78]

Let L be a self-adjoint operator in L^2 with $\sigma_c(L) \geq c > 0$ and $\dim(\sigma_p(L)) < \infty$, and denote the number of negative and zero eigenvalues of L by $n(L)$ and $z(L)$. Define L_c^2 as the subspace of L^2 by

$$L_c^2 = \{u \in L^2 : \{\langle u, v_j \rangle_{L^2} = 0\}_{j=1}^N\},$$

where $\{v_j\}_{j=1}^N$ is a set of linearly independent vectors. Let $A(\mu)$ be the matrix valued function defined by

$$\forall \mu \notin \sigma(L) : A_{i,j}(\mu) = \langle (\mu - L)^{-1} v_i, v_j \rangle_{L^2}, \quad i, j \in \{1, 2, \dots, N\}$$

Let n_0 , z_0 and p_0 be the numbers of negative, zero, and positive eigenvalues of $\lim_{\mu \rightarrow 0} A(\mu)$ and denote $z_\infty = N - n_0 - z_0 - p_0$. Then, the number of negative and zero eigenvalues of $L|_{L_c^2}$ are given by

$$\begin{aligned} n(L|_{L_c^2}) &= n(L) - p_0 - z_0, \\ z(L|_{L_c^2}) &= z(L) + z_0 - z_\infty \end{aligned}$$

Theorem A.4 (Implicit Function Theorem).

Let X , Y , and Z be Banach spaces and let $F(x, y) : X \times Y \mapsto Z$ be a C^1 map on an open neighborhood of the point $(x_0, y_0) \in X \times Y$. Assume that

$$F(x_0, y_0) = 0,$$

and that

$$D_x F(x_0, y_0) : X \mapsto Z \text{ is one-to-one and onto.}$$

There are $r > 0$ and $\delta > 0$ such that for each y with $\|y - y_0\| \leq \delta$ there exists a unique solution $x \in X$ of the operator equation $F(x, y) = 0$ with $\|x - x_0\| \leq r$. Moreover, the map $Y \ni y \mapsto x(y) \in X$ is C^1 near $y = y_0$.

Theorem A.5 (Banach Fixed Point Theorem).

Let M be a closed, non-empty subset in the Banach space X and let $A : M \mapsto M$ be a contraction operator, that is, for all $u, v \in M$ there exists $q \in [0, 1)$ satisfying $\|Au - Av\|_X \leq q\|u - v\|_X$. Then, there exists a unique $y \in M$ such that $A(y) = y$.

The following three propositions are formulated as Lemma 3.2 and claims (L1) and (L3) in Lemma 3.3 of [53]

Proposition A.1. Let $\alpha \in (\frac{1}{3}, 2]$ and $\psi \in H_{\text{per,odd}}^\alpha$ be a solution obtained in Theorem 6.3 and Corollary 6.1. An eigenfunction of \mathcal{H} defined by (6.4) and (6.17) corresponding to the n -th eigenvalue of \mathcal{H} for $n = 1, 2, 3$ changes its sign at most $2(n - 1)$ times over \mathbb{T} . An eigenfunction of $\mathcal{H}|_{L_{\text{even}}^2}$ for the n -th eigenvalue of $\mathcal{H}|_{L_{\text{even}}^2}$ changes its sign at most $2(n - 1)$ times over \mathbb{T} .

Proposition A.2. Assume $\alpha \in (\frac{1}{3}, 2]$ and $\psi \in H_{\text{per,odd}}^\alpha$ be a solution obtained in Theorem 6.3 and Corollary 6.1. If $\{1, \psi, \psi^2\} \in \text{Range}(\mathcal{H})$, then $\text{Ker}(\mathcal{H}) = \text{span}(\partial_x \psi)$.

Proposition A.3. Assume $\alpha \in (\frac{1}{3}, 2]$ and $\psi \in H_{\text{per,odd}}^\alpha$ be a solution obtained in Theorem 6.3 and Corollary 6.1. Then, $\partial_x \psi \in \text{Ker}(\mathcal{H})$ corresponds to the lowest eigenvalue of \mathcal{H} in the space of odd functions with respect to $x = \pi/2$.

Appendix B

Periodic Waves In The KdV And BO Equation

We verify the assumptions 4.17 in Theorem 4.1 of Chapter 4 for the KdV and BO equations.

The solution ϕ to the boundary-value problem (4.1) with $\alpha = 2$ is given by

$$\phi(x) = \frac{2K(k)^2}{\pi^2} \left[1 - 2k^2 - \sqrt{1 - k^2 + k^4} + 3k^2 \operatorname{cn}^2 \left(\frac{K(k)}{\pi} x; k \right) \right] \quad (\text{B.1})$$

where cn is the Jacobi elliptic function, $K(k)$ is a complete elliptic integral of the first kind, and $k \in (0, 1)$ is the elliptic modulus that parameterizes the wave speed c given by

$$c = \frac{4K(k)^2}{\pi^2} \sqrt{1 - k^2 + k^4}. \quad (\text{B.2})$$

The small-amplitude expansions (3.9) and (3.13) are recovered from (3.38)–(3.39) with the wave amplitude $a := 3k^2/4 + \mathcal{O}(k^4)$ as $k \rightarrow 0$.

We prove that the map $(0, 1) \ni k \mapsto c \in (1, \infty)$ is strictly increasing, hence the explicit solution (3.38)–(3.39) exists for every $c > 1$ (see also [14]). We also extend the inequalities (4.19) and (4.20) with $\alpha = 2$ for every $c > 1$.

Lemma B.1. *The map $(0, 1) \ni k \mapsto c \in (1, \infty)$ for the solution (B.1)–(B.2) is strictly increasing. In addition, for every $c > 1$, we have*

$$\int_{-\pi}^{\pi} \phi^3 dx < 0, \quad \int_{-\pi}^{\pi} \phi(\phi')^2 dx < 0. \quad (\text{B.3})$$

Proof. We have $\phi = 0$ and $c = 1$ at $k = 0$. Thanks to the smoothness of ϕ

and c in k , it holds from (3.39) by explicit differentiation:

$$\frac{\pi^2 \sqrt{1-k^2+k^4}}{4K(k)} \frac{dc}{dk} = 2(1-k^2+k^4) \frac{dK(k)}{dk} - k(1-2k^2)K(k).$$

By using the differential relation,

$$\frac{dK(k)}{dk} = \frac{E(k) - (1-k^2)K(k)}{k(1-k^2)},$$

the previous expression can be reduced to the form

$$\frac{\pi^2 k(1-k^2) \sqrt{1-k^2+k^4}}{4K(k)} \frac{dc}{dk} = 2(1-k^2+k^4)E(k) - (2-3k^2+k^4)K(k) =: I(k),$$

where $E(k)$ is a complete elliptic integral of the second kind and $I(k)$ is introduced for convenience. Note that $I(0) = 0$. We claim that the map $(0, 1) \ni k \mapsto I$ is strictly increasing. Indeed, by using the differential relation

$$\frac{dE(k)}{dk} = \frac{E(k) - K(k)}{k},$$

we obtain after straightforward computations

$$\frac{dI(k)}{dk} = 5k [(1-k^2)K(k) - (1-2k^2)E(k)] > 0,$$

where the last inequality follows from the fact that $K(k) > E(k)$ for every $k \in (0, 1)$. Since $I(0) = 0$, we have $I(k) > 0$ for every $k \in (0, 1)$, which implies that $\frac{dc}{dk} > 0$ for every $k \in (0, 1)$.

Let us now prove the inequalities (B.3) for every $c > 1$. Since ϕ and c are smooth in k , we differentiate the nonlinear equation in the boundary-value problem (4.1) with $\alpha = 2$ in k and obtain

$$[c + D_{\alpha=2} + 2\phi] \frac{\partial \phi}{\partial k} + \frac{dc}{dk} \phi = 0.$$

Multiplying this equation by ϕ and integrating on $[-\pi, \pi]$ imply that

$$\int_{-\pi}^{\pi} \phi^2 \frac{\partial \phi}{\partial k} dx = -\frac{dc}{dk} \int_{-\pi}^{\pi} \phi^3 dx,$$

where we have used the facts that $D_{\alpha=2}$ is self-adjoint in $L^2_{\text{per}}(-\pi, \pi)$ and $\phi, \partial_a \phi \in H^{\alpha=2}_{\text{per}}(-\pi, \pi)$. Since $\frac{dc}{dk} > 0$ for every $k \in (0, 1)$, the map $k \mapsto \int_{-\pi}^{\pi} \phi^3 dx$ is strictly decreasing with $\int_{-\pi}^{\pi} \phi^3 dx = 0$ at $k = 0$. Therefore, $\int_{-\pi}^{\pi} \phi^3 dx < 0$ for

$k \in (0, 1)$ by the continuity argument in k .

Finally, the inequality $\int_{-\pi}^{\pi} \phi(\phi')^2 dx < 0$ for every $c > 1$ follows from the boundary-value problem (4.1) with $\alpha = 2$:

$$\int_{-\pi}^{\pi} \phi(\phi')^2 dx = -\frac{1}{c} \left[\int_{-\pi}^{\pi} (\phi')^2 \phi'' dx + \int_{-\pi}^{\pi} \phi^2 (\phi')^2 dx \right],$$

where the first term in the right-hand side is zero thanks to the smoothness of ϕ . □

The next Lemma shows that the solution ϕ of the boundary value problem (4.1) when $\alpha = 1$ also satisfies assumption 4.17.

Lemma B.2. *Let*

$$\phi(x) = \frac{\cosh \gamma \cos x - 1}{\sinh \gamma (\cosh \gamma - \cos x)}, \quad c = \coth \gamma \tag{B.4}$$

be the solution of (4.1) with $\alpha = 1$ then the inequalities

$$\int_{-\pi}^{\pi} \phi^3 dx < 0, \quad \int_{-\pi}^{\pi} \phi(\phi')^2 dx < 0 \tag{B.5}$$

hold for every $c > 1$.

Proof. We notice that the small amplitude expansion (3.9) and (3.13) are recovered from (B.4) with the wave amplitude $a := 2e^{-\gamma} + \mathcal{O}(e^{-3\gamma})$ as $\gamma \rightarrow \infty$. Since the map $(0, \infty) \ni \gamma \mapsto c = \coth \gamma \in (1, \infty)$ is strictly decreasing, the explicit solution (B.4) exists for every $c > 1$.

Using the explicit formula (B.4) and symbolic computations with Wolfram’s Mathematica, we obtain

$$\int_{-\pi}^{\pi} \phi^3 dx = -\pi(c - 1)^2(2c + 1),$$

and

$$\int_{-\pi}^{\pi} \phi(\phi')^2 dx = \frac{\pi}{4}(c^1 - 1)^2,$$

from which the inequalities (B.5) hold for all $c > 1$. □

Bibliography

- [1] L. Abdelouhab, J. Bona, M. Felland, and J. C Saut, *Nonlocal models for nonlinear, dispersive wave*, Phys. D **40** (1989), 360–392.
- [2] M. J. Ablowitz, *Nonlinear dispersive waves: Asymptotic analysis and solitons*, Cambridge Texts in Applied Mathematics, Cambridge University Press, 2011.
- [3] G. B. Airy, *On the laws of the tides on the coasts of Ireland, as inferred from an extensive series of observations made in connection with the ordnance survey of Ireland*, Phil. Trans. R. Soc **135** (1845), 1–124.
- [4] G.B. Airy, *Tides and waves*, Encyclopædia Metropolitana, John Joseph Griffin and Company, 1849.
- [5] J. P. Albert, *Concentration compactness and the stability of solitary-wave solutions to nonlocal equations*, Contemporary Mathematics **221** (1999), 1–29.
- [6] J. Álvarez and A. Durán, *Petviashvili type methods for traveling wave computations: I. analysis of convergence*, J. Comput. Appl. Math. **266** (2014), 39–51.
- [7] J. Álvarez and A. Durán, *Petviashvili type methods for traveling wave computations: II. acceleration with vector extrapolation methods*, Math. Comput. Simulation (2016), 19–36.
- [8] J. Álvarez and A. Durán, *Numerical generation of periodic traveling wave solutions of some nonlinear dispersive wave systems*, J. Comput. Appl. Math. **316** (2017), no. 29–39.
- [9] G. Alves, F. Natali, and A. Pastor, *Sufficient conditions for orbital stability of periodic traveling waves*, J. Diff. Eqs. **267** (2019), 879–901.
- [10] V. Ambrosio, *On the existence of periodic solutions for a fractional Schrödinger equation*, Proc. ams **146**, 2018, pp. 3767–3775.
- [11] T. P. Andrade and A. Pastor, *Orbital stability of one-parameter periodic traveling waves for dispersive equations and applications*, J. Math. Anal. Appl **475** (2019), 1242–1275.
- [12] J. Angulo, *Non-linear stability of periodic travelling-wave solutions for the Schrödinger and modified Korteweg-de Vries equation*, J. Diff. Equat. **235** (2007), 1–30.
- [13] ———, *Stability properties of solitary waves for fractional KdV and BBM equations*, Nonlinearity **31** (2018), 920–956.
- [14] J. Angulo and F. Natali, *Positivity properties of the Fourier transform and the stability of periodic travelling-wave solutions*, SIAM J. Math. Anal **40** (2008), 1123–1151.
- [15] ———, *Instability of periodic traveling waves for dispersive models*, Diff. Int. Equat **29** (2016), 837–874.

-
- [16] K. I. Babenko, *Some remarks on the theory of surface waves of finite amplitude*, Dokl. Akad. Nauk SSSR **294** (1987), 1033–1037.
- [17] Z. Bai and H. Lü, *Positive solutions for boundary value problem of nonlinear fractional differential equation*, J Math. Anal. Appl **311** (2005), 495–505.
- [18] H. Bateman, *Higher transcendental functions*, Vol. III, McGraw-Hill Book Company, New York, 1953.
- [19] T. Brooke Benjamin, *Internal waves of permanent form in fluids of great depth*, Journal of Fluid Mechanics **29**, no. 3, 559–592.
- [20] J. L. Bona and H. Kalisch, *Singularity formation in the generalized Benjamin—Ono equation*, Disc.Contin. Dyn. Syst. **11** (2004), 27–45.
- [21] J. L. Bona, P. E. Souganidis, and W. A. Strauss, *Stability and instability of solitary waves of Korteweg-de Vries type*, Proc. Roy. Soc. London Ser. A **411** (1987), 395–412.
- [22] J. Boussinesq, *Théorie des ondes et des remous qui se propagent le long d’un canal rectangulaire horizontal, en communiquant au liquide contenu dans ce canal des vitesses sensiblement pareilles de la surface au fond.*, Journal de Mathématiques Pures et Appliquées (1872), 55–108.
- [23] ———, *Essai sur la théorie des eaux courantes; mémoires présentés par divers savants à l’acad. des Sci. Inst. Nat. France* **XXIII** (1877), 1–680.
- [24] H. Brezis, *Functional analysis, Sobolev spaces and partial differential equations*, Springer, New York, 2011.
- [25] J. C. Bronski and V. M. Hur, *Modulational instability and variational structure*, Stud. Appl. Math **132** (2014), 285–331.
- [26] H. Chen, *Existence of periodic traveling-wave solutions of nonlinear, dispersive wave equations*, Nonlinearity **17** (2004), 2041–2056.
- [27] H. Chen and J. Bona, *Periodic travelling wave solutions of nonlinear dispersive evolution equations*, Discr. Cont. Dynam. Syst **33** (2013), 4841–4873.
- [28] M. Chugunova and D. Pelinovsky, *Count of eigenvalues in the generalized eigenvalue problem*, J. Math. Phys **51** (2010), 052901 (19 pages).
- [29] M. Chugunova and D. E. Pelinovsky, *Two-pulse solutions in the fifth-order KdV equation: rigorous theory and numerical approximations*, Discr. Cont. Dynam. Syst. B **8** (2007), 773–800.
- [30] K. Claasen and M. Johnson, *Nondegeneracy and stability of antiperiodic bound states for fractional nonlinear Schrödinger equations*, J. Diff. Eqs. **266** (2019), 5664–5712.
- [31] D. Clamond and D. Dutykh, *Fast accurate computation of the fully nonlinear solitary surface gravity waves*, Comput. & Fluids **84** (2013), 35–38.
- [32] ———, *Accurate fast computation of steady two-dimensional surface gravity waves in arbitrary depth*, J. Fluid Mech. **844** (2018), 491–518.
- [33] J. Colliander, M. Keel, G. Staffilani, H. Takaoka, and T. Tao, *Sharp global well-posedness results for periodic and non-periodic KdV and modified KdV on \mathbb{R} and \mathbb{T}* , J. Amer. Math. Soc **16** (2003), 705–749.
- [34] R. J. Decker, A. Demirkaya, P. G. Kevrekidis, D. Iglesias, J. Severino, and Y. Shavit, *Kink dynamics in a nonlinear beam model*, 2020.

-
- [35] R. J. Decker, A. Demirkaya, N. S. Manton, and P. G. Kevrekidis, *Kink-antikink interaction forces and bound states in a biharmonic ϕ^4 model*, 2020.
- [36] B. Deconinck and T. Kapitula, *On the spectral and orbital stability of spatially periodic stationary solutions of generalized Korteweg-de Vries equations*, Hamiltonian partial diff eq. appl. (fields institute communications), 2015, pp. 285–322.
- [37] L. Demanet and W. Schlag, *Numerical verification of a gap condition for a linearized NLS equation*, Nonlinearity **19** (2006), 829–852.
- [38] Z. Du and C. Gui, *Further study on periodic solutions of elliptic equations with a fractional Laplacian*, Nonlinear Analysis **193** (2020), 111417 (16 pages).
- [39] A. Durán, *An efficient method to compute solitary wave solutions of fractional Korteweg-de Vries equations*, International Journal of Computer Mathematics **95** (2018), no. 6-7, 1362–1374.
- [40] D. Dutykh and D. Clamond, *Efficient computation of steady solitary gravity waves*, Wave Motion **51** (2014), 86–99.
- [41] S. A. Dyachenko, P. M. Lushnikov, and A. O. Korotkevich, *Complex singularity of a Stokes wave*, JETP Letters **98** (2014), 675–679.
- [42] R. L. Frank and E. Lenzmann, *Uniqueness of non-linear ground states for fractional Laplacian in \mathbb{R}* , Acta Math **210** (2013), 261–318.
- [43] T. Gallay and D. E. Pelinovsky, *Orbital stability in the cubic defocusing NLS equation. part i: Cnoidal periodic waves*, J. Diff. Eqs. **258** (2015), 3607–3638.
- [44] R. Garappa, *The Mittag-Leffler function (matlab central file exchange)*, Retrieved October 31 (2020).
- [45] L. Gavrilov, *Remark on the number of critical points on the period*, J. Diff. Eqs **101** (1993), 58–65.
- [46] R. Gorenflo, A. Kilbas, F. Mainardi, and S. Rogosin, *Mittag-Leffler functions, related topics and applications*, Springer-Verlag, Berlin, 2014.
- [47] M. Grillakis, J. Shatah, and W. Strauss, *Stability theory of solitary waves in the presence of symmetry i*, J. Funct. Anal **74** (1987), 160–197.
- [48] S. Hakkaev and A. G. Stefanov, *Stability of periodic waves for the fractional KdV and NLS equations*, Proc. R. Soc. Edinburgh, 2021. to be published.
- [49] M. Haragus, J. Li, and D. E. Pelinovsky, *Counting unstable eigenvalues in Hamiltonian spectral problems via commuting operators*, Comm. Math. Math **354** (2017), 247–268.
- [50] M. Hărăguș and T. Kapitula, *On the spectra of periodic waves for infinite-dimensional Hamiltonian systems*, Phys. D **237** (2008), 2649–2671.
- [51] D. Henry, J. F. Perez, and W. Wreszinski, *Stability theory for solitary-wave solutions of scalar field equation*, Comm. Math. Phys **85** (1982), 351–361.
- [52] V. Hur and M. A. Johnson, *Modulational instability in the Whitham equation for water waves*, Stud. Appl. Math **134** (2014), 120–143.
- [53] V. M. Hur and M. Johnson, *Stability of periodic traveling waves for nonlinear dispersive equations*, SIAM J. Math. Anal **47** (2015), 3528–3554.
- [54] M. A. Johnson, *Stability of small periodic waves in fractional KdV-type equations*, SIAM J. Math. Anal **45** (2013), 3168–3293.

- [55] T. Kapitula and K. Promislow, *Spectral and dynamical stability of nonlinear waves*, Applied Mathematical Science, Springer, New York, 2013.
- [56] T. Kapitula and A. Stefanov, *Hamiltonian–Krein (instability) index theory for kdv-like eigenvalue problems*, Stud. Appl. Math **132** (2014), 183–211.
- [57] T. Kato, *Perturbation theory for linear operators*, Classics in Mathematics, Springer-Verlag Berlin Heidelberg, Germany, 1995.
- [58] C. E. Kenig, Y. Martel, and L. Robbiano, *Local well-posedness and blow-up in the energy space for a class of l^2 critical dispersion generalized Benjamin-Ono equations*, Ann. Inst. H. Poincaré, Anal. Non Lin **28** (2011), 853–887.
- [59] C. E. Kenig and H. Takaoka, *Global well posedness of the modified Benjamin-Ono equation with initial data in $h^{1/2}$* , IMRN **2006** (2006), O95702.
- [60] A. A. Kilbas, H. M. Srivastava, and J. J. Trujillo, *Theory and application of fractional differential equations*, North-Holland Mathematics Studies, vol. 204, Elsevier, New York, 2006.
- [61] D. J. Korteweg and G. de Vries, *Xli. on the change of form of long waves advancing in a rectangular canal, and on a new type of long stationary waves*, The London, Edinburgh, and Dublin Philosophical Magazine and Journal of Science **39** (1895), no. 240, 422–443.
- [62] M. Kwasnicki, *Ten equivalent definitions of the fractional laplace operator*, Fractional Calculus and Applied Analysis **20** (2017), 51–7.
- [63] T. I. Lakoba and J. Yang, *A generalized petviashvili iteration method for scalar and vector Hamiltonian equations with arbitrary form of nonlinearity*, J. Comput. Phys **226** (2007), 1668–1692.
- [64] U. Le and D. E. Pelinovsky, *Convergence of Petviashvili’s method near periodic waves in the fractional Korteweg-de Vries equation*, SIAM J. Math. Anal **51** (2019), 2850–2883.
- [65] S. P. Levandosky, *A stability analysis of fifth-order water wave models*, Physica D **125** (1999), 222–240.
- [66] Z. Lin, *Instability of nonlinear dispersive solitary waves*, J. Funct. Anal **255** (2008), 1091–1124.
- [67] F. Linares, D. Pilod, and J. C. Saut, *Dispersive perturbations of Burgers and hyperbolic equations i: Local theory*, SIAM J. Math. Anal **46** (2014), 1505–1537.
- [68] ———, *Remarks on the orbital stability of ground state solutions of FKDV and related equations*, Adv. Diff. Eqs. **20** (2015), 835–858.
- [69] A. Lischke, G. Pang, M. Gulian, F. Song, C. Glusa, X. Zheng, Z. Mao, W. Cai, M. M. Meerschaert, M. Ainsworth, and G. E. Karniadakis, *What is the fractional Laplacian? a comparative review with new results*, J. Comp. Phys **404** (2020), 109009 (62 pages).
- [70] Y. Martel and D. Pilod, *Construction of a minimal mass blow up solution of the modified Benjamin–Ono equation*, Math. Ann **369** (2017), 153–245.
- [71] Y. Matsuno, *Bilinear transformation method*, Vol. 174, Academic Press, Mathematics in Science and Engineering, 1984.
- [72] M. G Mittag-Leffler, *Sur la nouvelle fonction $e_\alpha(x)$* , Acad. Sci. Paris **137** (1903), 554–558.

- [73] L. Molinet, D. Pilod, and S. Vento, *On well-posedness for some dispersive perturbations of Burgers equation*, Ann. I.H.Poincaré. **35** (2018), 1719–1756.
- [74] F. Natali, D. Pelinovsky, and U. Le, *New variational characterization of periodic waves in the fractional Korteweg–de Vries equation*, Nonlinearity **33** (2020), 1956–1986.
- [75] ———, *Periodic waves in the fractional modified Korteweg–de Vries equation*, arXiv, 2020.
- [76] J. J. Nieto, *Maximum principles for fractional differential equations derived from Mittag–Leffler functions*, appl. Math. Lett. **23** (2010), 1248–1251.
- [77] Hiroaki Ono, *Algebraic solitary waves in stratified fluids*, Journal of the Physical Society of Japan **39** (1975), no. 4, 1082–1091.
- [78] D. E. Pelinovsky, *Inertia law for spectral stability of solitary waves in coupled nonlinear Schrödinger equations*, Proc. Roy. Soc. Lond. A **461** (2005), 783–812.
- [79] ———, *Localization in periodic potentials: from Schrödinger operators to the Gross–Pitaevskii equation*, LMS Lecture Note Series, vol. 390, Cambridge University Press, Cambridge, 2011.
- [80] ———, *Spectral stability of nonlinear waves in KdV-type evolution equations*, Nonlinear physical systems: Spectral analysis, stability, and bifurcations, 2014, pp. 377–400.
- [81] D. E. Pelinovsky and Yu. A. Stepanyants, *Convergence of Petviashvili’s iteration method for numerical approximation of stationary solutions of nonlinear wave equations*, SIAM J. Numer. Anal **42** (2004), 1110–1127.
- [82] V.I. Petviashvili, *Equation of an extraordinary soliton*, Plasma Physics **2** (1976), p.469.
- [83] I. Podlubny, *Fractional differential equations*, Mathematics in Science and Engineering, vol. 198, Academic Press, California, 1998.
- [84] H. Pollard, *The complete monotonic character of the Mittag–Leffler function $e_\alpha(-x)$* , Bull. Amer. Math. Soc **54** (1948), 1115–1116.
- [85] A. P. Prudnikov, Y. A. Brychkov, and O. I. Marichev, *Integrals and series: Volume 1–elementary functions* (N.M. Queen Trans, ed.), Taylor & Francis, London, 2002.
- [86] L. Roncal and P. R. Stinga, *Fractional Laplacian on the torus*, Commu. Contemp. Math **18** (2016), 1550033 (26 pages).
- [87] A. O. Krotkevich S. A. Dyachenko P. M. Lushnikov, *Complex singularity of a Stokes wave*, JETP Letters **98** (2014), 675–679.
- [88] T. Simon, *On the Green’s functions of the killed fractional Laplacian on the periodic domain*, In prints.
- [89] J.A. Sanders S.N. Chow, *On the number of critical points of the period*, J. Diff. Eqs **64** (1986), 51–66.
- [90] G.G. Stokes, *On the theory of oscillatory waves*, University of Chicago, 1880.
- [91] P. J. Torres, *Existence of one-signed periodic solutions of some second-order differential equations via a Krasnoselskii fixed point theorem*, J. Diff. Eqs. **190** (2003), 643–662.
- [92] M. I. Weinstein, *Modulational stability of ground states of nonlinear Schrödinger equations*, SIAM J. Math. Anal **16** (1985), 472–491.
- [93] ———, *Lyapunov stability of ground states of nonlinear dispersive evolution equations*, Comm. Pure Appl. Math **39** (1986), 51–68.

- [94] E. Zeidler, *Applied functional analysis: Main principles and their applications*, Applied Mathematical Sciences, vol. 109, Springer-Verlag, New York.